

UCSF

UC San Francisco Electronic Theses and Dissertations

Title

Genetic Predictors of Bevacizumab-Induced Hypertension

Permalink

<https://escholarship.org/uc/item/5v75r4n9>

Author

Li, Megan S.

Publication Date

2017

Peer reviewed|Thesis/dissertation

Genetic Predictors of
Bevacizumab-Induced Hypertension

by

Megan S. Li

DISSERTATION

Submitted in partial satisfaction of the requirements for the degree of

DOCTOR OF PHILOSOPHY

in

Pharmaceutical Sciences and Pharmacogenomics

in the

GRADUATE DIVISION

**Copyright 2017
by
Megan S. Li**

Dedicated to Rufus,
who sat at my feet for countless hours while I studied and worked
and patiently listened to all my practice talks.

Acknowledgments

First and foremost, I thank my research advisor Dr. Deanna Kroetz, who has been incredibly supportive and encouraging while also challenging me to become an independent thinker and a better scientist. Deanna has played an instrumental part in making my completion of a Ph.D. a productive and rewarding experience, and I am extremely grateful to have her as a mentor.

I also thank my other faculty mentors for their time, input, and scientific expertise. Drs. Kathleen Giacomini and Pui-Yan Kwok, as members of my dissertation committee, have given valuable feedback and guidance throughout my research. Kathy and Pui, along with Drs. Nadav Ahituv and Laura van 't Veer, also oversaw my qualifying examination and provided scientific direction on my dissertation proposal.

Most of my research would not have been possible without the help of collaborators. I especially thank Dr. Kouros Owzar, Flora Mulkey, and Dr. Chen Jiang at the Alliance Statistics and Data Center for the great amount of time and help they have contributed for data curation and statistical analyses. I also acknowledge the UCSF Genomics Core for performing and providing support for the exome sequencing, Dr. Bert O'Neil for confirming our sequencing case phenotypes, Drs. Yukihide Momozawa and Michiaki Kubo for replication genotyping, Drs. Bryan Schneider and Fei Shen for comparison of ECOG-5103 results, Drs. Federico Innocenti and Alan Venook for valuable discussion, and everybody associated with the Alliance for Clinical Trials in Oncology and CALGB 80405 and 40502

who has helped coordinate sample transfers, data sharing, and review of abstracts and manuscripts.

I thank current and former members of the Kroetz lab for helping me settle into the lab, project discussion and presentation feedback, and technical support, especially Drs. Svetlana Markova, Aparna Chhibber, Michael Martin, Yingmei Liu, Sulggi Lee, and Katherina Chua. I also thank members of the Giacomini lab, especially Drs. Sook Wah Yee, Xiaomin Liang, and James Chien, for their willingness to help around the lab at a moment's notice.

I am grateful to my friends outside of graduate school for their constant encouragement and in helping me maintain some normalcy in my daily life. I am also appreciative of my PSPG classmates for being on this journey and surviving to the end with me.

And finally, I thank my parents for their love and unwavering support, and for instilling a love of learning in me. I am fortunate to have inherited some of your smart genes, but I am even luckier to have you as role models of kindness and hard work. I hope I have made you proud!

Genetic Predictors of Bevacizumab-Induced Hypertension

Megan Li

Bevacizumab is a vascular endothelial growth factor-specific angiogenesis inhibitor indicated as an adjunct to chemotherapy for the treatment of several types of cancer. Hypertension is commonly observed during bevacizumab treatment, and high-grade toxicity can limit therapy and lead to other cardiovascular complications. The factors that contribute to interindividual variability in blood pressure response to bevacizumab treatment are not well understood. To identify novel mechanisms of bevacizumab-induced hypertension, the research in this dissertation explored genetic variation associated with the toxicity. A sequencing analysis of whole exomes and candidate gene regulatory regions identified a genomic region between *SLC29A1* and *HSP90AB1* containing several variants associated with hypertension in colorectal cancer patients with extreme toxicity phenotypes. Functional experiments in human endothelial cells provide evidence that variation in *SLC29A1* (*ENT1*) expression is associated with altered adenosine signaling that modulates the synthesis of vasodilatory molecules during bevacizumab treatment. These results suggest that increased basal expression of *SLC29A1* and low extracellular adenosine levels may sensitive patients to a rise in blood pressure during bevacizumab exposure. Additionally, a genome-wide association study of a larger, independent cohort of breast cancer patients identified variants associated with cumulative bevacizumab dose at the first occurrence of hypertension. Several of these SNPs are located within or near genes of biological interest (*MSH6*, *SDC4*, *ASB5*, *SMYD5*) and may highlight additional mechanisms important in the pathogenesis of the toxicity. Collectively, the studies in this dissertation

identified novel genetic loci that potentially modify the risk of developing bevacizumab-induced hypertension. The results of this research will advance understanding of the biological mechanism of this adverse drug reaction and should be considered in the future use and development of angiogenesis inhibitors.

Table of Contents

Chapter 1: Hypertension as an Adverse Drug Reaction of Bevacizumab Treatment.....	1
1.1 Introduction	1
1.2 Bevacizumab.....	1
1.3 Bevacizumab-induced hypertension.....	3
1.4 Hypertension: Primary, secondary, and monogenic forms.....	7
1.5 Hypothesized mechanisms of bevacizumab-induced hypertension	13
1.6 Pharmacogenetics of bevacizumab and VEGF inhibitor toxicity	18
1.7 Hypertension as a marker of bevacizumab efficacy	22
1.8 Research motivation and focus of this dissertation	23
1.9 References	26
Chapter 2: Identification of Genomic Regions Associated with Bevacizumab-Induced Hypertension by Exome Sequencing	43
2.1 Abstract.....	43
2.2 Introduction	44
2.3 Materials and Methods.....	45
2.3.1 Patient population	45
2.3.2 Bevacizumab-induced hypertension phenotype.....	47
2.3.3 Sequencing	50
2.3.4 Read mapping, variant calling, and filtering.....	52
2.3.5 Sample quality control	53
2.3.6 Variant quality control.....	55
2.3.7 SNP-based association testing.....	56

2.3.8 Gene-based association testing.....	57
2.3.9 <i>In silico</i> functional analysis	60
2.3.10 Association of top SNPs in independent cohorts.....	60
2.4 Results	63
2.4.1 Subject selection and characteristics.....	63
2.4.2 Description of variant dataset	63
2.4.3 Candidate gene analysis	65
2.4.4 Exome-wide analysis	76
2.4.5 Analysis using other rare variant testing methods	83
2.4.6 Analysis of other variant subsets	84
2.4.7 <i>In silico</i> functional analysis	86
2.4.8 Replication analysis of top SNP associations	89
2.4.9 Association of top SNPs with secondary hypertension phenotypes.....	92
2.4.10 Analysis of previously reported SNP associations.....	97
2.5 Discussion	101
2.6 Conclusions	106
2.7 References	108
 Chapter 3: Functional Characterization of the Effects of Bevacizumab on Adenosine	
Signaling.....	119
3.1 Abstract.....	119
3.2 Introduction.....	120
3.3 Materials and Methods.....	125
3.3.1 Cell culture	125

3.3.2 Pharmacological treatment.....	126
3.3.3 Overexpression of SLC29A1	126
3.3.4 Measurement of cyclic AMP and nitric oxide.....	127
3.3.5 Statistical analysis.....	127
3.4 Results	128
3.4.1 Characterization of adenosine and VEGF signaling in HUVEC	128
3.4.2 Effect of bevacizumab on adenosine and VEGF signaling.....	132
3.4.3 Effect of ENT1 inhibition on adenosine and VEGF signaling.....	134
3.4.4 Effect of SLC29A1 overexpression on adenosine and VEGF signaling.....	136
3.5 Discussion	138
3.6 Conclusions	143
3.7 References	144
Chapter 4: Identification of Bevacizumab-Induced Hypertension Risk Variants by Genome-Wide Association	147
4.1 Abstract.....	147
4.2 Introduction.....	148
4.3 Materials and Methods.....	149
4.3.1 Patient population	149
4.3.2 Bevacizumab-induced hypertension phenotype.....	150
4.3.3 Genotyping.....	152
4.3.4 Statistical analyses.....	154
4.3.5 <i>In silico</i> functional analysis	154
4.3.6 Replication analysis of top associations.....	155

4.4 Results	157
4.4.1 Subject characteristics	157
4.4.2 Association with grade 2+ bevacizumab-induced hypertension	157
4.4.3 Association with grade 3+ bevacizumab-induced hypertension	163
4.4.4 <i>In silico</i> functional analysis	168
4.4.5 Replication analysis of top SNP associations	172
4.4.6 Analysis of previously reported SNP associations.....	177
4.5 Discussion	180
4.6 Conclusions	184
4.7 References	185
Chapter 5: Conclusions and Perspectives	195
5.1 Summary	195
5.2 Challenges and future directions	199
5.3 Conclusions	202
5.4 References	205

List of Tables

Table 1.1. Adverse effects of bevacizumab	5
Table 1.2. Assessment of hypertension in the National Cancer Institute’s Common Terminology Criteria for Adverse Events version 3	5
Table 1.3. Pathophysiological mechanisms of primary hypertension	9
Table 1.4. Major genome-wide association studies of hypertension and blood pressure	12
Table 1.5. Rare variant studies of primary hypertension and blood pressure.....	13
Table 1.6. Previous pharmacogenetic studies of bevacizumab-induced hypertension	21
Table 2.1. Assessment of hypertension in the National Cancer Institute’s Common Terminology Criteria for Adverse Events version 3	48
Table 2.2. Grade 3 hypertension events in the CALGB 80405 bevacizumab arm.....	48
Table 2.3. Analyzed candidate genes	51
Table 2.4. Quality of sequencing reads per sample	52
Table 2.5. SNPs excluded per GATK Best Practices v3.4 recommendations	53
Table 2.6. Quality control of sample data	55
Table 2.7. Quality control of variant data	56
Table 2.8. Post-QC quality per sample	56
Table 2.9. Gene-based rare variant association tests	59
Table 2.10. Replication and exploratory cohorts.....	62
Table 2.11. Characteristics of extreme phenotype patient subgroups	63
Table 2.12. Summary of variant filtering procedures	64
Table 2.13. Top SNP associations of candidate gene analysis	69
Table 2.14. Top gene associations of candidate gene analysis (MAF < 0.03).....	73

Table 2.15. Top gene associations of candidate gene analysis (all MAF)	74
Table 2.16. Function of individual variants in top genes of candidate gene analysis (MAF < 0.03).....	75
Table 2.17. Top SNP associations of exome-wide analysis	79
Table 2.18. Top gene associations of exome-wide analysis (MAF < 0.03)	80
Table 2.19. Top gene associations of exome-wide analysis (all MAF)	81
Table 2.20. Functional predictions and allele counts of variants in top genes of exome-wide analysis (MAF < 0.03).....	82
Table 2.21. Top candidate gene associations of non-SKAT analyses (MAF < 0.03)	83
Table 2.22. Top exome-wide gene associations of non-SKAT analyses (MAF < 0.03)	84
Table 2.23. Top gene associations of exploratory analyses (MAF < 0.03)	85
Table 2.24. Top gene associations of indel analyses.....	86
Table 2.25. Evidence of regulatory activity for top <i>SLC29A1-HSP90AB1</i> SNPs.....	88
Table 2.26. Replication analysis of top <i>SLC29A1-HSP90AB1</i> SNP associations in independent bevacizumab-treated cohorts.....	90
Table 2.27. Association of rs6902226 with secondary bevacizumab-induced hypertension phenotypes in larger cohorts.....	93
Table 2.28. Association of rs3734704 with secondary bevacizumab-induced hypertension phenotypes in larger cohorts.....	94
Table 2.29. Association of rs9381299 with secondary bevacizumab-induced hypertension phenotypes in larger cohorts.....	95
Table 2.30. Association of rs6929249 and rs834576 with secondary bevacizumab-induced hypertension phenotypes in CALGB 40502.....	96

Table 2.31. Previously reported SNP associations with bevacizumab-induced hypertension	98
Table 2.32. Associations of previously reported SNPs with early grade 3+ bevacizumab- induced hypertension in CALGB 80405	99
Table 2.33. Associations of previously reported SNPs with early grade 2+ bevacizumab- induced hypertension in CALGB 80405	100
Table 4.1. Assessment of hypertension in the National Cancer Institute’s Common Terminology Criteria for Adverse Events version 3	152
Table 4.2. Phenotype curation.....	152
Table 4.3. Quality control of genotyped samples	153
Table 4.4. Quality control of genotyped SNPs.....	153
Table 4.5. Summary of replication cohorts	156
Table 4.6. Characteristics of subjects included in discovery analyses	157
Table 4.7. Top SNP associations of grade 2+ hypertension analysis	160
Table 4.8. Top SNP associations of grade 3+ hypertension analysis	165
Table 4.9. rs1981431 eQTL associations with <i>SDC4</i> expression.....	172
Table 4.10. Replication analysis of top SNP associations in CALGB 80405	173
Table 4.11. Replication analysis of top SNP associations in CALGB 90401	173
Table 4.12. Lookup of top SNP associations with grade 3+ hypertension in ECOG-5103...	174
Table 4.13. Previously reported SNP associations with bevacizumab-induced hypertension	178
Table 4.14. Associations of previously reported SNPs with grade 2+ hypertension in CALGB 40502	179

Table 4.15. Associations of previously reported SNPs with grade 3+ hypertension in CALGB
40502 179

Table 4.16. Top *SV2C* SNP associations with grade 3+ hypertension in CALGB 40502 180

List of Figures

Figure 1.1. VEGF signaling and inhibition by bevacizumab.....	3
Figure 1.2. Mechanism of VEGF-mediated vasodilation.....	15
Figure 2.1. CALGB 80405 trial design and hypertension frequency.....	47
Figure 2.2. Subject selection from bevacizumab-induced hypertension extreme phenotypes in CALGB 80405 for exome sequencing	49
Figure 2.3. First and second principal components in sequenced samples.....	54
Figure 2.4. Distribution of SNP allele frequency.....	64
Figure 2.5. SNP functional annotation	65
Figure 2.6. Candidate gene analysis workflow.....	66
Figure 2.7. Quantile-quantile plot of candidate gene SNP-based analysis	67
Figure 2.8. Manhattan plot of candidate gene SNP-based analysis	68
Figure 2.9. Associations with bevacizumab-induced hypertension in the <i>SLC29A1</i> - <i>HSP90AB1</i> region.....	70
Figure 2.10. Linkage disequilibrium plot of <i>SLC29A1</i> - <i>HSP90AB1</i> intergenic region	71
Figure 2.11. Frequency of early grade 3 bevacizumab-induced hypertension in carriers of <i>SLC29A1</i> - <i>HSP90AB1</i> variants	72
Figure 2.12. Exome-wide analysis workflow	76
Figure 2.13. Quantile-quantile plot of exome-wide SNP-based analysis	77
Figure 2.14. Manhattan plot of exome-wide SNP-based analysis	78
Figure 2.15. Top <i>SLC29A1</i> - <i>HSP90AB1</i> SNPs are in predicted transcriptionally-active regions in human umbilical vein endothelial cells	87

Figure 2.16. Frequency of high-grade hypertension in replication cohorts stratified by variant allele carrier status.....	91
Figure 2.17. Frequency of secondary bevacizumab-induced hypertension phenotypes in carriers of <i>SLC29A1-HSP90AB1</i> risk variants in CALGB 40502 and CALGB 90401.....	97
Figure 3.1. Adenosine and adenosine receptor signaling.....	121
Figure 3.2. Effects of adenosine receptor signaling on the regulation of blood pressure ...	122
Figure 3.3. Adenosine signaling increases endothelial nitric oxide synthase activity and nitric oxide production.....	124
Figure 3.4. Effects of NECA and VEGF on adenosine and VEGF signaling in HUVEC	129
Figure 3.5. Effects of adenosine and VEGF on adenosine and VEGF signaling in HUVEC....	130
Figure 3.6. Effects of adenosine receptor blockade on adenosine and VEGF signaling in HUVEC.....	131
Figure 3.7. Effects of bevacizumab on adenosine and VEGF signaling in HUVEC	133
Figure 3.8. Effects of ENT1 inhibition on adenosine and VEGF signaling in HUVEC	135
Figure 3.9. Effects of SLC29A1-overexpression on adenosine and VEGF signaling in HUVEC	137
Figure 3.10. Hypothesized mechanism of increased ENT1 expression on bevacizumab-induced hypertension	141
Figure 4.1. CALGB 40502 trial design	150
Figure 4.2. Hypertension events in CALGB 40502.....	151
Figure 4.3. Quantile-quantile plot of grade 2+ hypertension analysis.....	158
Figure 4.4. Manhattan plot of grade 2+ hypertension analysis.....	159
Figure 4.5. Associations with grade 2+ hypertension in the rs2018541 genomic region...	161

Figure 4.6. rs2018541 is associated with increased incidence of grade 2+ hypertension .	162
Figure 4.7. Quantile-quantile plot of grade 3+ hypertension analysis.....	164
Figure 4.8. Manhattan plot of grade 3+ hypertension analysis.....	165
Figure 4.9. Associations with grade 3+ hypertension in the rs1981431 genomic region...	166
Figure 4.10. rs1981431 is associated with decreased incidence of grade 3+ hypertension	167
Figure 4.11. rs2018541 is in a genomic region 5' upstream of <i>MSH6</i> lacking predicted regulatory function.....	170
Figure 4.12. rs1981431 and rs2741454 are in a predicted enhancer region within an intron of <i>SDC4</i>	171
Figure 4.13. Frequency of early bevacizumab-induced hypertension in CALGB 80405 replication subjects stratified by carrier status of top discovery SNPs.....	175
Figure 4.14. Cumulative incidence of bevacizumab-induced hypertension in CALGB 90401 replication subjects stratified by genotypes of top discovery SNPs	176

Chapter 1: Hypertension as an Adverse Drug Reaction of Bevacizumab Treatment

1.1 Introduction

Bevacizumab is a vascular endothelial growth factor-specific angiogenesis inhibitor indicated as an adjunct to chemotherapy for the treatment of several types of cancer. Hypertension (HTN) is commonly observed during bevacizumab treatment, and high-grade toxicity can limit therapy and lead to other cardiovascular complications. The factors that contribute to interindividual variability in blood pressure (BP) response to bevacizumab treatment are not well understood. Here, we discuss the current literature regarding bevacizumab and the mechanisms and pharmacogenetics of bevacizumab-induced HTN.

1.2 Bevacizumab

Bevacizumab (Avastin®, Genentech/Roche) is an angiogenesis inhibitor that is approved for the treatment of patients with metastatic colorectal cancer, advanced nonsquamous non-small cell lung cancer, metastatic renal cell carcinoma, recurrent glioblastoma, advanced cervical cancer, and platinum-resistant ovarian cancer¹. It is also approved for treatment of metastatic breast cancer in the European Union and other non-U.S. countries and was approved for this indication in the United States between 2008 and 2011.

Bevacizumab is typically administered as a solution intravenously in the range of 5-15 mg/kg every 2 or 3 weeks². The addition of bevacizumab to standard chemotherapy regimens in the approved indications has been shown to significantly increase overall survival (OS), progression-free survival (PFS), and/or overall response rate¹.

Bevacizumab is a recombinant humanized monoclonal IgG1 antibody that binds to all isoforms and bioactive proteolytic fragments of human vascular endothelial growth factor-A (VEGF), which is essential for both normal and tumor angiogenesis. The antibody contains human framework regions with mutagenized murine-counterpart residues in six complementarity-determining regions³. By neutralizing VEGF, bevacizumab prevents the activation of VEGF tyrosine kinase receptors VEGFR1 (*FLT1*) and VEGFR2 (*KDR*) on endothelial cells. The anti-tumor effect of bevacizumab is primarily attributed to the inhibition of VEGFR2-mediated angiogenesis³ (Figure 1.1), slowing the growth of new blood vessels and effectively cutting off a tumor's supply of oxygen and nutrients. Inhibition of VEGF signaling also improves delivery of cytotoxic drugs by lowering tumor interstitial fluid pressure and by reducing the number of non-functional tumor blood vessels.

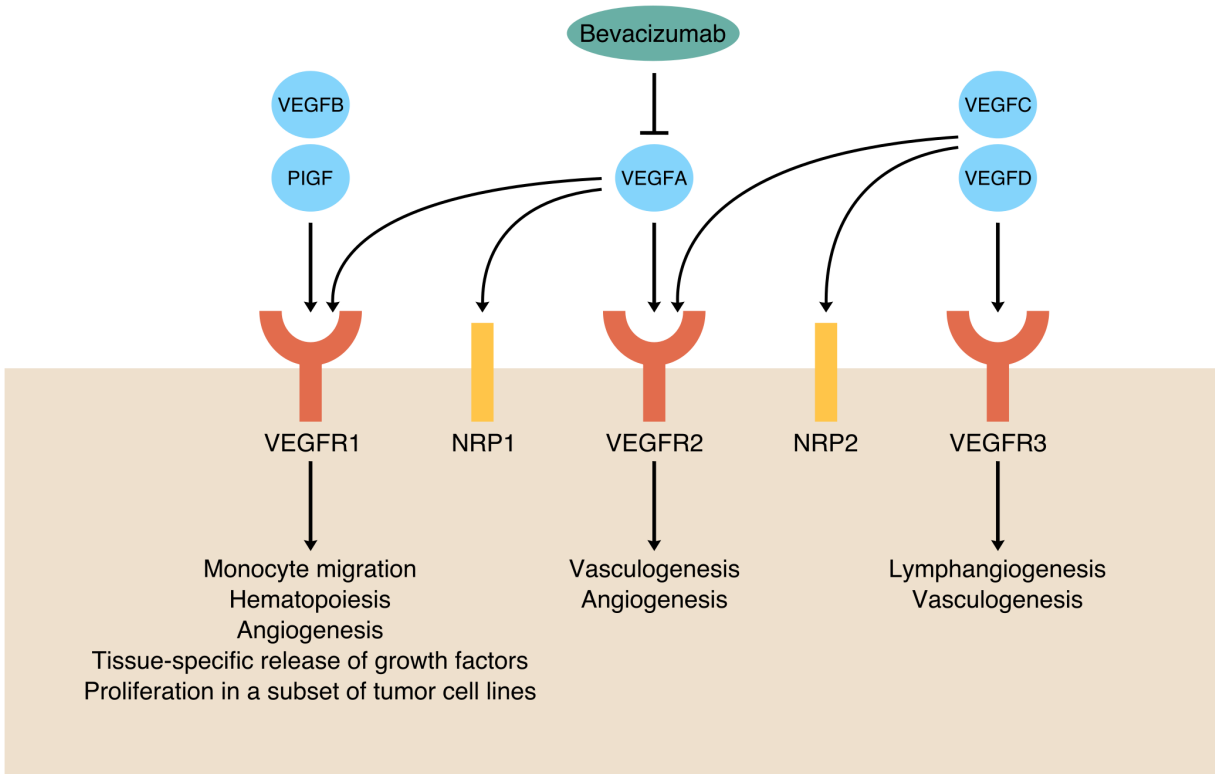


Figure 1.1. VEGF signaling and inhibition by bevacizumab. Vascular endothelial growth factor (VEGF) receptors are primarily expressed by endothelial cells. VEGFA binds both VEGFR1 and VEGFR2, though VEGFA-mediated angiogenesis is primarily mediated by VEGFR2, while VEGFR1 functions primarily as a decoy receptor for VEGFA. Placental growth factor (PIGF) and VEGFB bind selectively to VEGFR1, and VEGFC and VEGFD bind to VEGFR3, a key regulator of lymphangiogenesis. Neuropilin co-receptors NRP1 and NRP2 also regulate VEGFR signaling. Binding of VEGF by bevacizumab prevents VEGFA-activated receptor signaling. Adapted from Ferrara *et al*¹.

1.3 Bevacizumab-induced hypertension

The known adverse effects of bevacizumab² are listed in Table 1.1. HTN, or persistent elevation of arterial BP, is one of the more serious common drug reactions of bevacizumab treatment. While HTN itself is asymptomatic, unmanaged HTN can lead to cardiovascular complications. Rare cases of hypertensive crisis with encephalopathy^{4,5} and subarachnoid hemorrhage⁶⁻⁸ have also been reported for bevacizumab. All patients on bevacizumab treatment are recommended to have BP monitored every two to three weeks and to be

treated with appropriate antihypertensive therapy as needed. Bevacizumab is temporarily suspended in patients with uncontrollable severe HTN and discontinued in the event of hypertensive crisis or hypertensive encephalopathy, with no recommended dose reductions². Upon discontinuation of bevacizumab, BP typically returns to pre-treatment levels⁹.

Drug-induced HTN grades as defined by the National Cancer Institute's Common Terminology Criteria for Adverse Events (CTCAE)¹⁰ are listed in Table 1.2. HTN of all grades has been observed in up to 36% of patients treated with bevacizumab¹¹. The reported incidence of high-grade (grade 3–4) HTN ranges from 1.8 to 22%¹², with up to 1% of events being grade 4¹³. In a meta-analysis of twenty phase II and phase III clinical trials, bevacizumab was reported to increase the risk of high-grade HTN by up to 5.28-fold¹². Similar findings have been reported in other meta-analyses of trials of breast cancer¹⁴ and colorectal cancer¹⁵ and across multiple indications¹¹.

Table 1.1. Adverse effects of bevacizumab

Most serious adverse effects	Common side effects
<ul style="list-style-type: none"> • Gastrointestinal perforation • Surgery and wound healing complications • Hemorrhage • Fistula • Arterial thromboembolic events • Venous thromboembolic events • Hypertension • Posterior reversible encephalopathy syndrome • Proteinuria • Infusion reactions • Embryo-fetal toxicity • Ovarian failure 	<ul style="list-style-type: none"> • Epistaxis • Headache • Hypertension • Rhinitis • Proteinuria • Taste alteration • Dry skin • Rectal hemorrhage • Lacrimation disorder • Back pain • Exfoliative dermatitis

Table 1.2. Assessment of hypertension in the National Cancer Institute’s Common Terminology Criteria for Adverse Events version 3

Grade 1	Grade 2	Grade 3	Grade 4	Grade 5
Asymptomatic, transient (<24 hrs) increase by >20 mmHg (diastolic) or to >150/100 if previously WNL ¹	Recurrent or persistent (≥24 hrs) or symptomatic increase by >20 mmHg (diastolic) or to >150/100 if previously WNL ¹	Requiring more than one drug or more intensive therapy than previously	Life-threatening consequences (e.g., hypertensive crisis)	Death
Intervention not indicated	Monotherapy may be indicated			

¹WNL: Within normal limits

The time to BP elevation upon receiving bevacizumab varies but is frequently observed within the first cycle of therapy⁹. The toxicity appears to be dose-dependent, with a reported 7.5-fold increase in all-grade HTN risk in patients treated with high-dose (≥ 10 mg/kg) bevacizumab compared to a 3-fold increase in patients receiving low-dose (< 10

mg/kg) bevacizumab¹¹. In the same meta-analysis, the development of grade 3 HTN was observed in 8.7% of low-dose patients and 16.0% of high-dose patients. Development of HTN has also been associated with cumulative dose of bevacizumab¹⁶⁻¹⁸. Other studies have demonstrated no dose effect¹⁹. Regardless, high-grade HTN is still consistently observed at low doses^{11,12,19}.

HTN also occurs during treatment with other VEGF pathway inhibitors⁹, including aflibercept, a soluble decoy receptor that binds VEGF, and VEGF receptor tyrosine kinase inhibitors (RTKI) such as sunitinib, sorafenib, pazopanib, axitinib, cediranib, motesanib, and vandetanib. The frequency of HTN during treatment with VEGF RTKIs ranges from 15 to 60%²⁰, with a greater incidence observed during treatment with more potent inhibitors such as axitinib, cediranib, and pazopanib^{21,22}, suggesting that HTN is primarily an on-target effect of VEGF inhibition.

In most patients treated with VEGF inhibitors, elevated BP can be controlled with standard antihypertensive medications²³. Patients who develop HTN or a significant rise in BP from baseline are recommended to initiate antihypertensive therapy, have current antihypertensive therapy titrated to better control, or have another agent added⁹. Early initiation of antihypertensive therapy has been shown to reduce complications, even in life-threatening cases of encephalopathy²⁴, and to prevent or minimize HTN while continuing bevacizumab treatment^{25,26}. All major classes of antihypertensive agents, including angiotensin-converting enzyme (ACE) inhibitors, angiotensin II receptor blockers (ARBs), beta blockers, calcium channel blockers, and thiazide diuretics, have been successfully used

to treat angiogenesis inhibitor-induced HTN⁹. No specific antihypertensive agent provides superior control of bevacizumab-induced HTN, though different classes have been proposed or recommended against as first-line treatment, primarily for other related effects. For example, ACE inhibitors are recommended for treatment of proteinuria (also induced by bevacizumab)²⁷, while there is caution against use of the calcium channel blocker nifedipine, which has been shown to induce VEGF secretion²⁶. Long-acting oral nitrates have also been reported to successfully restore BP to baseline levels in patients with HTN refractory to combination treatment with ACE inhibitors and calcium channel blockers^{28,29}.

Demographic and clinical risk factors for VEGF inhibitor-induced HTN are derived from those of primary HTN, including age, body mass index (BMI) and abdominal obesity, family history of and/or preexisting cardiovascular disease, dyslipidemia, diabetes mellitus, preexisting renal conditions, and cigarette smoking^{9,22}. Preexisting HTN has been shown to correlate directly with the development of treatment-related HTN^{22,30,31}. Tumor type has also been suggested to have a role, with the highest risk of bevacizumab-induced HTN being reported in patients with renal cell carcinoma and breast cancers^{12,32}.

1.4 Hypertension: Primary, secondary, and monogenic forms

Bevacizumab-induced HTN is a type of secondary HTN, or HTN related to a specific known etiology. Primary or essential HTN is elevated BP of unknown etiology. While the mechanisms of drug-induced HTN may differ from those causing primary HTN, the pathophysiological and genetic factors contributing to both types may overlap, and any

factors underlying primary HTN may be exacerbated by drug treatment. Thus, an understanding of primary HTN is necessary to formulate questions related to bevacizumab-induced HTN.

HTN is generally defined as systolic BP \geq 140 mmHg or diastolic BP \geq 90 mmHg. Approximately one billion adults worldwide have HTN³³, and about one-third of adults (80 million) in the United States have high BP³⁴. Most patients have primary HTN, while about 10% of HTN cases result from secondary causes³⁵. While a rise in BP is generally asymptomatic, it becomes a major risk factor for cardiovascular disease and stroke, accounting for 9.4 million deaths worldwide each year³³.

Numerous risk factors for the development of primary HTN include age, race and ethnicity, family history, increased weight, physical inactivity, tobacco use, psychosocial stressors, lower education and socioeconomic status, and dietary factors (e.g., dietary fats, higher sodium intake, lower potassium intake, and excessive alcohol intake)³⁴. Common causes of secondary HTN are kidney disease, endocrine disease, congenital vascular defects, sleep apnea, and pharmacological causes³⁵. Drugs that can elevate BP include anti-cancer agents (including bevacizumab), nonsteroidal anti-inflammatory drugs and analgesics, antidepressants, glucocorticoids, licorice, sex hormones, immunosuppressive agents, erythropoietin, anti-retroviral treatment, cocaine, caffeine, alcohol, salt-containing medications, and certain herbal products³⁶.

Dysregulation of sodium and fluid balance and vasomotor tone have been implicated in the development of primary HTN, with multiple interacting pathophysiological mechanisms contributing to the alteration of both systems³⁷. A detailed list of such mechanisms is provided in Table 1.3.

Table 1.3. Pathophysiological mechanisms of primary hypertension

- Increased sympathetic nervous system activity and imbalance of the autonomic nervous system
- Overproduction of sodium-retaining hormones and vasoconstrictors
- Increased or inappropriate renin secretion inducing increased production of angiotensin II and aldosterone
- Deficiencies of vasodilators, such as prostacyclin, nitric oxide, and natriuretic peptides
- Alterations in expression of the kallikrein–kinin system that affect vascular tone and renal salt handling
- Abnormalities of resistance vessels, including selective lesions in the renal microvasculature
- Increased activity of vascular growth factors
- Alterations in adrenergic receptors that influence heart rate, cardiac output, and vascular tone
- Altered cellular ion transport
- Structural and functional abnormalities in the vasculature, including endothelial dysfunction, increased oxidative stress, vascular remodeling, and increased arterial stiffness

HTN has also been attributed to genetics. Family and twin studies estimate BP to be moderately heritable (30-50%)³⁸. The prevalence of HTN differs among racial groups, further suggesting a genetic contribution to HTN risk. Non-Hispanic blacks have a higher prevalence of HTN (42%) than non-Hispanic whites (28%), Hispanics (25%), and non-Hispanic Asians (25%)³⁹.

Monogenic forms of HTN have been mapped using linkage analysis and sequencing to at least 28 loci near genes primarily related to renal and adrenal mechanisms regulating sodium homeostasis³⁸. Many of these variants are gain-of-function mutations leading to increased mineralocorticoid activity or production. Exome sequencing has identified mutations in kelch-like 3 (*KLHL3*)^{40,41} and cullin 3 (*CUL3*)⁴⁰ proteins that cause pseudohypoaldosteronism type II, an autosomal dominant form of HTN associated with hyperkalemia, nonanion gap metabolic acidosis, and increased salt reabsorption by the kidney. Exome sequencing also identified gain-of-function somatic mutations in a K⁺ channel (*KCNJ5*)⁴² causing aldosterone-producing adenomas, a subtype of primary aldosteronism resulting from dysregulation of Na⁺ and Cl⁻ absorption and plasma volume.

While single, highly penetrant mutations causing monogenic syndromes are well characterized, the genetic architecture of primary HTN is still poorly understood. A Gaussian distribution of BP in the general population supports a polygenic basis for the trait, with monogenic diseases representing an extreme tail of the phenotype. Many genome-wide association studies (GWAS) have been performed to identify common single nucleotide polymorphisms (SNPs) with more modest effects on BP. Some of the earlier large-scale studies are summarized in Table 1.4. A number of more recent GWAS⁴³⁻⁴⁷ have brought the total count of genetic loci associated with primary HTN or BP to more than 100. Many of these loci are in or near genes that encode proteins within pathways or systems with a physiological relation to BP (e.g., renal salt handling or the renin-angiotensin system), although most are noncoding SNPs with unknown functional effects. All identified common variants together still only explain less than 5% of the total variance

in BP⁴⁸, leaving much of the genetic contribution to BP variability unexplained. More recently, studies of primary HTN using sequencing or exome arrays have been performed to identify rare variants contributing to variability in BP (Table 1.5). Future sequencing initiatives in substantially larger sample sizes may uncover even more low frequency variants associated with primary HTN.

Table 1.4. Major genome-wide association studies of hypertension and blood pressure

Study	Discovery cohort size	Loci containing top associations
Wellcome Trust Case Control Consortium (2007) ⁴⁹	1,952	No SNPs with genome-wide significance
Framingham Heart Study (2007) ⁵⁰	1,260	No SNPs with genome-wide significance
CHARGE Consortium (2009) ⁵¹	29,136	<i>ATP2B1, CYP17A1, PLEKHA7, SH2B3, CACNB2, CSK-ULK3, TBX3-TBX5, ULK4</i>
Global BPGen Consortium (2009) ⁵²	34,433	<i>CYP17A1, CYP1A2, FGF5, SH2B3, MTHFR, C10orf107, ZNF652, PLCD3</i>
International Consortium for Blood Pressure Genome-Wide Association Studies: Systolic BP, diastolic BP (2011) ⁵³	69,395	<i>SLC39A8, ATP2B1, GNAS-EDN3, CYP17A1-NT5C2, MTHFR-NPPB, HFE, C10orf107, FGF5, CYP1A1-ULK3, CACNB2 (3'), SH2B3, FURIN-FES, FLJ32810-TMEM133, PLEKHA7, ADM, NPR3-C5orf23, EBF1, PLCE1, BAT2-BAT5, MOV10, ZNF652, TBX5-TBX3, CACNB2 (5'), JAG1, GUCY1A3-GUCY1B3, MECOM, SLC4A7, GOSR2, ULK4</i>
International Consortium of Blood Pressure Genome-Wide Association Studies: Mean arterial pressure, pulse pressure (2011) ⁵⁴	74,064	<i>CHIC2, PIK3CG, NOV, ADAMTS8, MAP4, ADRB1, FIGN</i>
Asian Genetic Epidemiology Network Consortium: Systolic BP, diastolic BP (2011) ⁵⁵	19,608	<i>ST7L-CAPZA1, FIGN-GRB14, ENPEP, NPR3, TBX3</i>
Asian Genetic Epidemiology Network Consortium: Mean arterial pressure, pulse pressure (2013) ⁵⁶	26,600	<i>ATP2B1, NT5C2, CYP17A1, FGF5</i>
Continental Origins and Genetic Epidemiology Network (2013) ⁵⁷	29,378	<i>EVX1-HOXA, ULK4, RSPO3, PLEKHG1, SOX6</i>

Table 1.5. Rare variant studies of primary hypertension and blood pressure

Study	Study design	Discovery cohort size	Loci containing top associations
Ji <i>et al</i> (2008) ⁵⁸	Targeted sequencing	3,125	<i>SLC12A3, SLC12A1, KCNJ1</i>
Morrison <i>et al</i> (2014) ⁵⁹	Targeted sequencing	4,178	No significant findings
Yu <i>et al</i> (2016) ⁶⁰	Whole-exome sequencing	17,956	<i>CLCN6</i>
Liu <i>et al</i> (2016) ⁴⁷	Whole-exome array	146,562	<i>NPR1, DBH, TPMT1</i>
Surendran <i>et al</i> (2016) ⁴⁴	Whole-exome array	192,763	<i>RBM47, COL21A1, RRAS, A2ML1, ENPEP</i>

Several classes of drugs are used to treat primary HTN, including ACE inhibitors, ARBs, beta blockers, calcium channel blockers, and thiazide-type diuretics. Recommended treatment guidelines differ by racial subgroup⁶¹, and pharmacogenetic variants have been associated with response to HTN treatment⁶²⁻⁶⁴, further suggesting genetic differences contributing to HTN risk.

1.5 Hypothesized mechanisms of bevacizumab-induced hypertension

BP regulation entails complex physiology, and the mechanisms by which bevacizumab causes HTN remain unclear. The prevailing hypothesis for the mechanism of bevacizumab-induced HTN is an increase in vascular tone due to inhibition of VEGF-mediated vasodilation. Direct administration of VEGF has been shown to induce vasorelaxation and lower BP⁶⁵⁻⁶⁷. Bevacizumab inhibited VEGF-induced vasodilation, measured by outer vessel diameter, in pig retinal arterioles⁶⁸, and local administration of bevacizumab in humans rapidly decreased endothelium-dependent vasodilation⁶⁹. Thus, inhibition of VEGF

signaling and decreased endothelium-dependent vasodilation may result in overall vascular resistance and the development of HTN.

VEGF signaling through VEGFR2 promotes vascular permeability and vasodilation^{70,71} in endothelial cells via the downstream release of the vasodilator molecules nitric oxide (NO), produced by endothelial nitric oxide synthase (eNOS)^{72,73}, and prostacyclin (PGI₂)^{74,75}, generated from cyclooxygenase-catalyzed arachidonic acid metabolism (Figure 1.2). NO and PGI₂ act in a paracrine fashion on adjacent vascular smooth muscle cells to stimulate signaling that ultimately results in vasorelaxation⁷⁶. Addition of bevacizumab to human umbilical vein endothelial cells (HUVEC) has been shown to reduce VEGFR2 phosphorylation⁷⁷ and decrease NO production⁷⁸. Administration of an anti-VEGFR2 antibody in mice resulted in a rapid rise in BP as well as reduction of eNOS and neuronal NO synthase expression in the kidney⁷⁹.

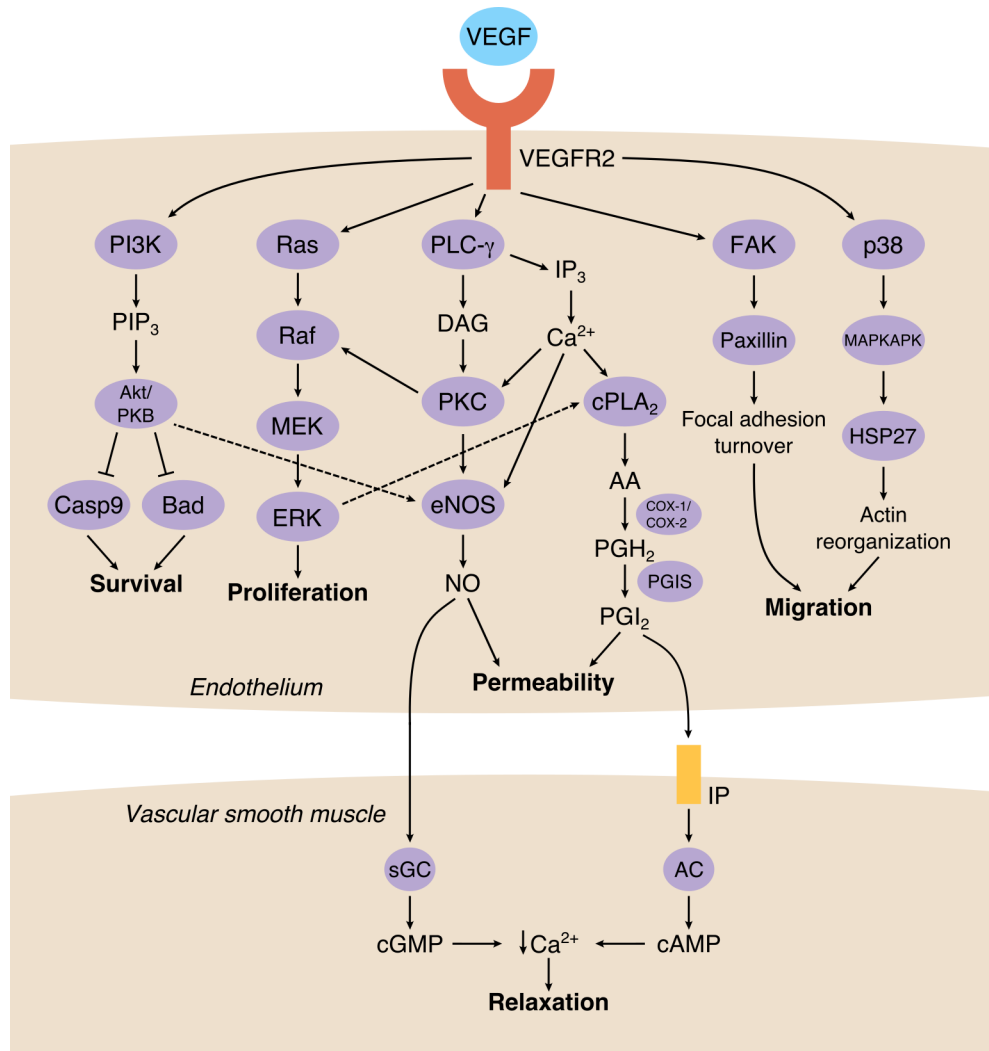


Figure 1.2. Mechanism of VEGF-mediated vasodilation. Activation of VEGF receptor 2 (VEGFR2) induces cell proliferation, migration and survival, and vascular permeability, leading to angiogenesis. Signaling through phospholipase C (PLC)- γ activates protein kinase C (PKC) by the generation of diacylglycerol (DAG) and increases the concentration of intracellular calcium (Ca^{2+}) via inositol 1,4,5-triphosphate (IP_3). PKC activation, increased Ca^{2+} , and activation of the PI3K-Akt pathway lead to phosphorylation and activation of endothelial nitric oxide synthase (eNOS) and generation of nitric oxide (NO). PKC also activates the Ras/MEK/ERK pathway, which in turn upregulates cytosolic phospholipase A2 (cPLA₂). cPLA₂ releases arachidonic acid (AA) from phospholipids, which is acted on by cyclooxygenases (COX-1/COX-2) to generate prostaglandin H₂ (PGH₂), which is then converted to prostacyclin (PGI₂) by prostacyclin synthase (PGIS). NO and PGI₂ diffuse to adjacent smooth muscle cells, where NO activates soluble guanylate cyclase (sGC), leading to cGMP synthesis. PGI₂ binds to prostacyclin receptors (IP), which activate adenylyl cyclase (AC) and increase cAMP synthesis. cGMP and cAMP lead to decreased intracellular Ca^{2+} concentrations, which induce vasorelaxation.

While many studies have shown a decrease in eNOS activity and NO production during VEGF pathway inhibition, others have shown that both NO-dependent and NO-independent vasodilation are reduced⁸⁰. Therefore, other endothelial signaling pathways adjacent to VEGF signaling have been proposed to contribute to a decrease in vasodilation. One such pathway focuses on the action of endothelin-1 (ET-1). ET-1 exerts its effects on neighboring vascular endothelial and smooth muscle cells via activation of ET_A and ET_B receptors⁸¹. In smooth muscle, where both ET_A and ET_B receptors are expressed, ET-1 acts as a vasoconstrictor, while in endothelial cells, which express only ET_B receptors, ET-1 promotes vasodilation⁸¹⁻⁸³. VEGF has been shown to influence ET-1 expression, though the relationship is not entirely understood. Plasma concentrations of ET-1 have been reported to increase following administration of the VEGF RTKI sunitinib in patients⁸⁴, but VEGF also induced ET-1 expression in cultured endothelial cells⁸⁰. Ongoing research is being conducted to elucidate the role of ET-1 in the onset of HTN during inhibition of VEGF signaling^{80,84,85}.

While inhibition of VEGF-mediated vasodilation is the dominant hypothesis for the pathophysiology of bevacizumab-induced HTN, it has yet to be established as the sole cause of the toxicity. Like primary HTN, bevacizumab-induced HTN could result from alterations in multiple tissue or organ systems. Other hypotheses proposed to contribute to bevacizumab-induced HTN include other sources of endothelial and vascular dysfunction. Microvascular rarefaction, or the reduction of capillary density, is a consequence of inhibiting VEGF^{86,87}, which is required for endothelial cell survival^{77,88}. Decreased microcapillary density may lead to increased systemic vascular resistance and pressure in

larger vessels. A rise in BP accompanied by a decrease in dermal capillary density has been observed after six months of bevacizumab treatment⁸⁹. Arterial stiffness, possibly resulting from changes to extracellular matrix or matrix-interacting proteins, can also contribute to a systemic rise in BP⁹⁰. Increased vascular stiffness has been observed in patients treated with the VEGFR2 inhibitor sorafenib⁹¹. Oxidative stress and the production of abnormal levels of reactive oxygen species (ROS) may also contribute to the development of HTN, possibly through ROS-mediated apoptosis of endothelial cells⁹² or excess oxidation of NO⁹³, decreasing its bioavailability for vasodilator tone.

Alterations in renal structure or function may also contribute to the development of bevacizumab-induced HTN. VEGF expression in kidney endothelial cells and podocytes is needed to maintain normal glomerular structure and function⁹⁴. Local genetic ablation of VEGF in kidney podocytes has been shown to lead to glomerular injury and elevated BP in mice⁹⁵. Other mechanisms similar to those that cause primary HTN, including disruption of the renin-angiotensin system or pressure-natriuresis relationship, may also underlie bevacizumab-induced HTN. These changes may be influenced by downregulation of NO, which directly affects tubuloglomerular feedback, pressure natriuresis, and sodium balance⁹⁶. Mice treated with a VEGFR2 inhibitor have displayed a reduction of kidney eNOS and neuronal NOS expression and a shift in the chronic pressure-natriuresis relationship⁷⁹. Similarly, administration of sunitinib in rats resulted in renal histological abnormalities and increased arterial pressure, and treatment of cultured human renal proximal tubular epithelial cells with sunitinib reduced VEGF-induced eNOS protein expression⁹⁷.

1.6 Pharmacogenetics of bevacizumab and VEGF inhibitor toxicity

While there already exists supporting evidence for the mechanism of bevacizumab-induced HTN, it remains unknown why such great interindividual variability in BP elevation exists among patients treated with bevacizumab. The consistent fraction of patients that developed high-grade HTN across multiple clinical trials of bevacizumab^{12,19} suggests that genetic variation may influence the risk and severity of bevacizumab toxicity.

The pharmacokinetics of bevacizumab are well-described by a linear two-compartment model⁹⁸. Bevacizumab elimination relies on proteolytic catabolism throughout the body and is also regulated by FcRn-receptor-mediated recycling¹³. Body weight and gender explain most of the interindividual variability in bevacizumab clearance and volume⁹⁸, and thus bevacizumab is administered on a mg/kg basis. Serum albumin, alkaline phosphatase (ALP), serum aspartate aminotransferase (AST), and tumor burden have also been reported to affect clearance rates⁹⁹. None of these factors are expected to have a significant impact on unbound VEGF levels or efficacy⁹⁸. Genetic variants affecting the binding affinities of VEGF¹⁰⁰ or FcRn⁹⁹ have been suggested to influence bevacizumab pharmacokinetics, but a significant correlation has yet to be established.

Studies of variation in bevacizumab pharmacodynamics also have not yet yielded any validated markers to predict bevacizumab efficacy or toxicity. Attempts to identify tumor-derived biomarkers have been unsuccessful¹⁰¹. Because bevacizumab targets host-mediated angiogenesis, predictors of both efficacy and toxicity are likely to be host factors. In searching for genetic biomarkers of bevacizumab-induced HTN, prior studies have

primarily focused on common functional SNPs in *VEGFA* and *KDR*, as these genes encode the most direct targets of bevacizumab, VEGF and VEGFR2. Several *VEGFA* polymorphisms (rs699947, rs833061, rs1570360, rs2010963, rs3025039) located in the promoter and 5' and 3' untranslated regions are associated with differential VEGF expression and serum levels¹⁰²⁻¹⁰⁸. Two nonsynonymous functional variants in *KDR* are also commonly examined in relation to bevacizumab-induced HTN. rs2305948 (V297I, exon 7) results in an amino acid change in the third immunoglobulin (Ig)-like domain of VEGFR2, which is critical for binding of the VEGF ligand^{109,110}. rs1870377 (H472Q, exon 11) affects the fifth VEGFR2 Ig-like domain, which contains structural features that inhibit VEGFR2 signaling in the absence of VEGF¹¹¹.

Previous studies of bevacizumab-induced HTN have identified significant associations between *VEGFA/KDR* SNPs and incidence of the toxicity (Table 1.6). Schneider *et al* identified associations between rs833061 and rs2010963 with incidence of grade 3–4 HTN in the ECOG-2100 trial of bevacizumab and first-line paclitaxel in patients with metastatic breast cancer¹⁰¹. Jain *et al* performed a meta-analysis of bevacizumab treated patients across six different trials and identified carriers of VEGFR2 H472Q (rs1870377) as having greater risk of developing grade 2+ HTN¹¹². Etienne-Grimaldi *et al* genotyped women with locally recurrent or metastatic breast cancer receiving bevacizumab-containing therapy and found a significant association between rs2010963 and all-grade HTN¹¹³, though with the opposite direction of effect as reported by Schneider *et al*. In an analysis of bevacizumab-treated patients with metastatic colorectal cancer, Morita *et al* identified rs699947 and rs833061 to be associated with early grade 2+ HTN (during the first two

months of treatment) and rs699947 and rs3025039 to be associated with grade 2+ HTN during the entire treatment period¹⁰⁸; the rs833061 effect direction agreed with that of Schneider *et al.* Sibertin-Blanc *et al* identified an association of rs3025039 with incidence of all-grade HTN in metastatic colorectal cancer patients¹¹⁴, with a direction of effect that contradicts that in the Morita *et al* study. Finally, Gampenrieder *et al* found an association between rs2010963 and the incidence of bevacizumab-induced HTN in metastatic breast cancer patients¹¹⁵, with a direction of effect that agrees with Schneider *et al* but not Etienne-Grimaldi *et al.*

More recent studies have expanded the set of examined genes beyond *VEGFA* and *KDR*. Lambrechts *et al* tested 236 SNPs in VEGF pathway and HTN-related genes in a meta-analysis of six trials of bevacizumab treatment¹¹⁶. No SNP surpassed the adjusted significance threshold, but SNPs in *EGLN3*, *EGF*, *WNK1*, and *KDR* had the strongest associations with all-grade HTN. Schneider *et al* expanded their initial study to a GWAS of bevacizumab-treated breast cancer patients in ECOG-5103. A SNP in *SV2C* associated with high systolic BP in the discovery study and was validated for association with grade 3–4 HTN in a subset of ECOG-2100 patients¹¹⁷.

Table 1.6. Previous pharmacogenetic studies of bevacizumab-induced hypertension

Study	N, subjects	N, SNPs tested	Associated SNP (allele/genotype)	HTN phenotype	HTN risk	Association P-value
Schneider <i>et al</i> (2008) ¹⁰¹	363	7	VEGFA rs833061 (TT)	Grade 3+	Decreased	0.022
			VEGFA rs2010963 (CC)	Grade 3+	Decreased	0.005
Jain <i>et al</i> (2010) ¹¹²	170	2	KDR rs1870377 (A)	Grade 2+	Increased (OR 2.3)	0.0154
Etienne-Grimaldi <i>et al</i> (2011) ¹¹³	137	5	VEGFA rs2010963 (C)	All-grade	Increased	0.01
			VEGFA rs699947 (CC)	Early grade 2+	Decreased	0.004
Morita <i>et al</i> (2012) ¹⁰⁸	60	5	VEGFA rs833061 (TT)	Grade 2+	Decreased	0.031
			VEGFA rs3025039 (CC)	Early grade 2+	Decreased	0.025
			EGLN3 rs1680695 (G)	Grade 2+	Decreased	0.043
Lambrechts <i>et al</i> (2014) ¹¹⁶	1,631	236	EGF rs4444903 (G)	All-grade	Increased (OR 1.50)	0.012
			KDR rs2305949 (T)	All-grade	Increased (OR 1.57)	0.0025
			WNK1 rs11064560 (T)	All-grade	Decreased (OR 0.62)	0.020
			SV2C rs6453204 (G)	All-grade	Increased (OR 1.41)	0.028
Schneider <i>et al</i> (2014) ¹¹⁷	582	810,372		SBP > 160 mmHg	Increased (OR 3.3, binary; HR 2.2, cumulative dose)	6.0 x 10 ⁻⁸ (binary); 4.7 x 10 ⁻⁸ (cumulative dose)
Sibertin-Blanc <i>et al</i> (2015) ¹¹⁴	89	10	VEGFA rs3025039 (CC)	All-grade	Increased (CT+TT: OR 0.159)	0.022
Gampenrieder <i>et al</i> (2016) ¹¹⁵	163	10	VEGFA rs2010963 (GG)	Grade 3+	Increased	0.031

Genetic associations with HTN toxicity have also been reported during treatment with VEGF RTKIs. SNPs in *VEGFA*, *KDR*, and *NOS3* (eNOS) are associated with sunitinib-induced HTN¹¹⁸⁻¹²¹. Variants in hepatic and renal drug metabolizing enzymes and transporters also associate with RTKI toxicities^{122,123}, though these are not expected to affect bevacizumab pharmacokinetics.

In summary, four regulatory *VEGFA* SNPs, a nonsynonymous *KDR* SNP, and an intronic variant in *SV2C* have been significantly associated with incidence of bevacizumab-induced HTN. An intronic *KDR* SNP and several SNPs in other VEGF (*EGLN3*) or HTN (*EGF*, *WNK1*) pathway genes were modestly associated with the toxicity. However, the effect directions of several of these findings are discordant, and no association has been replicated consistently across multiple studies. Given the complexity of primary HTN, the genetic architecture contributing to bevacizumab-induced HTN is also likely to be polygenic. Therefore, further research on this phenotype is warranted in additional cohorts and in an expanded set of genes.

1.7 Hypertension as a marker of bevacizumab efficacy

Clinical, radiological, and molecular markers have been examined to identify biomarkers or other surrogate markers to predict bevacizumab efficacy. Genetic markers, most of which consist of the *VEGFA* functional polymorphisms mentioned above, have been significantly associated with improved OS and PFS in several studies¹²⁴⁻¹²⁷. However, few of these pharmacogenetic findings have had consistent results.

The relationship between bevacizumab-induced HTN and efficacy has also been examined, with the development of HTN being proposed as a surrogate marker for the inhibition of the VEGF signaling pathway¹²⁸. Multiple studies and meta-analyses have identified associations between bevacizumab-induced HTN and longer PFS, OS, or response rate¹²⁹⁻¹³², though other studies found no consistent correlation between HTN and clinical benefit^{12,19}.

If the development of HTN is indeed predictive of improved clinical outcomes, cases of high-grade HTN that would normally prompt discontinuation of bevacizumab treatment may instead warrant more aggressive treatment of HTN. Dose titration of bevacizumab while closely monitoring BP has been proposed to improve outcomes¹³³. Because bevacizumab-induced HTN is hypothesized to be an on-target drug effect, identification of genetic variants that influence both BP and efficacy may enable prediction of both toxicity and efficacy prior to treatment.

1.8 Research motivation and focus of this dissertation

Bevacizumab is used for the treatment of multiple tumor types, with HTN being frequently observed during treatment. The development of high-grade HTN may put a patient at risk for serious cardiovascular events and damage to other organ systems. The toxicity may also require discontinuation of bevacizumab, limiting its therapeutic benefits. There are currently no validated biomarkers to predict bevacizumab toxicity, and the factors that contribute to interindividual variability in BP elevation during treatment are not well understood. Further research on the risk factors and mechanisms of bevacizumab-induced

HTN are necessary to minimize the number of patients impacted by this dose-limiting toxicity.

Although prior studies have identified common variants associated with bevacizumab-induced HTN, such findings have been inconsistent and require further validation. Given the heritable but complex nature of primary HTN, the genetic architecture underlying bevacizumab-induced HTN is also likely to be polygenic. Additional examination of genetic variation in non-VEGF pathways and of rare variants with potentially large phenotypic effects may identify novel mechanisms contributing to bevacizumab-induced HTN.

In this dissertation research, the hypothesis that genetic variation contributes to the risk of developing bevacizumab-induced HTN was tested with the following research aims:

1. Identify genomic regions associated with severe, early-onset bevacizumab-induced HTN by analyzing sequenced whole exomes and candidate gene regulatory regions of bevacizumab-treated colorectal cancer patients with extreme toxicity phenotypes (Chapter 2).
2. Identify common variants associated with bevacizumab-induced HTN by analyzing GWAS data from a larger, independent cohort of bevacizumab-treated breast cancer patients (Chapter 4). This approach accounted for cumulative bevacizumab dose and study discontinuation for non-HTN causes using a time-to-event outcome.
3. Examine the potential functional effects of top SNPs identified in Aims 1 and 2 through literature searches and *in silico* analyses using publicly available bioinformatics data (Chapters 2 and 4).

4. Replicate the top associations identified in Aims 1 and 2 by testing for association in independent bevacizumab-treated cohorts (Chapters 2 and 4).
5. Validate previously reported genetic associations with bevacizumab-induced HTN by testing for association in bevacizumab-treated cohorts (Chapters 2 and 4).
6. Determine whether the modulation of a gene identified in Aim 1 affects markers of VEGF-stimulated vasodilation following bevacizumab treatment in an *in vitro* system. Vascular endothelial cells were assayed for changes in NO and PGI₂ during overexpression or pharmacological inhibition of the target gene/protein (Chapter 3).

Collectively, these studies identified novel genetic loci associated with bevacizumab-induced HTN and provided functional evidence for a novel mechanism of this toxicity. The results of this research will advance understanding of the biological mechanism of bevacizumab-induced HTN and should be considered in the future use and development of angiogenesis inhibitors.

1.9 References

1. Ferrara N, Adamis AP. Ten years of anti-vascular endothelial growth factor therapy. *Nat Rev Drug Discov.* 2016;15(6):385–403.
2. Avastin [package insert]. South San Francisco, CA: Genentech, Inc.; 2016. Available from: https://www.gene.com/download/pdf/avastin_prescribing.pdf
3. Ferrara N, Hillan KJ, Gerber HP, Novotny W. Discovery and development of bevacizumab, an anti-VEGF antibody for treating cancer. *Nat Rev Drug Discov.* 2004;3(5):391–400.
4. Glusker P, Recht L, Lane B. Reversible posterior leukoencephalopathy syndrome and bevacizumab. *N Engl J Med.* 2006;354(9):980–2.
5. Ozcan C, Wong SJ, Hari P. Reversible posterior leukoencephalopathy syndrome and bevacizumab. *N Engl J Med.* 2006;354(9):980–2.
6. Baizabal-Carvallo JF, Alonso-Juárez M, Salas I. Pretruncal subarachnoid hemorrhage and high cerebral blood flow velocities with bevacizumab therapy. *Clin Neuropharmacol.* 2010;33(5):268–9.
7. Dissanayake AS, Ramakonar HH, Lind CRP. Diffuse, non-traumatic, non-aneurysmal subarachnoid haemorrhage during bevacizumab treatment of high grade glioma: case report and review of the literature. *Interdiscip Neurosurg.* 2015;2(2):65–8.
8. Zand R, Kazemi S, Barr J, Afshani M. Subarachnoid hemorrhage with severe vasospasm after bevacizumab therapy: a case report. *Neurology.* 2012;78(1 Suppl):P02.205.
9. Maitland ML, Bakris GL, Black HR, Chen HX, Durand JB, Elliott WJ, Ivy SP, Leier CV, Lindenfeld J, Liu G, Remick SC, Steingart R, Tang WHW, Cardiovascular Toxicities Panel, Convened by the Angiogenesis Task Force of the National Cancer Institute Investigational Drug Steering Committee. Initial assessment, surveillance, and management of blood pressure in patients receiving vascular endothelial growth factor signaling pathway inhibitors. *J Natl Cancer Inst.* 2010;102(9):596–604.
10. Common Terminology for Adverse Events v3.0 (CTCAE). Cancer Therapy Evaluation Program; 2003. Available from: <http://ctep.cancer.gov/reporting/ctc.html>
11. Zhu X, Wu S, Dahut WL, Parikh CR. Risks of proteinuria and hypertension with bevacizumab, an antibody against vascular endothelial growth factor: systematic review and meta-analysis. *Am J Kidney Dis.* 2007;49(2):186–93.
12. Ranpura V, Pulipati B, Chu D, Zhu X, Wu S. Increased risk of high-grade hypertension with bevacizumab in cancer patients: a meta-analysis. *Am J*

Hypertens. 2010;23(5):460–8.

13. Avastin: Summary of product characteristics. European Medicines Agency; [cited 2017 Mar 25]. Available from: http://www.ema.europa.eu/docs/en_GB/document_library/EPAR_-_Product_Information/human/000582/WC500029271.pdf
14. Cortes J, Calvo V, Ramírez-Merino N, O'Shaughnessy J, Brufsky A, Robert N, Vidal M, Muñoz E, Perez J, Dawood S, Saura C, Di Cosimo S, González-Martín A, Bellet M, Silva OE, Miles D, Llombart A, Baselga J. Adverse events risk associated with bevacizumab addition to breast cancer chemotherapy: a meta-analysis. *Ann Oncol.* 2012;23(5):1130–7.
15. Loupakis F, Bria E, Vaccaro V, Cuppone F, Milella M, Carlini P, Cremolini C, Salvatore L, Falcone A, Muti P, Sperduti I, Giannarelli D, Cognetti F. Magnitude of benefit of the addition of bevacizumab to first-line chemotherapy for metastatic colorectal cancer: meta-analysis of randomized clinical trials. *J Exp Clin Cancer Res.* 2010;29:58.
16. Mir O, Coriat R, Cabanes L, Ropert S, Billefont B, Alexandre J, Durand J-P, Treluyer J-M, Knebelmann B, Goldwasser F. An observational study of bevacizumab-induced hypertension as a clinical biomarker of antitumor activity. *Oncologist.* 2011;16(9):1325–32.
17. Feliu J, Salud A, Safont MJ, García-Girón C, Aparicio J, Losa F, Bosch C, Escudero P, Casado E, Jorge M, Bohn U, Pérez-Carrión R, Carmona A, Custodio AB, Maurel J. Correlation of hypertension and proteinuria with outcome in elderly bevacizumab-treated patients with metastatic colorectal cancer. *PLoS One.* 2015;10(1):e0116527.
18. Slusarz KM, Merker VL, Muzikansky A, Francis SA, Plotkin SR. Long-term toxicity of bevacizumab therapy in neurofibromatosis 2 patients. *Cancer Chemother Pharmacol.* 2014;73(6):1197–204.
19. Hurwitz HI, Douglas PS, Middleton JP, Sledge GW, Johnson DH, Reardon DA, Chen D, Rosen O. Analysis of early hypertension and clinical outcome with bevacizumab: results from seven phase III studies. *Oncologist.* 2013;18(3):273–80.
20. Verheul HMW, Pinedo HM. Possible molecular mechanisms involved in the toxicity of angiogenesis inhibition. *Nat Rev Cancer.* 2007;7(6):475–85.
21. Keefe D, Bowen J, Gibson R, Tan T, Okera M, Stringer A. Noncardiac vascular toxicities of vascular endothelial growth factor inhibitors in advanced cancer: a review. *Oncologist.* 2011;16(4):432–44.
22. Hamnvik OP, Choueiri TK, Turchin A, McKay RR, Goyal L, Davis M, Kaymakçalan MD, Williams JS. Clinical risk factors for the development of hypertension in

- patients treated with inhibitors of the VEGF signaling pathway. *Cancer*. 2015;121(2):311–9.
23. Wu S, Chen JJ, Kudelka A, Lu J, Zhu X. Incidence and risk of hypertension with sorafenib in patients with cancer: a systematic review and meta-analysis. *Lancet Oncol*. 2008;9(2):117–23.
 24. Seet RCS, Rabinstein AA. Clinical features and outcomes of posterior reversible encephalopathy syndrome following bevacizumab treatment. *Q J Med*. 2012;105:69–75.
 25. Langenberg MHG, van Herpen CML, De Bono J, Schellens JHM, Unger C, Hoekman K, Blum HE, Fiedler W, Dreves J, Le Maulf F, Fielding A, Robertson J, Voest EE. Effective strategies for management of hypertension after vascular endothelial growth factor signaling inhibition therapy: results from a phase II randomized, factorial, double-blind study of Cediranib in patients with advanced solid tumors. *J Clin Oncol*. 2009;27(36):6152–9.
 26. Izzedine H, Ederhy S, Goldwasser F, Soria JC, Milano G, Cohen A, Khayat D, Spano JP. Management of hypertension in angiogenesis inhibitor-treated patients. *Ann Oncol*. 2009;20(5):807–15.
 27. Dincer M, Altundag K. Angiotensin-converting enzyme inhibitors for bevacizumab-induced hypertension. *Ann Pharmacother*. 2006;40(12):2278–9.
 28. Dirix LY, Maes H, Sweldens C. Treatment of arterial hypertension (AHT) associated with angiogenesis inhibitors. *Ann Oncol*. 2007;18(6):1121–2.
 29. Kruzliak P, Kovacova G, Pechanova O. Therapeutic potential of nitric oxide donors in the prevention and treatment of angiogenesis-inhibitor-induced hypertension. *Angiogenesis*. 2013;16(2):289–95.
 30. Isobe T, Uchino K, Makiyama C, Ariyama H, Arita S, Tamura S, Komoda M, Kusaba H, Shirakawa T, Esaki T, Mitsugi K, Takaishi S, Akashi K, Baba E. Analysis of adverse events of bevacizumab-containing systemic chemotherapy for metastatic colorectal cancer in Japan. *Anticancer Res*. 2014;34(4):2035–40.
 31. Wicki A, Hermann F, Prêtre V, Winterhalder R, Kueng M, von Moos R, Rochlitz C, Herrmann R. Pre-existing antihypertensive treatment predicts early increase in blood pressure during bevacizumab therapy: the prospective AVALUE cohort study. *Oncol Res Treat*. 2014;37(5):230–6.
 32. An MM, Zou Z, Shen H, Liu P, Chen ML, Cao YB, Jiang YY. Incidence and risk of significantly raised blood pressure in cancer patients treated with bevacizumab: an updated meta-analysis. *Eur J Clin Pharmacol*. 2010;66(8):813–21.
 33. World Health Organization. A global brief on hypertension: silent killer, global

public health crisis. 2013.

34. Mozaffarian D, Benjamin EJ, Go AS, Arnett DK, Blaha MJ, Cushman M, Das SR, de Ferranti S, Després J-P, Fullerton HJ, Howard VJ, Huffman MD, Isasi CR, Jiménez MC, Judd SE, Kissela BM, Lichtman JH, Lisabeth LD, Liu S, Mackey RH, Magid DJ, McGuire DK, Mohler ER III, Moy CS, Muntner P, Mussolino ME, Nasir K, Neumar RW, Nichol G, Palaniappan L, Pandey DK, Reeves MJ, Rodriguez CJ, Rosamond W, Sorlie PD, Stein J, Towfighi A, Turan TN, Virani SS, Woo D, Yeh RW, Turner MB. Heart disease and stroke statistics—2016 update: a report from the American Heart Association. *Circulation*. 2016;133(4):e38–60.
35. The Japanese Society of Hypertension guidelines for the management of hypertension (JSH 2014). *Hypertens Res*. 2014;37:253–392.
36. Grossman A, Messerli FH, Grossman E. Drug induced hypertension – an unappreciated cause of secondary hypertension. *Eur J Pharmacol*. 2015;763(Pt A):15–22.
37. Oparil S, Zaman MA, Calhoun DA. Pathogenesis of hypertension. *Ann Intern Med*. 2003;139(9):761–76.
38. Padmanabhan S, Caulfield M, Dominiczak AF. Genetic and molecular aspects of hypertension. *Circ Res*. 2015;116(6):937–59.
39. Nwankwo T, Yoon SS, Burt V, Gu Q. Hypertension among adults in the United States: National Health and Nutrition Examination Survey, 2011-2012. *NCHS Data Brief*. 2013;133:1–8.
40. Boyden LM, Choi M, Choate KA, Nelson-Williams CJ, Farhi A, Toka HR, Tikhonova IR, Bjornson R, Mane SM, Colussi G, Lebel M, Gordon RD, Ben A Semmekrot, Poujol A, Välimäki MJ, De Ferrari ME, Sanjad SA, Gutkin M, Karet FE, Tucci JR, Stockigt JR, Keppler-Noreuil KM, Porter CC, Anand SK, Whiteford ML, Davis ID, Dewar SB, Bettinelli A, Fadrowski JJ, Belsha CW, Hunley TE, Nelson RD, Trachtman H, Cole TRP, Pinsk M, Bockenhauer D, Shenoy M, Vaidyanathan P, Foreman JW, Rasoulpour M, Thameem F, Al-Shahrouri HZ, Radhakrishnan J, Gharavi AG, Goilav B, Lifton RP. Mutations in kelch-like 3 and cullin 3 cause hypertension and electrolyte abnormalities. *Nature*. 2012;482(7383):98–102.
41. Louis-Dit-Picard H, Barc J, Trujillano D, Miserey-Lenkei S, Bouatia-Naji N, Pylypenko O, Beaurain G, Bonnefond A, Sand O, Simian C, Vidal-Petiot E, Soukaseum C, Mandet C, Broux F, Chabre O, Delahousse M, Esnault V, Fiquet B, Houillier P, Bagnis CI, Koenig J, Konrad M, Landais P, Mourani C, Niaudet P, Probst V, Thauvin C, Unwin RJ, Soroka SD, Ehret G, Ossowski S, Caulfield M, Bruneval P, Estivill X, Froguel P, Hadchouel J, Schott J-J, Jeunemaitre X. KLHL3 mutations cause familial hyperkalemic hypertension by impairing ion transport in the distal nephron. *Nat Genet*. 2012;44(4):456–60.

42. Choi M, Scholl UI, Yue P, Björklund P, Zhao B, Nelson-Williams C, Ji W, Cho Y, Patel A, Men CJ, Lolis E, Wisgerhof MV, Geller DS, Mane S, Hellman P, Westin G, Åkerström G, Wang W, Carling T, Lifton RP. K⁺ channel mutations in adrenal aldosterone-producing adenomas and hereditary hypertension. *Science*. 2011;331(6018):768–72.
43. Hoffmann TJ, Ehret GB, Nandakumar P, Ranatunga D, Schaefer C, Kwok P-Y, Iribarren C, Chakravarti A, Risch N. Genome-wide association analyses using electronic health records identify new loci influencing blood pressure variation. *Nat Genet*. 2017;49(1):54–64.
44. Surendran P, Drenos F, Young R, Warren H, Cook JP, Manning AK, Grarup N, Sim X, Barnes DR, Witkowska K, Staley JR, Tragante V, Tukiainen T, Yaghootkar H, Masca N, Freitag DF, Ferreira T, Giannakopoulou O, Tinker A, Harakalova M, Mihailov E, Liu C, Kraja AT, Nielsen SF, Rasheed A, Samuel M, Zhao W, Bonnycastle LL, Jackson AU, Narisu N, Swift AJ, Southam L, Marten J, Huyghe JR, Stančáková A, Fava C, Ohlsson T, Matchan A, Stirrups KE, Bork-Jensen J, Gjesing AP, Kontto J, Perola M, Shaw-Hawkins S, Havulinna AS, Zhang H, Donnelly LA, Groves CJ, Rayner NW, Neville MJ, Robertson NR, Ylörkas AM, Herzig K-H, Kajantie E, Zhang W, Willems SM, Lannfelt L, Malerba G, Soranzo N, Trabetti E, Verweij N, Evangelou E, Moayyeri A, Vergnaud A-C, Nelson CP, Poveda A, Varga TV, Caslake M, de Craen AJM, Trompet S, Luan J, Scott RA, Harris SE, Liewald DCM, Marioni R, Menni C, Farmaki A-E, Hallmans G, Renström F, Huffman JE, Hassinen M, Burgess S, Vasani RS, Felix JF, Uria-Nickelsen M, Malarstig A, Reilly DF, Hoek M, Vogt TF, Lin H, Lieb W, Traylor M, Markus HS, Highland HM, Justice AE, Marouli E, Lindström J, Uusitupa M, Komulainen P, Lakka TA, Rauramaa R, Polašek O, Rudan I, Rolandsson O, Franks PW, Dedoussis G, Spector TD, Jousilahti P, Männistö S, Deary IJ, Starr JM, Langenberg C, Wareham NJ, Brown MJ, Dominiczak AF, Connell JM, Jukema JW, Sattar N, Ford I, Packard CJ, Esko T, Mägi R, Metspalu A, de Boer RA, van der Meer P, van der Harst P, Gambaro G, Ingelsson E, Lind L, de Bakker PIW, Numans ME, Brandslund I, Christensen C, Petersen ERB, Korpi-Hyövälti E, Oksa H, Chambers JC, Kooner JS, Blakemore AIF, Franks S, Jarvelin M-R, Husemoen LL, Linneberg A, Skaaby T, Thuesen B, Karpe F, Tuomilehto J, Doney ASF, Morris AD, Palmer CNA, Holmen OL, Hveem K, Willer CJ, Tuomi T, Groop L, Käräjämäki A, Palotie A, Ripatti S, Salomaa V, Alam DS, Majumder AAS, Di Angelantonio E, Chowdhury R, McCarthy MI, Poulter N, Stanton AV, Sever P, Amouyel P, Arveiler D, Blankenberg S, Ferrières J, Kee F, Kuulasmaa K, Müller-Nurasyid M, Veronesi G, Virtamo J, Deloukas P, Elliott P, Zeggini E, Kathiresan S, Melander O, Kuusisto J, Laakso M, Padmanabhan S, Porteous DJ, Hayward C, Scotland G, Collins FS, Mohlke KL, Hansen T, Pedersen O, Boehnke M, Stringham HM, Frossard P, Newton-Cheh C, Tobin MD, Nordestgaard BG, Caulfield MJ, Mahajan A, Morris AP, Tomaszewski M, Samani NJ, Saleheen D, Asselbergs FW, Lindgren CM, Danesh J, Wain LV, Butterworth AS, Howson JMM, Munroe PB. Trans-ancestry meta-analyses identify rare and common variants associated with blood pressure and hypertension. *Nat Genet*. 2016;48(10):1151–61.

45. Ehret GB, Ferreira T, Chasman DI, Jackson AU, Schmidt EM, Johnson T, Thorleifsson G, Luan J, Donnelly LA, Kanoni S, Petersen A-K, Pihur V, Strawbridge RJ, Shungin D, Hughes MF, Meirelles O, Kaakinen M, Bouatia-Naji N, Kristiansson K, Shah S, Kleber ME, Guo X, Lyytikäinen L-P, Fava C, Eriksson N, Nolte IM, Magnusson PK, Salfati EL, Rallidis LS, Theusch E, Smith AJP, Folkersen L, Witkowska K, Pers TH, Joehanes R, Kim SK, Lataniotis L, Jansen R, Johnson AD, Warren H, Kim YJ, Zhao W, Wu Y, Tayo BO, Bochud M, Absher D, Adair LS, Amin N, Arking DE, Axelsson T, Baldassarre D, Balkau B, Bandinelli S, Barnes MR, Barroso I, Bevan S, Bis JC, Bjornsdottir G, Boehnke M, Boerwinkle E, Bonnycastle LL, Boomsma DI, Bornstein SR, Brown MJ, Burnier M, Cabrera CP, Chambers JC, Chang I-S, Cheng C-Y, Chines PS, Chung R-H, Collins FS, Connell JM, Döring A, Dallongeville J, Danesh J, de Faire U, Delgado G, Dominiczak AF, Doney ASF, Drenos F, Edkins S, Eicher JD, Elosua R, Enroth S, Erdmann J, Eriksson P, Esko T, Evangelou E, Evans A, Fall T, Farrall M, Felix JF, Ferrières J, Ferrucci L, Fornage M, Forrester T, Franceschini N, Franco OH, Franco-Cereceda A, Fraser RM, Ganesh SK, Gao H, Gertow K, Gianfagna F, Gigante B, Giulianini F, Goel A, Goodall AH, Goodarzi MO, Gorski M, Gräßler J, Groves CJ, Gudnason V, Gyllenstein U, Hallmans G, Hartikainen A-L, Hassinen M, Havulinna AS, Hayward C, Hercberg S, Herzig K-H, Hicks AA, Hingorani AD, Hirschhorn JN, Hofman A, Holmen J, Holmen OL, Hottenga J-J, Howard P, Hsiung CA, Hunt SC, Ikram MA, Illig T, Iribarren C, Jensen RA, Kähönen M, Kang HM, Kathiresan S, Keating BJ, Khaw K-T, Kim YK, Kim E, Kivimäki M, Klopp N, Kolovou G, Komulainen P, Kooner JS, Kosova G, Krauss RM, Kuh D, Kutalik Z, Kuusisto J, Kvaløy K, Lakka TA, Lee NR, Lee I-T, Lee W-J, Levy D, Li X, Liang K-W, Lin H, Lin L, Lindström J, Lobbens S, Männistö S, Müller G, Müller-Nurasyid M, Mach F, Markus HS, Marouli E, McCarthy MI, McKenzie CA, Meneton P, Menni C, Metspalu A, Mijatovic V, Moilanen L, Montasser ME, Morris AD, Morrison AC, Mulas A, Nagaraja R, Narisu N, Nikus K, O'Donnell CJ, O'Reilly PF, Ong KK, Paccaud F, Palmer CD, Parsa A, Pedersen NL, Penninx BW, Perola M, Peters A, Poulter N, Pramstaller PP, Psaty BM, Quertermous T, Rao DC, Rasheed A, Rayner NW, Renström F, Rettig R, Rice KM, Roberts R, Rose LM, Rossouw J, Samani NJ, Sanna S, Saramies J, Schunkert H, Sebert S, Sheu WH-H, Shin Y-A, Sim X, Smit JH, Smith AV, Sosa MX, Spector TD, Stančáková A, Stanton AV, Stirrups KE, Stringham HM, Sundström J, Swift AJ, Syvänen A-C, Tai ES, Tanaka T, Tarasov KV, Teumer A, Thorsteinsdottir U, Tobin MD, Tremoli E, Uitterlinden AG, Uusitupa M, Vaez A, Vaidya D, van Duijn CM, van Iperen EPA, Vasán RS, Verwoert GC, Virtamo J, Vitart V, Voight BF, Vollenweider P, Wagner A, Wain LV, Wareham NJ, Watkins H, Weder AB, Westra H-J, Wilks R, Wilsgaard T, Wilson JF, Wong TY, Yang T-P, Yao J, Yengo L, Zhang W, Zhao JH, Zhu X, Bovet P, Cooper RS, Mohlke KL, Saleheen D, Lee J-Y, Elliott P, Gierman HJ, Willer CJ, Franke L, Hovingh GK, Taylor KD, Dedoussis G, Sever P, Wong A, Lind L, Assimes TL, Njølstad I, Schwarz PEH, Langenberg C, Snieder H, Caulfield MJ, Melander O, Laakso M, Saltevo J, Rauramaa R, Tuomilehto J, Ingelsson E, Lehtimäki T, Hveem K, Palmas W, März W, Kumari M, Salomaa V, Chen Y-DI, Rotter JI, Froguel P, Jarvelin M-R, Lakatta EG, Kuulasmaa K, Franks PW, Hamsten A, Wichmann H-E, Palmer CNA, Stefansson K, Ridker PM, Loos RJJ, Chakravarti A, Deloukas P, Morris AP, Newton-Cheh C, Munroe PB. The genetics of blood pressure regulation and its target organs from association studies in 342,415 individuals. *Nat Genet.* 2016;48(10):1171–84.

46. Warren HR, Evangelou E, Cabrera CP, Gao H, Ren M, Mifsud B, Ntalla I, Surendran P, Liu C, Cook JP, Kraja AT, Drenos F, Loh M, Verweij N, Marten J, Karaman I, Lepe MPS, O'Reilly PF, Knight J, Snieder H, Kato N, He J, Tai ES, Said MA, Porteous D, Alver M, Poulter N, Farrall M, Gansevoort RT, Padmanabhan S, Mägi R, Stanton A, Connell J, Bakker SJL, Metspalu A, Shields DC, Thom S, Brown M, Sever P, Esko T, Hayward C, van der Harst P, Saleheen D, Chowdhury R, Chambers JC, Chasman DI, Chakravarti A, Newton-Cheh C, Lindgren CM, Levy D, Kooner JS, Keavney B, Tomaszewski M, Samani NJ, Howson JMM, Tobin MD, Munroe PB, Ehret GB, Wain LV. Genome-wide association analysis identifies novel blood pressure loci and offers biological insights into cardiovascular risk. *Nat Genet.* 2017;49(3):403–15.
47. Liu C, Kraja AT, Smith JA, Brody JA, Franceschini N, Bis JC, Rice K, Morrison AC, Lu Y, Weiss S, Guo X, Palmas W, Martin LW, Chen Y-DI, Surendran P, Drenos F, Cook JP, Auer PL, Chu AY, Giri A, Zhao W, Jakobsdottir J, Lin L-A, Stafford JM, Amin N, Mei H, Yao J, Voorman A, Larson MG, Grove ML, Smith AV, Hwang S-J, Chen H, Huan T, Kosova G, Stitzel NO, Kathiresan S, Samani N, Schunkert H, Deloukas P, Li M, Fuchsberger C, Pattaro C, Gorski M, Kooperberg C, Papanicolaou GJ, Rossouw JE, Faul JD, Kardia SLR, Bouchard C, Raffel LJ, Uitterlinden AG, Franco OH, Vasani RS, O'Donnell CJ, Taylor KD, Liu K, Bottinger EP, Gottesman O, Daw EW, Giulianini F, Ganesh S, Salfati E, Harris TB, Launer LJ, Dörr M, Felix SB, Rettig R, Völzke H, Kim E, Lee W-J, Lee I-T, Sheu WH-H, Tsosie KS, Edwards DRV, Liu Y, Correa A, Weir DR, Völker U, Ridker PM, Boerwinkle E, Gudnason V, Reiner AP, van Duijn CM, Borecki IB, Edwards TL, Chakravarti A, Rotter JI, Psaty BM, Loos Rjf, Fornage M, Ehret GB, Newton-Cheh C, Levy D, Chasman DI. Meta-analysis identifies common and rare variants influencing blood pressure and overlapping with metabolic trait loci. *Nat Genet.* 2016;48(10):1162–70.
48. Munroe PB, Barnes MR, Caulfield MJ. Advances in blood pressure genomics. *Circ Res.* 2013;112(10):1365–79.
49. The Wellcome Trust Case Control Consortium. Genome-wide association study of 14,000 cases of seven common diseases and 3,000 shared controls. *Nature.* 2007;447(7145):661–78.
50. Levy D, Larson MG, Benjamin EJ, Newton-Cheh C, Wang TJ, Hwang S-J, Vasani RS, Mitchell GF. Framingham Heart Study 100K Project: genome-wide associations for blood pressure and arterial stiffness. *BMC Med Genet.* 2007;8(Suppl 1):S3.
51. Levy D, Ehret GB, Rice K, Verwoert GC, Launer LJ, Dehghan A, Glazer NL, Morrison AC, Johnson AD, Aspelund T, Aulchenko Y, Lumley T, Köttgen A, Vasani RS, Rivadeneira F, Eiriksdottir G, Guo X, Arking DE, Mitchell GF, Mattace-Raso FUS, Smith AV, Taylor K, Scharpf RB, Hwang S-J, Sijbrands EJJ, Bis J, Harris TB, Ganesh SK, O'Donnell CJ, Hofman A, Rotter JI, Coresh J, Benjamin EJ, Uitterlinden AG, Heiss G, Fox CS, Witteman JCM, Boerwinkle E, Wang TJ, Gudnason V, Larson MG, Chakravarti A, Psaty BM, van Duijn CM. Genome-wide association study of blood pressure and hypertension. *Nat Genet.* 2009;41(6):677–87.

52. Newton-Cheh C, Johnson T, Gateva V, Tobin MD, Bochud M, Coin L, Najjar SS, Zhao JH, Heath SC, Eyheramendy S, Papadakis K, Voight BF, Scott LJ, Zhang F, Farrall M, Tanaka T, Wallace C, Chambers JC, Khaw K-T, Nilsson P, van der Harst P, Polidoro S, Grobbee DE, Onland-Moret NC, Bots ML, Wain LV, Elliott KS, Teumer A, Luan J, Lucas G, Kuusisto J, Burton PR, Hadley D, McArdle WL, Brown M, Dominiczak A, Newhouse SJ, Samani NJ, Webster J, Zeggini E, Beckmann JS, Bergmann S, Lim N, Song K, Vollenweider P, Waeber G, Waterworth DM, Yuan X, Groop L, Orholm-Melander M, Allione A, Di Gregorio A, Guarrera S, Panico S, Ricceri F, Romanazzi V, Sacerdote C, Vineis P, Barroso I, Sandhu MS, Luben RN, Crawford GJ, Jousilahti P, Perola M, Boehnke M, Bonnycastle LL, Collins FS, Jackson AU, Mohlke KL, Stringham HM, Valle TT, Willer CJ, Bergman RN, Morken MA, Döring A, Gieger C, Illig T, Meitinger T, Org E, Pfeufer A, Wichmann H-E, Kathiresan S, Marrugat J, O'Donnell CJ, Schwartz SM, Siscovick DS, Subirana I, Freimer NB, Hartikainen A-L, McCarthy MI, O'Reilly PF, Peltonen L, Pouta A, de Jong PE, Snieder H, van Gilst WH, Clarke R, Goel A, Hamsten A, Peden JF, Seedorf U, Syvänen A-C, Tognoni G, Lakatta EG, Sanna S, Scheet P, Schlessinger D, Scuteri A, Dörr M, Ernst F, Felix SB, Homuth G, Lorbeer R, Reffelmann T, Rettig R, Völker U, Galan P, Gut IG, Herberg S, Lathrop GM, Zelenika D, Deloukas P, Soranzo N, Williams FM, Zhai G, Salomaa V, Laakso M, Elosua R, Forouhi NG, Völzke H, Uiterwaal CS, van der Schouw YT, Numans ME, Matullo G, Navis G, Berglund G, Bingham SA, Kooner JS, Connell JM, Bandinelli S, Ferrucci L, Watkins H, Spector TD, Tuomilehto J, Altshuler DM, Strachan DP, Laan M, Meneton P, Wareham NJ, Uda M, Jarvelin M-R, Mooser V, Melander O, Loos RJ, Elliott P, Abecasis GR, Caulfield M, Munroe PB. Genome-wide association study identifies eight loci associated with blood pressure. *Nat Genet.* 2009;41(6):666–76.
53. The International Consortium for Blood Pressure Genome-Wide Association Studies. Genetic variants in novel pathways influence blood pressure and cardiovascular disease risk. *Nature.* 2011;478(7367):103–9.
54. Wain LV, Verwoert GC, O'Reilly PF, Shi G, Johnson T, Johnson AD, Bochud M, Rice KM, Henneman P, Smith AV, Ehret GB, Amin N, Larson MG, Mooser V, Hadley D, Dörr M, Bis JC, Aspelund T, Esko T, Janssens ACJW, Zhao JH, Heath S, Laan M, Fu J, Pistis G, Luan J, Arora P, Lucas G, Pirastu N, Pichler I, Jackson AU, Webster RJ, Zhang F, Peden JF, Schmidt H, Tanaka T, Campbell H, Igl W, Milaneschi Y, Hottenga J-J, Vitart V, Chasman DI, Trompet S, Bragg-Gresham JL, Alizadeh BZ, Chambers JC, Guo X, Lehtimäki T, Kühnel B, Lopez LM, Polašek O, Boban M, Nelson CP, Morrison AC, Pihur V, Ganesh SK, Hofman A, Kundu S, Mattace-Raso FUS, Rivadeneira F, Sijbrands EJG, Uitterlinden AG, Hwang S-J, Vasani RS, Wang TJ, Bergmann S, Vollenweider P, Waeber G, Laitinen J, Pouta A, Zitting P, McArdle WL, Kroemer HK, Völker U, Völzke H, Glazer NL, Taylor KD, Harris TB, Alavere H, Haller T, Keis A, Tammesoo M-L, Aulchenko Y, Barroso I, Khaw K-T, Galan P, Herberg S, Lathrop M, Eyheramendy S, Org E, Söber S, Lu X, Nolte IM, Penninx BW, Corre T, Masciullo C, Sala C, Groop L, Voight BF, Melander O, O'Donnell CJ, Salomaa V, d'Adamo AP, Fabretto A, Faletra F, Ulivi S, Del Greco M F, Facheris M, Collins FS, Bergman RN, Beilby JP, Hung J, Musk AW, Mangino M, Shin S-Y, Soranzo N, Watkins H, Goel A, Hamsten A, Gider P, Loitfelder M, Zeginigg M, Hernandez D, Najjar SS, Navarro P, Wild SH, Corsi AM,

- Singleton A, de Geus EJC, Willemsen G, Parker AN, Rose LM, Buckley B, Stott D, Orru M, Uda M, van der Klauw MM, Zhang W, Li X, Scott J, Chen Y-DI, Burke GL, Kähönen M, Viikari J, Döring A, Meitinger T, Davies G, Starr JM, Emilsson V, Plump A, Lindeman JH, Hoen PAC', König IR, Felix JF, Clarke R, Hopewell JC, Ongen H, Breteler M, DeBette S, DeStefano AL, Fornage M, Mitchell GF, Smith NL, Holm H, Stefansson K, Thorleifsson G, Thorsteinsdottir U, Samani NJ, Preuss M, Rudan I, Hayward C, Deary IJ, Wichmann H-E, Raitakari OT, Palmas W, Kooner JS, Stolk RP, Jukema JW, Wright AF, Boomsma DI, Bandinelli S, Gyllensten UB, Wilson JF, Ferrucci L, Schmidt R, Farrall M, Spector TD, Palmer LJ, Tuomilehto J, Pfeufer A, Gasparini P, Siscovick D, Altshuler DM, Loos RJJ, Toniolo D, Snieder H, Gieger C, Meneton P, Wareham NJ, Oostra BA, Metspalu A, Launer L, Rettig R, Strachan DP, Beckmann JS, Witteman JCM, Erdmann J, van Dijk KW, Boerwinkle E, Boehnke M, Ridker PM, Jarvelin M-R, Chakravarti A, Abecasis GR, Gudnason V, Newton-Cheh C, Levy D, Munroe PB, Psaty BM, Caulfield MJ, Rao DC, Tobin MD, Elliott P, van Duijn CM. Genome-wide association study identifies six new loci influencing pulse pressure and mean arterial pressure. *Nat Genet.* 2011;43(10):1005–11.
55. Kato N, Takeuchi F, Tabara Y, Kelly TN, Go MJ, Sim X, Tay WT, Chen C-H, Zhang Y, Yamamoto K, Katsuya T, Yokota M, Kim YJ, Ong RTH, Nabika T, Gu D, Chang L-C, KOKUBO Y, Huang W, Ohnaka K, Yamori Y, Nakashima E, Jaquish CE, Lee J-Y, Seielstad M, Isono M, Hixson JE, Chen Y-T, Miki T, Zhou X, Sugiyama T, Jeon J-P, Liu JJ, Takayanagi R, Kim SS, Aung T, Sung YJ, Zhang X, Wong TY, Han B-G, Kobayashi S, Ogihara T, Zhu D, Iwai N, Wu J-Y, Teo YY, Tai ES, Cho YS, He J. Meta-analysis of genome-wide association studies identifies common variants associated with blood pressure variation in east Asians. *Nat Genet.* 2011;43(6):531–8.
56. Kelly TN, Takeuchi F, Tabara Y, Edwards TL, Kim YJ, Chen P, Li H, Wu Y, Yang CF, Zhang Y, Gu D, Katsuya T, Ohkubo T, Gao YT, Go MJ, Teo YY, Lu L, Lee NR, Chang LC, Peng H, Zhao Q, Nakashima E, Kita Y, Shu XO, Kim NH, Tai ES, Wang Y, Adair LS, Chen CH, Zhang S, Li C, Nabika T, Umemura S, Cai Q, Cho YS, Wong TY, Zhu J, Wu JY, Gao X, Hixson JE, Cai H, Lee J, Cheng CY, Rao DC, Xiang YB, Cho MC, Han BG, Wang A, Tsai FJ, Mohlke K, Lin X, Ikram MK, Lee JY, Zheng W, Tetsuro M, Kato N, He J. Genome-wide association study meta-analysis reveals transethnic replication of mean arterial and pulse pressure loci. *Hypertension.* 2013;62(5):853–9.
57. Franceschini N, Fox E, Zhang Z, Edwards TL, Nalls MA, Sung YJ, Tayo BO, Sun YV, Gottesman O, Adeyemo A, Johnson AD, Young JH, Rice K, Duan Q, Chen F, Li Y, Tang H, Fornage M, Keene KL, Andrews JS, Smith JA, Faul JD, Guangfa Z, Guo W, Liu Y, Murray SS, Musani SK, Srinivasan S, Edwards DRV, Wang H, Becker LC, Bovet P, Bochud M, Broeckel U, Burnier M, Carty C, Chasman DI, Ehret G, Chen W-M, Chen G, Chen W, Ding J, Dreisbach AW, Evans MK, Guo X, Garcia ME, Jensen R, Keller MF, Lettre G, Lotay V, Martin LW, Moore JH, Morrison AC, Mosley TH, Ogunniyi A, Palmas W, Papanicolaou G, Penman A, Polak JF, Ridker PM, Salako B, Singleton AB, Shriner D, Taylor KD, Vasan R, Wiggins K, Williams SM, Yanek LR, Zhao W, Zonderman AB, Becker DM, Berenson G, Boerwinkle E, Bottinger E, Cushman M, Eaton C, Nyberg F, Heiss G, Hirschhorn JN, Howard VJ, Karczewsk KJ, Lanktree MB,

- Liu K, Liu Y, Loos R, Margolis K, Snyder M, Consortium TAGEN, Go MJ, Kim YJ, Lee J-Y, Jeon J-P, Kim SS, Han B-G, Cho YS, Sim X, Tay WT, Ong RTH, Seielstad M, Liu JJ, Aung T, Wong TY, Teo YY, Tai ES, Chen C-H, Chang L-C, Chen Y-T, Wu J-Y, Kelly TN, Gu D, Hixson JE, He J, Tabara Y, KOKUBO Y, Miki T, Iwai N, Kato N, Takeuchi F, Katsuya T, Nabika T, Sugiyama T, Zhang Y, Huang W, Zhang X, Zhou X, Jin L, Zhu D, Psaty BM, Schork NJ, Weir DR, Rotimi CN, Sale MM, Harris T, Kardina SLR, Hunt SC, Arnett D, Redline S, Cooper RS, Risch NJ, Rao DC, Rotter JI, Chakravarti A, Reiner AP, Levy D, Keating BJ, Zhu X. Genome-wide association analysis of blood-pressure traits in African-ancestry individuals reveals common associated genes in African and non-African populations. *Am J Hum Genet.* 2013;93(3):545–54.
58. Ji W, Foo JN, O'Roak BJ, Zhao H, Larson MG, Simon DB, Newton-Cheh C, State MW, Levy D, Lifton RP. Rare independent mutations in renal salt handling genes contribute to blood pressure variation. *Nat Genet.* 2008;40(5):592–9.
59. Morrison AC, Bis JC, Hwang S-J, Ehret GB, Lumley T, Rice K, Muzny D, Gibbs RA, Boerwinkle E, Psaty BM, Chakravarti A, Levy D. Sequence analysis of six blood pressure candidate regions in 4,178 individuals: the Cohorts for Heart and Aging Research in Genomic Epidemiology (CHARGE) targeted sequencing study. *PLoS One.* 2014;9(10):e109155.
60. Yu B, Pulit SL, Hwang S-J, Brody JA, Amin N, Auer PL, Bis JC, Boerwinkle E, Burke GL, Chakravarti A, Correa A, Dreisbach AW, Franco OH, Ehret GB, Franceschini N, Hofman A, Lin D-Y, Metcalf GA, Musani SK, Muzny D, Palmas W, Raffle L, Reiner A, Rice K, Rotter JI, Veeraraghavan N, Fox E, Guo X, North KE, Gibbs RA, van Duijn CM, Psaty BM, Levy D, Newton-Cheh C, Morrison AC, CHARGE Consortium and the National Heart, Lung, and Blood Institute GO ESP. Rare exome sequence variants in *CLCN6* reduce blood pressure levels and hypertension risk. *Circ Cardiovasc Genet.* 2016;9(1):64–70.
61. James PA, Oparil S, Carter BL, Cushman WC, Dennison-Himmelfarb C, Handler J, Lackland DT, LeFevre ML, MacKenzie TD, Ogedegbe O, Smith SC Jr, Svetkey LP, Taler SJ, Townsend RR, Wright JT Jr, Narva AS, Ortiz E. 2014 evidence-based guideline for the management of high blood pressure in adults: report from the panel members appointed to the Eighth Joint National Committee (JNC 8). *JAMA.* 2014;311(5):507–20.
62. Fontana V, Luizon MR, Sandrim VC. An update on the pharmacogenetics of treating hypertension. *J Hum Hypertens.* 2015;29(5):283–91.
63. Hiltunen TP, Donner KM, Sarin AP, Saarela J, Ripatti S, Chapman AB, Gums JG, Gong Y, Cooper-DeHoff RM, Frau F, Glorioso V, Zaninello R, Salvi E, Glorioso N, Boerwinkle E, Turner ST, Johnson JA, Kontula KK. Pharmacogenomics of hypertension: a genome-wide, placebo-controlled cross-over study, using four classes of antihypertensive drugs. *J Am Heart Assoc.* 2015;4(1):e001521.
64. Cabrera CP, Ng FL, Warren HR, Barnes MR, Munroe PB, Caulfield MJ. Exploring

hypertension genome-wide association studies findings and impact on pathophysiology, pathways, and pharmacogenetics. *Wiley Interdiscip Rev Syst Biol Med*. 2015;7(2):73–90.

65. Horowitz JR, Rivard A, van der Zee R, Hariawala M, Sheriff DD, Esakof DD, Chaudhry GM, Symes JF, Isner JM. Vascular endothelial growth factor/vascular permeability factor produces nitric oxide-dependent hypotension. Evidence for a maintenance role in quiescent adult endothelium. *Arterioscler Thromb Vasc Biol*. 1997;17(11):2793–800.
66. Henry TD, Rocha-Singh K, Isner JM, Kereiakes DJ, Giordano FJ, Simons M, Losordo DW, Hendel RC, Bonow RO, Eppler SM, Zioncheck TF, Holmgren EB, McCluskey ER. Intracoronary administration of recombinant human vascular endothelial growth factor to patients with coronary artery disease. *Am Heart J*. 2001;142(5):872–80.
67. Henry TD, Annex BH, McKendall GR, Azrin MA, Lopez JJ, Giordano FJ, Shah PK, Willerson JT, Benza RL, Berman DS, Gibson CM, Bajamonde A, Rundle AC, Fine J, McCluskey ER, VIVA Investigators. The VIVA trial: Vascular endothelial growth factor in Ischemia for Vascular Angiogenesis. *Circulation*. 2003;107(10):1359–65.
68. Su E-N, Cringle SJ, McAllister IL, Yu D-Y. An experimental study of VEGF induced changes in vasoactivity in pig retinal arterioles and the influence of an anti-VEGF agent. *BMC Ophthalmol*. 2012;12:10.
69. Thijs AMJ, van Herpen CML, Sweep FCGJ, Geurts-Moespot A, Smits P, van der Graaf WTA, Rongen GA. Role of endogenous vascular endothelial growth factor in endothelium-dependent vasodilation in humans. *Hypertension*. 2013;61(5):1060–5.
70. Ferrara N, Gerber HP, LeCouter J. The biology of VEGF and its receptors. *Nat Med*. 2003;9(6):669–76.
71. Li B, Ogasawara AK, Yang R, Wei W, He GW, Zioncheck TF, Bunting S, de Vos AM, Jin H. KDR (VEGF receptor 2) is the major mediator for the hypotensive effect of VEGF. *Hypertension*. 2002;39(6):1095–100.
72. Hood JD, Meininger CJ, Ziche M, Granger HJ. VEGF upregulates eNOS message, protein, and NO production in human endothelial cells. *Am J Physiol Heart Circ Physiol*. 1998;274(3 Pt 2):H1054–8.
73. Bouloumié A, Schini-Kerth VB, Busse R. Vascular endothelial growth factor upregulates nitric oxide synthase expression in endothelial cells. *Cardiovasc Res*. 1999;41(3):773–80.
74. Wheeler-Jones C, Abu-Ghazaleh R, Cospedal R, Houliston RA, Martin J, Zachary I. Vascular endothelial growth factor stimulates prostacyclin production and activation of cytosolic phospholipase A2 in endothelial cells via p42/p44 mitogen-

- activated protein kinase. *FEBS Lett.* 1997;420(1):28–32.
75. Neagoe P-E, Lemieux C, Sirois MG. Vascular endothelial growth factor (VEGF)-A165-induced prostacyclin synthesis requires the activation of VEGF receptor-1 and -2 heterodimer. *J Biol Chem.* 2005;280(11):9904–12.
 76. Robinson ES, Khankin EV, Karumanchi SA, Humphreys BD. Hypertension induced by vascular endothelial growth factor signaling pathway inhibition: mechanisms and potential use as a biomarker. *Semin Nephrol.* 2010;30(6):591–601.
 77. Lee S, Chen TT, Barber CL, Jordan MC, Murdock J, Desai S, Ferrara N, Nagy A, Roos KP, Iruela-Arispe ML. Autocrine VEGF signaling is required for vascular homeostasis. *Cell.* 2007;130(4):691–703.
 78. Wang Y, Fei D, Vanderlaan M, Song A. Biological activity of bevacizumab, a humanized anti-VEGF antibody in vitro. *Angiogenesis.* 2004;7(4):335–45.
 79. Facemire CS, Nixon AB, Griffiths R, Hurwitz H, Coffman TM. Vascular endothelial growth factor receptor 2 controls blood pressure by regulating nitric oxide synthase expression. *Hypertension.* 2009;54(3):652–8.
 80. Lankhorst S, Kappers MHW, van Esch JHM, Danser AHJ, van den Meiracker AH. Hypertension during vascular endothelial growth factor inhibition: focus on nitric oxide, endothelin-1, and oxidative stress. *Antioxid Redox Signal.* 2014;20(1):135–45.
 81. Vignon-Zellweger N, Heiden S, Miyauchi T, Emoto N. Endothelin and endothelin receptors in the renal and cardiovascular systems. *Life Sci.* 2012;91(13-14):490–500.
 82. Liu S, Premont RT, Kontos CD, Huang J, Rockey DC. Endothelin-1 activates endothelial cell nitric-oxide synthase via heterotrimeric G-protein betagamma subunit signaling to protein kinase B/Akt. *J Biol Chem.* 2003;278(50):49929–35.
 83. Lankhorst S, Kappers MHW, van Esch JHM, Danser AHJ, van den Meiracker AH. Mechanism of hypertension and proteinuria during angiogenesis inhibition: evolving role of endothelin-1. *J Hypertens.* 2013;31(3):444–54.
 84. Kappers MHW, van Esch JHM, Sluiter W, Sleijfer S, Danser AHJ, van den Meiracker AH. Hypertension induced by the tyrosine kinase inhibitor sunitinib is associated with increased circulating endothelin-1 levels. *Hypertension.* 2010;56(4):675–81.
 85. Kappers MHW, de Beer VJ, Zhou Z, Danser AHJ, Sleijfer S, Duncker DJ, van den Meiracker AH, Merkus D. Sunitinib-induced systemic vasoconstriction in swine is endothelin mediated and does not involve nitric oxide or oxidative stress. *Hypertension.* 2012;59(1):151–7.

86. Baffert F, Le T, Sennino B, Thurston G, Kuo CJ, Hu-Lowe D, McDonald DM. Cellular changes in normal blood capillaries undergoing regression after inhibition of VEGF signaling. *Am J Physiol Heart Circ Physiol*. 2006;290(2):H547–59.
87. Kamba T, Tam BYY, Hashizume H, Haskell A, Sennino B, Mancuso MR, Norberg SM, O'Brien SM, Davis RB, Gowen LC, Anderson KD, Thurston G, Joho S, Springer ML, Kuo CJ, McDonald DM. VEGF-dependent plasticity of fenestrated capillaries in the normal adult microvasculature. *Am J Physiol Heart Circ Physiol*. 2006;290(2):H560–76.
88. Gerber HP, McMurtrey A, Kowalski J, Yan M, Keyt BA, Dixit V, Ferrara N. Vascular endothelial growth factor regulates endothelial cell survival through the phosphatidylinositol 3'-kinase/Akt signal transduction pathway: requirement for Flk-1/KDR activation. *J Biol Chem*. 1998;273(46):30336–43.
89. Mourad JJ, des Guetz G, Debbabi H, Levy BI. Blood pressure rise following angiogenesis inhibition by bevacizumab: a crucial role for microcirculation. *Ann Oncol*. 2008;19(5):927–34.
90. Safar ME, Levy BI, Struijker-Boudier H. Current perspectives on arterial stiffness and pulse pressure in hypertension and cardiovascular diseases. *Circulation*. 2003;107(22):2864–9.
91. Veronese ML, Mosenkis A, Flaherty KT, Gallagher M, Stevenson JP, Townsend RR, O'Dwyer PJ. Mechanisms of hypertension associated with BAY 43-9006. *J Clin Oncol*. 2006;24(9):1363–9.
92. Case J, Ingram DA, Haneline LS. Oxidative stress impairs endothelial progenitor cell function. *Antioxid Redox Signal*. 2008;10(11):1895–907.
93. Schulz E, Jansen T, Wenzel P, Daiber A, Münzel T. Nitric oxide, tetrahydrobiopterin, oxidative stress, and endothelial dysfunction in hypertension. *Antioxid Redox Signal*. 2008;10(6):1115–26.
94. Coultas L, Chawengsaksophak K, Rossant J. Endothelial cells and VEGF in vascular development. *Nature*. 2005;438(7070):937–45.
95. Eremina V, Jefferson JA, Kowalewska J, Hochster H, Haas M, Weisstuch J, Richardson C, Kopp JB, Kabir MG, Backx PH, Gerber HP, Ferrara N, Barisoni L, Alpers CE, Quaggin SE. VEGF inhibition and renal thrombotic microangiopathy. *N Engl J Med*. 2008;358(11):1129–36.
96. Zou A-P, Cowley AW. Role of nitric oxide in the control of renal function and salt sensitivity. *Curr Hypertens Rep*. 1999;1(2):178–86.
97. Gu J-W, Manning RD, Young E, Shparago M, Sartin B, Bailey AP. Vascular endothelial growth factor receptor inhibitor enhances dietary salt-induced hypertension in

- Sprague-Dawley rats. *Am J Physiol Regul Integr Comp Physiol*. 2009;297(1):R142–8.
98. Lu J-F, Bruno R, Eppler S, Novotny W, Lum B, Gaudreault J. Clinical pharmacokinetics of bevacizumab in patients with solid tumors. *Cancer Chemother Pharmacol*. 2008;62(5):779–86.
 99. Kazazi-Hyseni F, Beijnen JH, Schellens JHM. Bevacizumab. *Oncologist*. 2010;15(8):819–25.
 100. Panoilia E, Schindler E, Samantas E, Aravantinos G, Kalofonos HP, Christodoulou C, Patrinos GP, Friberg LE, Sivolapenko G. A pharmacokinetic binding model for bevacizumab and VEGF165 in colorectal cancer patients. *Cancer Chemother Pharmacol*. 2015;75(4):791–803.
 101. Schneider BP, Wang M, Radovich M, Sledge GW, Badve S, Thor A, Flockhart DA, Hancock B, Davidson N, Gralow J, Dickler M, Perez EA, Cobleigh M, Shenkier T, Edgerton S, Miller KD, ECOG 2100. Association of vascular endothelial growth factor and vascular endothelial growth factor receptor-2 genetic polymorphisms with outcome in a trial of paclitaxel compared with paclitaxel plus bevacizumab in advanced breast cancer: ECOG 2100. *J Clin Oncol*. 2008;26(28):4672–8.
 102. Renner W, Kotschan S, Hoffmann C, Obermayer-Pietsch B, Pilger E. A common 936 C/T mutation in the gene for vascular endothelial growth factor is associated with vascular endothelial growth factor plasma levels. *J Vasc Res*. 2000;37(6):443–8.
 103. Awata T, Inoue K, Kurihara S, Ohkubo T, Watanabe M, Inukai K, Inoue I, Katayama S. A common polymorphism in the 5'-untranslated region of the VEGF gene is associated with diabetic retinopathy in type 2 diabetes. *Diabetes*. 2002;51(5):1635–9.
 104. Koukourakis MI, Papazoglou D, Giatromanolaki A, Bougioukas G, Maltezos E, Siviridis E. VEGF gene sequence variation defines VEGF gene expression status and angiogenic activity in non-small cell lung cancer. *Lung Cancer*. 2004;46(3):293–8.
 105. Abajo A, Rodriguez J, Bitarte N, Zarate R, Boni V, Ponz M, Chopitea A, Bandres E, Garcia-Foncillas J. Dose-finding study and pharmacogenomic analysis of fixed-rate infusion of gemcitabine, irinotecan and bevacizumab in pretreated metastatic colorectal cancer patients. *Br J Cancer*. 2010;103(10):1529–35.
 106. Steffensen KD, Waldstrøm M, Brandslund I, Jakobsen A. The relationship of VEGF polymorphisms with serum VEGF levels and progression-free survival in patients with epithelial ovarian cancer. *Gynecol Oncol*. 2010;117(1):109–16.
 107. Chen MH, Tzeng C-H, Chen P-M, Lin J-K, Lin T-C, Chen W-S, Jiang J-K, Wang H-S, Wang W-S. VEGF -460T → C polymorphism and its association with VEGF expression and outcome to FOLFOX-4 treatment in patients with colorectal

- carcinoma. *Pharmacogenomics J.* 2011;11(3):227–36.
108. Morita S, Uehara K, Nakayama G, Shibata T, Oguri T, Inada-Inoue M, Shimokata T, Sugishita M, Mitsuma A, Ando Y. Association between bevacizumab-related hypertension and vascular endothelial growth factor (VEGF) gene polymorphisms in Japanese patients with metastatic colorectal cancer. *Cancer Chemother Pharmacol.* 2013;71(2):405–11.
 109. Fuh G, Li B, Crowley C, Cunningham B, Wells JA. Requirements for binding and signaling of the kinase domain receptor for vascular endothelial growth factor. *J Biol Chem.* 1998;273(18):11197–204.
 110. Wang Y, Zheng Y, Zhang W, Yu H, Lou K, Zhang Y, Qin Q, Zhao B, Yang Y, Hui R. Polymorphisms of KDR gene are associated with coronary heart disease. *J Am Coll Cardiol.* 2007;50(8):760–7.
 111. Tao Q, Backer MV, Backer JM, Terman BI. Kinase insert domain receptor (KDR) extracellular immunoglobulin-like domains 4-7 contain structural features that block receptor dimerization and vascular endothelial growth factor-induced signaling. *J Biol Chem.* 2001;276(24):21916–23.
 112. Jain L, Sissung TM, Danesi R, Kohn EC, Dahut WL, Kummar S, Venzon D, Liewehr D, English BC, Baum CE, Yarchoan R, Giaccone G, Venitz J, Price DK, Figg WD. Hypertension and hand-foot skin reactions related to VEGFR2 genotype and improved clinical outcome following bevacizumab and sorafenib. *J Exp Clin Cancer Res.* 2010;29:95.
 113. Etienne-Grimaldi MC, Formento P, Degeorges A, Pierga JY, Delva R, Pivot X, Dalenc F, Espié M, Veyret C, Formento JL, Francoual M, Piutti M, de Crémoux P, Milano G. Prospective analysis of the impact of VEGF-A gene polymorphisms on the pharmacodynamics of bevacizumab-based therapy in metastatic breast cancer patients. *Br J Clin Pharmacol.* 2011;71(6):921–8.
 114. Sibertin-Blanc C, Mancini J, Fabre A, Lagarde A, Del Grande J, Levy N, Seitz JF, Olschwang S, Dahan L. Vascular Endothelial Growth Factor A c.*237C>T polymorphism is associated with bevacizumab efficacy and related hypertension in metastatic colorectal cancer. *Dig Liver Dis.* 2015;47(4):331–7.
 115. Gampenrieder SP, Hufnagl C, Brechelmacher S, Huemer F, Hackl H, Rinnerthaler G, Romeder F, Monzo Fuentes C, Morre P, Hauser-Kronberger C, Mlineritsch B, Greil R. Endothelin-1 genetic polymorphism as predictive marker for bevacizumab in metastatic breast cancer. *Pharmacogenomics J.* 2016. doi:10.1038/tpj.2016.25 [Epub ahead of print]
 116. Lambrechts D, Moisse M, Delmar P, Miles DW, Leigh N, Escudier B, Van Cutsem E, Bansal AT, Carmeliet P, Scherer SJ, de Haas S, Pallaud C. Genetic markers of bevacizumab-induced hypertension. *Angiogenesis.* 2014;17(3):685–94.

117. Schneider BP, Li L, Shen F, Miller KD, Radovich M, O'Neill A, Gray RJ, Lane D, Flockhart DA, Jiang G, Wang Z, Lai D, Koller D, Pratt JH, Dang CT, Northfelt D, Perez EA, Shenkier T, Cobleigh M, Smith ML, Railey E, Partridge A, Gralow J, Sparano J, Davidson NE, Foroud T, Sledge GW. Genetic variant predicts bevacizumab-induced hypertension in ECOG-5103 and ECOG-2100. *Br J Cancer*. 2014;111(6):1241–8.
118. Kim JJ, Vaziri SAJ, Rini BI, Elson P, Garcia JA, Wirka R, Dreicer R, Ganapathi MK, Ganapathi R. Association of VEGF and VEGFR2 single nucleotide polymorphisms with hypertension and clinical outcome in metastatic clear cell renal cell carcinoma patients treated with sunitinib. *Cancer*. 2012;118(7):1946–54.
119. van Erp NP, Eechoute K, van der Veldt AA, Haanen JB, Reyners AKL, Mathijssen RHJ, Boven E, van der Straaten T, Baak-Pablo RF, Wessels JAM, Guchelaar H-J, Gelderblom H. Pharmacogenetic pathway analysis for determination of sunitinib-induced toxicity. *J Clin Oncol*. 2009;27(26):4406–12.
120. Eechoute K, van der Veldt AAM, Oosting S, Kappers MHW, Wessels JAM, Gelderblom H, Guchelaar H-J, Reyners AKL, van Herpen CML, Haanen JB, Mathijssen RHJ, Boven E. Polymorphisms in endothelial nitric oxide synthase (eNOS) and vascular endothelial growth factor (VEGF) predict sunitinib-induced hypertension. *Clin Pharmacol Ther*. 2012;92(4):503–10.
121. Garcia-Donas J, Esteban E, Leandro-García LJ, Castellano DE, del Alba AG, Climent MA, Arranz JA, Gallardo E, Puente J, Bellmunt J, Mellado B, Martínez E, Moreno F, Font A, Robledo M, Rodríguez-Antona C. Single nucleotide polymorphism associations with response and toxic effects in patients with advanced renal-cell carcinoma treated with first-line sunitinib: a multicentre, observational, prospective study. *Lancet Oncol*. 2011;12(12):1143–50.
122. Semeniuk-Wojtaś A, Lubas A, Stec R, Szczylik C, Niemczyk S. Influence of tyrosine kinase inhibitors on hypertension and nephrotoxicity in metastatic renal cell cancer patients. *Int J Mol Sci*. 2016;17(12):2073.
123. Diekstra MHM, Swen JJ, Gelderblom H, Guchelaar H-J. A decade of pharmacogenomics research on tyrosine kinase inhibitors in metastatic renal cell cancer: a systematic review. *Expert Rev Mol Diagn*. 2016;16(5):605–18.
124. Jain L, Vargo CA, Danesi R, Sissung TM, Price DK, Venzon D, Venitz J, Figg WD. The role of vascular endothelial growth factor SNPs as predictive and prognostic markers for major solid tumors. *Mol Cancer Ther*. 2009;8(9):2496–508.
125. de Haas S, Delmar P, Bansal AT, Moisse M, Miles DW, Leighl N, Escudier B, Van Cutsem E, Carmeliet P, Scherer SJ, Pallaud C, Lambrechts D. Genetic variability of VEGF pathway genes in six randomized phase III trials assessing the addition of bevacizumab to standard therapy. *Angiogenesis*. 2014;17(4):909–20.
126. Lambrechts D, Lenz H-J, de Haas S, Carmeliet P, Scherer SJ. Markers of response for

- the antiangiogenic agent bevacizumab. *J Clin Oncol*. 2013;31(9):1219–30.
127. Eng L, Azad AK, Habbous S, Pang V, Xu W, Maitland-van der Zee AH, Savas S, Mackay HJ, Amir E, Liu G. Vascular endothelial growth factor pathway polymorphisms as prognostic and pharmacogenetic factors in cancer: a systematic review and meta-analysis. *Clin Cancer Res*. 2012;18(17):4526–37.
 128. Maitland ML, Moshier K, Imperial J, Kasza KE, Karrison T, Elliott W, Undevia SD, Stadler W, Desai AA, Ratain MJ. Blood pressure (BP) as a biomarker for sorafenib (S), an inhibitor of the vascular endothelial growth factor (VEGF) signaling pathway. *J Clin Oncol (Meeting Abstracts)*. 2006;24:2035.
 129. Jubb AM, Harris AL. Biomarkers to predict the clinical efficacy of bevacizumab in cancer. *Lancet Oncol*. 2010;11(12):1172–83.
 130. Mangoni AA, Woodman RJ, Kichenadasse G, Rowland A, Sorich MJ. Anti-VEGF-induced hypertension and cancer outcomes: translating research into clinical practice. *Expert Rev Precis Med Drug Dev*. 2016;1(2):125–7.
 131. Chen C, Sun P, Ye S, Weng HW, Dai QS. Hypertension as a predictive biomarker for efficacy of bevacizumab treatment in metastatic colorectal cancer: a meta-analysis. *J BUON*. 2014;19(4):917–24.
 132. Cai J, Ma H, Huang F, Zhu D, Bi J, Ke Y, Zhang T. Correlation of bevacizumab-induced hypertension and outcomes of metastatic colorectal cancer patients treated with bevacizumab: a systematic review and meta-analysis. *World J Surg Oncol*. 2013;11:306.
 133. Dewdney A, Cunningham D, Barbachano Y, Chau I. Correlation of bevacizumab-induced hypertension and outcome in the BOXER study, a phase II study of capecitabine, oxaliplatin (CAPOX) plus bevacizumab as peri-operative treatment in 45 patients with poor-risk colorectal liver-only metastases unsuitable for upfront resection. *Br J Cancer*. 2012;106(11):1718–21.

Chapter 2: Identification of Genomic Regions Associated with Bevacizumab-Induced Hypertension by Exome Sequencing

2.1 Abstract

Bevacizumab is a vascular endothelial growth factor-specific angiogenesis inhibitor indicated as an adjunct to chemotherapy for the treatment of several types of cancer. Hypertension (HTN) is commonly observed during bevacizumab treatment, and high-grade toxicity can limit therapy or lead to other cardiovascular complications. The factors that contribute to interindividual variability in blood pressure response to bevacizumab treatment are not well understood. To identify genomic regions associated with bevacizumab-induced HTN risk, sequencing of whole-exome and candidate gene regulatory regions was performed on 61 bevacizumab-treated colorectal cancer patients (19 cases who developed early-onset grade 3 HTN and 42 controls who had no reported HTN in the first six cycles of treatment). SNP-based tests for common variant associations and gene-based tests for rare variant associations were performed in 174 candidate genes. Additional subsets of variants were analyzed by exploratory approaches utilizing functional predictions and several rare variant association methods. Four variants in independent linkage disequilibrium blocks between *SLC29A1* and *HSP90AB1* showed substantial differences in allele frequency between cases and controls. Validation in larger bevacizumab-treated cohorts demonstrated association between one of these variants (rs9381299) with early grade 3+ HTN or with systolic blood pressure > 180 mmHg. These SNP regions are enriched for regulatory elements in vascular endothelial cells that may potentially increase gene expression. Although this study was not powered to detect

significant exome-wide associations, these results suggest that the genomic region between *SLC29A1* and *HSP90AB1* may be a key target for further investigation into the pathogenesis of bevacizumab-induced HTN.

2.2 Introduction

Bevacizumab is a recombinant humanized monoclonal antibody that targets human vascular endothelial growth factor-A (VEGF), preventing its binding to VEGF receptor 2 (VEGFR2)¹. The development of hypertension (HTN) is frequently observed^{2,3} during treatment with bevacizumab and may lead to serious cardiovascular complications. Upon blood pressure elevation, bevacizumab is either held temporarily or discontinued⁴, thereby limiting therapy that may otherwise be beneficial. There are currently no validated biomarkers to predict bevacizumab toxicity, and the factors that contribute to interindividual variability in blood pressure response to bevacizumab treatment are not well understood.

Prior studies have evaluated and identified associations between HTN incidence during bevacizumab treatment and common candidate single nucleotide polymorphisms (SNPs) in genes encoding VEGF (*VEGFA*)⁵⁻⁹ and VEGFR2 (*KDR*)¹⁰; however, the directions of effect for several of these findings are discordant. More recent studies utilizing expanded candidate gene and genome-wide strategies have identified a risk variant in *SV2C*¹¹ and modest associations in *EGLN3*, *EGF*, and *WNK1*¹². Given the heritable but complex nature of primary HTN, the genetic architecture underlying bevacizumab-induced HTN is also likely to be polygenic. Additional examination of genetic variation in non-VEGF pathways and of

rare variants with potentially large phenotypic effects may identify novel mechanisms contributing to bevacizumab-induced HTN.

The development of next generation sequencing methods permits direct interrogation of variants, including rare variants, which are not captured on genotyping arrays. Although whole genome data still presents bioinformatic challenges, restriction of sequencing to the protein-coding exome and regulatory regions reduces the bioinformatic complexity and focuses on variants that are most likely to be functional. Exome sequencing has been used to identify genetic associations in complex phenotypes including cholesterol levels¹³, myocardial infarction¹⁴, and schizophrenia¹⁵. Use of exome sequencing in pharmacogenetic traits has been recently reported for warfarin response¹⁶, clopidogrel response¹⁷, drug-induced long QT interval syndrome¹⁸, and gemcitabine/carboplatin-induced myelosuppression¹⁹. Therefore, this approach may also identify novel and rare variants in genes contributing to bevacizumab-induced HTN.

In this study, whole exomes and candidate gene regulatory regions were sequenced in bevacizumab-treated subjects with the objective of identifying genes harboring multiple variants associated with severe, early-onset bevacizumab-induced HTN. *In silico* functional analyses provide evidence for the potential involvement of the most significant genomic region in this dose-limiting toxicity.

2.3 Materials and Methods

2.3.1 Patient population

The patient cohort for this study was selected from the bevacizumab arm of CALGB 80405 (Alliance; NCT 00265850), a phase III trial conducted to determine if the addition of cetuximab to FOLFIRI or FOLFOX chemotherapy prolongs survival compared to FOLFIRI or FOLFOX with bevacizumab in patients with untreated advanced or metastatic colorectal cancer who have K-ras wild type tumors (Figure 2.1). This trial has been previously described in detail^{20,21}. All patients in the current study were also enrolled in a pharmacogenetic companion study (CALGB 60501) embedded within CALGB 80405. Subjects in the bevacizumab arm received 5 mg/kg bevacizumab IV every 2 weeks with FOLFOX or FOLFIRI every 2 weeks; each treatment cycle was 8 weeks. Out of 899 patients accrued into the bevacizumab arm, DNA was available from 581 patients. The protocol was approved by the National Cancer Institute's Adult Central Institutional Review Board and by local institutional review boards, as appropriate. All participants provided written informed consent for pharmacogenetic sample procurement and analysis.

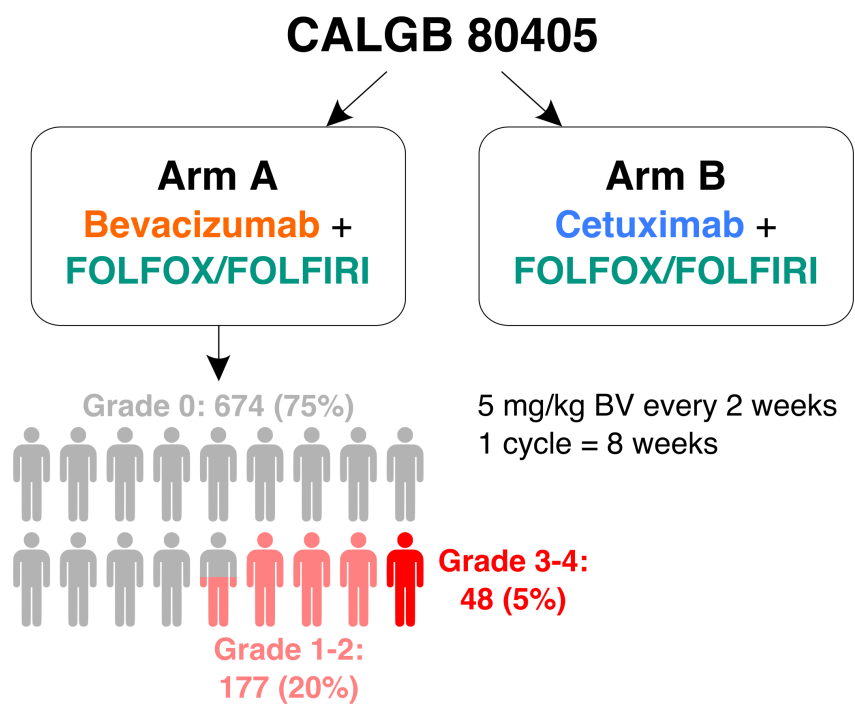


Figure 2.1. CALGB 80405 trial design and hypertension frequency. The current pharmacogenomic analysis utilized samples and toxicity phenotype data from a subset of patients on the bevacizumab (BV) arm of CALGB 80405. Frequencies of grade 0, 1-2, and 3-4 hypertension represent reported events during the first three treatment cycles in the bevacizumab arm.

2.3.2 Bevacizumab-induced hypertension phenotype

Blood pressure was measured prior to the trial, at Day 1 of each treatment cycle, and every two weeks during treatment. Eligibility criteria required that patients with preexisting HTN remain on antihypertensive medications and be normotensive upon study initiation. Serious adverse events, including HTN, were reported during each treatment cycle. The severity of HTN was recorded on a scale of 0–5 according to the National Cancer Institute’s Common Terminology Criteria for Adverse Events version 3²² (Table 2.1). Most grade 3+ HTN developed within the first two treatment cycles (Table 2.2).

Table 2.1. Assessment of hypertension in the National Cancer Institute’s Common Terminology Criteria for Adverse Events version 3

Grade 1	Grade 2	Grade 3	Grade 4	Grade 5
Asymptomatic, transient (<24 hrs) increase by >20 mmHg (diastolic) or to >150/100 if previously WNL ¹ Intervention not indicated	Recurrent or persistent (≥24 hrs) or symptomatic increase by >20 mmHg (diastolic) or to >150/100 if previously WNL ¹ Monotherapy may be indicated	Requiring more than one drug or more intensive therapy than previously	Life-threatening consequences (e.g., hypertensive crisis)	Death

¹WNL: Within normal limits

Table 2.2. Grade 3 hypertension events in the CALGB 80405 bevacizumab arm

Treatment Cycle	N, HTN events ¹	N, potential cases ²	N, sequenced cases ³
1	23	17	12
2	30	14	10
3	15	4	3
4	11		
5	9		
6	8		
7	6		

¹Some patients are represented more than once, having had events in more than one cycle.

²Potential cases with pharmacogenetic consent.

³Subset of potential cases with available DNA.

Cases and controls were selected using an extreme phenotype design to compare severe, early-onset HTN patients to those with no reported HTN (Figure 2.2). Extreme phenotype designs enrich sampling of causal variants with large effect sizes and increase statistical power²³. Such an approach takes advantage of the hypothesis that the genetic loads of variants contributing to drug sensitivity or resistance are expected to be highest at the tails

of the phenotypic distribution. Extreme phenotypes have been used in sequencing studies of similar sized cohorts to identify novel variants associated with *P. aeruginosa* infection²⁴ and the pharmacogenetic traits mentioned above¹⁶⁻¹⁹.

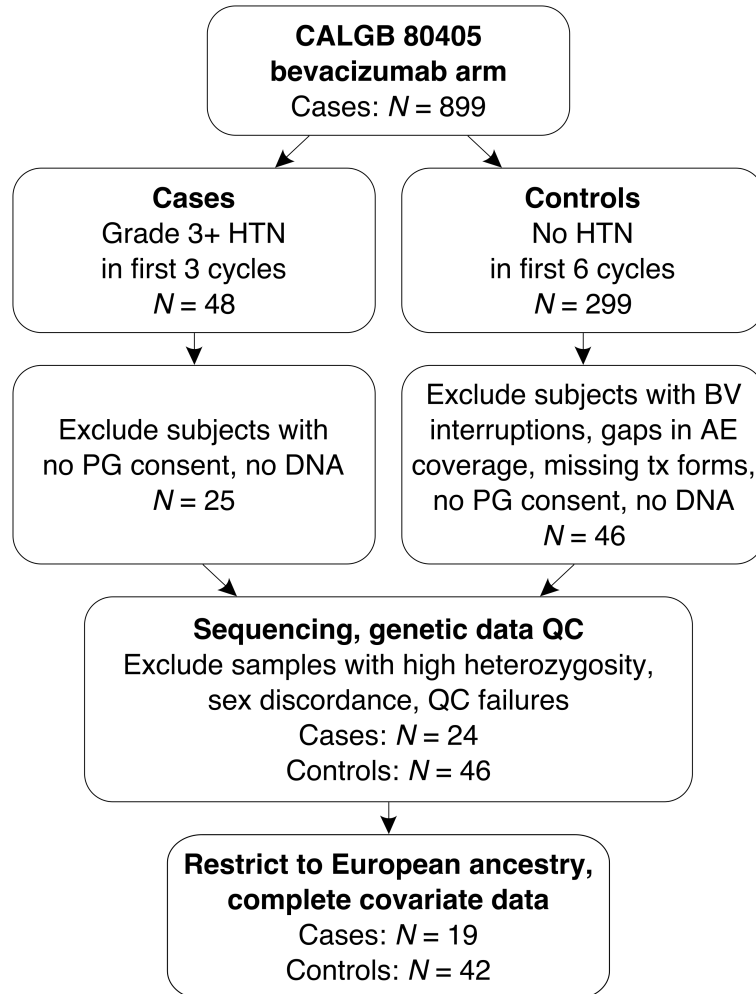


Figure 2.2. Subject selection from bevacizumab-induced hypertension extreme phenotypes in CALGB 80405 for exome sequencing. Abbreviations used: HTN, hypertension; PG, pharmacogenetic; BV, bevacizumab; AE, adverse event; tx, treatment.

Cases were defined as having at least one grade 3 or higher HTN event during the first three treatment cycles. Forty-eight cases were confirmed by extensive chart reviews, with 35 having consented to pharmacogenetic studies and 25 having available DNA. Controls

were defined as having no reported HTN during the first six treatment cycles while completing a minimum of four uninterrupted cycles with no gaps in adverse event form coverage. From 299 subjects who completed at least four treatment cycles, 53 potential controls remained after exclusion for one or more of the following: bevacizumab interruptions ($N = 204$), any grade HTN during the first six cycles ($N = 37$), gaps in AE form coverage ($N = 4$), missing treatment forms ($N = 1$). Forty-six controls had both pharmacogenetic consent and available DNA.

2.3.3 Sequencing

Genomic DNA (1.2 μ g) extracted from blood samples was provided by the Alliance Pathology Coordinating Office, and sequencing was performed by the UCSF Genomics Core Facility. Custom probes were designed to target intronic, UTR, and 50 kb regions upstream and downstream of selected candidate genes (Table 2.3) for a total target size of 85 Mb (64 Mb standard exome + 21 Mb custom regions). Candidate genes were selected based on their documented role in VEGF signaling ($N = 78$), endothelial cell biology ($N = 31$), nitric oxide signaling ($N = 23$), or hypertension ($N = 42$), as defined by Gene Ontology (GO, <http://www.geneontology.org/>) Consortium and KEGG (<http://www.genome.jp/kegg/pathway.html>). Sequencing libraries were constructed using the KAPA Library Preparation Kit (Illumina, San Diego, CA) and captured for enrichment of the target regions using the SeqCap EZ Exome Plus Kit (Roche NimbleGen, Madison, WI). Enriched libraries were sequenced on the HiSeq2500 System (Illumina) using paired-end 100 bp runs. FastQC (<http://www.bioinformatics.babraham.ac.uk/projects/fastqc/>) was used to perform quality control checks on sequencing reads. Samples were required to

meet a minimum of 20X coverage over 80% of the target. A mean of 117 million reads were sequenced for each individual, and a mean target coverage of 65X was achieved for all samples, with 89% of the target reads having $\geq 20X$ coverage. Read quality data are summarized in Table 2.4.

Table 2.3. Analyzed candidate genes

Pathway	Genes
Vascular endothelial growth factor signaling (N = 78)	<i>AKT1, AKT3, ARNT, BAD, CASP9, CAV1, CDC42, EGLN3, EPAS1, FLT1, FLT4, HIF1A, HRAS, HSP90AA1, HSPB1, KDR, KRAS, MAP2K1, MAP2K2, MAPK1, MAPK11, MAPK12, MAPK13, MAPK14, MAPK3, MAPKAPK2, MAPKAPK3, NFATC2, NOS3, NRAS, NRP1, NRP2, PGF, PIK3CA, PIK3CB, PIK3CD, PIK3CG, PIK3R1, PIK3R2, PIK3R3, PIK3R5, PLA2G10, PLA2G12A, PLA2G12B, PLA2G1B, PLA2G2A, PLA2G2D, PLA2G2E, PLA2G2F, PLA2G3, PLA2G4A, PLA2G4B, PLA2G5, PLA2G6, PLCG1, PLCG2, PPP3CA, PPP3CB, PPP3CC, PPP3R1, PPP3R2, PRKCA, PRKCB, PRKCG, PTGS2, PTK2, PXN, RAC1, RAC2, RAF1, SH2D2A, SHC2, SPHK1, SPHK2, SRC, VEGFA, VEGFB, VEGFC</i>
Nitric oxide signaling (N = 23)	<i>ALOX12, APOE, ARG2, CYGB, EGFR, GCH1, GCHFR, HSP90AB1, IL10, INS, KRT1, MT3, NCF1, NCF2, NOS1, NOS1AP, NOS2, NOX5, NQO1, PRKAR1B, SOD1, SOD2, VIMP</i>
Endothelial cell biology (N = 31)	<i>ACE, AGT, AGTR1, ANGPT1, CCL2, CDH5, EDN1, EDN2, EDNRA, FASLG, FGF1, ICAM1, IL11, IL1B, IL6, ITGA5, ITGAV, ITGB3, KLK3, NPPB, NPR1, PDGFRA, PECAM1, PF4, PLA2G4C, PTGIS, RHOB, SERPINE1, TEK, THBS1, TNFAIP3</i>
Hypertension (N = 42)	<i>ACTA2, ADM, ADRA1B, ADRA1D, ADRB1, AVPR1A, AVPR1B, BDKRB2, BMPR2, CACNA1C, CALCA, CHRNA1, CLIC4, CPS1, DRD3, ECE1, EDNRB, EGF, EPHX2, GUCY1A3, GUCY1B3, ITPR1, ITPR2, KCNMA1, KNG1, MYLK, MYLK2, MYLK3, NOSIP, NOSTRIN, P2RX4, PDE3A, PDE3B, PRKG1, PRKG2, PTGIR, PTGS1, REN, S1PR1, SLC7A1, UTS2, WNK1</i>

Table 2.4. Quality of sequencing reads per sample

	Mean	Range
Total reads	117 million	84–277 million
Reads mapped to hg19 reference	117 million (99.4%)	83–276 million (98.7–99.6%)
Library complexity ¹	57%	55–60%
Capture efficiency ²	69%	66–73%
Mean target coverage	65X	50–82X
Target base coverage ≥ 10x	94%	93–95%
Target base coverage ≥ 20x	89%	85–92%
Heterozygous / homozygous ratio	1.1	0.8–1.3 ³

¹Ratio of unique reads versus total reads mapped to target.

²Ratio of reads mapped to target versus reads mapped to reference.

³Excluding outlier sample with het/hom ratio of 1.8.

2.3.4 Read mapping, variant calling, and filtering

Sequencing reads were mapped to the hg19 reference genome using Burrows-Wheeler Aligner²³ (BWA-MEM v0.7.5). BAM files summarizing sequence alignments were refined by local indel realignment and duplicate marking using Picard (<http://broadinstitute.github.io/picard/>) and SAMtools²⁵. Base quality scores were recalibrated using Genome Analysis Toolkit²⁶ (GATK v2.6-5). This procedure trained an adaptive error model using known variant sites from dbSNP 132, HapMap v3.3, the Omni 2.5 chip array from the 1000 Genomes Project, and natural indels identified by Mills *et al*²⁷ to differentiate true variants from machine artifacts.

Variant discovery was performed on all samples with the GATK HaplotypeCaller using the joint calling function and formatted to the variant call format (VCF). Multi-allelic sites were split into single, unique variants, and indels were left-normalized. Variant calls were hard-

filtered for sites of low quality (Phred-scaled quality < 30) and in line with GATK v3.4 Best Practices recommendations^{28,29} (Table 2.5).

Table 2.5. SNPs excluded per GATK Best Practices v3.4 recommendations

	Filtering criteria	N, failed SNPs
Quality	QUAL < 30	0 ¹
	QD < 2.0	9,596
Strand bias	FS > 60.0	2,545
	SOR > 4.0	7,433
Mapping quality	MQ < 40.0	15,470
	MQRankSum < -12.5	11,465
Read position	ReadPosRankSum < -8.0	4,344

¹Already filtered at calling step.

2.3.5 Sample quality control

Individual sequence data were further assessed for call rate, mean read depth, heterozygosity, transition/transversion ratios, nonsynonymous/synonymous ratios, private variant counts, and novel (absent from dbSNP 147) variant counts. A call rate \geq 95% was required, and a value beyond six standard deviations calculated for the cohort was considered an outlier.

The degree of relatedness between individuals was estimated after filtering SNPs with minor allele frequency (MAF) < 0.05 and pruning SNPs in linkage disequilibrium (LD, $r^2 > 0.5$). Kinship data were used to confirm that all individuals were unrelated ($\pi\text{-hat} < 0.125$). X chromosome homozygosity was estimated, and self-reported sex was checked against that inferred from sequence data. Concordance checks between sequencing variants that overlapped with variants previously genotyped on genome-wide SNP arrays were

performed; samples were confirmed to have concordance rates > 90%. Principal component analysis (PCA) was previously performed on these samples using genotyped data, and self-reported race of the samples was compared with ancestry inferred from PCA (Figure 2.3). Results of sample QC are summarized in Table 2.6.

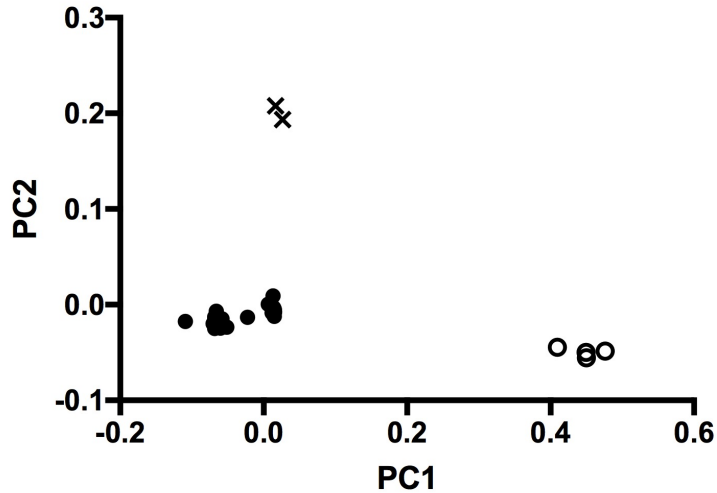


Figure 2.3. First and second principal components in sequenced samples. Principal components were estimated using previously generated genome-wide genotype data. Each symbol represents a sample from the sequenced cohort ($N = 71$). Closed circles indicate self-reported Caucasian subjects; open circles indicate self-reported African American subjects; X indicates self-reported Caucasian subjects removed from analysis.

Table 2.6. Quality control of sample data

	Filtering criteria	N, failed samples
Call rate	< 95%	0
Read depth	Statistical outliers	0
Heterozygosity	Statistical outliers	1 ³
Transition / transversion ratio ¹	Statistical outliers	0
Nonsynonymous / synonymous ratio ²	Statistical outliers	0
Number of private variants	Statistical outliers	0
Number of novel variants	Statistical outliers	0
Relatedness (IBD)	Pi-hat > 0.125	0
Sex	Genetic ≠ Self-reported	1 ³
GWAS concordance	< 90%	1 ³
Ancestry (PCA)	Genetic ≠ Self-reported	2

¹Expected range: 2.1–2.8.

²Expected: Slightly below 1.0.

³The same sample failed heterozygosity, sex concordance, and GWAS concordance.

2.3.6 Variant quality control

SNPs and indels were separated prior to additional quality control steps. Going forward, except where indicated, summarized data pertain only to SNPs. To retain only high quality genotypes, variant sites were excluded from subsequent analyses if they exhibited > 10% missingness, low average quality (QD < 5.0), an outlier distribution of base quality for sites supporting the reference and alternate alleles (BaseQRankSum), or significant deviation from Hardy-Weinberg equilibrium (Table 2.7). SNP quality metrics following QC are summarized in Table 2.8.

Table 2.7. Quality control of variant data

	Filtering criteria	N, failed SNPs
Call rate	< 90%	1,907
Read depth	Statistical outliers	0
Quality by depth	QD < 5.0	3,014
Base quality score distribution	Statistical outliers	15
HWE (MAF \geq 0.05, controls only)	$P < 0.05$ (Bonferroni-adjusted)	1,090

Table 2.8. Post-QC quality per sample

	Mean	Range	Total (across all samples)
Call rate	99.97%	99.94–100%	
Read depth	65X	48–80X	
Heterozygosity	0.01	-0.04–0.19	
Transition / transversion ratio	2.34	2.32–2.36	
Nonsynonymous / synonymous ratio	0.86	0.84–0.88	
All SNPs ¹	87,893	82,900–89,592	327,184
Private SNPs	1,559	1,250–2,832	96,638
Novel SNPs (absent from dbSNP 147)	273	158–653	16,950

¹Non-reference calls only.

VCF files were processed and filtered using VCFtools³⁰, BCFtools (<https://samtools.github.io/bcftools/>), and PLINK 1.9³¹. The final variant list was annotated with RefSeq gene names and functional consequences using ANNOVAR³² (v2016Feb01).

2.3.7 SNP-based association testing

Variants were filtered for MAF \geq 0.10 (threshold chosen based on limited sample size) and LD-pruned at $r^2 > 0.8$ before testing each variant independently for case-control association

using logistic regression under an additive genetic model. Tests were adjusted for sex, age, BMI ≥ 25 , preexisting HTN, and preexisting diabetes, based on published data describing clinical predictors of the toxicity³³. Associations with Bonferroni-adjusted P -values < 0.05 were considered statistically significant. Tests were run using the PLINK/SEQ genetics library (<http://atgu.mgh.harvard.edu/plinkseq/>).

2.3.8 Gene-based association testing

Association testing was conducted at the gene level to evaluate combined effects from multiple rare and low frequency variants (MAF < 0.03) in each gene. Burden tests collapse variants within each gene and compare cases to controls for an excess of rare alleles. Adaptive burden tests operate similarly using data-adaptive weights or thresholds. Burden approaches are powerful when a large proportion of variants have the same directionality and magnitude of effect³⁴.

The Sequence Kernel Association Test (SKAT) is a variance-component test that aggregates associations between variants and the phenotype through a kernel matrix³⁵. In contrast to the burden test, which aggregates variants before performing regression, SKAT models SNP effects linearly then aggregates individual variant-score test statistics across the gene. Hence, SKAT is robust to the heterogeneity of effect sizes within a gene. SKAT-O³⁶ is an extension of SKAT that combines SKAT and the burden test into a single framework and adaptively selects the best linear combination of the two test statistics to maximize power. The CommonRare function in SKAT allows for a combined analysis of rare and common variants.

SKAT-O, implemented using the R statistical environment³⁷, was used as the primary gene-based test in this study. Variants of MAF < 0.03 were aggregated across genes and tested for case-control association. Only genes containing more than one observed variant allele were included. Genes containing variants of all frequencies were tested using the SKAT CommonRare function. Other gene-based tests, including burden and adaptive burden tests, were performed using PLINK/SEQ (Table 2.9). All tests were adjusted for sex, age, BMI \geq 25, preexisting HTN, and preexisting diabetes. Associations with Bonferroni-adjusted *P*-values < 0.05 were considered statistically significant.

Table 2.9. Gene-based rare variant association tests

Test	Description	Directionality	Reference
BURDEN	Excess of rare alleles in cases compared to controls	1-sided	NA
UNIQ	Count of case-unique rare alleles	1-sided	NA
VT	Variable threshold test	1-sided	Price <i>et al</i> (2010) ³⁸
FQRWGT	Frequency-weighted test	1-sided	Madsen and Browning (2009) ³⁹
CALPHA	C-alpha test	2-sided	Neale <i>et al</i> (2011) ⁴⁰
SUMSTAT	Sum of single-site statistics	2-sided	Hoh <i>et al</i> (2001) ⁴¹
SKAT-O	Sequence kernel association test “optimal” method	2-sided	Lee <i>et al</i> (2012) ³⁶
SKAT-CommonRare	Sequence kernel association test for combined effect of common and rare variants	2-sided	Ionita-Laza <i>et al</i> (2013) ⁴²

2.3.9 In silico functional analysis

Functional annotations of variants with the smallest association P -values and their proxies ($r^2 > 0.8$) were summarized in HaploReg⁴³ and RegulomeDB⁴⁴. Predictions of functional impact were obtained from computational algorithms including SIFT⁴⁵, PolyPhen-2⁴⁶, GERP++⁴⁷, and CADD⁴⁸. Variant allele frequencies were compared to those reported in large European population datasets including the 1000 Genomes Project EUR super-population⁴⁹, the NHLBI GO Exome Sequencing Project European-American group⁵⁰, and the Exome Aggregation Consortium (ExAC) Non-Finnish European group⁵¹. Noncoding variants were assessed primarily by overlap with predicted functional elements from RNA-seq, CHIP-seq, and DNase I hypersensitivity peak calls in the ENCODE Project^{52,53} and the Roadmap Epigenomics Project⁵⁴. SNPs were queried against SCAN (<http://www.scandb.org/>), the Genotype-Tissue Expression (GTEx) Project Portal⁵⁵, ExSNP⁵⁶, and PhenoScanner⁵⁷ for previously published expression quantitative trait loci (eQTL) associations. Gene enrichment analyses were performed using ConsensusPathDB⁵⁸ and ToppGene⁵⁹ to detect functional enrichment in curated databases of biochemical pathways, ontology gene sets, disease and drug associations, and other features.

2.3.10 Association of top SNPs in independent cohorts

Top SNP associations were tested for replication in two larger, independent cohorts of bevacizumab-treated patients from clinical trials CALGB 40502⁶⁰ (described in Chapter 4) and CALGB 90401⁶¹. Associations with systolic blood pressure (SBP) > 180 mmHg or grade 3+ HTN for available SNPs were also looked up in the GWAS results of a third independent cohort in the ECOG-5103 trial¹¹. Additional exploratory analyses included associations with

grade 2+ and grade 3+ HTN (in all treatment cycles) and early grade 2+ HTN in the CALGB populations. Here, CALGB 80405 samples not selected for the exome sequencing analysis were also included.

CALGB 40502 is a phase III trial of paclitaxel compared with nab-paclitaxel or ixabepilone with bevacizumab for locally recurrent or metastatic breast cancer. CALGB 90401 is a phase III trial comparing docetaxel and prednisone with or without bevacizumab in men with hormone refractory prostate cancer. ECOG-5103 is a phase III adjuvant breast cancer trial of doxorubicin and cyclophosphamide followed by paclitaxel with or without bevacizumab. Sample sizes used in the analysis of these cohorts are listed in Table 2.10.

CALGB 80405 samples were previously genotyped on the Human OmniExpress and OmniExpressExome arrays (Illumina), and CALGB 90401 samples were genotyped on the Human610-Quad array (Illumina) at the RIKEN Center for Integrative Medical Sciences; rs9381299 genotypes were extracted from these existing GWAS data. Imputed genotypes (generated by the Michigan Imputation Server⁶²) for rs6929249 and rs834576 were also available in CALGB 40502. rs3734704 and rs6902226 (proxy for rs6929249 at a physical distance of 346 bp and $r^2 = 0.98$ in 1000G EUR) were individually genotyped in the CALGB populations at RIKEN. SNPs were tested for case-control association using logistic regression under an additive genetic model. Tests were implemented through R using the glm function. Early HTN was defined as HTN occurring within the number of treatment cycles equaling the same total exposure of bevacizumab (60 mg/kg) in the first three treatment cycles of CALGB 80405. Tests were adjusted for the same covariates as in the

discovery analysis, where available (Table 2.10). Associations with Bonferroni-adjusted P -values $< 0.05/N$ (where N was the number of variants tested or looked up) were considered statistically significant.

Table 2.10. Replication and exploratory cohorts

Study	Covariates	Phenotype ¹	Replication (R) or Exploratory (E)	N^2 , cases	N^2 , controls
CALGB 80405	Preexisting HTN	Early grade 2+ HTN ³	E	70	399
CALGB 40502	Age, BMI \geq 25, preexisting HTN, preexisting diabetes	Early grade 3+ HTN	R	29	386
		Early grade 2+ HTN	E	74	341
		Grade 3+ HTN	E	43	372
		Grade 2+ HTN	E	122	293
CALGB 90401	Age, BMI \geq 25, preexisting diabetes	Early grade 3+ HTN	R	16	600
		Early grade 2+ HTN	E	39	577
		Grade 3+ HTN	E	25	591
		Grade 2+ HTN	E	63	553
ECOG-5103	Age $>$ 50, BMI $>$ 30 (subjects with preexisting HTN excluded)	SBP $>$ 180 mmHg	R	39	391
		Grade 3+ HTN	E	177	387

¹Early HTN: HTN occurring within the number of treatment cycles equaling the same total exposure of bevacizumab (60 mg/kg) in the first three treatment cycles of CALGB 80405.

² N : Genotyped samples from genetic European, bevacizumab-treated patients.

³Samples not analyzed in exome analysis: 51 cases, 356 controls.

2.4 Results

2.4.1 Subject selection and characteristics

Seventy-one samples (25 cases and 46 controls) were selected for sequencing. Following quality control procedures, one sample was excluded due to sample contamination (detected by high heterozygosity, low concordance with GWAS data, and discordant gender). The discovery analysis was limited to genetic Europeans to minimize effects associated with population stratification that may lead to spurious associations; 19 cases and 42 controls with complete sequence, phenotype, and covariate data were retained for analysis. Demographic and clinical characteristics of the analyzed cohort are listed in Table 2.11 and, with the exception of preexisting HTN, are similar between cases and controls.

Table 2.11. Characteristics of extreme phenotype patient subgroups

	Cases (N = 19)	Controls (N = 42)
Female (N, %)	9 (47%)	14 (33%)
Age (mean, range)	61 (32–80)	60 (37–82)
BMI (mean, range)	26.9 (17.7–40.8)	28.4 (18.6–58.4)
Preexisting diabetes (N, %)	3 (16%)	4 (10%)
Preexisting hypertension (N, %)	14 (74%)	12 (29%)

All analyzed subjects (total N = 61) are genetic European.

2.4.2 Description of variant dataset

After processing and quality control of 402,302 called variants, the final variant call-set included 327,184 SNPs and 30,678 indels in 22,998 genes (Table 2.12). Of the SNPs, 46% have MAF < 0.03 in the analysis cohort (Figure 2.4). A total of 72,607 (22%) SNPs were in protein-coding regions, with 53% of those being nonsynonymous, stop-gain, or stop-loss mutations. The remaining noncoding SNPs were annotated to intronic (47%), intergenic

(17%), 5' or 3' UTR (7%), noncoding RNA (5%), upstream or downstream (2%), or splicing (0.1%) regions. A total of 16,950 novel SNPs were identified. Variant functions are summarized in Figure 2.5.

Table 2.12. Summary of variant filtering procedures

Filtering step	SNPs remaining	Indels remaining
Called in GATK	363,180	39,122
Hard-filtered (GATK Best Practices)	332,368	29,657
Multi-allelic sites split	333,034	39,119
Left-normalized	NA	39,119
QC	327,184	(7,542 re-aligned) 30,678

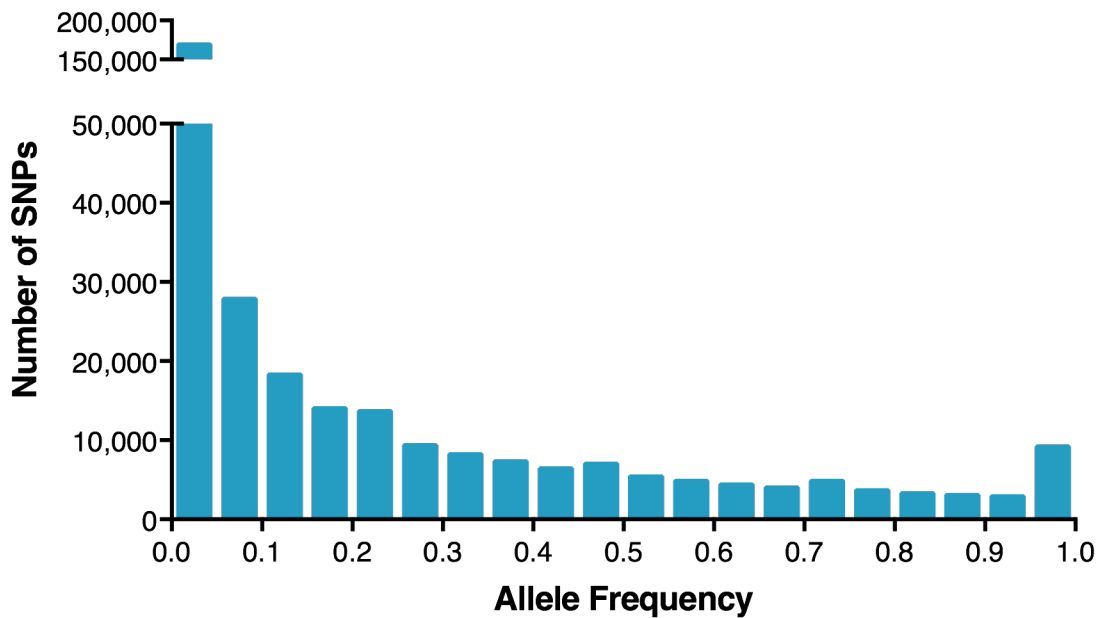


Figure 2.4. Distribution of SNP allele frequency. Of the SNPs passing QC, 151,157 (46%) have MAF < 0.03 in the analysis cohort.

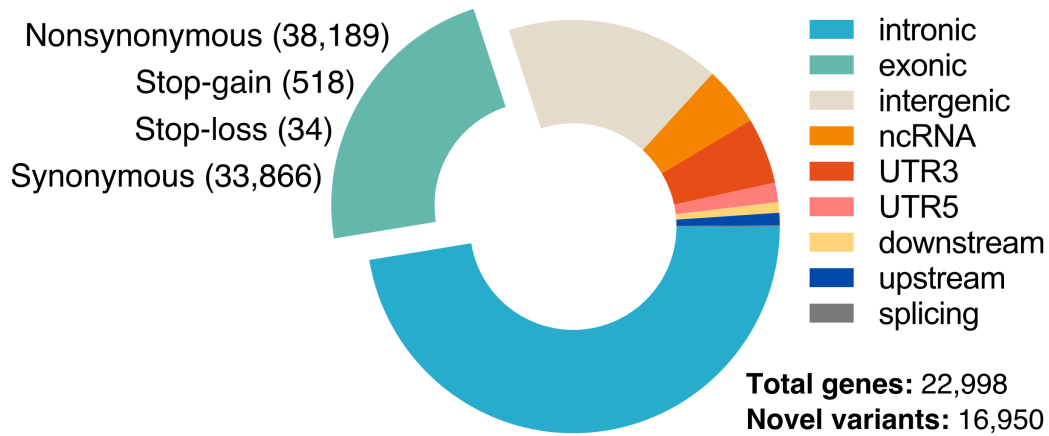


Figure 2.5. SNP functional annotation. SNPs passing QC were annotated based on mapping to hg19 using ANNOVAR. Exonic SNPs were further classified based on their amino acid changes.

2.4.3 Candidate gene analysis

In a targeted analysis of 174 pre-specified candidate genes for which additional intronic, UTR, and flanking regions were sequenced, association testing was performed on 92,886 coding and noncoding variants (Figure 2.6). Genes from pathways of VEGF signaling, nitric oxide (NO) signaling, endothelial cell biology, and HTN risk were included (Table 2.3). Common variants ($MAF \geq 0.10$, $N = 9,356$) were analyzed in SNP-based association tests (Figures 2.7 and 2.8). Since a genetic European population was selected based on genome-wide SNP data, the atypical behavior in the QQ plot (Figure 2.7) most likely reflects the limited power of the small cohort and not population stratification. No SNP met the Bonferroni-corrected significance level ($P = 5.3 \times 10^{-6}$). Within the ten strongest associations (Table 2.13), four SNPs were located in an intergenic region downstream of *SLC29A1* and upstream of *HSP90AB1*: rs6929249 ($P = 1 \times 10^{-4}$, OR 38), rs3734704 ($P = 6 \times 10^{-4}$, OR 29), rs834576 ($P = 0.002$, OR 19), and rs9381299 ($P = 0.004$, OR 8.8). These SNPs span 9.9 kb and are in three separate LD blocks (Figures 2.9 and 2.10). For all four SNPs,

the frequency of early grade 3 HTN in minor allele carriers was consistently higher (58–70%) than in non-carriers (6–24%) (Figure 2.11).

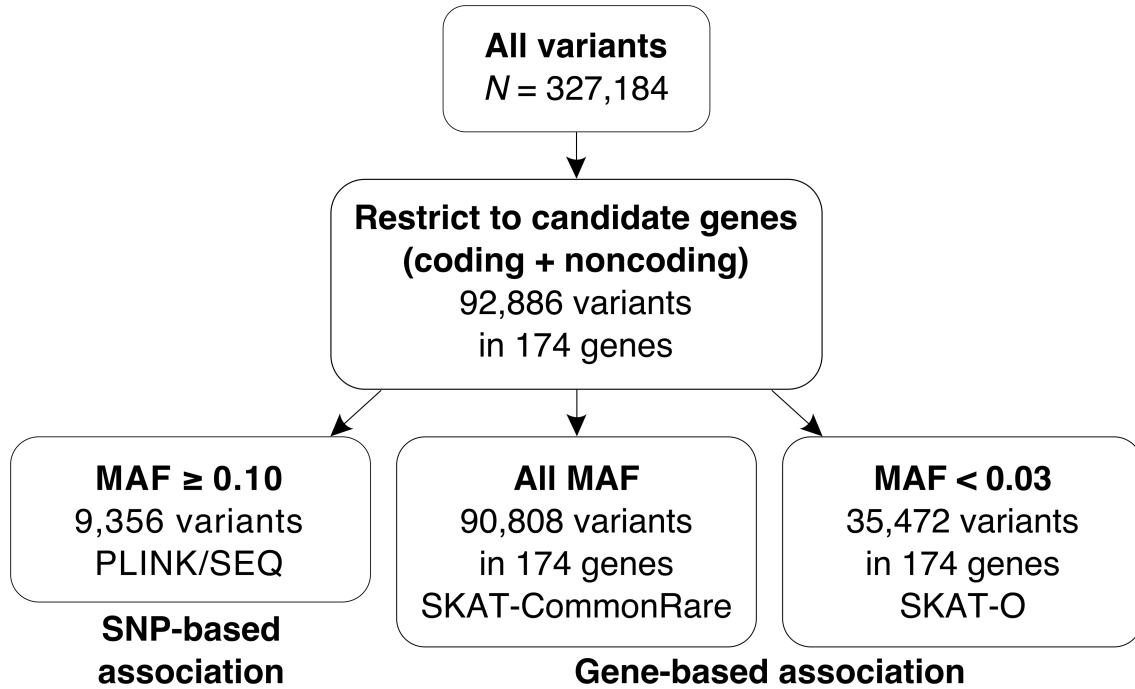


Figure 2.6. Candidate gene analysis workflow. Variants were restricted to candidate gene regions. Common variants were analyzed by SNP-based association tests, and rare and low frequency variants were analyzed by gene-based association tests either alone or combined with common variants.

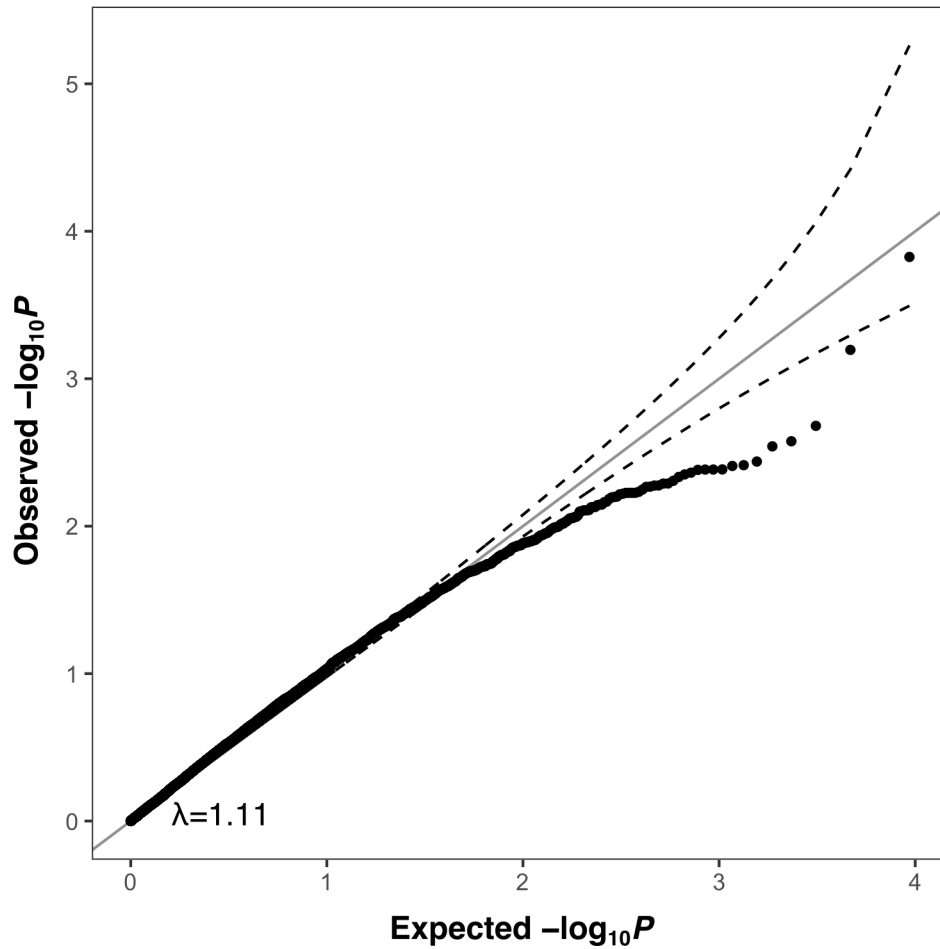


Figure 2.7. Quantile-quantile plot of candidate gene SNP-based analysis. Observed and predicted P -value relationships are plotted for the association with bevacizumab-induced hypertension. The solid line shows the expected distribution assuming no inflation of statistics and the dashed lines show the 95% confidence intervals for the expected distribution. The genomic inflation factor is noted on the graph.

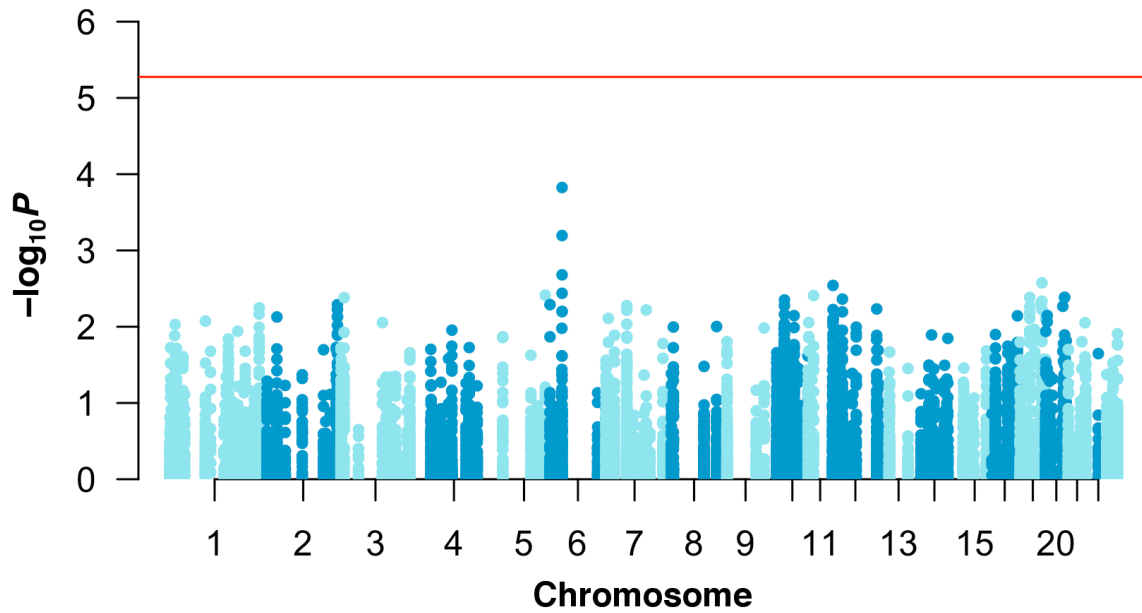


Figure 2.8. Manhattan plot of candidate gene SNP-based analysis. The distribution of $-\log_{10}$ transformed unadjusted P -values for the association with bevacizumab-induced hypertension is plotted as a function of the chromosomal location of all tested SNPs ($N = 9,356$). No SNPs surpassed the Bonferroni-corrected significance threshold of $P = 5.3 \times 10^{-6}$.

Table 2.13. Top SNP associations of candidate gene analysis

SNP (ref/var)	Case genotype counts ¹	Control genotype counts ¹	Case MAF	Control MAF	OR (95% CI)	P ²	Candidate Gene ³	Function
rs6929249 (A/G)	5/13/1	36/6/0	0.39	0.07	37.8 (5.8–247)	1 x 10 ⁻⁴	HSP90AB1	upstream
rs3734704 (A/C)	2/14/3	31/10/1	0.53	0.14	28.9 (4.2–199)	6 x 10 ⁻⁴	HSP90AB1	upstream
rs834576 (C/A)	12/6/1	37/5/0	0.21	0.06	19.3 (2.9–127)	0.002	HSP90AB1	upstream
rs59189065 (G/A)	7/11/1	35/7/0	0.34	0.08	9.9 (2.2–44.3)	0.003	PRKCA	intronic
rs2470417 (C/T)	6/12/1	33/9/0	0.37	0.10	12.7 (2.4–67.5)	0.003	CACNA1C	upstream
rs9381299 (T/C)	9/8/2	35/7/0	0.32	0.08	8.8 (2.0–37.8)	0.004	HSP90AB1	upstream
rs11651806 (C/G)	13/6/0	11/27/4	0.16	0.41	0.1 (0.0–0.5)	0.004	CCL2	upstream
rs72869749 (C/T)	9/9/1	35/7/0	0.29	0.08	26.1 (2.8–239)	0.004	PDE3B	intronic
rs142385484 (C/T)	12/7/0	38/3/1	0.18	0.06	13.9 (2.3–84.2)	0.004	NOS1P	downstream
rs11739214 (G/C)	10/6/3	33/9/0	0.32	0.10	10.1 (2.1–48.9)	0.004	FLT4	downstream

¹Genotype counts: Homozygous reference / heterozygous / homozygous variant.

²Unadjusted P-value from logistic regression under an additive genetic model and adjusted for sex, age, BMI ≥ 25, preexisting hypertension, and preexisting diabetes.

³Represents candidate gene ± 50 kb flanking region containing the sequenced variant. In some cases, this may not be the nearest gene to the variant.

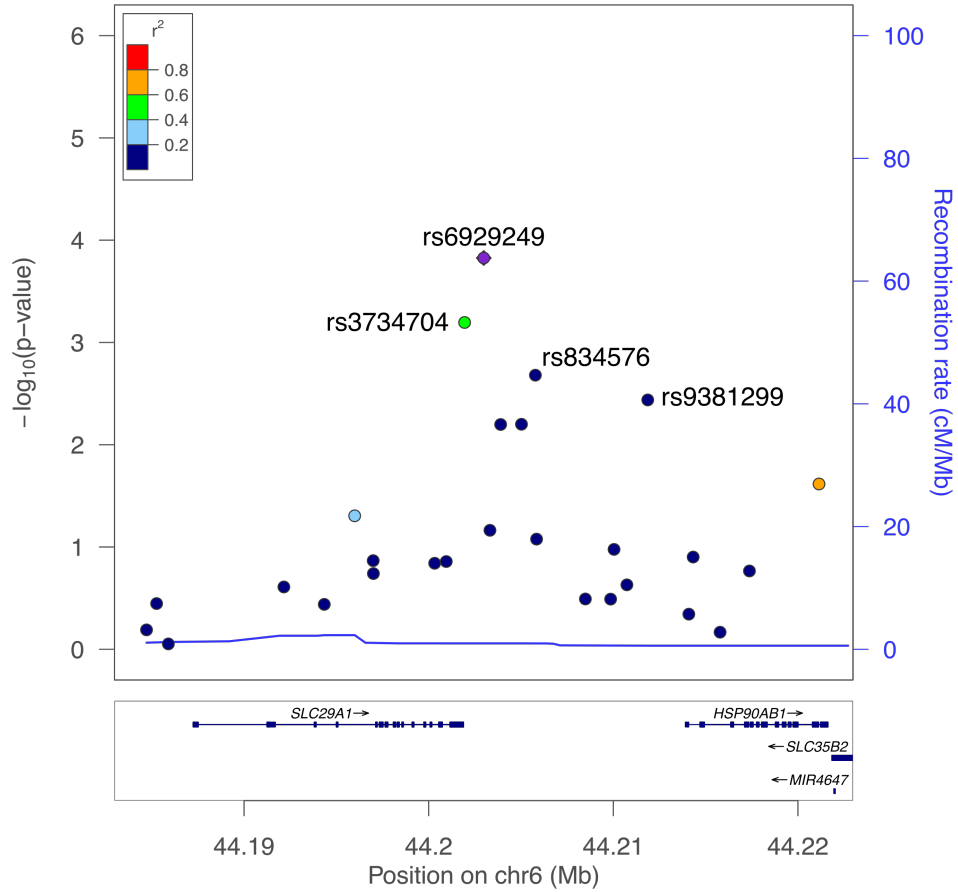


Figure 2.9. Associations with bevacizumab-induced hypertension in the *SLC29A1*-*HSP90AB1* region. Associations with bevacizumab-induced hypertension for analyzed SNPs are shown on a $-\log_{10}P$ scale. Dot color indicates the strength of linkage disequilibrium (r^2) between rs6929249 and each SNP. Plot was produced using LocusZoom (<http://locuszoom.sph.umich.edu/>).

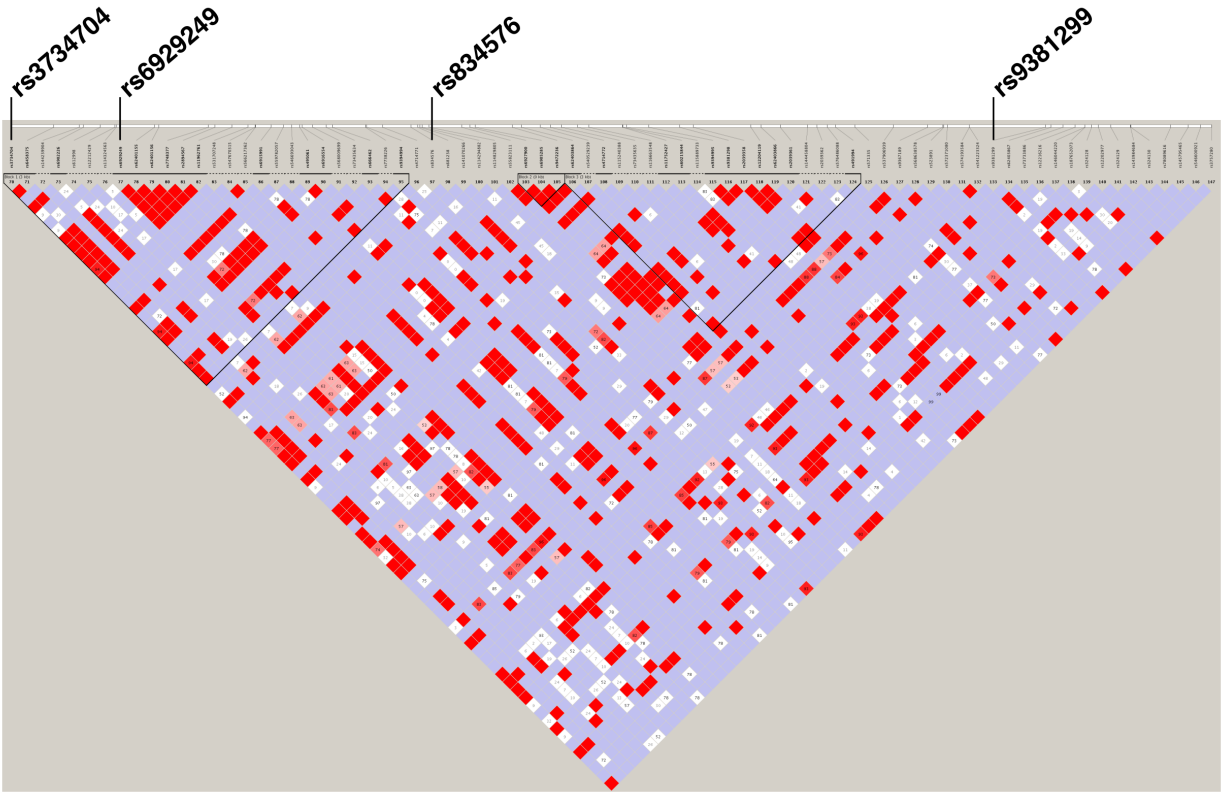


Figure 2.10. Linkage disequilibrium plot of *SLC29A1-HSP90AB1* intergenic region. Linkage disequilibrium (LD) structure of SNPs from the 1000 Genomes CEU population, with top exome analysis SNPs marked. Red: $D' = 1$, $\text{LOD} \geq 2$; blue: $D' = 1$, $\text{LOD} < 2$; pink: $D' < 1$, $\text{LOD} \geq 2$; white: $D' < 1$, $\text{LOD} < 2$. Plot was produced using Haploview (<https://www.broadinstitute.org/haploview/haploview>).

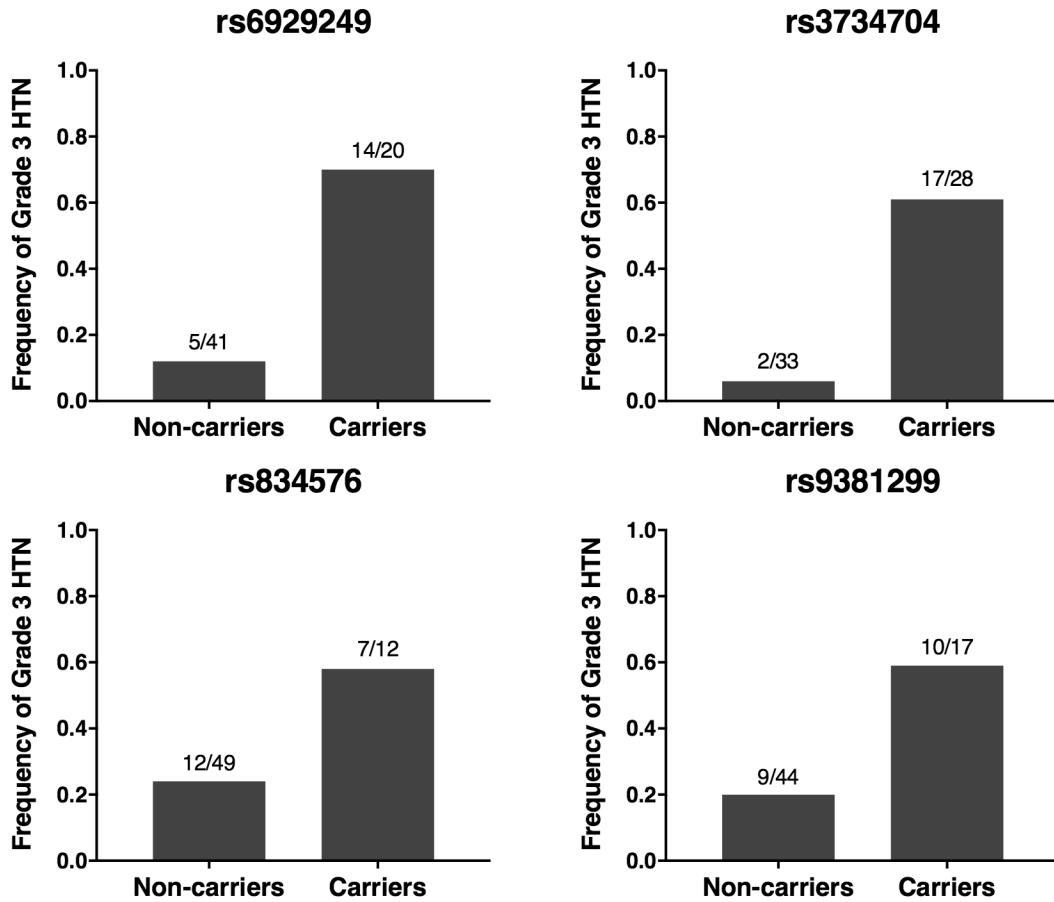


Figure 2.11. Frequency of early grade 3 bevacizumab-induced hypertension in carriers of *SLC29A1-HSP90AB1* variants. Variant alleles of each SNP are associated with higher incidence of early grade 3 hypertension (HTN) in sequenced CALGB 80405 subjects. Fractions represent the number of HTN cases over the total number of subjects for each carrier status.

To test the possibility that individual genes harboring multiple rare and low frequency variants contribute to toxicity risk, a total of 35,472 variants with MAF < 0.03 in the 174 candidate gene regions were tested using SKAT-O, and 90,808 rare and common variants were tested with SKAT-CommonRare (Figure 2.6). No gene associations met statistical significance after Bonferroni correction ($P = 2.9 \times 10^{-4}$; Tables 2.14 and 2.15). The top hits from the MAF < 0.03 analysis and the all-MAF analysis are *CPS1* ($P = 0.01$) and *FLT1* ($P = 0.006$), respectively. Functional annotations of individual variants within the top genes of the MAF < 0.03 analysis are summarized in Table 2.16. As expected, each of these genes had a small number of potentially functional (nonsynonymous or regulatory) rare SNPs.

Table 2.14. Top gene associations of candidate gene analysis (MAF < 0.03)

Gene	P^1	N, tested variants per gene
<i>CPS1</i>	0.01	276
<i>THBS1</i>	0.01	208
<i>CALCA</i>	0.02	127
<i>NOSIP</i>	0.02	113
<i>PDGFRA</i>	0.03	132
<i>PECAM1</i>	0.03	62
<i>ACE</i>	0.03	146
<i>NOS1AP</i>	0.03	542
<i>NRP2</i>	0.04	341
<i>AKT3</i>	0.05	354

¹Unadjusted P -value from SKAT-O analysis adjusted for sex, age, BMI ≥ 25 , preexisting hypertension, and preexisting diabetes.

Table 2.15. Top gene associations of candidate gene analysis (all MAF)

Gene	<i>P</i>¹	<i>N</i>, tested variants per gene	<i>N</i>, tested rare variants per gene	<i>N</i>, tested common variants per gene
<i>FLT1</i>	0.006	838	527	311
<i>ITGA5</i>	0.009	185	101	84
<i>CYGB</i>	0.01	351	179	172
<i>NOS1AP</i>	0.02	1476	799	677
<i>SPHK1</i>	0.02	214	141	73
<i>ACE</i>	0.02	280	168	112
<i>CPS1</i>	0.02	752	390	362
<i>CLIC4</i>	0.02	362	195	167
<i>PRKCG</i>	0.02	201	145	56
<i>UTS2</i>	0.03	379	189	190

¹Unadjusted *P*-value from SKAT-CommonRare analysis adjusted for sex, age, BMI \geq 25, preexisting hypertension, and preexisting diabetes.

Table 2.16. Function of individual variants in top genes of candidate gene analysis (MAF < 0.03)

Gene	Intergenic	Intronic	5'-UTR	3'-UTR	Nonsynonymous	Synonymous
<i>CPS1</i>	78	187	2	1	2	2
<i>THBS1</i>	201	13		3	1	2
<i>CALCA</i>	122	5	1	2	1	
<i>NOSIP</i>	82	29		2		
<i>PDGFRA</i>	79	46		4	2	1
<i>PECAM1</i>	46	8		8	1	
<i>ACE</i>	116	24			3	7
<i>NOS1AP</i>	121	414	8	2		1
<i>NRP2</i>	145	185	1	8	2	2
<i>AKT3</i>	110	255		8		

2.4.4 Exome-wide analysis

To analyze variants across the genome that are most likely to be deleterious, nonsynonymous, stop codon, and splice-site variants ($N = 39,981$) were identified in all sequenced genes (Figure 2.12). SNP-based association testing was performed on 8,254 common variants ($MAF \geq 0.10$) within this subset (Figures 2.13 and 2.14). As with the candidate gene analysis, the atypical QQ plot most likely reflects the small sample size. There were no SNPs that met the Bonferroni-adjusted statistical threshold ($P = 6.1 \times 10^{-6}$); the strongest association is with rs6007344 ($P = 0.002$), a nonsynonymous SNP in *ARHGAP8* (Table 2.17). The rs6007344 minor allele is observed in 10 of 19 (53%) patients who developed grade 3 HTN and in 8 of 42 (19%) patients who did not develop HTN.

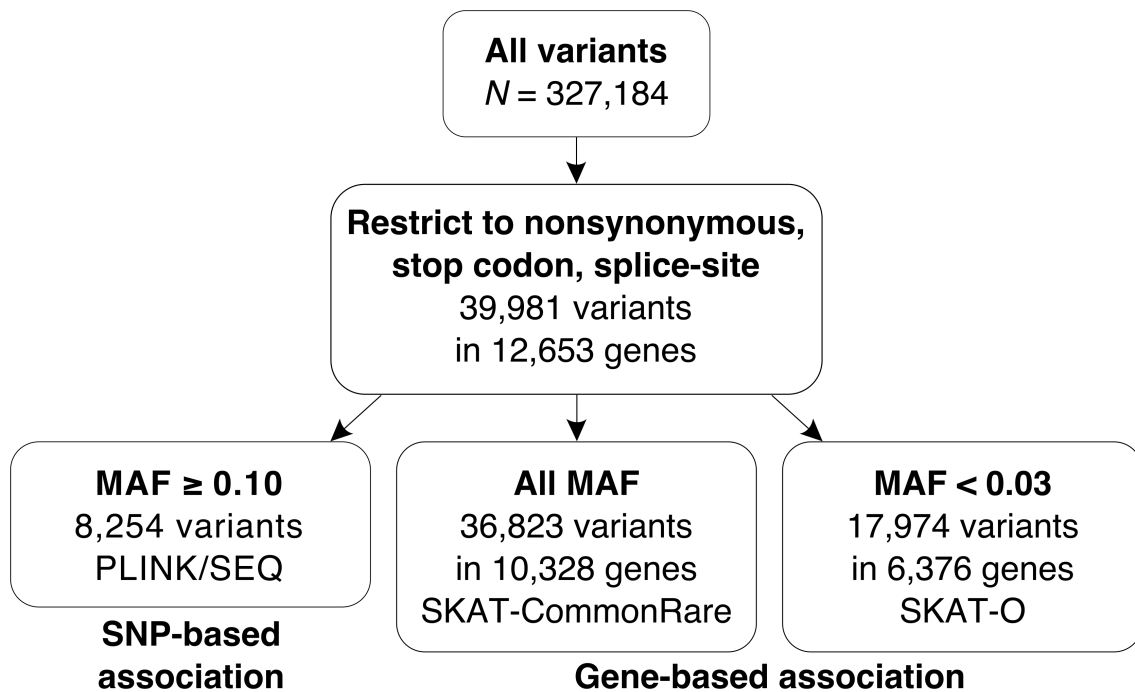


Figure 2.12. Exome-wide analysis workflow. Variants were restricted to nonsynonymous, stop codon, and splice-site variants. Common variants were analyzed by SNP-based association tests, and rare and low frequency variants were analyzed by gene-based association tests either alone or combined with common variants.

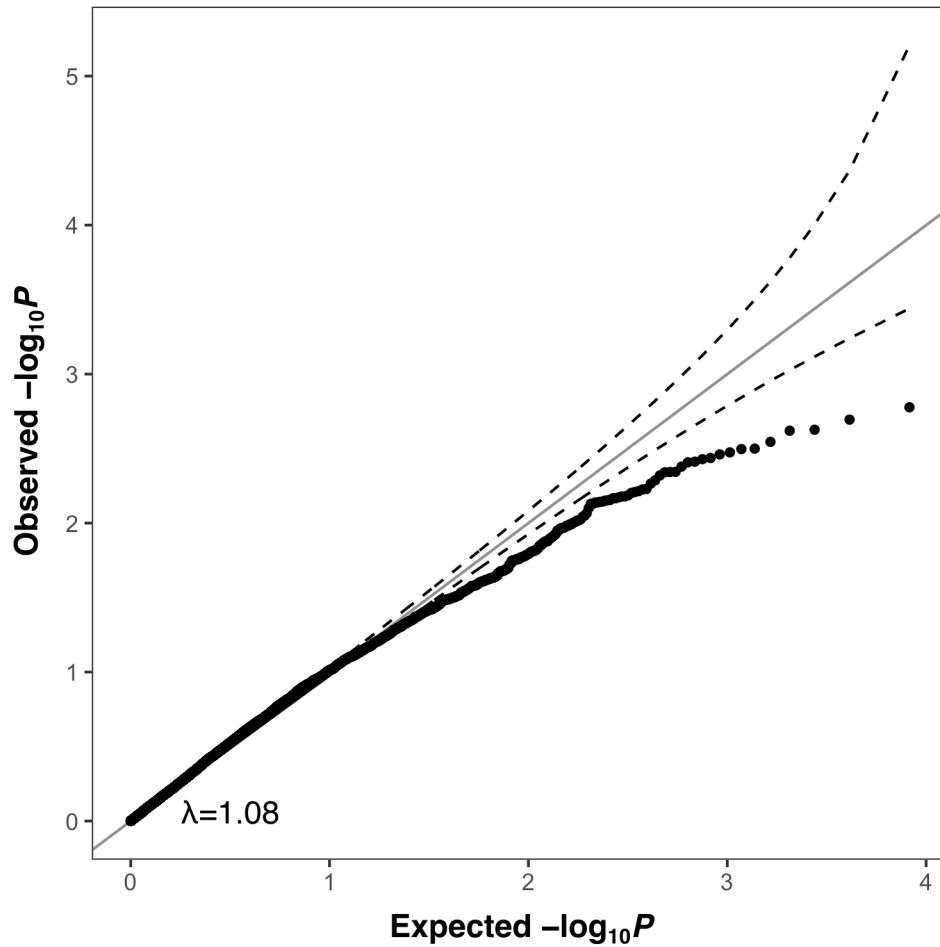


Figure 2.13. Quantile-quantile plot of exome-wide SNP-based analysis. Observed and predicted P -value relationships are plotted for the association with bevacizumab-induced hypertension. The solid line shows the expected distribution assuming no inflation of statistics and the dashed lines show the 95% confidence intervals for the expected distribution. The genomic inflation factor is noted on the graph.

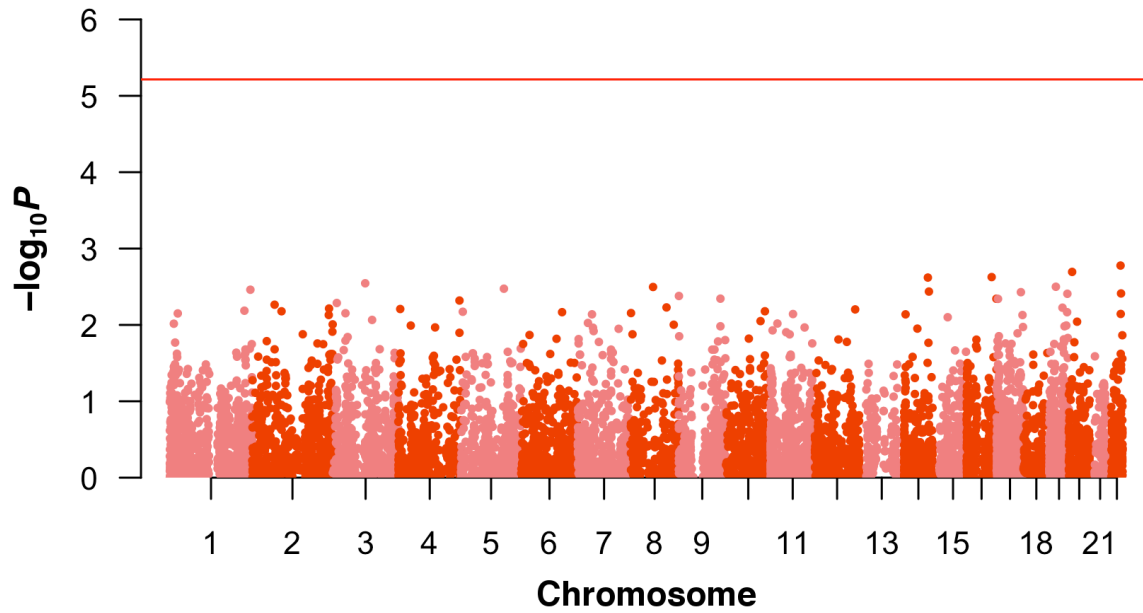


Figure 2.14. Manhattan plot of exome-wide SNP-based analysis. The distribution of $-\log_{10}$ transformed unadjusted P -values for the association with bevacizumab-induced hypertension is plotted as a function of the chromosomal location of all tested SNPs ($N = 8,254$). No SNPs surpassed the Bonferroni-corrected significance threshold of $P = 6.1 \times 10^{-6}$.

Table 2.17. Top SNP associations of exome-wide analysis

SNP (ref/var)	Case genotype counts ¹	Control genotype counts ¹	Case MAF	Control MAF	OR (95% CI)	P ²	Gene	Function
rs6007344 (G/C)	9/10/0	34/8/0	0.26	0.09	48.4 (4.3–544)	0.002	ARHGAP8	nonsynonymous
rs6087119 (G/A)	11/7/1	35/7/0	0.24	0.08	14.6 (2.7–79.7)	0.002	ANKEF1	nonsynonymous
rs3743598 (G/T)	15/4/0	20/18/4	0.11	0.30	0.1 (0.0–0.4)	0.002	ADAT1	nonsynonymous
rs4900072 (C/T)	3/8/8	24/12/6	0.63	0.28	6.2 (1.9–19.9)	0.002	C14orf159	nonsynonymous
rs4241468 (G/A)	2/5/12	10/24/8	0.76	0.47	5.7 (1.8–17.7)	0.003	OR5H14	nonsynonymous
rs17679334 (C/T)	11/8/0	38/4/0	0.21	0.05	74.7 (4.3–1311)	0.003	ZNF682	nonsynonymous
rs17343819 (T/C)	11/7/1	39/3/0	0.24	0.03	12.5 (2.3–66.6)	0.003	CPA6	nonsynonymous
rs11749126 (A/T)	8/9/2	34/8/0	0.34	0.09	11.9 (2.3–62.0)	0.003	ADAMTS19	nonsynonymous
rs2275155 (A/T)	13/5/1	14/21/7	0.18	0.41	0.1 (0.0–0.5)	0.003	SDCCAG8	nonsynonymous
rs1303 (T/G)	9/8/2	24/18/0	0.32	0.21	10.5 (2.1–51.1)	0.004	SERPINA1	nonsynonymous

¹Genotype counts: Homozygous reference / heterozygous / homozygous variant.

²Unadjusted P-value from logistic regression under an additive genetic model and adjusted for sex, age, BMI ≥ 25, preexisting hypertension, and preexisting diabetes.

Gene-based association testing with SKAT was performed on 17,974 rare and low frequency variants (MAF < 0.03) in 6,376 genes, and on 36,823 common and rare variants in 10,328 genes (Figure 2.12); variants were assigned to genes as defined by RefSeq. No gene association met statistical significance after Bonferroni correction ($P = 7.8 \times 10^{-6}$ and 4.8×10^{-6} , respectively; Tables 2.18 and 2.19). The top hits from the MAF < 0.03 analysis and the all-MAF analysis are *ANO2* ($P = 5 \times 10^{-5}$) and *CRYBB2* ($P = 4 \times 10^{-4}$), respectively. Functional annotations and case and control allele counts of individual variants within the top genes of the MAF < 0.03 analysis are summarized in Table 2.20. The total number of variants in each of these genes was low and there is no evidence for enrichment of deleterious rare variants in the cases.

Table 2.18. Top gene associations of exome-wide analysis (MAF < 0.03)

Gene	P^1	N, tested variants per gene
<i>ANO2</i>	5×10^{-5}	4
<i>FARP2</i>	3×10^{-4}	3
<i>CRYBB2</i>	4×10^{-4}	1
<i>DDIAS</i>	4×10^{-4}	3
<i>ZMIZ2</i>	5×10^{-4}	2
<i>SCO1</i>	9×10^{-4}	4
<i>C9orf57</i>	0.001	1
<i>SPIRE2</i>	0.001	2
<i>TCL1A</i>	0.001	2
<i>GOT2</i>	0.001	3

¹Unadjusted P -value from SKAT-O analysis adjusted for sex, age, BMI ≥ 25 , preexisting hypertension, and preexisting diabetes.

Table 2.19. Top gene associations of exome-wide analysis (all MAF)

Gene	<i>P</i>¹	<i>N</i>, tested rare variants per gene	<i>N</i>, tested common variants per gene
<i>CRYBB2</i>	4 x 10 ⁻⁴	1	0
<i>NAALAD2</i>	5 x 10 ⁻⁴	3	1
<i>C5orf58</i>	6 x 10 ⁻⁴	0	1
<i>PLPP2</i>	7 x 10 ⁻⁴	2	1
<i>OR5R1</i>	9 x 10 ⁻⁴	5	5
<i>C9orf57</i>	9 x 10 ⁻⁴	1	0
<i>CST5</i>	0.001	0	1
<i>ZMIZ2</i>	0.001	2	0
<i>BTN3A1</i>	0.001	1	2
<i>ANO2</i>	0.001	5	2

¹Unadjusted *P*-value from SKAT-CommonRare analysis adjusted for sex, age, BMI ≥ 25, preexisting hypertension, and preexisting diabetes.

Table 2.20. Functional predictions and allele counts of variants in top genes of exome-wide analysis (MAF < 0.03)

Gene	SNP	SIFT	PP2	CADD	ExAC NFE MAF	Case AC	Control AC
ANO2	rs144224656	D	D	33.0	0.006	0	1
	rs200078432	T	B	9.4	0.01	1	1
	rs200918253	T	P	25.5	0.001	0	2
	rs199618060	T	B	0.0	2×10^{-4}	0	1
	rs61739702	T	D	29.1	0.03	0	1
FARP2	rs61739735	T	B	13.3	0.006	0	1
	rs769768522	T	P	20.3	9×10^{-5}	0	1
	rs16986560	T	B	10.6	0.01	1	2
DDIAS	rs143776868	T	B	0.9	0.002	1	1
	rs781115475	T	B	0.1	2×10^{-5}	1	0
	rs141656476	T	B	0.3	0.002	0	1
	chr7:44805175 (C/A)	D	P	21.6	NA	0	1
ZMIZ2	rs71548246	D	P	20.8	0.01	0	2
	rs139771078	T	P	12.8	4×10^{-4}	0	1
	chr17:10599144 (A/G)	D	D	25.3	NA	0	1
SCO1	rs61753148	D	B	8.3	0.006	0	1
	rs147487151	D	D	26.4	5×10^{-4}	1	0
	rs201522474	D	B	22.3	0.002	1	2
C9orf57	rs756702934	T	B	0.1	8×10^{-5}	0	1
	rs141817469	T	B	0.1	0.07	0	3
SPIRE2	rs17093294	T	B	0.5	0.02	0	2
	rs146705048	D	D	24.9	6×10^{-4}	0	1
	rs368397369	T	B	12.7	1×10^{-4}	0	1
GOT2	rs139235307	D	D	26.4	0.0176	0	3
	rs149988435	D	P	26.2	0.0016	1	0

SIFT: D=Damaging, T=Tolerated; PP2 (PolyPhen-2): B=Benign, P=Probably Damaging, D=Damaging; CADD: Phred-scaled scores (>10 considered deleterious); ExAC NFE MAF = Non-Finnish European minor allele frequency; AC = allele count.

2.4.5 Analysis using other rare variant testing methods

In SKAT, variants are weighted by default by the MAF in the analyzed cohort, with rarer variants being upweighted. Custom weights based on MAF in the sequenced controls, MAF in the 1000 Genomes Project (EUR), PolyPhen-2 scores, GERP++ scores, and CADD Phred-scaled scores were each applied to SKAT testing. The resulting top genes and *P*-values did not vary substantially across the different weighting schemes, and no *P*-value exceeded the *P*-values of the top associations in the default weighted analyses (data not shown).

Additional rare variant methods listed in Table 2.9 were used to test gene-based associations within the candidate gene and exome-wide subsets described above. In general, burden and adaptive burden test results differed from the results of the two-sided tests (SKAT, C-alpha, SUMSTAT), but no statistically significant associations were identified using any method (Tables 2.21 and 2.22).

Table 2.21. Top candidate gene associations of non-SKAT analyses (MAF < 0.03)

Test	Top gene	<i>P</i>	<i>N</i>, tested variants per gene
BURDEN	<i>HRAS</i>	0.02	162
UNIQ	<i>AGTR1</i>	0.02	144
VT	<i>ITGB3</i>	0.001	229
FRQWGT	<i>HRAS</i>	0.01	162
CALPHA	<i>CCL2</i>	0.008	115
SUMSTAT	<i>AGTR1</i>	0.01	144

Table 2.22. Top exome-wide gene associations of non-SKAT analyses (MAF < 0.03)

Test	Top gene	P	N, tested variants per gene
BURDEN	<i>DNAH14</i>	0.0006	12
UNIQ	<i>KIZ</i>	0.001	4
VT	<i>DNAH14</i>	0.001	12
FRQWGT	<i>DNAH14</i>	0.0004	12
CALPHA	<i>KIZ</i>	0.001	4
SUMSTAT	<i>KIZ</i>	0.001	4

2.4.6 Analysis of other variant subsets

Additional subsets of variants were analyzed by several exploratory approaches. Rare variants in the candidate gene analysis were further grouped and tested by SKAT-O within seven gene sets: Blood pressure, endothelial cell biology, endothelin signaling, NO signaling, prostacyclin signaling, vascular process, and VEGF signaling. Variants were also filtered by Phred-scaled CADD scores and tested using SKAT-O. Variants identified as pathogenic or probable-pathogenic for disease or drug response in the NCBI ClinVar database were analyzed with burden testing. The top associations of these analyses are summarized in Table 2.23. No associations met the respective Bonferroni-corrected significance levels.

Table 2.23. Top gene associations of exploratory analyses (MAF < 0.03)

Analyzed variants	Test	Top gene/set	<i>P</i>	<i>N</i> , tested variants per gene
Candidate gene sets (coding + noncoding)	SKAT-O	Blood pressure	0.23	2771
Candidate gene sets (nonsynonymous, stop codon, splice-site)	SKAT-O	Blood pressure	0.21	40
CADD > 10	SKAT-O	<i>CHURC1-FNTB, RAB15</i>	0.0002	2
CADD > 15	SKAT-O	<i>ZMIZ2</i>	0.0006	2
CADD > 20	SKAT-O	<i>UTRN</i>	0.0006	6
ClinVar pathogenic + probable-pathogenic + drug response	Burden	<i>GALT</i>	0.04	2

Finally, an analysis of the 30,678 sequenced indels was performed. Indel lengths ranged from -208 to 164 bp, with a majority being ≤ 6 bp. A total of 12,006 (39%) indels had MAF < 0.03 in the analysis cohort. As with the SNPs, indels were sorted into subsets based on function or gene: Coding (exonic and splicing), coding frameshift, and candidate gene. Single-variant association tests were used to examine coding ($N = 1,740$) and coding frameshift ($N = 735$) indels, of which there were too few to perform gene-based testing. The top association of both analyses was with rs146317894, a frameshift insertion in *OR52D1* ($P = 0.02$, OR 0.1). No statistically significant associations were identified in the gene-based indel analyses (Table 2.24).

Table 2.24. Top gene associations of indel analyses

Analyzed indels	N, indels	Top gene	P	N, tested variants per gene
All	7,666 indels in 4,361 genes	<i>SCNN1A</i>	0.001	4
Candidate gene (coding + noncoding)	2,310 indels in 173 genes	<i>EDN2</i>	0.007	12

2.4.7 In silico functional analysis

The four SNPs between *SLC29A1* and *HSP90AB1* identified in the primary candidate gene analysis are noncoding, and all proxy SNPs ($r^2 > 0.8$) are also in noncoding regions. These SNPs were examined for overlap with regulatory elements inferred from functional data generated in human umbilical vein endothelial cells (HUVEC) from the ENCODE Project^{52,53} (Figure 2.15). rs6929249 and rs3734704 are located within 1 kb downstream of the 3' end of *SLC29A1* in a moderately transcribed region enriched for histone modifications linked to gene activation (H3K4me1, H3K27ac, H3K36me3, H3K79me2) and binding of CTCF, which can act as an insulator. rs834576 is in a region approximately 3.8 kb downstream of *SLC29A1* that is also enriched for H3K4me1, H3K27ac, and CTCF as well as additional activating histone modifications (H3K4me2, H3K4me3, H3K9ac, H2A.Z) and binding of RNA polymerase II; the variant site also maps to a CpG island, a feature often associated with promoters. rs3734704 and rs834576 also overlap with DNase I hypersensitivity peaks representing regions of open chromatin. rs3734704 and rs834576 are in genomic segments predicted by ChromHMM⁶³ to be strong enhancers, rs6929249 in a predicted region of transcriptional transition, and rs9381299 in a predicted region of weak transcription. Similar data from the Roadmap Epigenomics Project⁵⁴ corroborated the

ENCODE predictions (Table 2.25). rs3734704 is predicted by CADD to be deleterious, and rs834576 is predicted by RegulomeDB as likely to affect binding. In a search of previously published eQTL analyses, the risk allele of rs9381299 was found to be associated with increased *SLC29A1* expression in monocytes ($P = 3.8 \times 10^{-5}$, $\beta = 0.18$)⁶⁴.

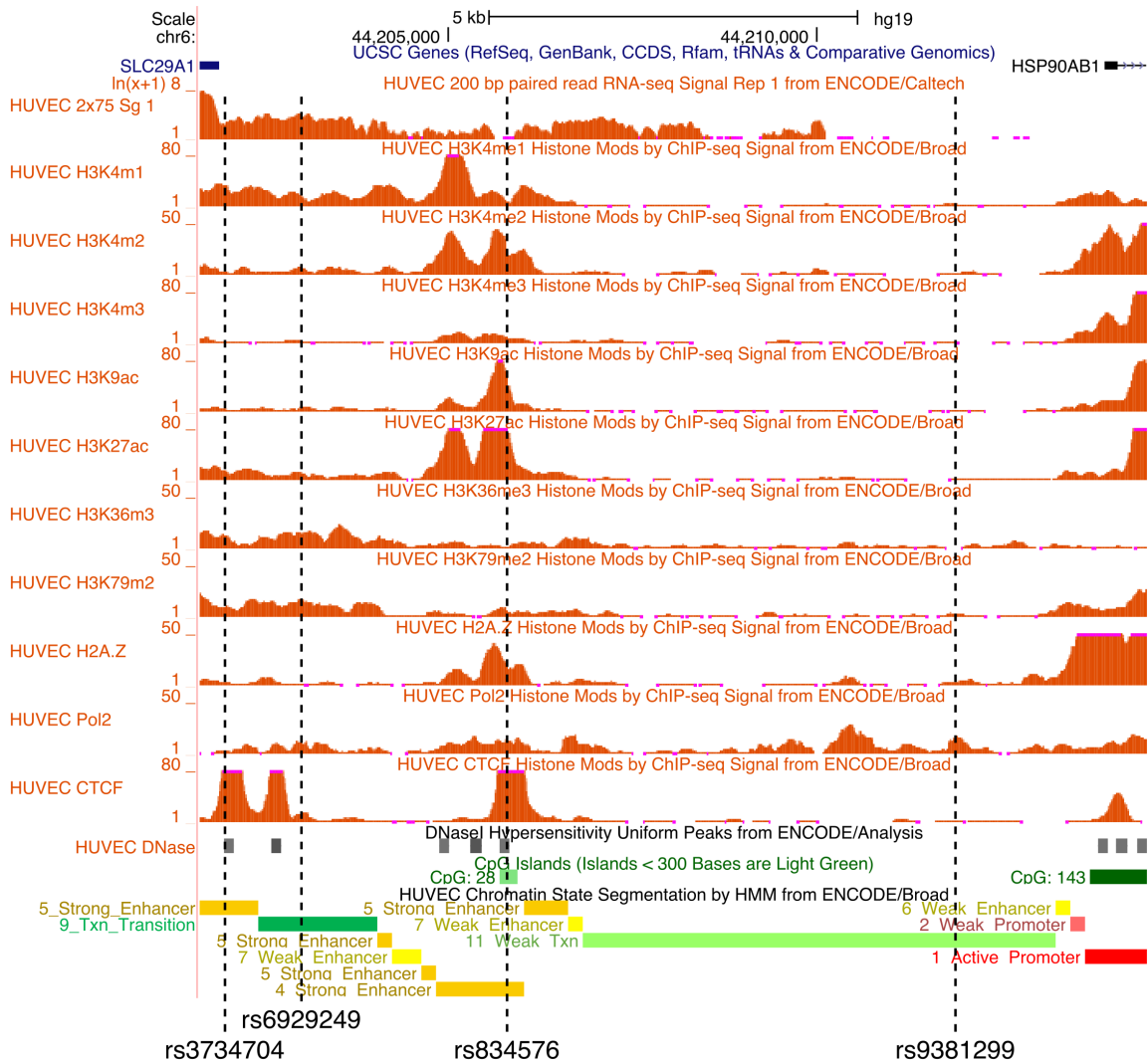


Figure 2.15. Top *SLC29A1*-*HSP90AB1* SNPs are in predicted transcriptionally-active regions in human umbilical vein endothelial cells. Tracks (top to bottom): UCSC Genes, HUVEC 200 bp paired read RNA-seq Signal Rep 1 from ENCODE/Caltech, HUVEC Histone Modifications by ChIP-seq Signal from ENCODE/Broad (H3K4me1, H3K4me2, H3K4me3, H3K9ac, H3K27ac, H3K36me3, H3K79me2, H2A.Z, Pol2, CTCF), HUVEC DNase I Hypersensitivity Uniform Peaks from ENCODE/Analysis, CpG Islands, and HUVEC Chromatin State Segmentation by HMM from ENCODE/Broad.

Table 2.25. Evidence of regulatory activity for top SLC29A1-HSP90AB1 SNPs

	rs6929249	rs3734704	rs834576	rs9381299
RegulomeDB score	5	4	2b	6
CADD Phred-scaled score	2.6	10.9	9.8	1.1
Conserved region	No	Yes (GERP++)	No	No
HUVEC Chromatin State	9_Txn_Transition (ENCODE) 6_EnhG (Roadmap)	5_Strong_Enhancer (ENCODE) 6_EnhG (Roadmap)	4_Strong_Enhancer (ENCODE) 7_Enh (Roadmap)	11_Weak_Txn (ENCODE)
HUVEC Chromatin Marks (ENCODE, Roadmap)	H3K4me1_Enh, H3K27ac_Enh, H3K9ac_Pro	H3K4me1_Enh, H3K27ac_Enh, H3K9ac_Pro	H3K4me1_Enh, H3K4me3_Pro, H3K27ac_Enh, H3K9ac_Pro	None
HUVEC DNase Hypersensitive (ENCODE, Roadmap)	No	Yes	Yes	No
HUVEC TF Binding (ENCODE)	None	CTCF	POLR2A, CTCF	None

Data from publicly available databases are summarized for the four SNPs in the SLC29A1-HSP90AB1 region. Red text indicates strong evidence for regulatory function.

2.4.8 Replication analysis of top SNP associations

rs9381299, rs3734704, rs834576, and a proxy SNP of rs6929249 were tested for association with early grade 3+ HTN in independent bevacizumab-treated cohorts from CALGB 40502 and CALGB 90401 (Table 2.26). Association of rs9381299 with SBP > 180 mmHg was also examined in ECOG-5103 GWAS results, with SBP > 180 being an even more extreme phenotype than grade 3 HTN, which typically occurs at SBP > 160. Other SNPs were not available for lookup in ECOG-5103.

rs9381299 significantly associated with early grade 3+ HTN in CALGB 40502 ($P = 0.01$, OR 2.4) and with SBP > 180 in ECOG-5103 ($P = 0.02$, OR 2.1). rs834576 also nominally associated with early grade 3+ HTN in CALGB 40502 ($P = 0.03$, OR 2.9). Although the other associations did not replicate, frequency of HTN was consistently higher in variant allele carriers versus non-carriers: 8–16% vs. 5–6% in CALGB 40502, 3–4% vs. 2% in CALGB 90401, and 16% vs. 7% in ECOG-5103 (Figure 2.16).

Table 2.26. Replication analysis of top SLC29A1-HSP90AB1 SNP associations in independent bevacizumab-treated cohorts

Study	Phenotype ¹	SNP	Case genotype counts ²	Control genotype counts ²	Case MAF	Control MAF	OR (95% CI)	P ³
CALGB 40502	Early grade 3+ HTN	rs6902226 ⁴	19/9/1	276/100/10	0.19	0.16	1.2 (0.6–2.4)	0.56
		rs6929249 ⁵	19/10/0	278/98/10	0.17	0.15	1.1 (0.5–2.2)	0.81
		rs3734704	11/17/1	222/134/30	0.33	0.25	1.5 (0.8–2.6)	0.20
CALGB 90401	Early grade 3+ HTN	rs834576 ⁵	23/6/0	355/30/1	0.10	0.04	2.9 (1.0–7.6)	0.03
		rs9381299	16/13/0	303/76/7	0.22	0.12	2.4 (1.2–4.9)	0.01
		rs6902226 ⁴	10/6/0	410/173/16	0.19	0.17	1.1 (0.4–2.7)	0.77
ECOG-5103	SBP > 180 mmHg	rs3734704	7/7/2	321/241/37	0.34	0.26	1.5 (0.7–3.2)	0.30
		rs9381299	10/6/0	469/125/6	0.19	0.11	1.8 (0.6–4.4)	0.22
ECOG-5103	SBP > 180 mmHg	rs9381299	23/16/0	308/79/4	0.21	0.11	2.1 (1.1–3.7)	0.02

¹Early HTN: HTN occurring within the number of treatment cycles equaling the same total exposure of bevacizumab (60 mg/kg) in the first three treatment cycles of CALGB 80405.

²Genotype counts: Homozygous reference / heterozygous / homozygous variant.

³Unadjusted P-value from logistic regression under an additive genetic model and adjusted for covariates listed in Table 2.10.

⁴rs6902226 is a proxy for rs6929249 ($r^2 = 0.98$).

⁵rs6929249 and rs834576 genotypes were imputed using genome-wide genotyping data and sequencing data from the 1000 Genomes Project. The imputation accuracy for these two SNPs was excellent: rs6929249: $R^2 = 0.949$; rs834576: $R^2 = 0.936$.

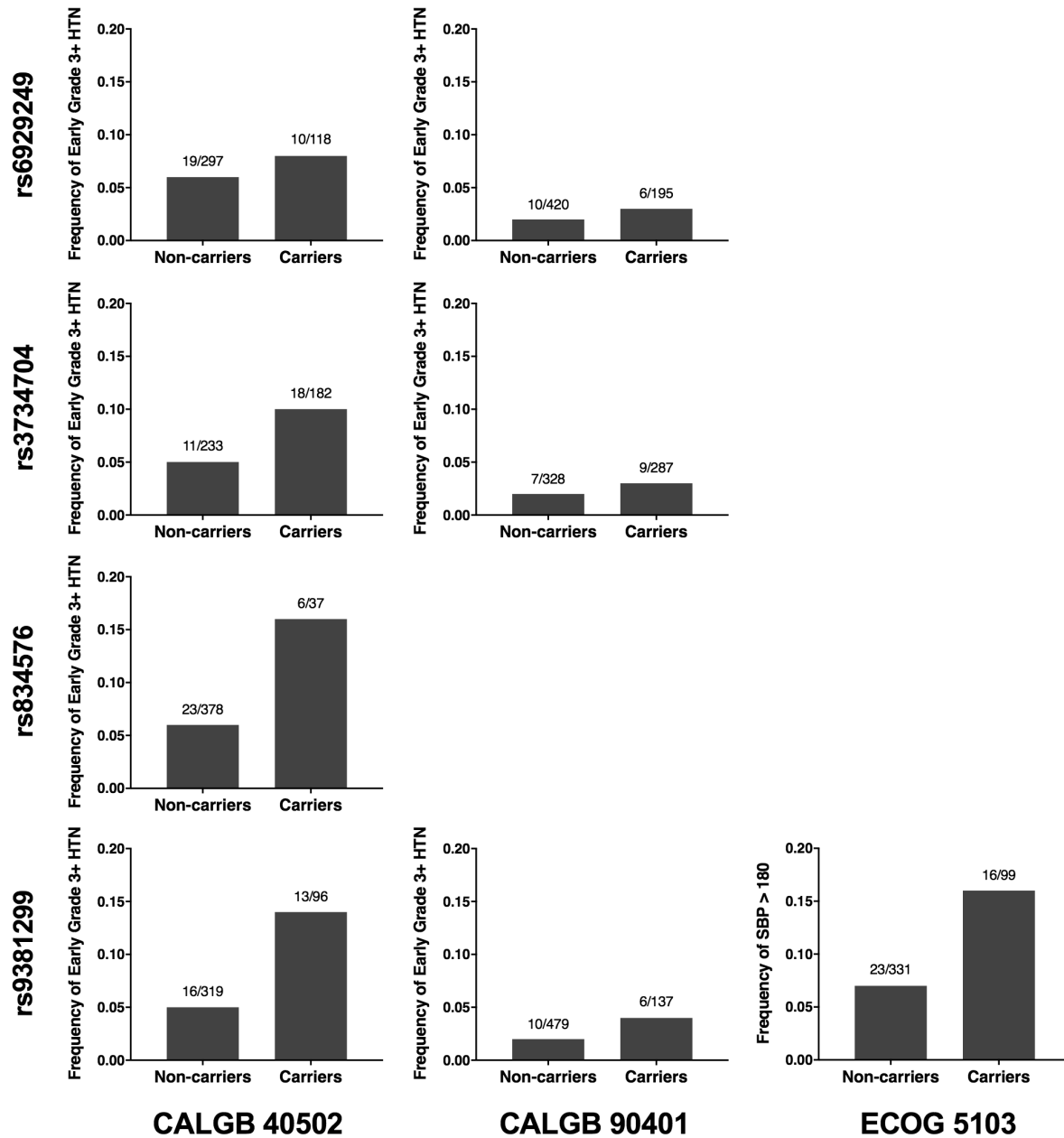


Figure 2.16. Frequency of high-grade hypertension in replication cohorts stratified by variant allele carrier status. Variant alleles are more commonly found in subjects with high-grade hypertension (HTN), defined as early grade 3+ HTN in CALGB 40502 and CALGB 90401, or SBP > 180 mmHg in ECOG-5103. Top to bottom: rs6929249 (or rs6902226 as a proxy in CALGB 90401), rs3734704, rs834576, rs9381299. Fractions represent the number of HTN cases over the total number of subjects for each carrier status.

2.4.9 Association of top SNPs with secondary hypertension phenotypes

As an exploratory analysis, top SNPs in the *SLC29A1-HSP90AB1* intergenic region were also tested for association with secondary HTN phenotypes (Tables 2.27–2.30). Most notably, rs9381299 associated with the development of grade 2+ HTN in any treatment cycle in CALGB 90401 ($P = 0.007$, OR 2.0) and CALGB 40502 ($P = 0.02$, OR 1.7). rs3734704 associated with grade 2+ HTN ($P = 0.007$, OR 1.8) and early grade 2+ HTN ($P = 0.02$, OR 1.8) in CALGB 90401 (Figure 2.17).

Table 2.27. Association of rs6902226¹ with secondary bevacizumab-induced hypertension phenotypes in larger cohorts

Study	Phenotype ²	Case genotype counts ³	Control genotype counts ³	Case MAF	Control MAF	OR (95% CI)	P ⁴
CALGB 80405	Early grade 2+ HTN	34/15/2	233/113/10	0.19	0.19	1.0 (0.6–1.7)	0.98
	Early grade 2+ HTN	49/23/2	246/86/9	0.18	0.15	1.2 (0.8–1.9)	0.41
CALGB 40502	Grade 3+ HTN	28/13/2	267/96/9	0.20	0.15	1.3 (0.7–2.4)	0.32
	Grade 2+ HTN	82/37/3	213/72/8	0.18	0.15	1.2 (0.8–1.7)	0.45
CALGB 90401	Early grade 2+ HTN	23/13/3	397/166/13	0.24	0.17	1.7 (0.9–2.9)	0.06
	Grade 3+ HTN	18/7/0	402/172/16	0.14	0.17	0.8 (0.3–1.7)	0.55
	Grade 2+ HTN	38/22/3	382/157/13	0.22	0.17	1.5 (0.9–2.3)	0.09

¹rs6902226 is a proxy for rs6929249 ($r^2 = 0.98$).

²Early HTN: HTN occurring within the number of treatment cycles equaling the same total exposure of bevacizumab (60 mg/kg) in the first three treatment cycles of CALGB 80405.

³Genotype counts: Homozygous reference / heterozygous / homozygous variant.

⁴Unadjusted P-value from logistic regression under an additive genetic model and adjusted for covariates listed in Table 2.10.

Table 2.28. Association of rs3734704 with secondary bevacizumab-induced hypertension phenotypes in larger cohorts

Study	Phenotype ¹	Case genotype counts ²	Control genotype counts ²	Case MAF	Control MAF	OR (95% CI)	P ³
CALGB 80405	Early grade 2+ HTN	30/18/3	179/150/27	0.24	0.29	0.8 (0.5–1.2)	0.27
	Early grade 2+ HTN	36/36/2	197/115/29	0.27	0.25	1.1 (0.7–1.6)	0.70
CALGB 40502	Grade 3+ HTN	18/23/2	215/128/29	0.31	0.25	1.4 (0.8–2.3)	0.20
	Grade 2+ HTN	59/54/9	174/97/22	0.30	0.24	1.3 (0.9–1.8)	0.13
CALGB 90401	Early grade 2+ HTN	15/19/5	313/229/34	0.37	0.26	1.8 (1.1–2.9)	0.02
	Grade 3+ HTN	12/11/2	316/237/37	0.30	0.26	1.2 (0.6–2.2)	0.59
	Grade 2+ HTN	24/32/7	304/216/32	0.37	0.25	1.8 (1.2–2.6)	0.007

¹Early HTN: HTN occurring within the number of treatment cycles equaling the same total exposure of bevacizumab (60 mg/kg) in the first three treatment cycles of CALGB 80405.

²Genotype counts: Homozygous reference / heterozygous / homozygous variant.

³Unadjusted P-value from logistic regression under an additive genetic model and adjusted for covariates listed in Table 2.10.

Table 2.29. Association of rs9381299 with secondary bevacizumab-induced hypertension phenotypes in larger cohorts

Study	Phenotype ¹	Case genotype counts ²	Control genotype counts ²	Case MAF	Control MAF	OR (95% CI)	P ³
CALGB 80405	Early grade 2+ HTN	41/9/1	253/92/6	0.11	0.15	0.7 (0.3–1.3)	0.26
	Early grade 2+ HTN	53/21/0	266/68/7	0.14	0.12	1.2 (0.7–2.1)	0.44
	Grade 3+ HTN	27/16/0	292/73/7	0.19	0.12	1.9 (1.0–3.5)	0.05
CALGB 40502	Grade 2+ HTN	83/38/1	236/51/6	0.16	0.11	1.7 (1.1–2.6)	0.02
	Early grade 2+ HTN	25/14/0	454/117/6	0.18	0.11	1.8 (0.9–3.3)	0.07
	Grade 3+ HTN	15/10/0	464/121/6	0.20	0.11	2.0 (0.9–4.1)	0.07
CALGB 90401	Grade 2+ HTN	39/24/0	440/107/6	0.19	0.11	2.0 (1.2–3.3)	0.007
	Grade 3+ HTN	133/41/3	304/79/4	0.13	0.11	1.2 (0.8–1.8)	0.28

¹Early HTN: HTN occurring within the number of treatment cycles equaling the same total exposure of bevacizumab (60 mg/kg) in the first three treatment cycles of CALGB 80405.

²Genotype counts: Homozygous reference / heterozygous / homozygous variant.

³Unadjusted P-value from logistic regression under an additive genetic model and adjusted for covariates listed in Table 2.10.

Table 2.30. Association of rs6929249 and rs834576 with secondary bevacizumab-induced hypertension phenotypes in CALGB 40502

SNP ¹	Phenotype ²	Case genotype counts ³	Control genotype counts ³	Case MAF	Control MAF	OR (95% CI)	P ⁴
rs6929249	Early grade 2+ HTN	49/24/1	248/84/9	0.18	0.15	1.2 (0.7–1.9)	0.50
	Grade 3+ HTN	28/14/1	269/94/9	0.19	0.15	1.2 (0.7–2.2)	0.48
	Grade 2+ HTN	82/38/2	215/70/8	0.17	0.15	1.2 (0.8–1.7)	0.48
rs834576	Early grade 2+ HTN	64/10/0	314/26/1	0.07	0.04	1.7 (0.8–3.6)	0.16
	Grade 3+ HTN	35/8/0	343/28/1	0.09	0.04	2.7 (1.1–6.2)	0.03
	Grade 2+ HTN	107/15/0	271/21/1	0.06	0.04	1.6 (0.8–3.1)	0.17

¹rs6929249 and rs834576 genotypes were imputed using genome-wide genotyping data and sequencing data from the 1000 Genomes Project. The imputation accuracy for these two SNPs was excellent: rs6929249: R² = 0.949; rs834576: R² = 0.936.

²Early HTN: HTN occurring within the number of treatment cycles equaling the same total exposure of bevacizumab (60 mg/kg) in the first three treatment cycles of CALGB 80405.

³Genotype counts: Homozygous reference / heterozygous / homozygous variant.

⁴Unadjusted P-value from logistic regression under an additive genetic model and adjusted for covariates listed in Table 2.10.

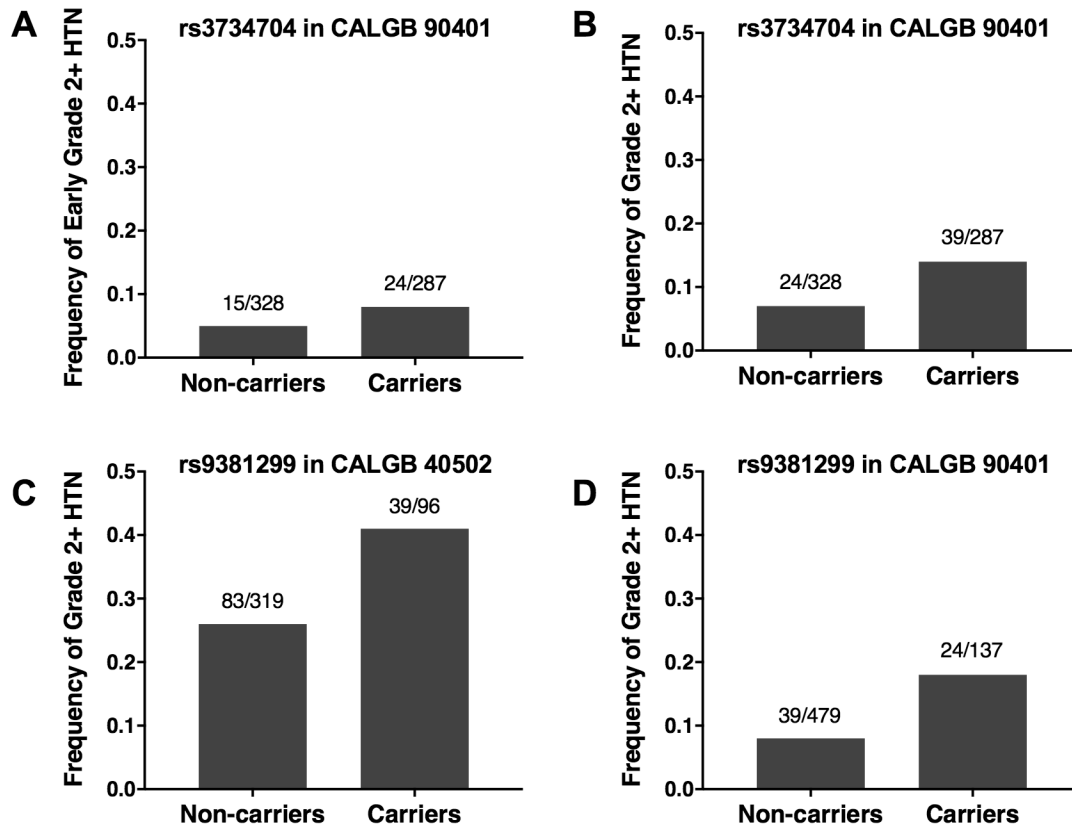


Figure 2.17. Frequency of secondary bevacizumab-induced hypertension phenotypes in carriers of *SLC29A1-HSP90AB1* risk variants in CALGB 40502 and CALGB 90401. Top (rs3734704): A) Early grade 2+ and B) grade 2+ HTN frequencies in CALGB 90401. Bottom (rs9381299): Grade 2+ HTN frequencies in C) CALGB 40502 and D) CALGB 90401. Fractions represent the number of HTN cases over the total number of subjects for each carrier status.

2.4.10 Analysis of previously reported SNP associations

Previously identified SNPs from published candidate gene and genome-wide association studies of bevacizumab-induced HTN (Table 2.31) were tested for associations with early grade 3+ and early grade 2+ HTN in the CALGB 80405 GWAS cohort (Tables 2.32 and 2.33). None of these associations replicated. The allele frequencies of rs3025039 (*VEGFA*), rs2305948 (*KDR*), and rs1870377 (*KDR*) differed substantially between cases and controls, but these differences may be due to sparse allele counts in the cases.

Table 2.31. Previously reported SNP associations with bevacizumab-induced hypertension

SNP	Gene	Function	Association with bev-induced HTN	Study
rs699947 (A/C)	VEGFA	promoter	CC: Decreased risk (early grade 2+, grade 2+)	Morita <i>et al</i> (2012) ⁷
rs833061 (C/T)	VEGFA	promoter	TT: Decreased risk (grade 3+)	Schneider <i>et al</i> (2008) ⁵
			TT: Decreased risk (early grade 2+)	Morita <i>et al</i> (2012) ⁷
rs2010963 (G/C)	VEGFA	5'-UTR	CC: Decreased risk (grade 3+)	Schneider <i>et al</i> (2008) ⁵
			C: Increased risk (all-grade)	Etienne-Grimaldi <i>et al</i> (2011) ⁶
			GG: Increased risk (grade 3+)	Gampenrieder <i>et al</i> (2016) ⁹
rs3025039 (T/C)	VEGFA	3'-UTR	CC: Decreased risk (grade 2+)	Morita <i>et al</i> (2012) ⁷
			CC: Increased risk (all-grade)	Sibertin-Blanc <i>et al</i> (2015) ⁸
rs2305949 (C/T)	KDR	intronic	T: Decreased risk (all-grade)	Lambrechts <i>et al</i> (2014) ¹²
rs1870377 (T/A)	KDR	nonsynonymous	A: Increased risk (grade 2+)	Jain <i>et al</i> (2010) ¹⁰
rs1680695 (T/G)	EGLN3	intronic	G: Increased risk (all-grade)	Lambrechts <i>et al</i> (2014) ¹²
rs4444903 (A/G)	EGF	5'-UTR	G: Increased risk (all-grade)	Lambrechts <i>et al</i> (2014) ¹²
rs11064560 (T/G)	WNK1	intronic	T: Increased risk (all-grade)	Lambrechts <i>et al</i> (2014) ¹²
rs6453204 (A/G)	SV2C	intronic	G: Increased risk (SBP > 160 mmHg, grade 3+)	Schneider <i>et al</i> (2014) ¹¹

Table 2.32. Associations of previously reported SNPs with early grade 3+ bevacizumab-induced hypertension in CALGB 80405

SNP	Proxy SNP	Case genotype counts ¹	Control genotype counts ¹	Case MAF	Control MAF	OR (95% CI)	P ²
rs699947 (A/C)	rs833070 ($r^2 = 1.00$)	7/7/7	115/227/101	0.50	0.48	1.1 (0.6–2.1)	0.73
rs833061 (C/T)	rs833070 ($r^2 = 0.97$)	7/7/7	115/227/101	0.50	0.48	1.1 (0.6–2.1)	0.73
rs2010963 (G/C)	rs833069 ($r^2 = 0.97$)	10/10/1	207/194/42	0.29	0.31	0.8 (0.4–1.5)	0.48
rs3025039 (T/C)		19/2/0	329/105/9	0.05	0.14	0.3 (0.1–1.0)	0.11
rs2305949 (C/T)	rs2305948 ($D' = 0.98$)	20/1/0	352/82/9	0.02	0.11	0.2 (0.0–0.9)	0.11
rs1870377 (T/A)		13/7/0	266/145/32	0.18	0.24	0.7 (0.3–1.5)	0.44
rs1680695 (T/G)	rs1384372 ($r^2 = 0.93$)	8/1/1/2	200/192/51	0.36	0.33	1.1 (0.6–2.1)	0.77
rs4444903 (A/G)		8/9/4	148/220/75	0.40	0.42	1.0 (0.5–1.8)	0.92
rs11064560 (T/G)		6/2/2	103/102/23	0.30	0.32	0.8 (0.3–2.1)	0.70
rs6453204 (A/G)	None	NA	NA	NA	NA	NA	NA

¹Genotype counts: Homozygous reference / heterozygous / homozygous variant.

²Unadjusted P-value from logistic regression under an additive genetic model and adjusted for sex, age, BMI ≥ 25 , preexisting hypertension, and preexisting diabetes.

Table 2.33. Associations of previously reported SNPs with early grade 2+ bevacizumab-induced hypertension in CALGB 80405

SNP	Proxy SNP	Case genotype counts ¹	Control genotype counts ¹	Case MAF	Control MAF	OR (95% CI)	P ²
rs699947 (A/C)	rs833070 ($r^2 = 1.00$)	23/30/17	99/204/91	0.46	0.49	0.9 (0.6–1.3)	0.57
rs833061 (C/T)	rs833070 ($r^2 = 0.97$)	23/30/17	99/204/91	0.46	0.49	0.9 (0.6–1.3)	0.57
rs2010963 (G/C)	rs833069 ($r^2 = 0.97$)	32/32/6	185/172/37	0.31	0.31	1.0 (0.6–1.4)	0.86
rs3025039 (T/C)		57/13/0	291/94/9	0.09	0.14	0.6 (0.3–1.1)	0.11
rs2305949 (C/T)	rs2305948 ($D' = 0.98$)	60/8/2	312/75/7	0.09	0.11	0.8 (0.4–1.4)	0.41
rs1870377 (T/A)		47/18/4	232/134/28	0.19	0.24	0.8 (0.5–1.2)	0.25
rs1680695 (T/G)	rs1384372 ($r^2 = 0.93$)	31/29/10	177/174/43	0.35	0.33	1.1 (0.7–1.6)	0.65
rs4444903 (A/G)		24/31/15	132/198/64	0.44	0.41	1.1 (0.8–1.6)	0.58
rs11064560 (T/G)		18/17/6	91/87/19	0.35	0.32	1.1 (0.7–1.9)	0.60
rs6453204 (A/G)	None	NA	NA	NA	NA	NA	NA

¹Genotype counts: Homozygous reference / heterozygous / homozygous variant.

²Unadjusted P-value from logistic regression under an additive genetic model and adjusted for sex, age, BMI ≥ 25 , preexisting hypertension, and preexisting diabetes.

2.5 Discussion

The present study used exome sequencing to discover genes that potentially contribute to bevacizumab-induced HTN. Although no associations achieved genome-wide significance, our analyses identified a genomic region containing multiple SNPs that may have regulatory effects on biological pathways related to the phenotype.

Due to limited cases and a small sample size, this study was not powered to detect significant associations. Due to lack of consent or available DNA, many potential subjects could not be sequenced. Rare variant analyses, especially those studying complex traits, are inherently underpowered, and in general, sample sizes of over 10,000 exomes would be required to identify a true genetic association. Furthermore, preexisting HTN was significantly correlated with on-treatment HTN ($P = 0.002$, OR 6.7), with 14 of 19 (74%) cases having preexisting HTN compared to 12 of 42 (29%) controls. This association is possibly confounding, though genetic models were adjusted for preexisting HTN to minimize this effect and phenotype data was rigorously reviewed to confirm drug-induced HTN events. To increase statistical power within our few cases, an extreme phenotype study design was utilized. Limiting our phenotype to HTN that occurred in the first three treatment cycles removed later cases of HTN that are more likely to be attributed to other factors, as bevacizumab-induced HTN has been shown to develop early³³. Nevertheless, we recognized the limitations of the study and approached these analyses largely as a discovery-based study.

A targeted analysis examined variants within and flanking preselected candidate genes. The top hits from the gene-based SKAT tests were *CPS1* and *FLT1*. *CPS1* encodes carbamoyl-phosphate synthase 1, an enzyme believed to be involved in NO synthesis and vasodilation. *FLT1* encodes VEGF receptor 1, which binds VEGF and acts as a decoy receptor to modulate VEGFR2 signaling. The top ten variant associations with bevacizumab-induced HTN included four SNPs located between *SLC29A1* and *HSP90AB1*. These SNPs are not in strong LD, suggesting that they could have independent effects on the toxicity. While the discovery of common variants was not the original strategy of this sequencing analysis, other than rs9381299, these SNPs are not tagged on any standard commercial GWAS or exome arrays, demonstrating the added potential of examining variants of all allele frequencies identified from sequencing data.

SLC29A1 encodes the equilibrative nucleoside transporter ENT1. ENT1 is responsible for regulating circulating levels of adenosine, which increases endothelial nitric oxide synthase (eNOS)-dependent activity via adenosine receptor signaling⁶⁵. eNOS also lies downstream of VEGF signaling, and activation of eNOS produces NO, which functions as a vasodilator and has been implicated in HTN resulting from VEGF inhibition⁶⁶. Increased circulating adenosine levels have been observed in ENT1^{-/-} mice⁶⁷, and increased extracellular adenosine concentrations have been observed with reduced ENT1 expression in HUVEC⁶⁸ and human placenta microvascular endothelial cells⁶⁹. From this, we hypothesize that variation in *SLC29A1* expression is associated with altered adenosine signaling that modulates the synthesis of NO during bevacizumab treatment.

HSP90AB1 encodes a constitutively expressed, cytosolic isoform of Hsp90, a molecular chaperone that facilitates normal folding, stability, activation, function, and proteolytic turnover of many key regulators of cell growth and survival⁷⁰. Reduced Hsp90 expression in primary HUVEC has been observed during preeclampsia⁷¹, a complication of pregnancy that is characterized by high blood pressure. Hypertension has also presented as a common adverse event during early clinical trials of Hsp90 inhibitor treatment^{72,73}. Hsp90 binds to eNOS and enhances its NO-synthesizing activity⁷⁴. Disruption of Hsp90 signaling, either by chemical inhibition or mutagenesis, has been shown to attenuate VEGF-stimulated binding of Hsp90 to eNOS, NO production, and endothelium-dependent relaxation of isolated blood vessels⁷⁴⁻⁷⁷. Thus, variants modulating the expression or function of Hsp90 may decrease baseline eNOS activity, which could be further reduced upon VEGF inhibition by bevacizumab.

Based on data from our *in silico* analyses, the identified *SLC29A1-HSP90AB1* SNPs are located in putative regulatory regions in HUVEC. Three of the four SNPs are in moderately transcribed regions just downstream of *SLC29A1* that are enriched for epigenetic marks, RNA polymerase II binding, and other genomic features associated with transcriptional activity. Collectively, these data suggest that this region may be part of an unannotated *SLC29A1* splice variant or contain an enhancer that regulates expression of a nearby gene. Variants that alter CTCF binding sites may disrupt insulator activity and permit promoter-enhancer interactions in this region. The fourth SNP, rs9381299, while not in a predicted strong transcriptionally active region, was found to be associated with increased *SLC29A1* expression in monocytes but not in other more relevant tissues like the artery. Functional

studies in vascular endothelial cell models are needed to better assess the SNP effects on both SLC29A1 and HSP90AB1 expression.

An exome-wide strategy was also used to interrogate potentially deleterious variants, including examination of associations for the aggregation of rare and low frequency variants across all genes. This analysis focused on nonsynonymous, stop codon, and splice-site variants, which are most likely to disrupt protein function; it yielded no significant findings in either the SNP-based or gene-based tests. However, the top associations in these analyses may be of interest in future studies of this phenotype. A nonsynonymous SNP in *ARHGAP8* was the top association in the SNP-based analysis. *ARHGAP8* encodes a Rho GTPase activating protein (Rho GAP) that is highly expressed in the kidney⁵⁵. Although the function of *ARHGAP8* is largely unknown, other Rho GAPs have been implicated in renal function and hypertension^{78,79}. The variant, rs6007344, was previously associated with hypertension in a study of 1503 subjects⁸⁰. It encodes a glycine to arginine change in the Rho GAP domain but is predicted to be benign by SIFT, PolyPhen-2, and CADD. *ANO2*, the top hit from the gene-based analysis, encodes anoctamin-2, a calcium-activated chloride channel. A related protein, ANO1 (TMEM16A), is implicated in hypertension, but ANO2 appears to have a role in olfactory signal transduction and mediates light perception amplification in retina.

Additional rare variant association methods and analyses of other variant subsets, including indels, were performed but did not yield significant or biologically interesting results. Indels remain a rich source of causal variants, but their analysis still poses

challenges as they are difficult to describe in a standard fashion with respect to any given reference genome, and they are prone to sequencing and annotation errors. Left-normalization was applied to the indel set to increase annotation accuracy, but methods to improve indel detection and analysis are still needed for high-confidence calls.

The *SLC29A1-HSP90AB1* SNPs identified in the candidate gene analysis were tested for association in larger, independent bevacizumab-treated cohorts. The associations of rs9381299 with early grade 3+ HTN (CALGB 40502) and SBP > 180 mmHg (ECOG-5103), and rs834576 with early grade 3+ HTN (CALGB 40502) support the discovery results. Other SNPs were not validated at a statistically significant level. The sample sizes of the three replication cohorts had 72–99% power to detect effects at a nominal significance level of 0.05 for the SNP effect sizes observed in the discovery analysis (G*Power 3⁸¹). However, these effect sizes are most likely inflated due to the small sample size of the exome sequencing cohort. Assuming a more realistic difference of 10% MAF between cases and controls, power to detect associations at $\alpha < 0.05$ is only 18–34% in the replication cohorts.

Because of the small proportion of cases in CALGB 90401, differences in clinical trial design and bevacizumab dosing, as well as demographic, clinical, and phenotypic differences between study populations, we also expanded our definition of HTN and tested associations with secondary HTN phenotypes to examine the general effects of these SNPs on HTN. rs9381299 associated with grade 2+ HTN in CALGB 90401 and CALGB 40502, and

rs3734704 associated with early grade 2+ and grade 2+ HTN in CALGB 90401. Additional validation in other populations is needed to extend these current findings.

Prior studies have identified several common SNPs associated with HTN incidence during bevacizumab treatment. None of these associations replicated in CALGB 80405, although the allele frequencies of rs3025039 (*VEGFA*), rs2305948 (*KDR*), and rs1870377 (*KDR*) differ among the toxicity subgroups. The variant allele of rs1870377 encodes a change that has been reported to increase VEGFR2 phosphorylation⁸² and binding efficiency⁸³, which may be protective against bevacizumab-induced HTN. This variant was previously associated with higher incidence of grade 2+ HTN¹⁰ but is enriched within our controls in CALGB 80405.

2.6 Conclusions

The study of genetic variation in bevacizumab-induced HTN has been mostly limited to the examination of only a small number of candidate SNPs. This is the first study to date using whole-exome sequencing to examine this toxicity. Although this study was not powered to detect significant exome-wide associations, our results suggest that variation in a novel region between *SLC29A1* and *HSP90AB1* may modify the risk of developing bevacizumab-induced HTN. This region should be prioritized for follow-up in higher-powered replication studies and in functional characterization studies to define the role of these genes in the regulation of vasodilation upon bevacizumab exposure. The prioritized lists of genes generated through multiple exploratory approaches in this study can also be compared

with those from other studies of this toxicity. These findings will contribute to a better understanding of the genetic architecture and mechanism of bevacizumab-induced HTN.

2.7 References

1. Ferrara N, Hillan KJ, Gerber HP, Novotny W. Discovery and development of bevacizumab, an anti-VEGF antibody for treating cancer. *Nat Rev Drug Discov.* 2004;3(5):391–400.
2. Zhu X, Wu S, Dahut WL, Parikh CR. Risks of proteinuria and hypertension with bevacizumab, an antibody against vascular endothelial growth factor: systematic review and meta-analysis. *Am J Kidney Dis.* 2007;49(2):186–93.
3. Ranpura V, Pulipati B, Chu D, Zhu X, Wu S. Increased risk of high-grade hypertension with bevacizumab in cancer patients: a meta-analysis. *Am J Hypertens.* 2010;23(5):460–8.
4. Avastin [package insert]. South San Francisco, CA: Genentech, Inc.; 2016. Available from: https://www.gene.com/download/pdf/avastin_prescribing.pdf
5. Schneider BP, Wang M, Radovich M, Sledge GW, Badve S, Thor A, Flockhart DA, Hancock B, Davidson N, Gralow J, Dickler M, Perez EA, Cobleigh M, Shenkier T, Edgerton S, Miller KD, ECOG 2100. Association of vascular endothelial growth factor and vascular endothelial growth factor receptor-2 genetic polymorphisms with outcome in a trial of paclitaxel compared with paclitaxel plus bevacizumab in advanced breast cancer: ECOG 2100. *J Clin Oncol.* 2008;26(28):4672–8.
6. Etienne-Grimaldi MC, Formento P, Degeorges A, Pierga JY, Delva R, Pivot X, Dalenc F, Espié M, Veyret C, Formento JL, Francoual M, Piutti M, de Crémoux P, Milano G. Prospective analysis of the impact of VEGF-A gene polymorphisms on the pharmacodynamics of bevacizumab-based therapy in metastatic breast cancer patients. *Br J Clin Pharmacol.* 2011;71(6):921–8.
7. Morita S, Uehara K, Nakayama G, Shibata T, Oguri T, Inada-Inoue M, Shimokata T, Sugishita M, Mitsuma A, Ando Y. Association between bevacizumab-related hypertension and vascular endothelial growth factor (VEGF) gene polymorphisms in Japanese patients with metastatic colorectal cancer. *Cancer Chemother Pharmacol.* 2013;71(2):405–11.
8. Sibertin-Blanc C, Mancini J, Fabre A, Lagarde A, Del Grande J, Levy N, Seitz JF, Olschwang S, Dahan L. Vascular Endothelial Growth Factor A c.*237C>T polymorphism is associated with bevacizumab efficacy and related hypertension in metastatic colorectal cancer. *Dig Liver Dis.* 2015;47(4):331–7.
9. Gampenrieder SP, Hufnagl C, Brechelmacher S, Huemer F, Hackl H, Rinnerthaler G, Romeder F, Monzo Fuentes C, Morre P, Hauser-Kronberger C, Mlineritsch B, Greil R. Endothelin-1 genetic polymorphism as predictive marker for bevacizumab in metastatic breast cancer. *Pharmacogenomics J.* 2016. doi:10.1038/tpj.2016.25 [Epub ahead of print]

10. Jain L, Sissung TM, Danesi R, Kohn EC, Dahut WL, Kummar S, Venzon D, Liewehr D, English BC, Baum CE, Yarchoan R, Giaccone G, Venitz J, Price DK, Figg WD. Hypertension and hand-foot skin reactions related to VEGFR2 genotype and improved clinical outcome following bevacizumab and sorafenib. *J Exp Clin Cancer Res.* 2010;29:95.
11. Schneider BP, Li L, Shen F, Miller KD, Radovich M, O'Neill A, Gray RJ, Lane D, Flockhart DA, Jiang G, Wang Z, Lai D, Koller D, Pratt JH, Dang CT, Northfelt D, Perez EA, Shenkier T, Cobleigh M, Smith ML, Railey E, Partridge A, Gralow J, Sparano J, Davidson NE, Foroud T, Sledge GW. Genetic variant predicts bevacizumab-induced hypertension in ECOG-5103 and ECOG-2100. *Br J Cancer.* 2014;111(6):1241–8.
12. Lambrechts D, Moisse M, Delmar P, Miles DW, Leighl N, Escudier B, Van Cutsem E, Bansal AT, Carmeliet P, Scherer SJ, de Haas S, Pallaud C. Genetic markers of bevacizumab-induced hypertension. *Angiogenesis.* 2014;17(3):685–94.
13. Lange LA, Hu Y, Zhang H, Xue C, Schmidt EM, Tang Z-Z, Bizon C, Lange EM, Smith JD, Turner EH, Jun G, Kang HM, Peloso G, Auer PL, Li K-P, Flannick J, Zhang J, Fuchsberger C, Gaulton K, Lindgren C, Locke A, Manning A, Sim X, Rivas MA, Holmen OL, Gottesman O, Lu Y, Ruderfer D, Stahl EA, Duan Q, Li Y, Durda P, Jiao S, Isaacs A, Hofman A, Bis JC, Correa A, Griswold ME, Jakobsdottir J, Smith AV, Schreiner PJ, Feitosa MF, Zhang Q, Huffman JE, Crosby J, Wassel CL, Do R, Franceschini N, Martin LW, Robinson JG, Assimes TL, Crosslin DR, Rosenthal EA, Tsai M, Rieder MJ, Farlow DN, Folsom AR, Lumley T, Fox ER, Carlson CS, Peters U, Jackson RD, van Duijn CM, Uitterlinden AG, Levy D, Rotter JI, Taylor HA, Gudnason VJ, Siscovick DS, Fornage M, Borecki IB, Hayward C, Rudan I, Chen YE, Bottinger EP, Loos RJJ, Sætrum P, Hveem K, Boehnke M, Groop L, McCarthy M, Meitinger T, Ballantyne CM, Gabriel SB, O'Donnell CJ, Post WS, North KE, Reiner AP, Boerwinkle E, Psaty BM, Altshuler DM, Kathiresan S, Lin D-Y, Jarvik GP, Cupples LA, Kooperberg C, Wilson JG, Nickerson DA, Abecasis GR, Rich SS, Tracy RP, Willer CJ. Whole-exome sequencing identifies rare and low-frequency coding variants associated with LDL cholesterol. *Am J Hum Genet.* 2014;94(2):233–45.
14. Do R, Stitzel NO, Won H-H, Jorgensen AB, Duga S, Angelica Merlini P, Kiezun A, Farrall M, Goel A, Zuk O, Guella I, Asselta R, Lange LA, Peloso GM, Auer PL, Project NES, Girelli D, Martinelli N, Farlow DN, DePristo MA, Roberts R, Stewart AFR, Saleheen D, Danesh J, Epstein SE, Sivapalaratnam S, Kees Hovingh G, Kastelein JJ, Samani NJ, Schunkert H, Erdmann J, Shah SH, Kraus WE, Davies R, Nikpay M, Johansen CT, Wang J, Hegele RA, Hechter E, März W, Kleber ME, Huang J, Johnson AD, Li M, Burke GL, Gross M, Liu Y, Assimes TL, Heiss G, Lange EM, Folsom AR, Taylor HA, Olivieri O, Hamsten A, Clarke R, Reilly DF, Yin W, Rivas MA, Donnelly P, Rossouw JE, Psaty BM, Herrington DM, Wilson JG, Rich SS, Bamshad MJ, Tracy RP, Adrienne Cupples L, Rader DJ, Reilly MP, Spertus JA, Cresci S, Hartiala J, Wilson Tang WH, Hazen SL, Allayee H, Reiner AP, Carlson CS, Kooperberg C, Jackson RD, Boerwinkle E, Lander ES, Schwartz SM, Siscovick DS, McPherson R, Tybjaerg-Hansen A, Abecasis GR, Watkins H, Nickerson DA, Ardissino D, Sunyaev SR, O'Donnell CJ, Altshuler DM,

- Gabriel S, Kathiresan S. Exome sequencing identifies rare LDLR and APOA5 alleles conferring risk for myocardial infarction. *Nature*. 2015;518(7537):102–6.
15. Purcell SM, Moran JL, Fromer M, Ruderfer D, Solovieff N, Roussos P, O’Dushlaine C, Chambert K, Bergen SE, Kähler A, Duncan L, Stahl E, Genovese G, Fernández E, Collins MO, Komiyama NH, Choudhary JS, Magnusson PKE, Banks E, Shakir K, Garimella K, Fennell T, DePristo M, Grant SGN, Haggarty SJ, Gabriel S, Scolnick EM, Lander ES, Hultman CM, Sullivan PF, McCarroll SA, Sklar P. A polygenic burden of rare disruptive mutations in schizophrenia. *Nature*. 2014;506(7487):185–90.
 16. Daneshjou R, Gamazon ER, Burkley B, Cavallari LH, Johnson JA, Klein TE, Limdi N, Hillenmeyer S, Percha B, Karczewski KJ, Langae T, Patel SR, Bustamante CD, Altman RB, Perera MA. Genetic variant in folate homeostasis is associated with lower warfarin dose in African Americans. *Blood*. 2014;124(14):2298–305.
 17. Scott SA, Collet J-P, Baber U, Yang Y, Peter I, Linderman M, Sload J, Qiao W, Kini AS, Sharma SK, Desnick RJ, Fuster V, Hajjar RJ, Montalescot G, Hulot J-S. Exome sequencing of extreme clopidogrel response phenotypes identifies B4GALT2 as a determinant of on-treatment platelet reactivity. *Clin Pharmacol Ther*. 2016;100(3):287–94.
 18. Weeke P, Mosley JD, Hanna D, Delaney JT, Shaffer C, Wells QS, Van Driest S, Karnes JH, Ingram C, Guo Y, Shyr Y, Norris K, Kannankeril PJ, Ramirez AH, Smith JD, Mardis ER, Nickerson D, George AL Jr, Roden DM. Exome sequencing implicates an increased burden of rare potassium channel variants in the risk of drug-induced long QT interval syndrome. *J Am Coll Cardiol*. 2014;63(14):1430–7.
 19. Gréen H, Hasmats J, Kupersmidt I, Edsgård D, de Petris L, Lewensohn R, Blackhall F, Vikingsson S, Besse B, Lindgren A, Brandén E, Koyi H, Peterson C, Lundeborg J. Using whole-exome sequencing to identify genetic markers for carboplatin and gemcitabine-induced toxicities. *Clin Cancer Res*. 2016;22(2):366–73.
 20. Venook AP, Blanke CD, Niedzwiecki D, Lenz H-J, Taylor JR, Hollis DR, Sutherland S, Goldberg RM. Revisiting the Cancer and Leukemia Group B/Southwest Oncology Group 80405 Trial: a phase III trial of chemotherapy and biologic agents for patients with untreated advanced colorectal adenocarcinoma. *Clin Colorectal Cancer*. 2007;6(7):536–8.
 21. Venook AP, Niedzwiecki D, Lenz H-J, Innocenti F, Mahoney MR, O’Neil BH, Shaw JE, Polite BN, Hochster HS, Atkins JN, Goldberg RM, Mayer RJ, Schilsky RL, Bertagnolli MM, Blanke CD. CALGB/SWOG 80405: Phase III trial of irinotecan/5-FU/leucovorin (FOLFIRI) or oxaliplatin/5-FU/leucovorin (mFOLFOX6) with bevacizumab (BV) or cetuximab (CET) for patients (pts) with KRAS wild-type (wt) untreated metastatic adenocarcinoma of the colon or rectum (MCR). *J Clin Oncol*. 2014;32:5s.
 22. Common Terminology for Adverse Events v3.0 (CTCAE). Cancer Therapy Evaluation Program; 2003. Available from: <http://ctep.cancer.gov/reporting/ctc.html>

23. Barnett IJ, Lee S, Lin X. Detecting rare variant effects using extreme phenotype sampling in sequencing association studies. *Genet Epidemiol.* 2013;37(2):142–51.
24. Emond MJ, Louie T, Emerson J, Zhao W, Mathias RA, Knowles MR, Wright FA, Rieder MJ, Tabor HK, Nickerson DA, Barnes KC, National Heart, Lung, and Blood Institute (NHLBI) GO Exome Sequencing Project, Lung GO, Gibson RL, Bamshad MJ. Exome sequencing of extreme phenotypes identifies DCTN4 as a modifier of chronic *Pseudomonas aeruginosa* infection in cystic fibrosis. *Nat Genet.* 2012;44(8):886–9.
25. Li H, Handsaker B, Wysoker A, Fennell T, Ruan J, Homer N, Marth G, Abecasis GR, Durbin R, 1000 Genome Project Data Processing Subgroup. The Sequence Alignment/Map format and SAMtools. *Bioinformatics.* 2009;25(16):2078–9.
26. McKenna A, Hanna M, Banks E, Sivachenko A, Cibulskis K, Kernytsky A, Garimella K, Altshuler DM, Gabriel S, Daly M, DePristo MA. The Genome Analysis Toolkit: a MapReduce framework for analyzing next-generation DNA sequencing data. *Genome Res.* 2010;20(9):1297–303.
27. Mills RE, Pittard WS, Mullaney JM, Farooq U, Creasy TH, Mahurkar AA, Kemeza DM, Strassler DS, Ponting CP, Webber C, Devine SE. Natural genetic variation caused by small insertions and deletions in the human genome. *Genome Res.* 2011;21(6):830–9.
28. DePristo MA, Banks E, Poplin R, Garimella KV, Maguire JR, Hartl C, Philippakis AA, del Angel G, Rivas MA, Hanna M, McKenna A, Fennell TJ, Kernytsky AM, Sivachenko AY, Cibulskis K, Gabriel SB, Altshuler DM, Daly MJ. A framework for variation discovery and genotyping using next-generation DNA sequencing data. *Nat Genet.* 2011;43(5):491–8.
29. Van der Auwera GA, Carneiro MO, Hartl C, Poplin R, del Angel G, Levy-Moonshine A, Jordan T, Shakir K, Roazen D, Thibault J, Banks E, Garimella KV, Altshuler DM, Gabriel S, DePristo MA. From FastQ data to high confidence variant calls: the Genome Analysis Toolkit best practices pipeline. *Curr Protoc Bioinformatics.* 2013;43:11.10.1–33.
30. Danecek P, Auton A, Abecasis GR, Albers CA, Banks E, DePristo MA, Handsaker RE, Lunter G, Marth GT, Sherry ST, McVean G, Durbin R, 1000 Genomes Project Analysis Group. The variant call format and VCFtools. *Bioinformatics.* 2011;27(15):2156–8.
31. Chang CC, Chow CC, Tellier LC, Vattikuti S, Purcell SM, Lee JJ. Second-generation PLINK: rising to the challenge of larger and richer datasets. *Gigascience.* 2015;4(1):1–16.
32. Wang K, Li M, Hakonarson H. ANNOVAR: functional annotation of genetic variants from high-throughput sequencing data. *Nucleic Acids Res.* 2010;38(16):e164.
33. Maitland ML, Bakris GL, Black HR, Chen HX, Durand JB, Elliott WJ, Ivy SP, Leier CV,

- Lindenfeld J, Liu G, Remick SC, Steingart R, Tang WHW, Cardiovascular Toxicities Panel, Convened by the Angiogenesis Task Force of the National Cancer Institute Investigational Drug Steering Committee. Initial assessment, surveillance, and management of blood pressure in patients receiving vascular endothelial growth factor signaling pathway inhibitors. *J Natl Cancer Inst.* 2010;102(9):596–604.
34. Lee S, Abecasis GR, Boehnke M, Lin X. Rare-variant association analysis: study designs and statistical tests. *Am J Hum Genet.* 2014;95(1):5–23.
 35. Wu MC, Lee S, Cai T, Li Y, Boehnke M, Lin X. Rare-variant association testing for sequencing data with the sequence kernel association test. *Am J Hum Genet.* 2011;89(1):82–93.
 36. Lee S, Emond MJ, Bamshad MJ, Barnes KC, Rieder MJ, Nickerson DA, NHLBI GO Exome Sequencing Project—ESP Lung Project Team, Christiani DC, Wurfel MM, Lin X. Optimal unified approach for rare-variant association testing with application to small-sample case-control whole-exome sequencing studies. *Am J Hum Genet.* 2012;91(2):224–37.
 37. R Core Team. R: A language and environment for statistical computing. Vienna, Austria: R Foundation for Statistical Computing; 2013. Available from: <https://www.R-project.org/>
 38. Price AL, Kryukov GV, de Bakker PIW, Purcell SM, Staples J, Wei L-J, Sunyaev SR. Pooled association tests for rare variants in exon-resequencing studies. *Am J Hum Genet.* 2010;86(6):832–8.
 39. Madsen BE, Browning SR. A groupwise association test for rare mutations using a weighted sum statistic. *PLoS Genet.* 2009;5(2):e1000384.
 40. Neale BM, Rivas MA, Voight BF, Altshuler DM, Devlin B, Orho-Melander M, Kathiresan S, Purcell SM, Roeder K, Daly MJ. Testing for an unusual distribution of rare variants. *PLoS Genet.* 2011;7(3):e1001322.
 41. Hoh J, Wille A, Ott J. Trimming, weighting, and grouping SNPs in human case-control association studies. *Genome Res.* 2001;11(12):2115–9.
 42. Ionita-Laza I, Lee S, Makarov V, Buxbaum JD, Lin X. Sequence kernel association tests for the combined effect of rare and common variants. *Am J Hum Genet.* 2013;92(6):841–53.
 43. Ward LD, Kellis M. HaploReg: a resource for exploring chromatin states, conservation, and regulatory motif alterations within sets of genetically linked variants. *Nucleic Acids Res.* 2012;40(Database issue):D930–4.
 44. Boyle AP, Hong EL, Hariharan M, Cheng Y, Schaub MA, Kasowski M, Karczewski KJ, Park J, Hitz BC, Weng S, Cherry JM, Snyder M. Annotation of functional variation in

- personal genomes using RegulomeDB. *Genome Res.* 2012;22(9):1790–7.
45. Kumar P, Henikoff S, Ng PC. Predicting the effects of coding non-synonymous variants on protein function using the SIFT algorithm. *Nat Protoc.* 2009;4(8):1073–81.
 46. Adzhubei IA, Schmidt S, Peshkin L, Ramensky VE, Gerasimova A, Bork P, Kondrashov AS, Sunyaev SR. A method and server for predicting damaging missense mutations. *Nat Methods.* 2010;7(4):248–9.
 47. Davydov EV, Goode DL, Sirota M, Cooper GM, Sidow A, Batzoglou S. Identifying a high fraction of the human genome to be under selective constraint using GERP++. *PLoS Comput Biol.* 2010;6(12):e1001025.
 48. Kircher M, Witten DM, Jain P, O’Roak BJ, Cooper GM, Shendure J. A general framework for estimating the relative pathogenicity of human genetic variants. *Nat Genet.* 2014;46(3):310–5.
 49. 1000 Genomes Project Consortium, Auton A, Brooks LD, Durbin RM, Garrison EP, Kang HM, Korbel JO, Marchini JL, McCarthy S, McVean GA, Abecasis GR. A global reference for human genetic variation. *Nature.* 2015;526(7571):68–74.
 50. Exome Variant Server. Seattle, WA: NHLBI GO Exome Sequencing Project (ESP). [cited 2016 Dec 26]. Available from: <http://evs.gs.washington.edu/EVS/>
 51. Lek M, Karczewski KJ, Minikel EV, Samocha KE, Banks E, Fennell T, O’Donnell-Luria AH, Ware JS, Hill AJ, Cummings BB, Tukiainen T, Birnbaum DP, Kosmicki JA, Duncan LE, Estrada K, Zhao F, Zou J, Pierce-Hoffman E, Berghout J, Cooper DN, Deflaux N, DePristo M, Do R, Flannick J, Fromer M, Gauthier L, Goldstein J, Gupta N, Howrigan D, Kiezun A, Kurki MI, Moonshine AL, Natarajan P, Orozco L, Peloso GM, Poplin R, Rivas MA, Ruano-Rubio V, Rose SA, Ruderfer DM, Shakir K, Stenson PD, Stevens C, Thomas BP, Tiao G, Tusie-Luna MT, Ben Weisburd, Won H-H, Yu D, Altshuler DM, Ardissino D, Boehnke M, Danesh J, Donnelly S, Elosua R, Florez JC, Gabriel SB, Getz G, Glatt SJ, Hultman CM, Kathiresan S, Laakso M, McCarroll S, McCarthy MI, McGovern D, McPherson R, Neale BM, Palotie A, Purcell SM, Saleheen D, Scharf JM, Sklar P, Sullivan PF, Tuomilehto J, Tsuang MT, Watkins HC, Wilson JG, Daly MJ, MacArthur DG. Analysis of protein-coding genetic variation in 60,706 humans. *Nat Rev Drug Discov.* 2016;536(7616):285–91.
 52. ENCODE Project Consortium. An integrated encyclopedia of DNA elements in the human genome. *Nature.* 2012;489(7414):57–74.
 53. Rosenbloom KR, Sloan CA, Malladi VS, Dreszer TR, Learned K, Kirkup VM, Wong MC, Maddren M, Fang R, Heitner SG, Lee BT, Barber GP, Harte RA, Diekhans M, Long JC, Wilder SP, Zweig AS, Karolchik D, Kuhn RM, Haussler D, Kent WJ. ENCODE data in the UCSC Genome Browser: year 5 update. *Nucleic Acids Res.* 2013;41(Database issue):D56–63.

54. Kundaje A, Meuleman W, Bilenky M, Yen A, Kheradpour P, Zhang Z, Wang J, Amin V, Whitaker JW, Ward LD, Sarkar A, Sandstrom RS, Eaton ML, Pfenning A, Wang X, Claussnitzer Yaping Liu M, Alan Harris R, Epstein CB, David Hawkins R, Lister R, Hong C, Mungall AJ, Canfield TK, Scott Hansen R, Kaul R, Bansal MS, Farh K-H, Feizi S, Karlic R, Kim A-R, Lowdon R, Elliott G, Mercer TR, Polak P, Rajagopal N, Sallari RC, Siebenthall KT, Stevens M, Thurman RE, Wu J, Zhang B, Zhou X, Abdennur N, Adli M, Akerman M, Barrera L, Antosiewicz-Bourget J, Ballinger T, Barnes MJ, Bates D, Bell RJA, Bennett DA, Bianco K, Bock C, Boyle P, Brinchmann J, Caballero-Campo P, Camahort R, Carrasco-Alfonso MJ, Charnecki T, Chen H, Chen Z, Cheng JB, Cho S, Chu A, Chung W-Y, Cowan C, Athena Deng Q, Deshpande V, Diegel M, Ding B, Durham T, Echipare L, Edsall L, Flowers D, Genbacev-Krtolica O, Gifford C, Gillespie S, Giste E, Glass IA, Gnirke A, Gormley M, Gu H, Gu J, Hafler DA, Hangauer MJ, Hariharan M, Hatan M, Haugen E, He Y, Heimfeld S, Herlofsen S, Hou Z, Humbert R, Issner R, Jackson AR, Jia H, Jiang P, Johnson AK, Kadlec T, Kamoh B, Kapidzic M, Kent J, Kim A, Kleinewietfeld M, Klugman S, Krishnan J, Kuan S, Kutayavin T, Lee A-Y, Lee K, Li J, Li N, Li Y, Ligon KL, Lin S, Lin Y, Liu J, Liu Y, Luckey CJ, Ma YP, Maire C, Marson A, Mattick JS, Mayo M, McMaster M, Metsky H, Mikkelsen T, Miller D, Miri M, Mukame E, Nagarajan RP, Neri F, Nery J, Nguyen T, O'Geen H, Paithankar S, Papayannopoulou T, Pelizzola M, Plettner P, Propson NE, Raghuraman S, Raney BJ, Raubitschek A, Reynolds AP, Richards H, Riehle K, Rinaudo P, Robinson JF, Rockweiler NB, Rosen E, Rynes E, Schein J, Sears R, Sejnowski T, Shafer A, Shen L, Shoemaker R, Sigaroudinia M, Slukvin I, Stehling-Sun S, Stewart R, Subramanian SL, Suknuntha K, Swanson S, Tian S, Tilden H, Tsai L, Urich M, Vaughn I, Vierstra J, Vong S, Wagner U, Wang H, Wang T, Wang Y, Weiss A, Whitton H, Wildberg A, Witt H, Won K-J, Xie M, Xing X, Xu I, Xuan Z, Ye Z, Yen C-A, Yu P, Zhang X, Zhang X, Zhao J, Zhou Y, Zhu J, Zhu Y, Ziegler S, Beaudet AE, Boyer LA, De Jager PL, Farnham PJ, Fisher SJ, Haussler D, Jones SJM, Li W, Marra MA, McManus MT, Thomson JA, Tlsty TD, Tsai L-H, Wang W, Waterland RA, Zhang MQ, Chadwick LH, Bernstein BE, Costello JF, Ecker JR, Hirst M, Meissner A, Milosavljevic A, Ren B, Stamatoyannopoulos JA, Wang T, Kellis M, Ernst J, Heravi-Moussavi A, Wang J, Ziller MJ, Schultz MD, Quon G, Wu Y-C, Pfenning AR, Claussnitzer M, Liu Y, Coarfa C, Harris RA, Shores N, Gjoneska E, Leung D, Xie W, Hawkins RD, Gascard P, Mungall AJ, Moore R, Chuah E, Tam A, Hansen RS, Sabo PJ, Carles A, Dixon JR, Kulkarni A, Li D, Neph SJ, Onuchic V, Ray P, Sinnott-Armstrong NA, Wu J, Zhang B, Zhou X, Beaudet AE, Boyer LA, De Jager PL, Farnham PJ, Fisher SJ, Haussler D, Jones SJM, Li W, Marra MA, McManus MT, Sunyaev S, Thomson JA, Tlsty TD, Tsai L-H, Wang W, Waterland RA, Zhang MQ, Chadwick LH, Costello JF, Ecker JR, Hirst M, Meissner A, Milosavljevic A, Ren B, Stamatoyannopoulos JA, Wang T. Integrative analysis of 111 reference human epigenomes. *Nature*. 2015;518(7539):317–30.
55. Lonsdale J, Thomas J, Salvatore M, Phillips R, Lo E, Shad S, Hasz R, Walters G, Garcia F, Young N, Foster B, Moser M, Karasik E, Gillard B, Ramsey K, Sullivan S, Bridge J, Magazine H, Syron J, Fleming J, Siminoff L, Traino H, Mosavel M, Barker L, Jewell S, Rohrer D, Maxim D, Filkins D, Harbach P, Cortadillo E, Berghuis B, Turner L, Hudson E, Feenstra K, Sobin L, Robb J, Branton P, Korzeniewski G, Shive C, Tabor D, Qi L, Groch K, Nampally S, Buia S, Zimmerman A, Smith A, Burges R, Robinson K, Valentino K, Bradbury D, Cosentino M, Diaz-Mayoral N, Kennedy M, Engel T, Williams P,

- Erickson K, Ardlie K, Winckler W, Getz G, DeLuca D, MacArthur D, Kellis M, Thomson A, Young T, Gelfand E, Donovan M, Meng Y, Grant G, Mash D, Marcus Y, Basile M, Liu J, Zhu J, Tu Z, Cox NJ, Nicolae DL, Gamazon ER, Im HK, Konkashbaev A, Pritchard J, Stevens M, Flutre T, Wen X, Dermitzakis ET, Lappalainen T, Guigo R, Monlong J, Sammeth M, Koller D, Battle A, Mostafavi S, McCarthy M, Rivas M, Maller J, Rusyn I, Nobel A, Wright F, Shabalin A, Feolo M, Sharopova N, Sturcke A, Paschal J, Anderson JM, Wilder EL, Derr LK, Green ED, Struewing JP, Temple G, Volpi S, Boyer JT, Thomson EJ, Guyer MS, Ng C, Abdallah A, Colantuoni D, Insel TR, Koester SE, Little AR, Bender PK, Lehner T, Yao Y, Compton CC, Vaught JB, Sawyer S, Lockhart NC, Demchok J, Moore HF. The Genotype-Tissue Expression (GTEx) project. *Nat Genet.* 2013;45(6):580–5.
56. Yu CH, Pal LR, Moulton J. Consensus genome-wide expression quantitative trait loci and their relationship with human complex trait disease. *OMICS.* 2016;20(7):400–14.
 57. Staley JR, Blackshaw J, Kamat MA, Ellis S, Surendran P, Sun BB, Paul DS, Freitag D, Burgess S, Danesh J, Young R, Butterworth AS. PhenoScanner: a database of human genotype–phenotype associations. *Bioinformatics.* 2016;32(20):3207–9.
 58. Kamburov A, Pentchev K, Galicka H, Wierling C, Lehrach H, Herwig R. ConsensusPathDB: toward a more complete picture of cell biology. *Nucleic Acids Res.* 2011;39(Database issue):D712–7.
 59. Chen J, Bardes EE, Aronow BJ, Jegga AG. ToppGene Suite for gene list enrichment analysis and candidate gene prioritization. *Nucleic Acids Res.* 2009;37(Web Server issue):W305–11.
 60. Rugo HS, Barry WT, Moreno-Aspitia A, Lyss AP, Cirrincione C, Leung E, Mayer EL, Naughton M, Toppmeyer D, Carey LA, Perez EA, Hudis C, Winer EP. Randomized phase III trial of paclitaxel once per week compared with nanoparticle albumin-bound nab-paclitaxel once per week or ixabepilone with bevacizumab as first-line chemotherapy for locally recurrent or metastatic breast cancer: CALGB 40502/NCCTG N063H (Alliance). *J Clin Oncol.* 2015;33(21):2361–9.
 61. Kelly WK, Halabi S, Carducci M, George D, Mahoney JF, Stadler WM, Morris M, Kantoff P, Monk JP, Kaplan E, Vogelzang NJ, Small EJ. Randomized, double-blind, placebo-controlled phase III trial comparing docetaxel and prednisone with or without bevacizumab in men with metastatic castration-resistant prostate cancer: CALGB 90401. *J Clin Oncol.* 2012;30(13):1534–40.
 62. Das S, Forer L, Schönherr S, Sidore C, Locke AE, Kwong A, Vrieze SI, Chew EY, Levy S, McGue M, Schlessinger D, Stambolian D, Loh P-R, Iacono WG, Swaroop A, Scott LJ, Cucca F, Kronenberg F, Boehnke M, Abecasis GR, Fuchsberger C. Next-generation genotype imputation service and methods. *Nat Genet.* 2016;48(10):1284–7.
 63. Ernst J, Kellis M. ChromHMM: automating chromatin-state discovery and characterization. *Nat Methods.* 2012;9(3):215–6.

64. Fairfax BP, Makino S, Radhakrishnan J, Plant K, Leslie S, Dilthey A, Ellis P, Langford C, Vannberg FO, Knight JC. Genetics of gene expression in primary immune cells identifies cell type-specific master regulators and roles of HLA alleles. *Nat Genet.* 2012;44(5):502–10.
65. San Martín R, Sobrevia L. Gestational diabetes and the adenosine/L-arginine/nitric oxide (ALANO) pathway in human umbilical vein endothelium. *Placenta.* 2006;27(1):1–10.
66. Facemire CS, Nixon AB, Griffiths R, Hurwitz H, Coffman TM. Vascular endothelial growth factor receptor 2 controls blood pressure by regulating nitric oxide synthase expression. *Hypertension.* 2009;54(3):652–8.
67. Rose JB, Naydenova Z, Bang A, Ramadan A, Klawitter J, Schram K, Sweeney G, Grenz A, Eltzschig H, Hammond J, Choi D-S, Coe IR. Absence of equilibrative nucleoside transporter 1 in ENT1 knockout mice leads to altered nucleoside levels following hypoxic challenge. *Life Sci.* 2011;89(17-18):621–30.
68. Vásquez G, Sanhueza F, Vásquez R, González M, San Martín R, Casanello P, Sobrevia L. Role of adenosine transport in gestational diabetes-induced L-arginine transport and nitric oxide synthesis in human umbilical vein endothelium. *J Physiol.* 2004;560(Pt 1):111–22.
69. Escudero C, Casanello P, Sobrevia L. Human equilibrative nucleoside transporters 1 and 2 may be differentially modulated by A2B adenosine receptors in placenta microvascular endothelial cells from pre-eclampsia. *Placenta.* 2008;29(9):816–25.
70. Taipale M, Jarosz DF, Lindquist S. HSP90 at the hub of protein homeostasis: emerging mechanistic insights. *Nat Rev Mol Cell Biol.* 2010;11(7):515–28.
71. Gu Y, Lewis DF, Zhang Y, Groome LJ, Wang Y. Increased superoxide generation and decreased stress protein Hsp90 expression in human umbilical cord vein endothelial cells (HUVECs) from pregnancies complicated by preeclampsia. *Hypertens Pregnancy.* 2006;25(3):169–82.
72. Yong K, Cavet J, Johnson P, Morgan G, Williams C, Nakashima D, Akinaga S, Oakervee H, Cavenagh J. Phase I study of KW-2478, a novel Hsp90 inhibitor, in patients with B-cell malignancies. *Br J Cancer.* 2016;114(1):7–13.
73. Maddocks K, Hertlein E, Chen TL, Wagner AJ, Ling Y, Flynn J, Phelps M, Johnson AJ, Byrd JC, Jones JA. A phase I trial of the intravenous Hsp90 inhibitor alvespimycin (17-DMAG) in patients with relapsed chronic lymphocytic leukemia/small lymphocytic lymphoma. *Leuk Lymphoma.* 2016;57(9):2212–5.
74. García-Cardena G, Fan R, Shah V, Sorrentino R, Cirino G, Papapetropoulos A, Sessa WC. Dynamic activation of endothelial nitric oxide synthase by Hsp90. *Nature.* 1998;392:821–4.

75. Papapetropoulos A, García-Cardeña G, Madri JA, Sessa WC. Nitric oxide production contributes to the angiogenic properties of vascular endothelial growth factor in human endothelial cells. *J Clin Invest*. 1997;100(12):3131–9.
76. Miao RQ, Fontana J, Fulton D, Lin MI, Harrison KD, Sessa WC. Dominant-negative Hsp90 reduces VEGF-stimulated nitric oxide release and migration in endothelial cells. *Arterioscler Thromb Vasc Biol*. 2008;28(1):105–11.
77. Duval M, Le Bœuf F, Huot J, Gratton J-P. Src-mediated phosphorylation of Hsp90 in response to vascular endothelial growth factor (VEGF) is required for VEGF receptor-2 signaling to endothelial NO synthase. *Mol Biol Cell*. 2007;18(11):4659–68.
78. Kato N, Loh M, Takeuchi F, Verweij N, Wang X, Zhang W, Kelly TN, Saleheen D, Lehne B, Leach IM, Drong AW, Abbott J, Wahl S, Tan S-T, Scott WR, Campanella G, Chadeau-Hyam M, Afzal U, Ahluwalia TS, Bonder MJ, Chen P, Dehghan A, Edwards TL, Esko T, Go MJ, Harris SE, Hartiala J, Kasela S, Kasturiratne A, Khor C-C, Kleber ME, Li H, Mok ZY, Nakatochi M, Sapari NS, Saxena R, Stewart AFR, Stolk L, Tabara Y, Teh AL, Wu Y, Wu J-Y, Zhang Y, Aits I, Da Silva Couto Alves A, Das S, Dorajoo R, Hopewell JC, Kim YK, Koivula RW, Luan J, Lyytikäinen L-P, Nguyen QN, Pereira MA, Postmus I, Raitakari OT, Bryan MS, Scott RA, Sorice R, Tragante V, Traglia M, White J, Yamamoto K, Zhang Y, Adair LS, Ahmed A, Akiyama K, Asif R, Aung T, Barroso I, Bjornnes A, Braun TR, Cai H, Chang L-C, Chen C-H, Cheng C-Y, Chong Y-S, Collins R, Courtney R, Davies G, Delgado G, Do LD, Doevendans PA, Gansevoort RT, Gao Y-T, Grammer TB, Grarup N, Grewal J, Gu D, Wander GS, Hartikainen A-L, Hazen SL, He J, Heng C-K, Hixson JE, Hofman A, Hsu C, Huang W, Husemoen LLN, Hwang J-Y, Ichihara S, Igase M, Isono M, Justesen JM, Katsuya T, Kibriya MG, Kim YJ, Kishimoto M, Koh W-P, Kohara K, Kumari M, Kwek K, Lee NR, Lee J, Liao J, Lieb W, Liewald DCM, Matsubara T, Matsushita Y, Meitinger T, Mihailov E, Milani L, Mills R, Mononen N, Müller-Nurasyid M, Nabika T, Nakashima E, Ng HK, Nikus K, Nutile T, Ohkubo T, Ohnaka K, Parish S, Paternoster L, Peng H, Peters A, Pham ST, Pinidiyapathirage MJ, Rahman M, Rakugi H, Rolandsson O, Rozario MA, Ruggiero D, Sala CF, Sarju R, Shimokawa K, Snieder H, Sparsø T, Spiering W, Starr JM, Stott DJ, Stram DO, Sugiyama T, Szymczak S, Tang WHW, Tong L, Trompet S, Turjanmaa V, Ueshima H, Uitterlinden AG, Umemura S, Vaarasmaki M, van Dam RM, van Gilst WH, van Veldhuisen DJ, Viikari JS, Waldenberger M, Wang Y, Wang A, Wilson R, Wong TY, Xiang Y-B, Yamaguchi S, Ye X, Young RD, Young TL, Yuan J-M, Zhou X, Asselbergs FW, Ciullo M, Clarke R, Deloukas P, Franke A, Franks PW, Franks S, Friedlander Y, Gross MD, Guo Z, Hansen T, Jarvelin M-R, Jørgensen T, Jukema JW, Kähönen M, Kajio H, Kivimaki M, Lee J-Y, Lehtimäki T, Linneberg A, Miki T, Pedersen O, Samani NJ, Sørensen TIA, Takayanagi R, Toniolo D, Ahsan H, Allayee H, Chen Y-T, Danesh J, Deary IJ, Franco OH, Franke L, Heijman BT, Holbrook JD, Isaacs A, Kim B-J, Lin X, Liu J, März W, Metspalu A, Mohlke KL, Sanghera DK, Shu X-O, van Meurs JBJ, Vithana E, Wickremasinghe AR, Wijmenga C, Wolffenbuttel BHW, Yokota M, Zheng W, Zhu D, Vineis P, Kyrtopoulos SA, Kleinjans JCS, McCarthy MI, Soong R, Gieger C, Scott J, Teo YY, He J, Elliott P, Tai ES, van der Harst P, Kooner JS, Chambers JC. Trans-ancestry genome-wide association study identifies 12 genetic loci influencing blood pressure and implicates a role for DNA methylation. *Nat Genet*.

2015;47(11):1282–93.

79. Loirand G, Pacaud P. Involvement of Rho GTPases and their regulators in the pathogenesis of hypertension. *Small GTPases*. 2014;5(4):e983866.
80. Akasaka H, Katsuya T, Saitoh S, Rakugi H, Ura N, Ogihara T, Shimamoto K. Rho GTPase activating protein 8 gene polymorphism and genetic predisposition to hypertension: the Tanno Sobetsu Study. *Circ J*. 2005;69(Suppl I):560.
81. Faul F, Erdfelder E, Lang A-G, Buchner A. G*Power 3: a flexible statistical power analysis program for the social, behavioral, and biomedical sciences. *Behav Res Methods*. 2007;39(2):175–91.
82. Glubb DM, Cerri E, Giese A, Zhang W, Mirza O, Thompson EE, Chen P, Das S, Jassem J, Rzyman W, Lingen MW, Salgia R, Hirsch FR, Dziadziuszko R, Ballmer-Hofer K, Innocenti F. Novel functional germline variants in the VEGF receptor 2 gene and their effect on gene expression and microvessel density in lung cancer. *Clin Cancer Res*. 2011;17(16):5257–67.
83. Wang Y, Zheng Y, Zhang W, Yu H, Lou K, Zhang Y, Qin Q, Zhao B, Yang Y, Hui R. Polymorphisms of KDR gene are associated with coronary heart disease. *J Am Coll Cardiol*. 2007;50(8):760–7.

Chapter 3: Functional Characterization of the Effects of Bevacizumab on Adenosine Signaling

3.1 Abstract

Bevacizumab-induced hypertension (HTN) is a common dose-limiting toxicity that can lead to other cardiovascular complications. The sequencing analysis described in Chapter 2 identified putative regulatory variants near *SLC29A1* associated with bevacizumab-induced HTN. *SLC29A1* encodes ENT1, a member of the endothelial nucleoside transporter family that regulates extracellular adenosine levels and therefore adenosine signaling. To examine the role of ENT1 in the pathogenesis of bevacizumab-induced HTN, studies were performed to measure the effects of adenosine and bevacizumab treatment on human umbilical vein endothelial cells. Pharmacological inhibition of ENT1 increased levels of cyclic AMP (cAMP), a marker of adenosine receptor activation, and levels of the vasodilatory molecule nitric oxide (NO), confirming that ENT1 inhibition increases adenosine signaling. Overexpression of *SLC29A1* disrupted adenosine signaling and resulted in decreased NO levels, with a greater reduction in NO following bevacizumab treatment under conditions of elevated *SLC29A1* expression. These early results support the hypothesis that variation in *SLC29A1* expression contributes to interindividual variability in bevacizumab-induced HTN, and low adenosine levels during angiogenesis inhibition may sensitize patients to a rise in blood pressure during bevacizumab treatment.

3.2 Introduction

Adenosine is an endogenous purine nucleoside that is a building block for nucleic acids and adenosine triphosphate (ATP), an essential molecule for cellular energy transfer.

Adenosine also plays an important role as a signaling molecule in many physiological processes, with general effects on tissue protection and repair¹. Basal extracellular adenosine concentrations normally range from 30–200 nM, and can reach levels of up to 30 μ M in response to cellular damage such as hypoxia, ischemia, and inflammation² and local concentrations as high as 100 μ M³. One of adenosine's effects is the promotion of vasodilation, and adenosine infusion has been shown to decrease arterial blood pressure⁴.

Adenosine signals through four subtypes of G-protein-coupled receptors: A_1 , A_{2A} , A_{2B} , and A_3 ¹ (Figure 3.1). Adenosine-stimulated vasodilation in most arteries and vascular beds is primarily mediated by the A_{2A} receptor and, to a lesser extent, the A_{2B} receptor⁵. Activation of A_2 receptors on vascular endothelial and smooth muscle cells increases adenylyl cyclase activity and results in an increase in intracellular cyclic AMP (cAMP)⁵ (Figure 3.2).

Adenosine-induced release of endothelial nitric oxide synthase (eNOS)-dependent nitric oxide (NO) from endothelial cells as well as opening of K^+ channels in smooth muscle cells both contribute to vasodilation⁵. Adenosine has also been reported to increase endothelial synthesis of prostacyclin (PGI_2)⁶, another vasodilatory molecule.

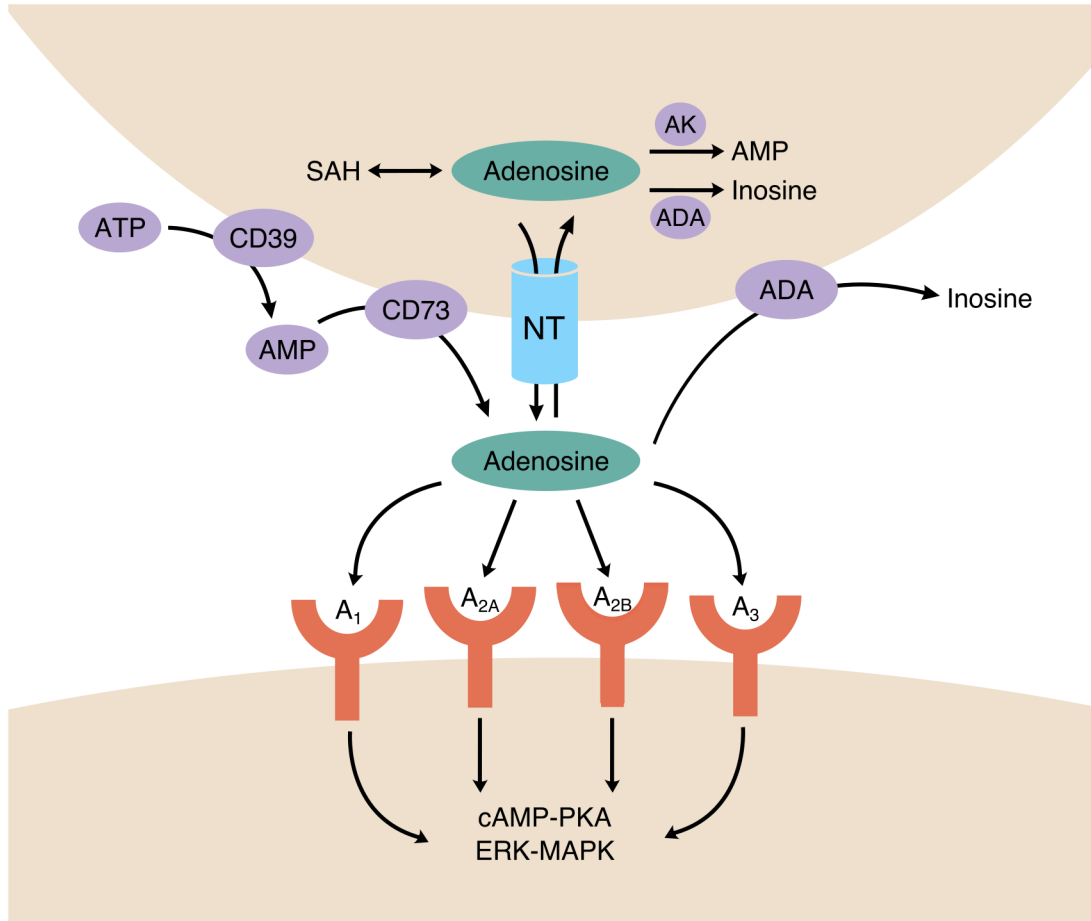
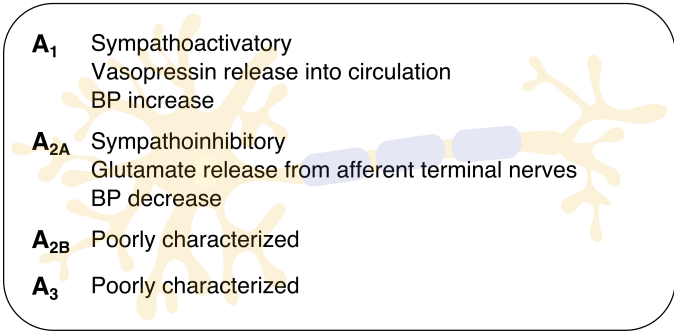
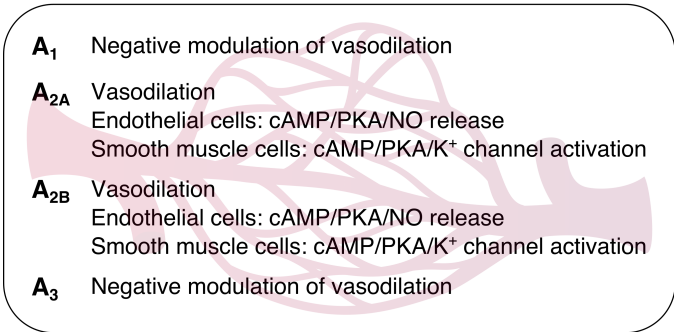


Figure 3.1. Adenosine and adenosine receptor signaling. Extracellular adenosine is primarily derived from the conversion of ATP to AMP by CD39, and AMP to adenosine by CD73. Adenosine is metabolized to inosine by adenosine deaminase (ADA), to AMP by adenosine kinase (AK), or to S-adenosylhomocysteine (SAH). Extracellular adenosine concentrations are further regulated by the activity of nucleoside transporters (NT). Adenosine can bind to four different G-protein-coupled receptor subtypes (A₁, A_{2A}, A_{2B}, A₃), activating secondary messenger pathways. cAMP, cyclic AMP; PKA, protein kinase A; ERK, extracellular signal-regulated kinase; MAPK, mitogen-activated protein kinase.

Brain and peripheral nervous system

- 
- A₁** Sympathoactivatory
Vasopressin release into circulation
BP increase
 - A_{2A}** Sympathoinhibitory
Glutamate release from afferent terminal nerves
BP decrease
 - A_{2B}** Poorly characterized
 - A₃** Poorly characterized

Blood vessels

- 
- A₁** Negative modulation of vasodilation
 - A_{2A}** Vasodilation
Endothelial cells: cAMP/PKA/NO release
Smooth muscle cells: cAMP/PKA/K⁺ channel activation
 - A_{2B}** Vasodilation
Endothelial cells: cAMP/PKA/NO release
Smooth muscle cells: cAMP/PKA/K⁺ channel activation
 - A₃** Negative modulation of vasodilation

Kidneys

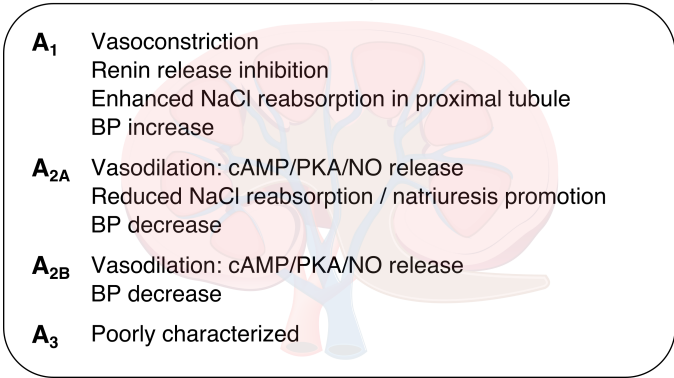
- 
- A₁** Vasoconstriction
Renin release inhibition
Enhanced NaCl reabsorption in proximal tubule
BP increase
 - A_{2A}** Vasodilation: cAMP/PKA/NO release
Reduced NaCl reabsorption / natriuresis promotion
BP decrease
 - A_{2B}** Vasodilation: cAMP/PKA/NO release
BP decrease
 - A₃** Poorly characterized

Figure 3.2. Effects of adenosine receptor signaling on the regulation of blood pressure.
Adapted from Zapata-Sudo *et al*⁶.

NO and PGI₂ also lie downstream of vascular endothelial growth factor (VEGF) signaling and have been implicated in hypertension (HTN) resulting from VEGF inhibition⁷.

Concentration-dependent increases in VEGF expression have been shown to be mediated by adenosine A₂ receptor signaling in cultured endothelial cells^{8,9}, and direct infusion of

adenosine increased plasma VEGF concentrations in humans⁴. In this way, adenosine may promote NO and PGI₂ synthesis both directly and through upregulation of VEGF expression.

Extracellular adenosine concentrations are regulated by ectonucleotidase-mediated hydrolysis of adenine nucleotides at the extracellular surface of tissues, metabolism by adenosine kinase or adenosine deaminase, or by transporter-mediated movement across cell membranes^{1,2} (Figure 3.1). Such transporters include equilibrative nucleoside transporters (ENTs) and concentrative nucleoside transporters (CNTs). ENTs regulate circulating levels of adenosine by mediating bidirectional transport across membranes via facilitated diffusion down a concentration gradient¹⁰. ENT1, one of four members of the ENT family, is ubiquitously but differentially expressed across tissues¹¹. Endothelial cells express both ENT1 and ENT2, but ENT1 is responsible for approximately 80% of adenosine transport in endothelial cells, with ENT2 mediating the remaining 20%¹². Elevated circulating adenosine levels have been detected in ENT1^{-/-} mice^{13,14}, and increased extracellular adenosine concentrations have been observed with reduced ENT1 expression in human endothelial cells^{15,16}. From this, it may be expected that decreases in ENT1 expression or function would then increase adenosine-mediated NO synthesis via an accumulation of extracellular adenosine (Figure 3.3).

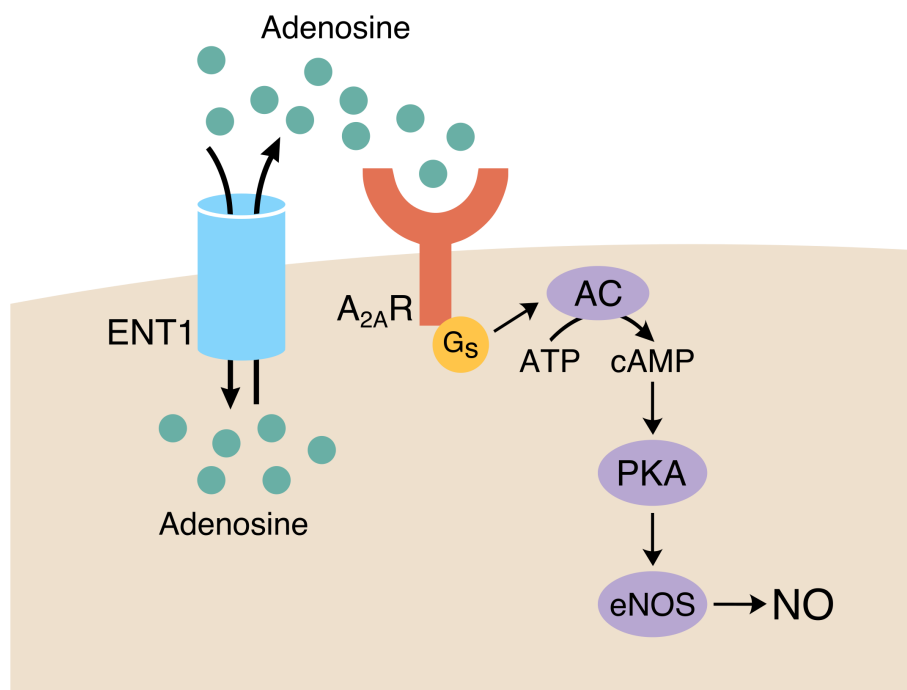


Figure 3.3. Adenosine signaling increases endothelial nitric oxide synthase activity and nitric oxide production. Extracellular adenosine is partially regulated by transport of adenosine across endothelial cell membranes by equilibrative nucleoside transporter 1 (ENT1). Adenosine-activated, G_s -coupled A_{2A} receptor ($A_{2A}R$) signaling leads to endothelial nitric oxide synthase (eNOS)-dependent nitric oxide (NO) synthesis. AC, adenylyl cyclase; cAMP; cyclic AMP; PKA, protein kinase A.

ENT1 is encoded by *SLC29A1*, which contains relatively few common polymorphisms¹⁷. A single haplotype, ENT1*1, accounted for 91.3% of an ethnically diverse DNA sample set¹⁸, and only six coding variants, two nonsynonymous and four synonymous, have been reported, all at low allele frequencies¹⁷. The two nonsynonymous variants (I216T, E391K) display normal nucleoside and nucleoside drug uptake kinetics¹⁸. However, *SLC29A1* mRNA and ENT1 protein expression are highly variable among individuals and across tissue types^{19,20}, which could be due in part to genetic variation in regulatory regions. The *SLC29A1* promoter contains many putative transcription factor binding sites¹⁹, and ENT1 expression has been shown to be regulated by a variety of factors including cell cycle phase,

cell differentiation, deoxynucleotide levels, hypoxia, and phorbol ester treatment¹¹. ENT1 expression is also downregulated in several pathological conditions including gestational diabetes, diabetes mellitus, hyperglycemia, and preeclampsia²¹ Expression in biopsy samples also varies across cancer types and has been correlated with sensitivity to cytotoxic nucleoside analogs^{11,20}.

The known effects of VEGF, adenosine, and ENT1 on vasodilation suggest that variation in ENT1 expression and function could influence blood pressure during VEGF inhibition with bevacizumab. The sequencing analysis described in Chapter 2 identified putative regulatory variants near *SLC29A1* associated with bevacizumab-induced HTN. The evidence that SNPs in this region could alter *SLC29A1* expression led to the hypothesis that increased basal levels of ENT1 are associated with reduced adenosine signaling that modulates the response of endothelial cells to bevacizumab treatment. To functionally characterize the role of ENT1 in the pathogenesis of bevacizumab-induced HTN, studies were performed in cultured human endothelial cells exposed to bevacizumab. Markers of adenosine and vasodilatory signaling were measured upon modulation of adenosine receptor function, VEGF receptor function, ENT1 function, or *SLC29A1* expression.

3.3 Materials and Methods

3.3.1 Cell culture

Human umbilical vein endothelial cells (HUVEC; C0035C; Thermo Fisher Scientific Inc., Waltham, MA) were maintained in endothelial cell growth medium-2 (EGM-2; Lonza,

Walkersville, MD) at 37 °C with 5% CO₂. Cells within passages 2–5 were seeded on 24-well collagen-coated plates for experiments.

3.3.2 Pharmacological treatment

HUVEC were serum-starved overnight in endothelial basal medium-2 (EBM-2; Lonza) with 0.5% fetal bovine serum. Cells were then treated for one hour at 37 °C with adenosine (Sigma-Aldrich, St. Louis, MO) or 5'-N-ethylcarboxamidoadenosine (NECA; Abcam, Cambridge, MA). Where indicated, human VEGF165 (50 ng/mL; Sigma-Aldrich) and bevacizumab (at 10X molar ratio of VEGF; provided by Genentech, South San Francisco, CA) were added during the 1-hour treatment period.

For inhibitor experiments, cells were pre-incubated for 30 minutes at 37 °C with non-selective adenosine receptor antagonist CGS-15943 (1 μM; Tocris Bioscience, Bristol, UK), VEGFR2 inhibitor ZM323881 hydrochloride (HCl) (1 μM; Tocris Bioscience), or ENT1 inhibitor *S*-(4-Nitrobenzyl)-6-thioinosine (NBTI, 1 μM; Sigma-Aldrich). Inhibitors were added at the same concentrations during the 1-hour treatment period.

3.3.3 Overexpression of SLC29A1

At approximately 90% confluency, HUVEC were transiently transfected according to the manufacturer's protocol with 0.75 μL/well Lipofectamine 3000 (Thermo Fisher), 1 μL/well P3000 reagent (Thermo Fisher), and 500 ng/well plasmid DNA in EGM-2. Cells were transfected with pcDNA3.1(+) vector containing human SLC29A1 cDNA (ORF clone ID OHu16500D; GenScript, Piscataway, NJ). HUVEC transfected with empty pcDNA3.1(+)

vector (Thermo Fisher) were used as negative controls. Cells were incubated at 37 °C for 20 hours following transfection, then serum-starved for four hours (instead of overnight as in untransfected cells) prior to pharmacological treatment.

To confirm SLC29A1 overexpression, RNA was isolated using the RNeasy Mini Kit (Qiagen, Valencia, CA) and reverse transcribed using the iScript cDNA Synthesis Kit (Bio-Rad, Hercules, CA), according to the manufacturers' protocols. Quantitative real-time PCR reactions prepared with Maxima SYBR Green/ROX qPCR Master Mix (Thermo Fisher) were run on the 7900HT Fast Real-time PCR System (Applied Biosystems, Foster City, CA) at 95 °C for 10 min, followed by 40 cycles at 95 °C for 15 s and 60 °C for 1 min. qRT-PCR data were analyzed by SDS software v2.4 (Applied Biosystems).

3.3.4 Measurement of cyclic AMP and nitric oxide

Intracellular cAMP levels were measured with a Human cAMP ELISA kit (ab133051; Abcam) following sample acetylation. Total nitrate and nitrite levels, as a measure of nitric oxide, were measured with a colorimetric Nitric Oxide Assay kit (ab65328; Abcam). Levels of 6-keto-Prostaglandin F₁ alpha (6k-PGF₁ alpha) and 2,3-dinor-6-keto-Prostaglandin F₁ alpha (2,3d-6k-PGF₁ alpha), the two major metabolites of prostacyclin, were measured with a Urinary Prostacyclin ELISA kit (ab133032; Abcam).

3.3.5 Statistical analysis

Linear trends across levels of adenosine or NECA were assessed by a Cochran-Armitage test. Differences between groups were analyzed using unpaired t-test, two-way analysis of

variance (ANOVA), or three-way ANOVA, as appropriate. Differences with two-sided P -values < 0.05 were considered statistically significant. Statistical analyses and visualization were conducted using the R statistical environment²² and ggplot2²³.

3.4 Results

3.4.1 Characterization of adenosine and VEGF signaling in HUVEC

To establish the dose-dependent effects of adenosine in HUVEC, cells were treated with increasing concentrations of either adenosine or NECA, an adenosine analog. cAMP levels, as a measure of adenosine receptor signaling, increased as a function of NECA concentration (Figure 3.4A). Increases in levels of NO and PGI₂ (Figures 3.4B and 3.4C) also showed NECA dose dependency. VEGF (50 ng/mL) was added to increase the robustness of VEGF signaling, and the levels of NO and PGI₂ were generally higher in the presence of exogenous VEGF (Figure 3.4). Increases in cAMP, NO, and PGI₂ were similar between NECA and adenosine treatment, and a dose-dependent response to adenosine in the presence of VEGF was still observed for cAMP, NO, and PGI₂ levels (Figure 3.5).

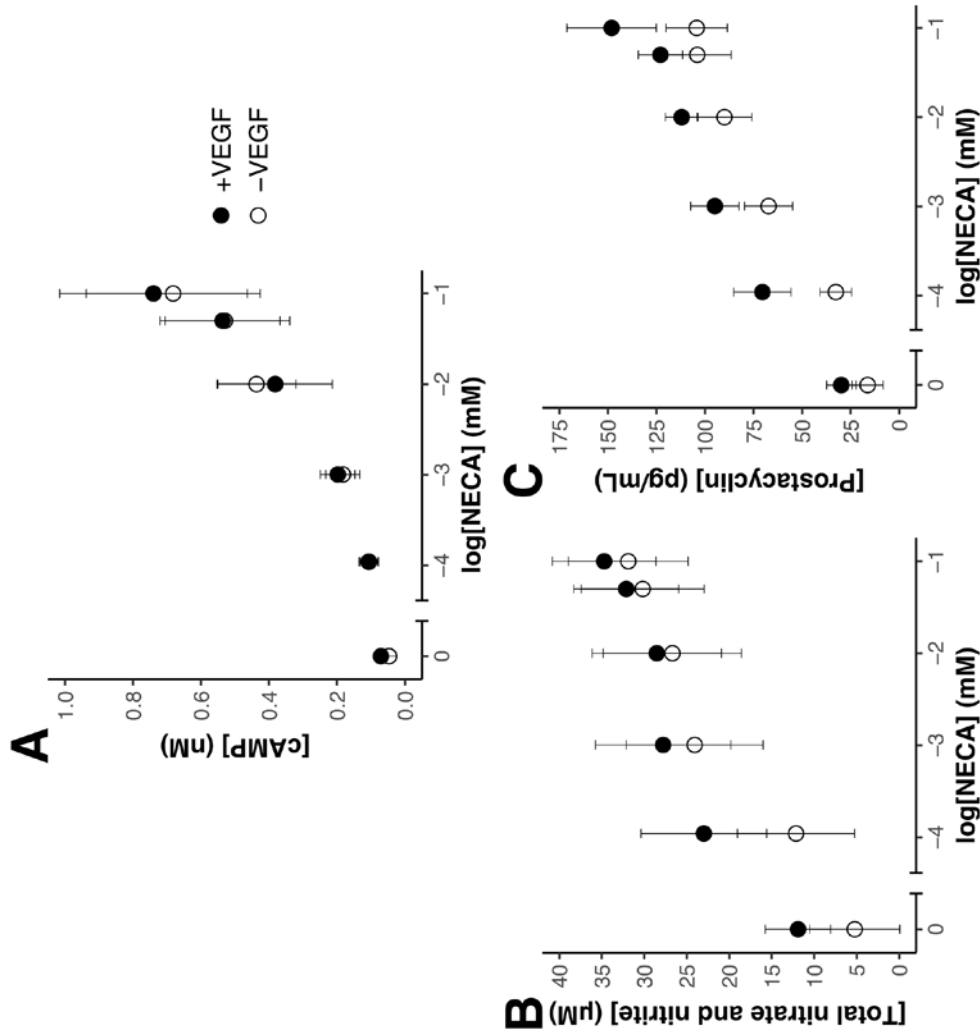


Figure 3.4. Effects of NECA and VEGF on adenosine and VEGF signaling in HUVEC. Treatment of HUVEC with the adenosine analog NECA increased levels of A) cyclic AMP (cAMP; $P = 0.001$), B) nitric oxide (NO; $P = 0.01$), and C) prostacyclin (PGI_2 ; $P = 0.02$) in a NECA dose-dependent manner. The addition of 50 ng/mL exogenous VEGF increased production of NO ($P = 0.04$) and PGI_2 ($P = 1 \times 10^{-5}$) but not cAMP. Values are expressed as means \pm standard deviations from three or four independent experiments. The increase in each marker across NECA concentrations was assessed by a Cochran-Armitage trend test. Differences between VEGF-treated and untreated cells at each NECA concentration were analyzed by two-way ANOVA.

To determine how much of the measured effects on cAMP, NO and PGI₂ were stimulated through adenosine receptor signaling, HUVEC were treated with the non-selective adenosine receptor antagonist CGS-15943 prior to and during exposure to adenosine and VEGF. cAMP levels decreased by over 80% upon treatment with CGS-15943 (Figure 3.6A), demonstrating minimal non-adenosine-stimulated cAMP levels in the system. NO levels were decreased by half in the presence of CGS-15943 (Figure 3.6B). Preliminary results show that CGS-15943 also reduces PGI₂ levels by approximately 25% in the presence of 10 μM NECA (data not shown).

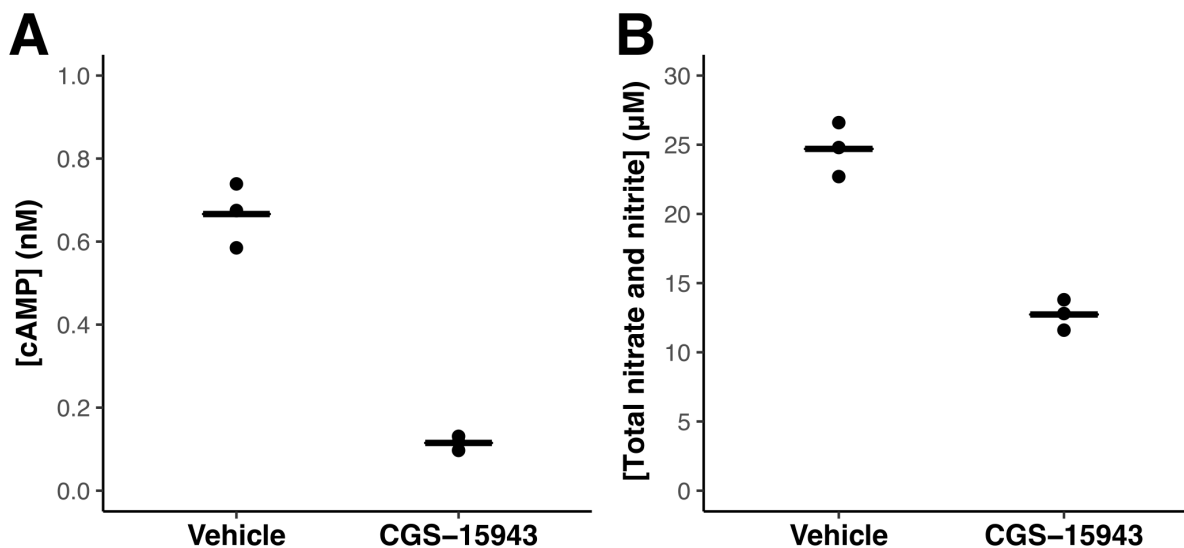


Figure 3.6. Effects of adenosine receptor blockade on adenosine and VEGF signaling in HUVEC. Treatment of HUVEC with the non-selective adenosine receptor antagonist CGS-15943 (1 μM) in the presence of 10 μM adenosine and 50 ng/mL VEGF decreased levels of A) cyclic AMP (cAMP; $P = 0.005$) and B) nitric oxide ($P = 0.002$). Points represent means from three independent experiments; lines represent group means. Differences between CGS-15943-treated and vehicle-treated cells were analyzed by an unpaired t-test.

HUVEC were also treated with the VEGFR2 inhibitor ZM323881 HCl to determine the contribution of VEGFR2 signaling to each measured effect. Preliminary data show that ZM323881 HCl had no effect on cAMP but decreased both NO and PGI₂ levels. Furthermore,

treatment of HUVEC with both CGS-15943 and ZM323881 HCl had additive effects on NO levels, almost completely abolishing its production. cAMP levels were similar to those in cells treated only with CGS-15943, suggesting that VEGFR2 inhibition has no effect on adenosine receptor activity. PGI₂ levels were similar to those in cells treated only with ZM 323881 HCl, indicating that PGI₂ production does not depend on adenosine receptor signaling.

3.4.2 Effect of bevacizumab on adenosine and VEGF signaling

The effects of bevacizumab on cAMP, NO, and PGI₂ were examined in the presence of adenosine and VEGF. Bevacizumab treatment decreased NO levels at all tested adenosine concentrations but had no effect on cAMP (Figure 3.7). Preliminary data also showed a decrease in PGI₂ levels. These results suggest that bevacizumab has no direct effect on adenosine receptor signaling and that NO and PGI₂ levels reflect both adenosine and VEGF signaling.

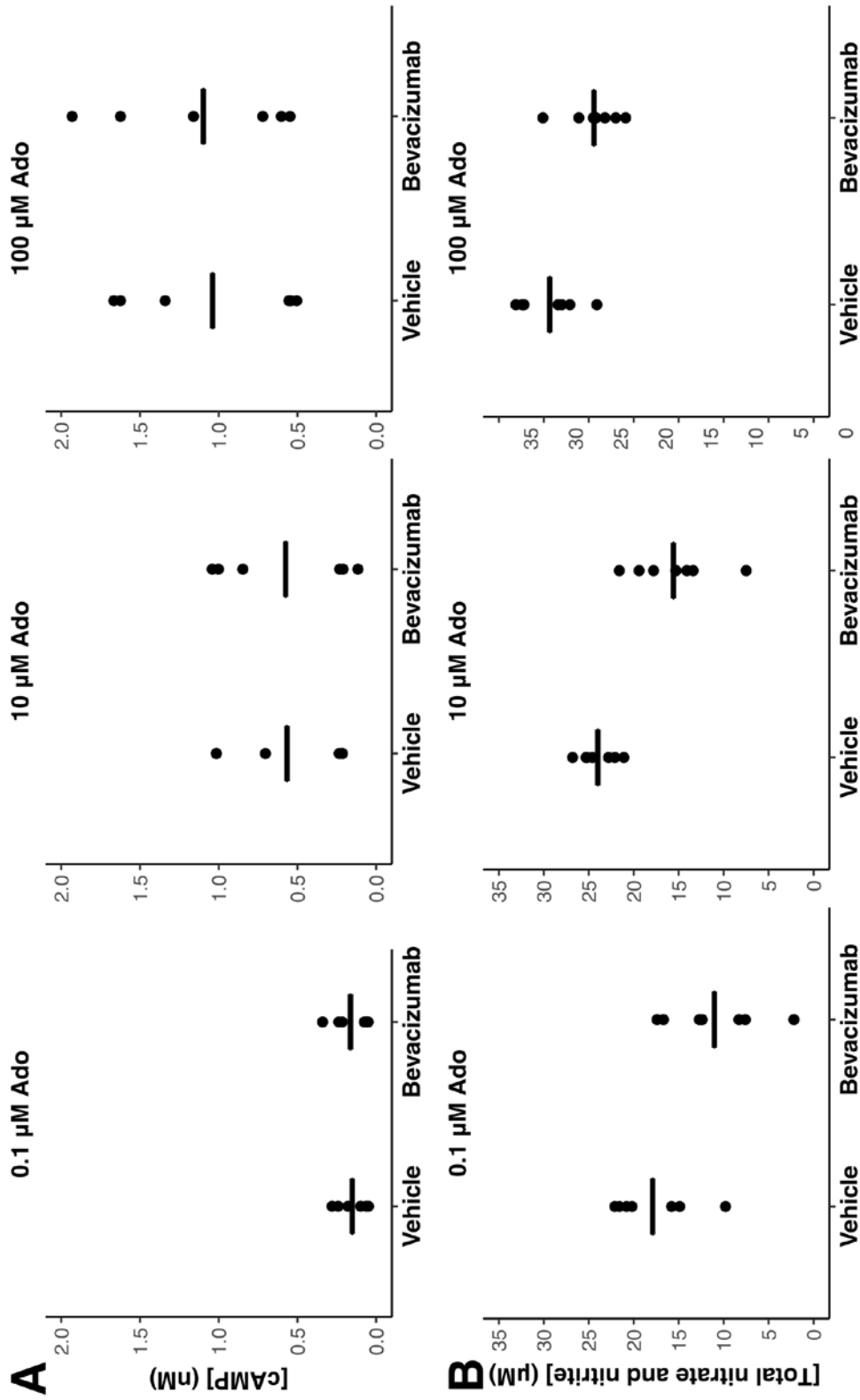


Figure 3.7. Effects of bevacizumab on adenosine and VEGF signaling in HUVEC. HUVEC were incubated in 50 ng/mL VEGF and adenosine (0.1, 10, 100 μM). Bevacizumab was added at a molar concentration 10X greater than VEGF. Exposure to bevacizumab decreased levels of nitric oxide ($P = 1 \times 10^{-11}$) compared to vehicle-treated cells at all adenosine concentrations, but had no effect on cyclic AMP (cAMP). Points represent means from six or seven independent experiments; lines represent group means. Differences between bevacizumab-treated and vehicle-treated cells at each adenosine concentration were analyzed by two-way ANOVA.

3.4.3 Effect of ENT1 inhibition on adenosine and VEGF signaling

The effect of ENT1 inhibition with NBTI on adenosine and VEGF signaling was tested in the presence of adenosine and VEGF. NBTI-treated cells showed increased cAMP levels compared to vehicle-treated controls at all tested adenosine concentrations (Figure 3.8A), indicating an increase in adenosine receptor signaling. NBTI also increased NO levels (Figure 3.8B) and slightly increased PGI₂ levels (preliminary data only; not shown) compared to controls. The addition of bevacizumab resulted in small but significant decreases in NO and PGI₂ levels both in the presence and absence of NBTI, but had no effect on cAMP levels.

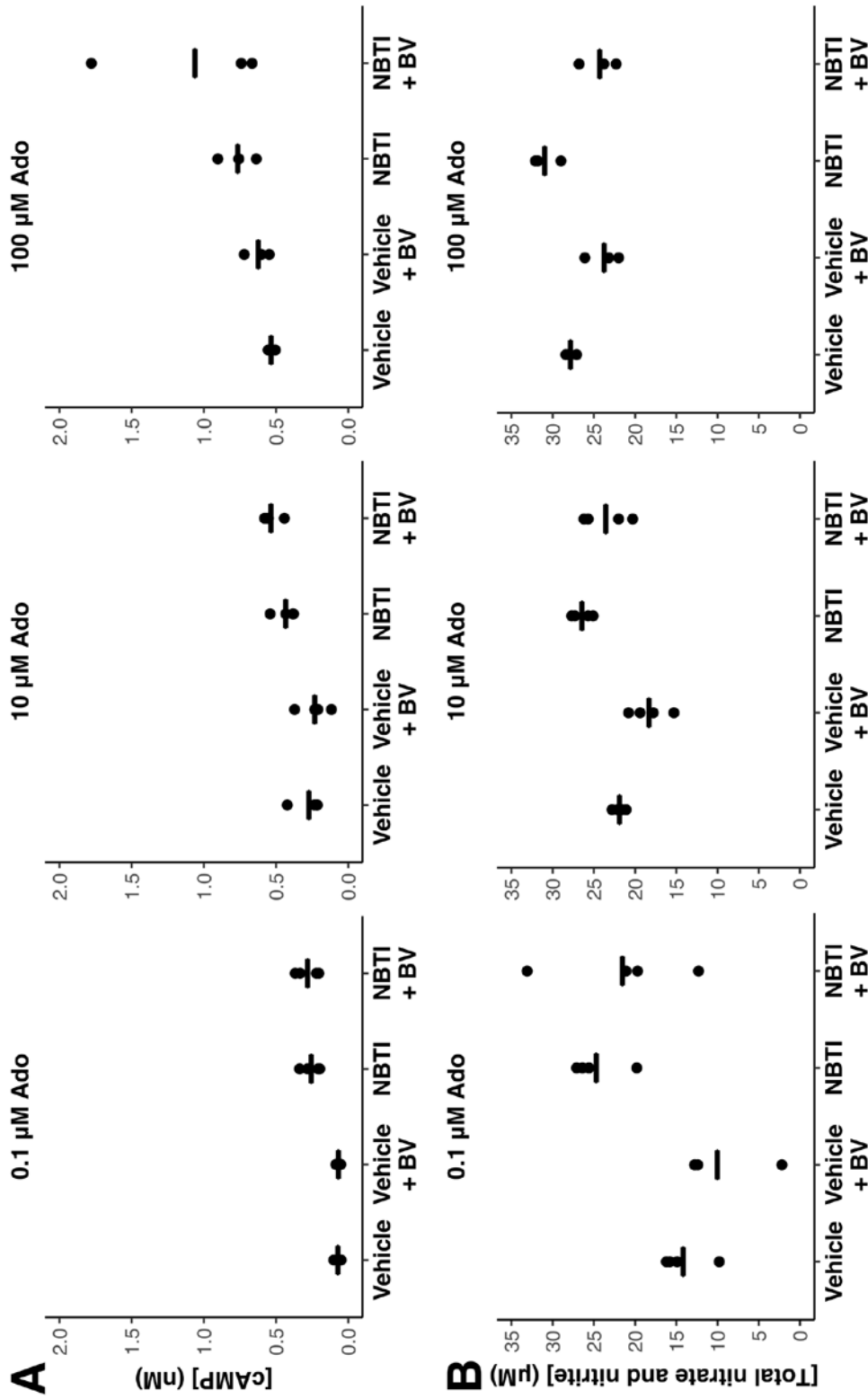


Figure 3.8. Effects of ENT1 inhibition on adenosine and VEGF signaling in HUVEC. HUVEC were incubated in 50 ng/mL VEGF and adenosine (0.1, 10, 100 µM). Treatment with the ENT1 inhibitor NBTI (1 µM) increased levels of A) cyclic AMP (cAMP; $P = 1 \times 10^{-10}$) and B) nitric oxide (NO; $P = 6 \times 10^{-13}$) compared to vehicle-treated cells at all adenosine concentrations. Exposure to bevacizumab (BV; 10X molar ratio of VEGF) had no effect on cAMP but decreased NO levels ($P = 5 \times 10^{-6}$). There was no difference in the effect of BV on NBTI-treated versus vehicle-treated cells. Points represent means from three or four independent experiments; lines represent group means. The effects of NBTI treatment and the comparison of BV exposure between NBTI-treated and vehicle-treated groups at each adenosine concentration were analyzed by three-way ANOVA.

3.4.4 Effect of SLC29A1 overexpression on adenosine and VEGF signaling

The functional effects of increased SLC29A1 expression were evaluated in HUVEC transfected with SLC29A1 cDNA. SLC29A1-transfected HUVEC were confirmed to consistently have more than a 100-fold increase in SLC29A1 mRNA expression compared to empty vector-transfected control cells (difference of mean relative expression: $P = 0.0002$).

SLC29A1-overexpressing HUVEC, in the presence of adenosine and VEGF, decreased the generation of cAMP when compared to empty vector-transfected controls at all tested adenosine concentrations (Figure 3.9A), indicating a decrease in adenosine receptor signaling. SLC29A1-overexpressing HUVEC also showed decreased NO levels (Figure 3.9B), while PGI₂ levels were reduced only slightly by SLC29A1 overexpression (preliminary data only; not shown). The addition of bevacizumab further reduced NO and PGI₂ levels in all cells but had no effect on cAMP levels. The inhibitory effect of bevacizumab on NO levels ranged from an 18–44% decrease in empty vector-transfected cells compared to a 50–75% decrease in SLC29A1-transfected cells, demonstrating a greater reduction in NO following bevacizumab treatment under conditions of high SLC29A1 expression.

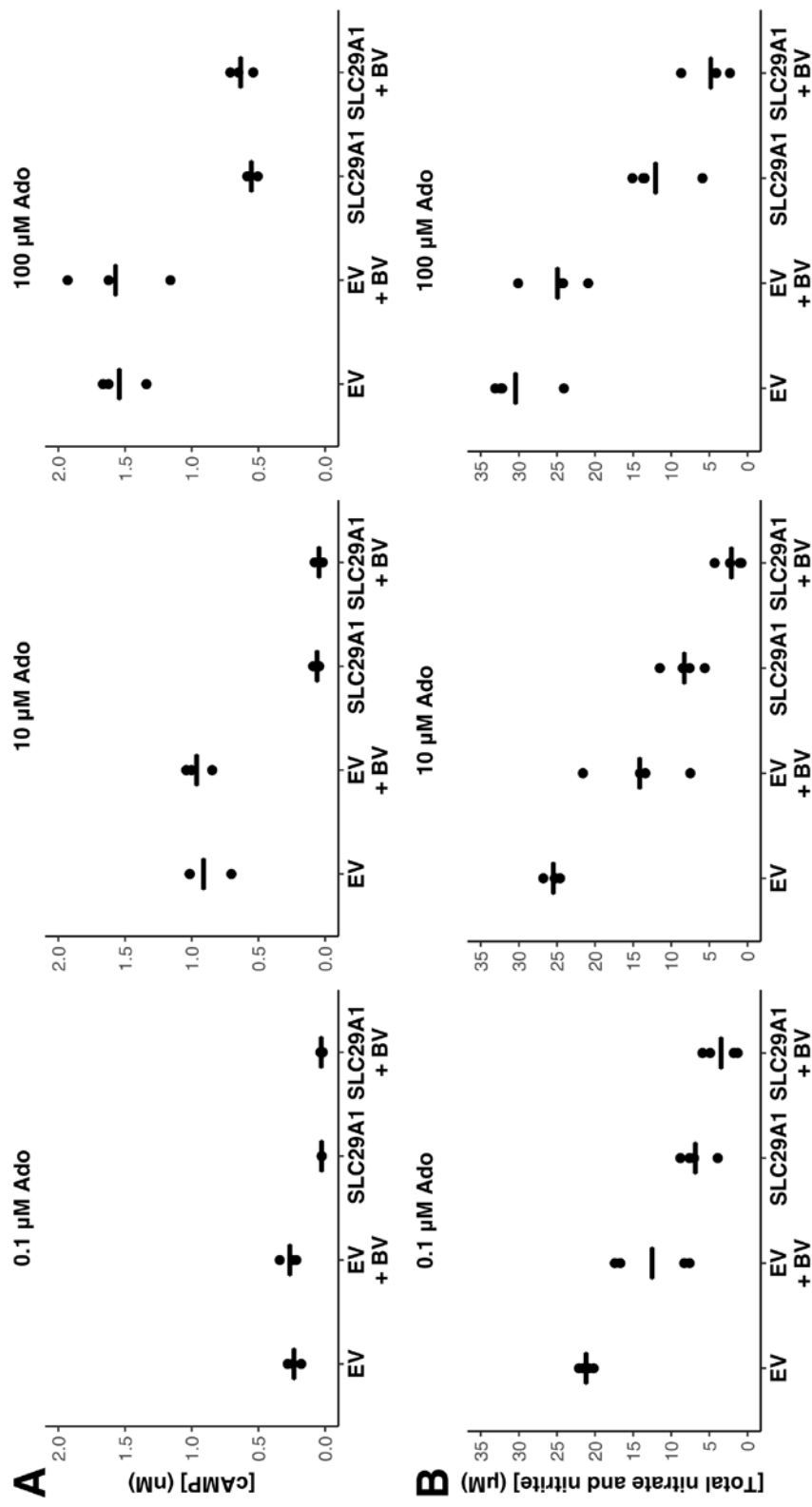


Figure 3.9. Effects of SLC29A1-overexpression on adenosine and VEGF signaling in HUVEC. An expression vector encoding SLC29A1 cDNA was transfected into HUVEC. Empty vector was transfected into HUVEC as a negative control (EV). Transfected HUVEC were incubated in 50 ng/mL VEGF and adenosine (0.1, 10, 100 µM). A) SLC29A1 overexpression decreased the generation of cyclic AMP (cAMP) in response to adenosine when compared to EV-transfected HUVEC ($P < 2 \times 10^{-16}$). Exposure to bevacizumab (BV; 10X molar ratio of VEGF) had no effect on cAMP in either group. B) SLC29A1 overexpression decreased the release of nitric oxide (NO) when compared to EV-transfected HUVEC ($P < 2 \times 10^{-16}$). Exposure to BV reduced NO levels in both groups and had a greater inhibitory effect in the SLC29A1-transfected cells ($P = 0.02$ compared to BV effect in EV). Points represent means from three or four independent experiments; lines represent group means. The effects of SLC29A1 overexpression and the comparison of BV exposure between SLC29A1-transfected and EV-transfected groups at each adenosine concentration were analyzed by three-way ANOVA.

3.5 Discussion

In this study, the effects of ENT1 and bevacizumab on vasodilatory signaling pathways were examined to better understand how changes in adenosine and VEGF signaling may contribute to bevacizumab-induced HTN. A HUVEC model was developed that responded to adenosine treatment as expected, with dose-dependent increases in cAMP, NO and PGI₂ production. Bevacizumab appears to have no direct effects on adenosine receptor activity, as indicated by the insensitivity of cAMP generation to bevacizumab treatment.

Pharmacological inhibition of ENT1 was confirmed to increase adenosine receptor signaling and NO synthesis. Furthermore, overexpression of SLC29A1 decreased adenosine receptor signaling and NO synthesis. Bevacizumab treatment reduced NO levels, with enhanced sensitivity under conditions of elevated SLC29A1 expression. Preliminary data suggest that the effects of ENT1 inhibition and SLC29A1 overexpression on PGI₂ levels follow the same trends as NO levels, but while NO is generated as a result of both adenosine and VEGF signaling, PGI₂ synthesis appears to be driven primarily by VEGF signaling and is less sensitive to changes in adenosine. Our data also suggest that a combination of SLC29A1 overexpression, low extracellular adenosine, and bevacizumab treatment (or low basal VEGF) may all interact to downregulate NO synthesis, although additional studies are required to rigorously test this hypothesis.

These results represent work that is still in progress, as measurement of ENT1 protein expression levels and additional functional testing are still needed. A major limitation of this study is the lack of measured adenosine levels and adenosine uptake. Adenosine levels fluctuate and are known to be difficult to measure accurately, due to ATP release and

hydrolysis during sample handling and rapid adenosine phosphorylation by adenosine kinase or metabolism by adenosine deaminase^{1,2,9}. Instead, cAMP levels were used as a marker of adenosine receptor activation, with minimal levels of cAMP detected when adenosine receptor signaling was chemically blocked. However, assessment of cellular adenosine uptake in this system is still required to truly understand the effects of ENT1 expression.

Another limitation of our endothelial cell model is the inability to account for the pleiotropic effects of adenosine in other cell types and tissues, including regulation of vasodilation through paracrine effects on vascular smooth muscle cells. A combined vascular endothelial and smooth muscle cell model would enable detection of the effects of bevacizumab on measures of contractility in smooth muscle. However, any *in vitro* system is still unable to accurately predict *in vivo* effects. Although modulation of ENT1 showed rapid changes in adenosine signaling and NO levels in our model, the body is likely to develop compensatory mechanisms to adapt to differences in adenosine flux and maintain homeostasis. An increase in adenosine deaminase and A_{2A} receptor expression was previously reported in microvascular endothelial cells and skeletal muscle of ENT1^{-/-} mice compared to wildtype mice²⁴, and although ENT1^{-/-} mice had increased plasma adenosine concentrations, their mean arterial blood pressure was similar to ENT1^{+/+} mice^{13,14}. Changes in ENT1 expression or adenosine levels may also affect the expression or activity of other nucleoside transporters, adenosine receptors, or adenosine-generating or metabolizing enzymes, possibly attenuating the response to altered ENT1 expression.

While there is expected to be a tight regulation of adenosine receptor signaling under normal conditions, exposure to bevacizumab could perturb this homeostatic balance (Figure 3.10). Increased ENT1 expression may impair the endothelium's ability to maintain a necessary amount of adenosine-stimulated NO production while under reduced VEGF signaling. Decreased PGI₂ production from VEGF inhibition would further contribute to vasoconstriction. NO itself has been reported to reduce *SLC29A1* promoter activity in HUVEC²⁵, so a downregulation of NO synthesis may sustain increased ENT1 expression levels. Patients with increased basal ENT1 expression and function would therefore be more sensitive to VEGF inhibition by bevacizumab. *In vivo* studies are needed to confirm this hypothesis, and extended treatment periods with bevacizumab should be tested to determine whether the same effects manifest over a longer time scale.

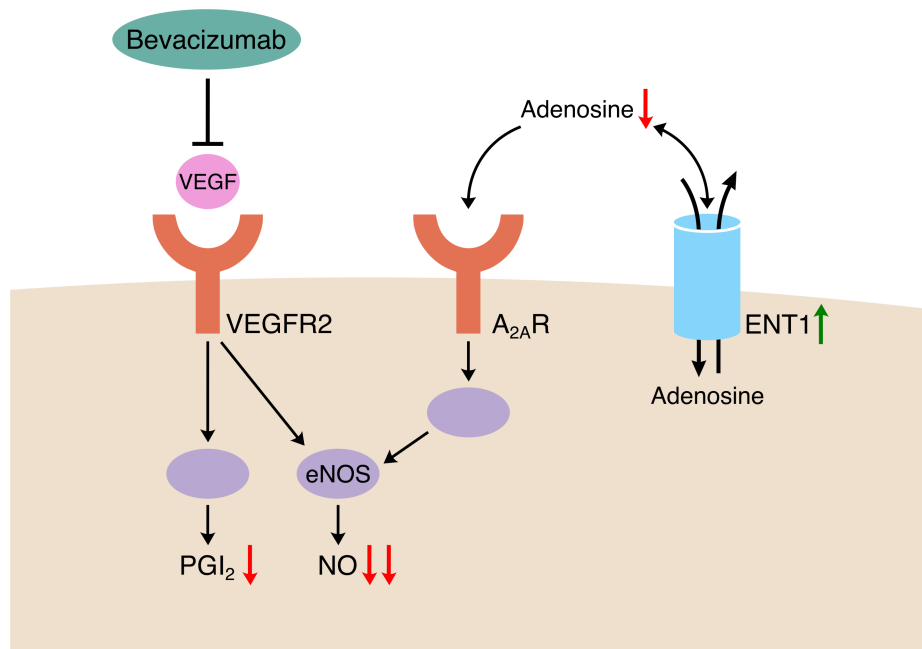


Figure 3.10. Hypothesized mechanism of increased ENT1 expression on bevacizumab-induced hypertension. In a normal vascular endothelial cell, equilibrative nucleoside transporter 1 (ENT1) allows for movement of adenosine across the cell membrane. Extracellular vascular endothelial growth factor (VEGF) and adenosine signal through VEGF receptor 2 (VEGFR2) and A_{2A} adenosine receptor ($A_{2A}R$), respectively, to upregulate endothelial nitric oxide synthase (eNOS) activity and increase nitric oxide (NO) synthesis. VEGFR2 activation also promotes prostacyclin (PGI_2) synthesis. When ENT1 expression is increased, extracellular adenosine and $A_{2A}R$ activity decrease, resulting in reduced NO levels. Bevacizumab, which binds VEGF, downregulates VEGFR2 signaling and reduces both NO and PGI_2 levels. The combined effects of reduced adenosine and VEGF signaling may contribute to vasoconstriction and overall systemic resistance in the blood vessels.

Based on data from *in silico* analyses, the top SNPs associated with bevacizumab-induced HTN reported in Chapter 2 are located in putative regulatory regions in HUVEC. Three of the four SNPs are in moderately transcribed regions just downstream of *SLC29A1* that are enriched for genomic features indicative of enhancer activity. A fourth SNP, while not in a predicted strong transcriptionally active region, was found to be associated with increased *SLC29A1* expression in monocytes. While additional studies are needed to determine the effects of these SNPs on *SLC29A1* expression, increased *SLC29A1* expression would support our hypothesized model. Similar changes in sensitivity to bevacizumab treatment

could also occur following changes in ENT1 expression or function as a result of epigenetic regulation of *SLC29A1* or drug interactions.

Adenosine transport kinetics could also play a role in bevacizumab sensitivity. While increased extracellular adenosine concentrations have been consistently observed with reduced ENT1 expression, the bidirectional and equilibrative nature of ENT1-mediated adenosine transport may complicate this relationship. A decreased V_{\max} for ENT1-mediated adenosine uptake has been reported in both HUVEC during gestational diabetes²⁶ and human placental microvascular endothelial cells during preeclampsia¹⁶ when compared to normal cells, though apparent K_m values did not change. The extent to which ENT1 modulates adenosine signaling will also be dependent on adenosine concentrations in the system, which can exceed the dissociation constant (K_d : $\sim 40 \mu\text{M}$) of ENT1 for adenosine²⁷ during pathogenic conditions but are much lower under normal conditions. Adenosine concentrations can also regulate receptor binding; A_{2A} receptors have high binding affinity (K_d : $0.1\text{--}1.0 \mu\text{M}$) for adenosine while A_{2B} receptors have lower affinity (K_d : $\geq 10 \mu\text{M}$)²⁸. Therefore, adenosine signals primarily through the A_{2A} receptor in the presence of low extracellular adenosine levels and shifts toward A_{2B} receptor signaling as adenosine levels increase, as has been observed in pathological states. Changes in rates of adenosine formation and degradation would also alter its extracellular concentrations. Direct effects on adenosine transport rates, receptor binding affinities, or enzyme kinetics modulated by genetic effects or drug interactions should be considered during future functional studies of bevacizumab treatment.

Altered adenosine signaling and nucleoside transporter expression have also been investigated in the development of preeclampsia, a complication of pregnancy that is characterized by high blood pressure. Increased adenosine concentrations and decreased SLC29A1 expression and ENT1 transport activity have been observed during preeclampsia^{16,29}. Although the association of increased adenosine with increased blood pressure contradicts our hypothesized mechanism, our findings still support the idea of dysregulated adenosine transport having a large effect on blood pressure. Other observations during preeclampsia include increased CD39 and CD73 activity²⁹ and upregulation of soluble VEGFR1 (sFlt-1)³⁰, which binds to VEGF as bevacizumab does. Enhanced A_{2B} receptor signaling has been associated with both increased sFlt-1 secretion³¹ and decreased ENT1 expression¹⁶. Although pregnancy and cancer are likely to exert different physiological influences on adenosine signaling, such mechanisms may be worth investigating in the context of bevacizumab-induced HTN.

3.6 Conclusions

In this study, the effects of ENT1 and bevacizumab on vasodilatory signaling pathways were examined to better understand how the interaction of adenosine and VEGF signaling may contribute to bevacizumab-induced HTN. These results represent work still in progress, but the data presented support the hypothesis that basal levels of SLC29A1 expression contribute to interindividual variability in bevacizumab-induced HTN. If true, low extracellular adenosine levels during angiogenesis inhibition may sensitize patients to a rise in blood pressure during bevacizumab exposure.

3.7 References

1. Jacobson KA, Gao Z-G. Adenosine receptors as therapeutic targets. *Nat Rev Drug Discov.* 2006;5(3):247–64.
2. Chen J-F, Eltzschig HK, Fredholm BB. Adenosine receptors as drug targets — what are the challenges? *Nat Rev Drug Discov.* 2013;12(4):265–86.
3. Sottofattori E, Anzaldi M, Ottonello L. HPLC determination of adenosine in human synovial fluid. *J Pharm Biomed Anal.* 2001;24(5-6):1143–6.
4. Adair TH, Cotten R, Gu J-W, Pryor JS, Bennett KR, McMullan MR, McDonnell P, Montani J-P. Adenosine infusion increases plasma levels of VEGF in humans. *BMC Physiol.* 2005;5:10.
5. Zapata-Sudo G, Sudo SZ, Alencar AKN, Sudo RT. Targeting of the adenosine receptors as a novel strategy for the treatment of arterial hypertension. *J Neurol Neurophysiol.* 2014;5:243.
6. Ray CJ, Abbas MR, Coney AM, Marshall JM. Interactions of adenosine, prostaglandins and nitric oxide in hypoxia-induced vasodilatation: in vivo and in vitro studies. *J Physiol.* 2002;544(Pt 1):195–209.
7. Facemire CS, Nixon AB, Griffiths R, Hurwitz H, Coffman TM. Vascular endothelial growth factor receptor 2 controls blood pressure by regulating nitric oxide synthase expression. *Hypertension.* 2009;54(3):652–8.
8. Escudero C, Roberts JM, Myatt L, Feoktistov I. Impaired adenosine-mediated angiogenesis in preeclampsia: potential implications for fetal programming. *Front Pharmacol.* 2014;5:134.
9. Adair TH. Growth regulation of the vascular system: an emerging role for adenosine. *Am J Physiol Regul Integr Comp Physiol.* 2005;289(2):R283–96.
10. Baldwin SA, Beal PR, Yao SYM, King AE, Cass CE, Young JD. The equilibrative nucleoside transporter family, SLC29. *Pflugers Arch.* 2004;447(5):735–43.
11. Young JD, Yao SYM, Sun L, Cass CE, Baldwin SA. Human equilibrative nucleoside transporter (ENT) family of nucleoside and nucleobase transporter proteins. *Xenobiotica.* 2008;38(7-8):995–1021.
12. San Martín R, Sobrevia L. Gestational diabetes and the adenosine/L-arginine/nitric oxide (ALANO) pathway in human umbilical vein endothelium. *Placenta.* 2006;27(1):1–10.
13. Rose JB, Naydenova Z, Bang A, Ramadan A, Klawitter J, Schram K, Sweeney G, Grenz A, Eltzschig H, Hammond J, Choi D-S, Coe IR. Absence of equilibrative nucleoside

- transporter 1 in ENT1 knockout mice leads to altered nucleoside levels following hypoxic challenge. *Life Sci.* 2011;89(17-18):621–30.
14. Li L, Mizel D, Huang Y, Eisner C, Hoerl M, Thiel M, Schnermann J. Tubuloglomerular feedback and renal function in mice with targeted deletion of the type 1 equilibrative nucleoside transporter. *Am J Physiol Renal Physiol.* 2013;304(4):F382–9.
 15. Vásquez G, Sanhueza F, Vásquez R, González M, San Martín R, Casanello P, Sobrevia L. Role of adenosine transport in gestational diabetes-induced L-arginine transport and nitric oxide synthesis in human umbilical vein endothelium. *J Physiol.* 2004;560(Pt 1):111–22.
 16. Escudero C, Casanello P, Sobrevia L. Human equilibrative nucleoside transporters 1 and 2 may be differentially modulated by A2B adenosine receptors in placenta microvascular endothelial cells from pre-eclampsia. *Placenta.* 2008;29(9):816–25.
 17. Pharmacogenetics of Membrane Transporters Database. UCSF Pharmacogenetics of Membrane Transporters. 2015 [cited 2017 Jan 10]. Available from: <http://pharmacogenetics.ucsf.edu/>
 18. Osato DH, Huang CC, Kawamoto M, Johns SJ, Stryke D, Wang J, Ferrin TE, Herskowitz I, Giacomini KM. Functional characterization in yeast of genetic variants in the human equilibrative nucleoside transporter, ENT1. *Pharmacogenetics.* 2003;13(5):297–301.
 19. Abdulla P, Coe IR. Characterization and functional analysis of the promoter for the human equilibrative nucleoside transporter gene, hENT1. *Nucleosides Nucleotides Nucleic Acids.* 2007;26(1):99–110.
 20. Pennycooke M, Chaudary N, Shuralyova I, Zhang Y, Coe IR. Differential expression of human nucleoside transporters in normal and tumor tissue. *Biochem Biophys Res Commun.* 2001;280(3):951–9.
 21. Vega JL, Puebla C, Vasquez R, Farias M, Alarcon J, Pastor-Anglada M, Krause B, Casanello P, Sobrevia L. TGF- 1 inhibits expression and activity of hENT1 in a nitric oxide-dependent manner in human umbilical vein endothelium. *Cardiovasc Res.* 2009;82(3):458–67.
 22. R Core Team. R: A language and environment for statistical computing. Vienna, Austria: R Foundation for Statistical Computing; 2013. Available from: <https://www.R-project.org/>
 23. Wickham H. *ggplot2: Elegant Graphics for Data Analysis.* Springer; 2009.
 24. Bone DBJ, Choi DS, Coe IR, Hammond JR. Nucleoside/nucleobase transport and metabolism by microvascular endothelial cells isolated from ENT1-/- mice. *Am J Physiol Heart Circ Physiol.* 2010;299(3):H847–56.

25. Farías M, San Martín R, Puebla C, Pearson JD, Casado JF, Pastor-Anglada M, Casanello P, Sobrevia L. Nitric oxide reduces adenosine transporter ENT1 gene (SLC29A1) promoter activity in human fetal endothelium from gestational diabetes. *J Cell Physiol.* 2006;208(2):451–60.
26. Westermeier F, Salomon C, Farías M, Arroyo P, Fuenzalida B, Sáez T, Salsoso R, Sanhueza C, Guzmán-Gutiérrez E, Pardo F, Leiva A, Sobrevia L. Insulin requires normal expression and signaling of insulin receptor A to reverse gestational diabetes-reduced adenosine transport in human umbilical vein endothelium. *FASEB J.* 2015;29(1):37–49.
27. Carrier EJ, Auchampach JA, Hillard CJ. Inhibition of an equilibrative nucleoside transporter by cannabidiol: a mechanism of cannabinoid immunosuppression. *Proc Natl Acad Sci.* 2006;103(20):7895–900.
28. Daly JW, Butts-Lamb P, Padgett W. Subclasses of adenosine receptors in the central nervous system: interaction with caffeine and related methylxanthines. *Cell Mol Neurobiol.* 1983;3(1):69–80.
29. Salsoso R, Farías M, Gutiérrez J, Pardo F, Chiarello DI, Toledo F, Leiva A, Mate A, Vázquez CM, Sobrevia L. Adenosine and preeclampsia. *Mol Aspects Med.* 2017. doi:10.1016/j.mam.2016.12.003 [Epub ahead of print]
30. Powe CE, Levine RJ, Karumanchi SA. Preeclampsia, a disease of the maternal endothelium: the role of antiangiogenic factors and implications for later cardiovascular disease. *Circulation.* 2011;123(24):2856–69.
31. Iriyama T, Sun K, Parchim NF, Li J, Zhao C, Song A, Hart LA, Blackwell SC, Sibai BM, Chan L-NL, Chan T-S, Hicks MJ, Blackburn MR, Kellems RE, Xia Y. Elevated placental adenosine signaling contributes to the pathogenesis of preeclampsia. *Circulation.* 2015;131(8):730–41.

Chapter 4: Identification of Bevacizumab-Induced Hypertension Risk Variants by Genome-Wide Association

4.1 Abstract

Bevacizumab is a vascular endothelial growth factor (VEGF)-specific angiogenesis inhibitor indicated as an adjunct to chemotherapy for the treatment of several types of cancer. Hypertension (HTN) is commonly observed during bevacizumab treatment, and high-grade toxicity can limit therapy or lead to other cardiovascular complications. The factors that contribute to interindividual variability in blood pressure response to bevacizumab treatment are not well understood. A genome-wide association study was conducted on 415 breast cancer patients from a clinical study of paclitaxel, nab-paclitaxel, or ixabepilone combined with bevacizumab treatment. Cox proportional hazards models with the cumulative bevacizumab exposure to the first occurrence of grade 2+ HTN or grade 3+ HTN were used to identify variants associated with bevacizumab-induced HTN. The top hits of these respective analyses included a locus upstream of *MSH6* (rs2018541: $P = 1.6 \times 10^{-7}$, HR 2.9, 95% CI 1.9–4.3) associated with grade 2+ HTN, and an intronic SNP in *SDC4* (rs1981431: $P = 2.1 \times 10^{-7}$, HR 0.3, 95% CI 0.2–0.4) associated with grade 3+ HTN. Both of these genes have been previously implicated in the regulation of VEGF or blood pressure. Other top associations of potential biological interest include a SNP in *ASB5* and a SNP associated with *SMYD5* expression. While these findings require independent validation, these results suggest that genetic variation in these genes may influence the risk of developing HTN while being treated with bevacizumab. Further studies are warranted to

determine the specific role that these genes play in the pathogenesis of bevacizumab-induced HTN.

4.2 Introduction

Bevacizumab is a recombinant humanized monoclonal antibody that targets human vascular endothelial growth factor-A (VEGF), preventing its binding to VEGF receptor 2 (VEGFR2)¹. The development of hypertension (HTN) is frequently observed^{2,3} during treatment with bevacizumab and may lead to serious cardiovascular complications. Upon blood pressure elevation, bevacizumab is either held temporarily or discontinued⁴, thereby limiting therapy that may otherwise be beneficial. There are currently no validated biomarkers to predict bevacizumab toxicity, and the factors that contribute to interindividual variability in blood pressure response to bevacizumab treatment are not well understood.

Prior studies have evaluated and identified associations between HTN incidence during bevacizumab treatment and common candidate single nucleotide polymorphisms (SNPs) in genes encoding VEGF (*VEGFA*)⁵⁻⁹ and VEGFR2 (*KDR*)¹⁰; however, the directions of effect for several of these findings are discordant. More recent studies utilizing expanded candidate gene and genome-wide strategies have identified a risk variant in *SV2C*¹¹ and modest associations in *EGLN3*, *EGF*, and *WNK1*¹². Given the heritable but complex nature of primary HTN, the genetic architecture underlying bevacizumab-induced HTN is also likely to be polygenic. Additional examination of genetic variation in non-VEGF pathways may identify potential novel mechanisms contributing to bevacizumab-induced HTN.

Large effect phenotypes exhibited by some pharmacogenetic traits have provided great statistical power for genetic association studies in relatively small sample sizes. Genome-wide association studies (GWAS) have been successful in identifying variants associated with drug toxicities, including statin-induced myopathy¹³, flucloxacillin-induced liver injury¹⁴, and carbamazepine-induced hypersensitivity and skin reactions^{15,16}. Only one prior study¹¹ of bevacizumab-induced HTN has used a genome-wide approach, while other studies have been limited to genotyping of candidate variants.

This GWAS aims to identify novel genetic predictors of bevacizumab-induced HTN in a cohort of breast cancer patients. This serves as a complementary but independent study to the exome sequencing study described in Chapter 2, in which a binary outcome of extreme toxicity phenotypes was analyzed in a small cohort. The larger population examined in this GWAS lends more statistical power to detect common variant associations using a cumulative dose model.

4.3 Materials and Methods

4.3.1 Patient population

The patient cohort for this study was selected from Cancer and Leukemia Group B (CALGB) 40502 (Alliance; NCT00785291), a phase III trial comparing weekly paclitaxel to weekly nab-paclitaxel or ixabepilone combined with bevacizumab as first-line treatment of locally recurrent or metastatic breast cancer¹⁷ (Figure 4.1). Patients were randomized to treatment with paclitaxel (90 mg/m²), nab-paclitaxel (150 mg/m²), or ixabepilone (16 mg/m²), on Days 1, 8, and 15 of each 28-day treatment cycle. If elected to be treated with

bevacizumab, patients received 10 mg/kg IV on Days 1 and 15 of each cycle. Of 799 patients accrued to the trial, 783 received chemotherapy and 97% received bevacizumab. A total of 669 women provided written informed consent for sample procurement and analysis, as part of a pharmacogenetic correlative substudy within the parent protocol, and 635 participants had DNA available in the CALGB/Alliance sample repository. All studies were approved by the National Cancer Institute's Institutional Review Board and by local institutional review boards, as appropriate.

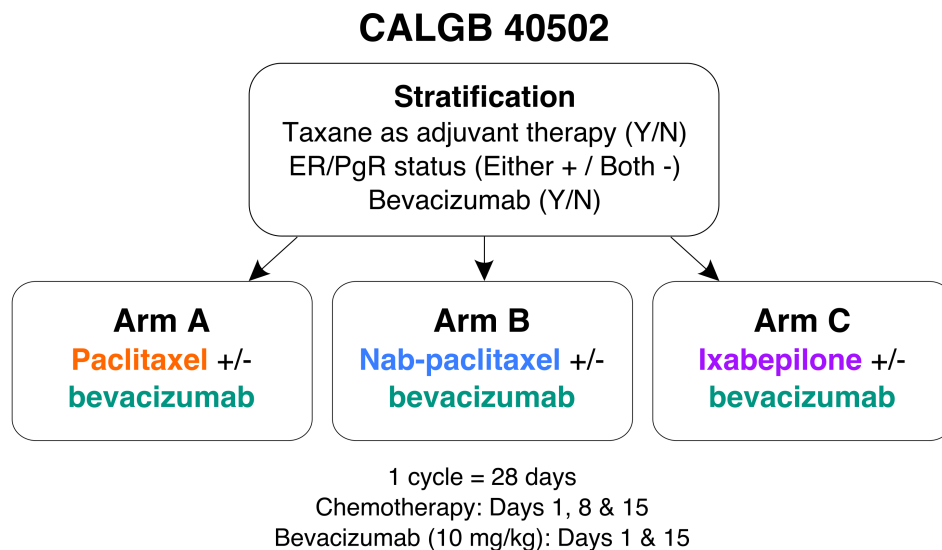


Figure 4.1. CALGB 40502 trial design. The current pharmacogenomic analysis utilized samples and toxicity phenotype data from a subset of the patients participating in CALGB 40502.

4.3.2 Bevacizumab-induced hypertension phenotype

Demographic and clinical data were collected from all patients and reviewed extensively for accurate reporting of adverse events and bevacizumab dosing for each treatment cycle (Figure 4.2). Eligibility criteria required no history of uncontrolled HTN, defined as systolic blood pressure > 150 mmHg and/or diastolic blood pressure > 90 mmHg on

antihypertensive medications, or any prior history of hypertensive crisis or hypertensive encephalopathy. Blood pressure was measured prior to registration, and a history of high blood pressure was self-reported by patients at registration. Toxicity data were collected on Day 1 of each treatment cycle. The severity of HTN was recorded on a scale of 0–5 according to the National Cancer Institute’s Common Terminology Criteria for Adverse Events version 3¹⁸ (Table 4.1). Patients not treated with bevacizumab were removed from the analysis. From the patients without at least one reported HTN event, those with missing AE forms were also excluded from analysis (Table 4.2).

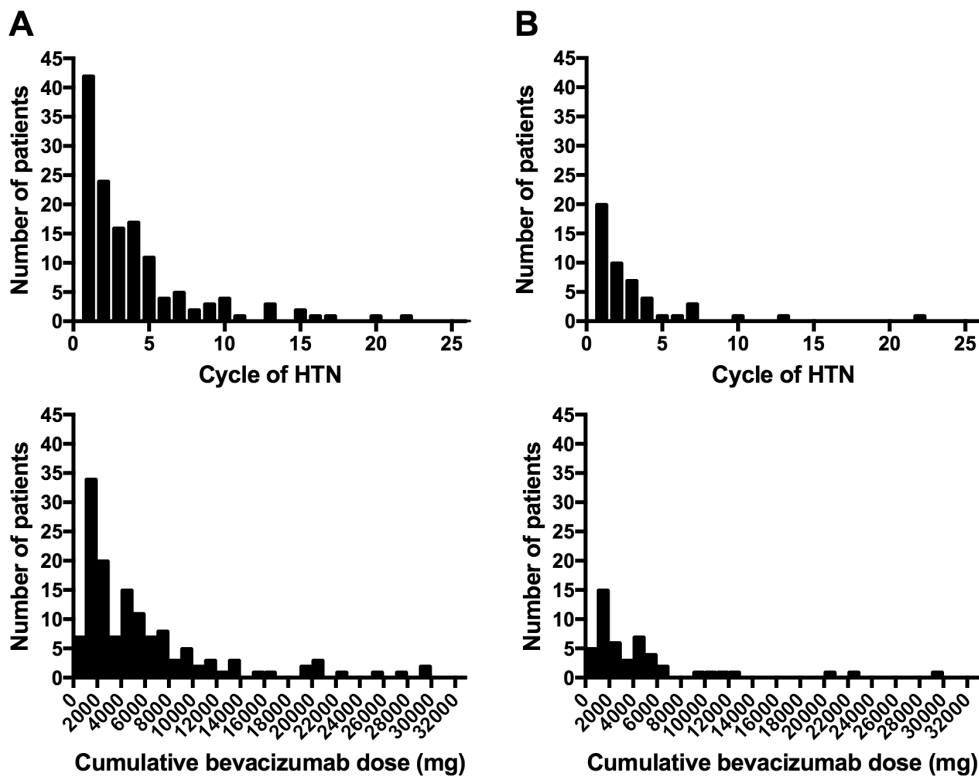


Figure 4.2. Hypertension events in CALGB 40502. Distribution of cycle number (top) or cumulative dose of bevacizumab (bottom) to first occurrence of A) grade 2+ or B) grade 3+ hypertension.

Table 4.1. Assessment of hypertension in the National Cancer Institute’s Common Terminology Criteria for Adverse Events version 3

Grade 1	Grade 2	Grade 3	Grade 4	Grade 5
Asymptomatic, transient (<24 hrs) increase by >20 mmHg (diastolic) or to >150/100 if previously WNL ¹	Recurrent or persistent (≥24 hrs) or symptomatic increase by >20 mmHg (diastolic) or to >150/100 if previously WNL ¹	Requiring more than one drug or more intensive therapy than previously	Life-threatening consequences (e.g., hypertensive crisis)	Death
Intervention not indicated	Monotherapy may be indicated			

¹WNL: Within normal limits

Table 4.2. Phenotype curation

	N, excluded subjects	N, remaining subjects
All subjects		799
Treated with bevacizumab	49	750
Missing AE forms (only if no HTN event)	8	742
Genetic European	288	454

4.3.3 Genotyping

Genomic DNA from consented subjects was extracted from whole blood samples using standard DNA extraction techniques. Genotyping was performed on the OmniExpressExome BeadChip (Illumina, San Diego, CA), which interrogated 964,055 variants, at the RIKEN Center for Integrative Medical Sciences. Sample replicates, genotyping controls, and samples with discordant X-chromosome heterozygosity were removed. To address potential confounding arising from population stratification, a principal component analysis implemented through an Identity-by-State method in

GenABEL¹⁹ and verified by EIGENSTRAT²⁰ was performed to identify 478 genetic European subjects; of these genetic Europeans, 444 had curated HTN phenotype data (Table 4.3).

Table 4.3. Quality control of genotyped samples

	N, excluded samples	N, remaining samples
DNA samples		651
Successfully genotyped	2	649
Duplicates/genotyping controls	18	631
Mismatched sex	3	628
Genetic European	150	478
Curated toxicity phenotype data available	34	444
Complete phenotype data (including covariates) available	29	415

To eliminate suboptimal markers, genotypes were limited to autosomal SNPs with call rate > 99%, no significant deviation from Hardy-Weinberg equilibrium ($P > 1 \times 10^{-8}$), and minor allele frequency (MAF) > 0.05. Following application of these filters, 574,465 SNPs were retained for analysis (Table 4.4). Imputed genotypes using genome-wide genotyping data and sequencing data from the 1000 Genomes Project (generated by the Michigan Imputation Server²¹) were used to examine loci of interest following the primary analysis.

Table 4.4. Quality control of genotyped SNPs

	N, excluded	N, remaining
Pre-QC		964,055
Autosomal	26,313	937,742
Call rate > 99%	58,396	879,346
Deviation from Hardy-Weinberg equilibrium	4	879,342
MAF > 5%	304,877	574,465

4.3.4 Statistical analyses

Analyses were conducted with Cox proportional hazards models that accounted for early treatment discontinuation due to non-HTN causes. The primary endpoints were the cumulative bevacizumab dose (mg) at the first reported occurrence of grade 2+ HTN or the cumulative bevacizumab dose at the first reported occurrence of grade 3+ HTN. In both models, the total study bevacizumab exposure was used for patients who did not experience a grade 2+ or 3+ event. All patients were uninformatively censored at two years, or 26 treatment cycles. Models were stratified by treatment arm and adjusted for age, BMI \geq 25, preexisting HTN, and preexisting diabetes, based on published data describing clinical predictors of the toxicity²². Genetic models were assumed to be additive. Associations with Bonferroni-adjusted *P*-values $<$ 0.05 were considered statistically significant. Cox models were implemented using the survival²³ package in the R statistical environment²⁴.

4.3.5 In silico functional analysis

Functional annotations of variants with the smallest association *P*-values and their proxies ($r^2 >$ 0.8) were summarized in HaploReg²⁵ and RegulomeDB²⁶. Predictions of functional impact were obtained from computational algorithms including SIFT²⁷, PolyPhen-2²⁸, GERP++²⁹, and CADD³⁰. Allele frequencies were compared to those reported in 1000 Genomes Project EUR super-population³¹. Noncoding variants were assessed primarily by overlap with predicted functional elements from RNA-seq, ChIP-seq, and DNase I hypersensitivity peak calls in the ENCODE Project^{32,33} and the Roadmap Epigenomics Project³⁴. SNPs were queried against SCAN (<http://www.scandb.org/>), the Genotype-

Tissue Expression (GTEx) Project Portal³⁵, ExSNP³⁶, and PhenoScanner³⁷ for previously published expression quantitative trait loci (eQTL) associations.

4.3.6 Replication analysis of top associations

Top SNP associations were tested for replication in two independent cohorts of bevacizumab-treated patients from clinical trials CALGB 80405^{38,39} (described in Chapter 2) and CALGB 90401⁴⁰. Associations with grade 3+ HTN for available SNPs were also looked up in the GWAS results of a third independent cohort in the ECOG-5103 trial¹¹.

CALGB 80405 is a phase III trial conducted to determine if the addition of cetuximab to FOLFIRI or FOLFOX chemotherapy prolongs survival compared to FOLFIRI or FOLFOX with bevacizumab in patients with untreated advanced or metastatic colorectal cancer. CALGB 90401 is a phase III trial comparing docetaxel and prednisone with or without bevacizumab in men with hormone refractory prostate cancer. ECOG-5103 is a phase III adjuvant breast cancer trial of doxorubicin and cyclophosphamide followed by paclitaxel with or bevacizumab. Sample sizes used in the analysis of these cohorts are listed in Table 4.5. CALGB 80405 samples were previously genotyped on the Human OmniExpress and OmniExpressExome arrays (Illumina), and CALGB 90401 samples were genotyped on the Human610-Quad array (Illumina) at the RIKEN Center for Integrative Medical Sciences.

Table 4.5. Summary of replication cohorts

Study	Covariates	Phenotype ¹	N ² , cases	N ² , controls
CALGB 80405	Preexisting HTN	Early grade 3+ HTN	21	448
		Early grade 2+ HTN	70	399
CALGB 90401	Age, BMI ≥ 25, preexisting diabetes	Grade 3+ HTN	25	591
		Grade 2+ HTN	63	553
ECOG-5103	Age > 50, BMI > 30 (subjects with preexisting HTN excluded)	Grade 3+ HTN	177	387

¹Early HTN: HTN occurring within the first three treatment cycles (cumulative bevacizumab dose: 60 mg/kg).

²N = Genotyped samples from genetic European, bevacizumab-treated patients.

Cox proportional hazards models, as described for the discovery analysis, were used to evaluate associations in CALGB 90401 subjects. The number of cycles of bevacizumab treatment was used in place of cumulative dose; subjects received 15 mg/kg bevacizumab once per 21-day cycle. In CALGB 80405, for which toxicity data was available only for the first three 8-week treatment cycles (cumulative dose 60 mg/kg), SNPs were tested with a binary model for association with early grade 2+ or grade 3+ HTN using logistic regression (glm function implemented in R²⁴). Tests were adjusted for the same covariates as in the discovery analysis, where available (Table 4.5). Cumulative dose model associations from existing ECOG-5103 GWAS results are reported here; analysis methods have been previously described¹¹. Associations with Bonferroni-adjusted P -values $< 0.05/N$ (where N was the number of variants tested) were considered statistically significant.

4.4 Results

4.4.1 Subject characteristics

Of 444 subjects, 139 (31%) developed on-treatment grade 2+ HTN, and 49 (11%) developed grade 3+ HTN. Of 415 subjects with non-missing covariate data, 121 grade 2+ HTN events (29%) and 43 grade 3+ HTN events (10%) were analyzed. The demographic and clinical characteristics of the analyzed cohort are summarized in Table 4.6.

Table 4.6. Characteristics of subjects included in discovery analyses

	All (N = 415)	Grade 2+ HTN (N = 121)	Grade 3+ HTN (N = 43)
Age (mean, range)	57 (28–86)	56 (28–78)	57 (37–77)
BMI (mean, range)	29.6 (15.1–73.5)	30.0 (19.5–73.5)	32.0 (19.5–73.5)
Preexisting diabetes (N, %)	46 (11%)	13 (11%)	5 (12%)
Preexisting hypertension (N, %)	154 (37%)	52 (43%)	28 (65%)

All analyzed subjects are genetic European and female.

4.4.2 Association with grade 2+ bevacizumab-induced hypertension

Following quality control procedures, 574,465 SNPs were tested for association with the cumulative bevacizumab dose to the first occurrence of grade 2+ HTN (Figures 4.3 and 4.4). No associations met genome-wide statistical significance after adjustment for multiple testing ($P = 8.7 \times 10^{-8}$). Of the four SNPs with $P < 10^{-5}$ (Table 4.7), rs2018541 had the strongest association ($P = 1.6 \times 10^{-7}$, HR 2.9, 95% CI 1.9–4.3; Figure 4.5). Individuals carrying this variant allele developed HTN at a lower cumulative bevacizumab dose, and the overall incidence of grade 2+ HTN in carriers of the rs2018541 variant allele was higher than in non-carriers (Figure 4.6).

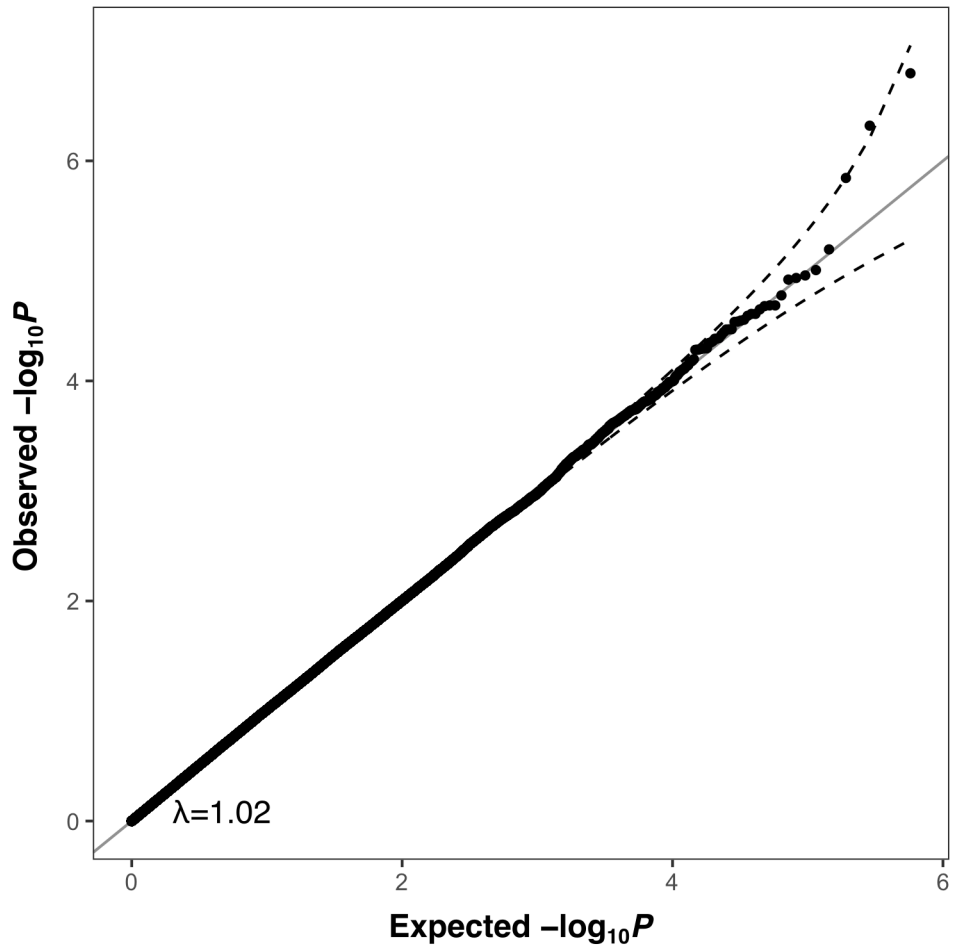


Figure 4.3. Quantile-quantile plot of grade 2+ hypertension analysis. Observed and expected P -value relationships are plotted for the association with grade 2+ hypertension. The solid line shows the expected distribution assuming no inflation of statistics and the dashed lines show the 95% confidence intervals for the expected distribution. The genomic inflation factor λ of 1.02 indicates no significant population stratification.

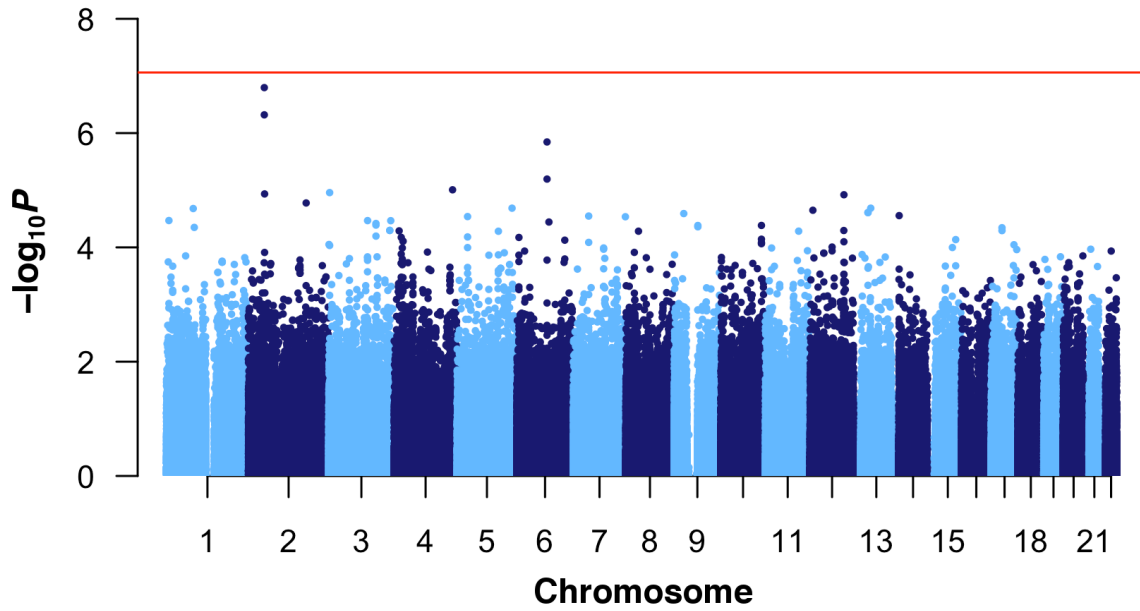


Figure 4.4. Manhattan plot of grade 2+ hypertension analysis. The distribution of $-\log_{10}$ transformed unadjusted P -values for the association with cumulative bevacizumab dose at the first occurrence of grade 2+ hypertension is plotted as a function of the chromosomal location of all tested SNPs ($N = 574,465$). No SNPs surpassed the Bonferroni-corrected significance threshold of $P = 8.7 \times 10^{-8}$.

Table 4.7. Top SNP associations of grade 2+ hypertension analysis

SNP	HR (95% CI)	<i>P</i>¹	MAF	Nearest gene	Function
rs2018541	2.9 (1.9–4.3)	1.6 x 10 ⁻⁷	0.06	<i>MSH6</i>	upstream
rs711272	1.9 (1.5–2.4)	1.4 x 10 ⁻⁶	0.27	<i>MAP3K7</i>	upstream
rs1145786	1.8 (1.4–2.3)	6.4 x 10 ⁻⁶	0.33	<i>MAP3K7</i>	upstream
rs17679314	2.4 (1.6–3.6)	9.8 x 10 ⁻⁶	0.09	<i>ASB5</i>	intronic
rs2728041	0.4 (0.2–0.6)	1.1 x 10 ⁻⁵	0.17	<i>CNTN4</i>	intronic
rs6752945	2.4 (1.6–3.6)	1.2 x 10 ⁻⁵	0.08	<i>STON1-GTF2A1L</i>	intronic
rs12821878	1.9 (1.4–2.5)	1.2 x 10 ⁻⁵	0.25	<i>IGF1</i>	intronic
rs867458	2.1 (1.5–2.9)	1.7 x 10 ⁻⁵	0.13	<i>SP3</i>	downstream
rs10070095	2.5 (1.6–3.8)	2.1 x 10 ⁻⁵	0.05	<i>ODZ2</i>	upstream
rs2273816	2.0 (1.5–2.8)	2.1 x 10 ⁻⁵	0.13	<i>KPNA3</i>	intronic

¹Unadjusted *P*-value from Cox proportional hazards analysis under an additive genetic model and adjusted for age, BMI ≥ 25, preexisting hypertension, and preexisting diabetes.

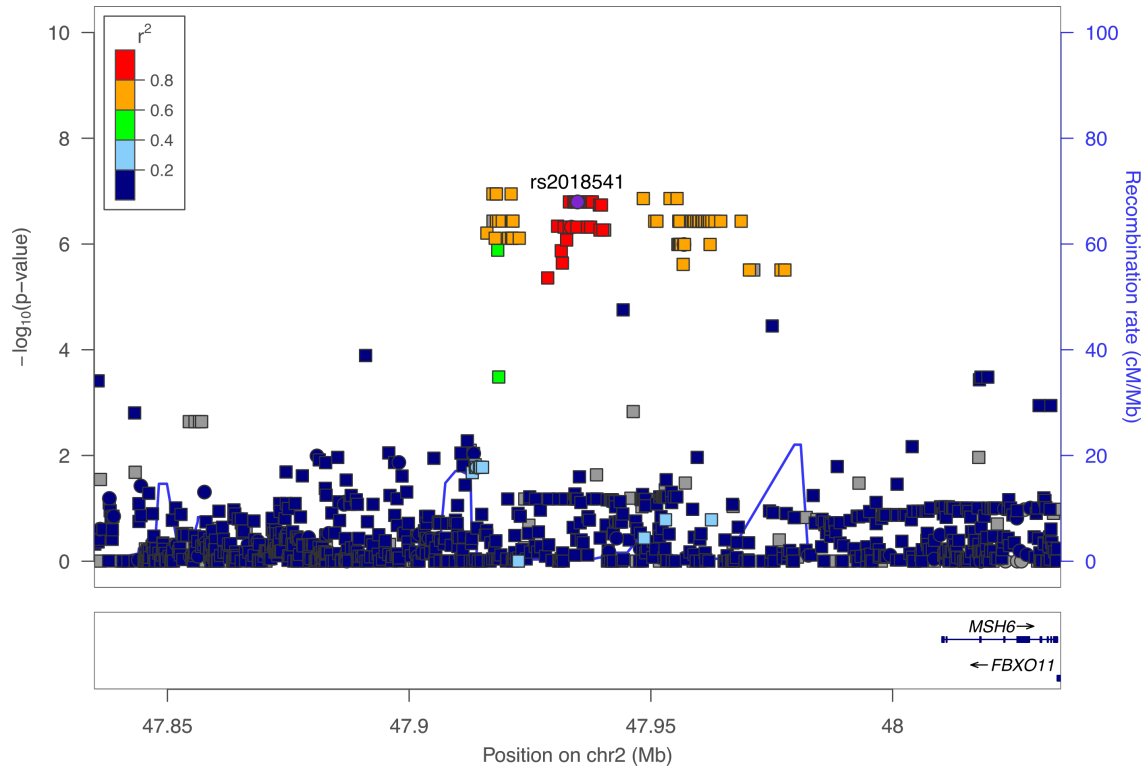
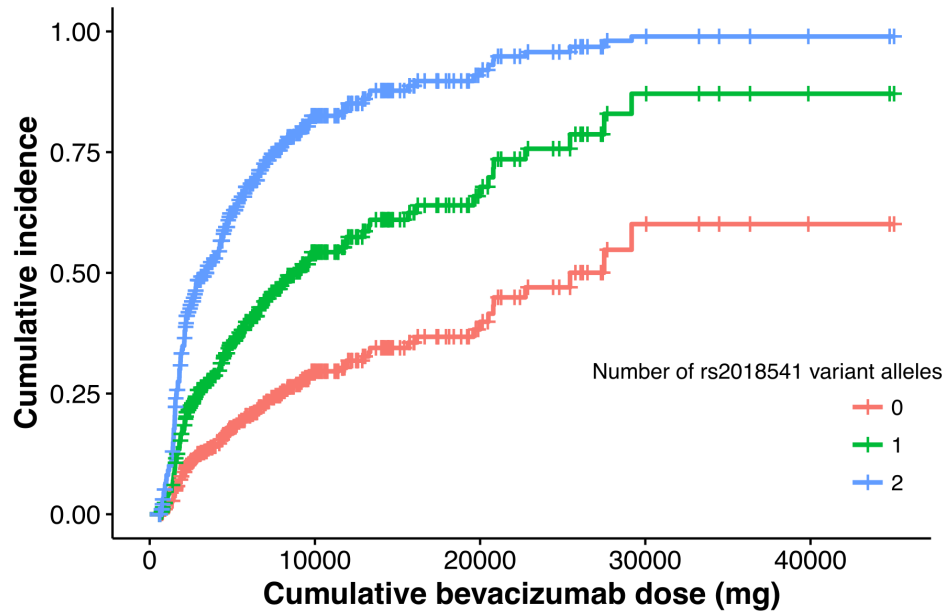


Figure 4.5. Associations with grade 2+ hypertension in the rs2018541 genomic region. Associations with grade 2+ hypertension are shown on a $-\log_{10}P$ scale. Circles indicate genotyped SNPs; squares indicate imputed SNPs. Dot color indicates the strength of linkage disequilibrium (r^2) between rs2018541 (purple) and each SNP. Plot was produced using LocusZoom (<http://locuszoom.sph.umich.edu/>).



Genotype	<i>N</i> , subjects	<i>N</i> , events
rs2018541=0 (AA)	366	94
rs2018541=1 (AG)	45	26
rs2018541=2 (GG)	4	1

Figure 4.6. rs2018541 is associated with increased incidence of grade 2+ hypertension.

The cumulative incidence of grade 2+ hypertension (HTN) as a function of cumulative bevacizumab dose at the first occurrence of toxicity is plotted for each genotype. The number of patients and grade 2+ HTN events per genotype are listed below. The variant allele increased toxicity risk compared with wild-type patients, although there were too few homozygous patients ($N = 4$) to draw meaningful conclusions in this group.

4.4.3 Association with grade 3+ bevacizumab-induced hypertension

The same 574,465 SNPs were tested for association with the cumulative bevacizumab dose to the first occurrence of grade 3+ HTN (Figures 4.7 and 4.8). No associations met genome-wide statistical significance after adjustment for multiple testing ($P = 8.7 \times 10^{-8}$). Five SNPs with $P < 10^{-5}$ are shown in Table 4.8. The strongest and only association exceeding $P < 10^{-6}$ is with rs1981431 ($P = 2.1 \times 10^{-7}$, HR 0.3, 95% CI 0.2–0.4; Figure 4.9). The SNP appears to have a protective effect, with only 1 of 101 individuals with the homozygous variant genotype developing grade 3+ HTN compared to 22 of 96 subjects with the homozygous reference genotype (Figure 4.10).

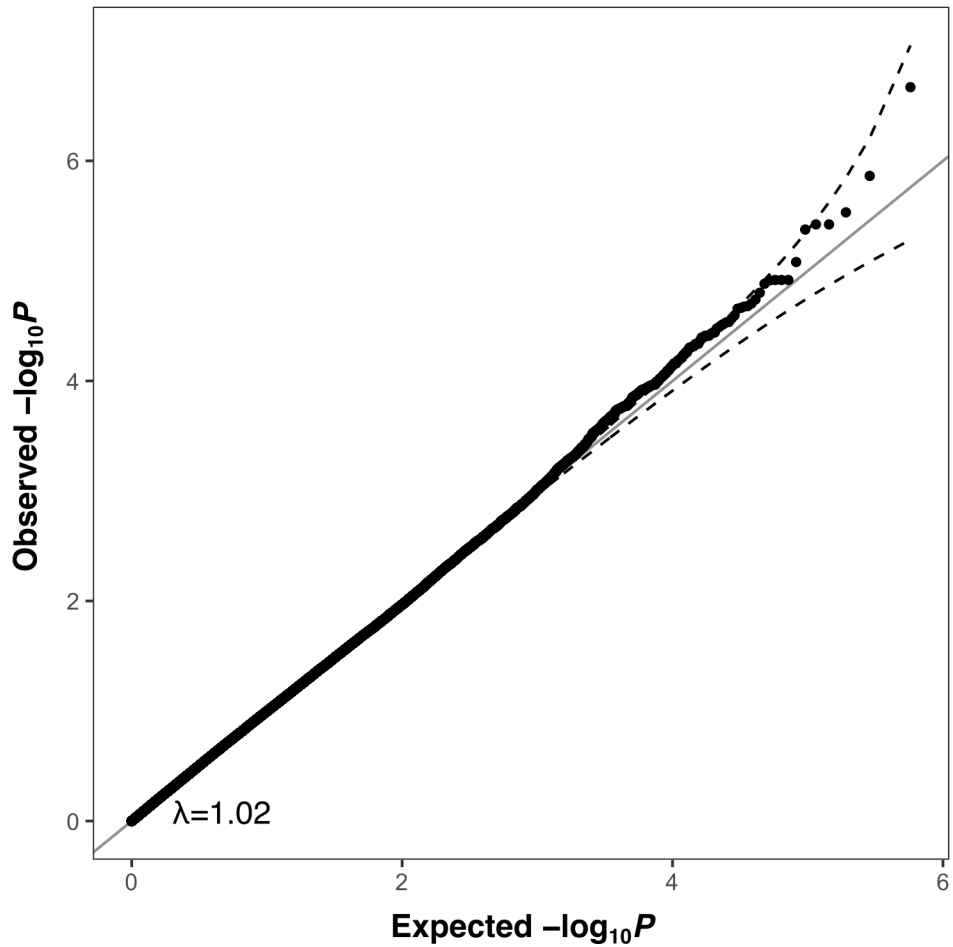


Figure 4.7. Quantile-quantile plot of grade 3+ hypertension analysis. Observed and expected P -value relationships are plotted for the association with grade 3+ hypertension. The solid line shows the expected distribution assuming no inflation of statistics and the dashed lines show the 95% confidence intervals for the expected distribution. The genomic inflation factor λ of 1.02 indicates no significant population stratification.

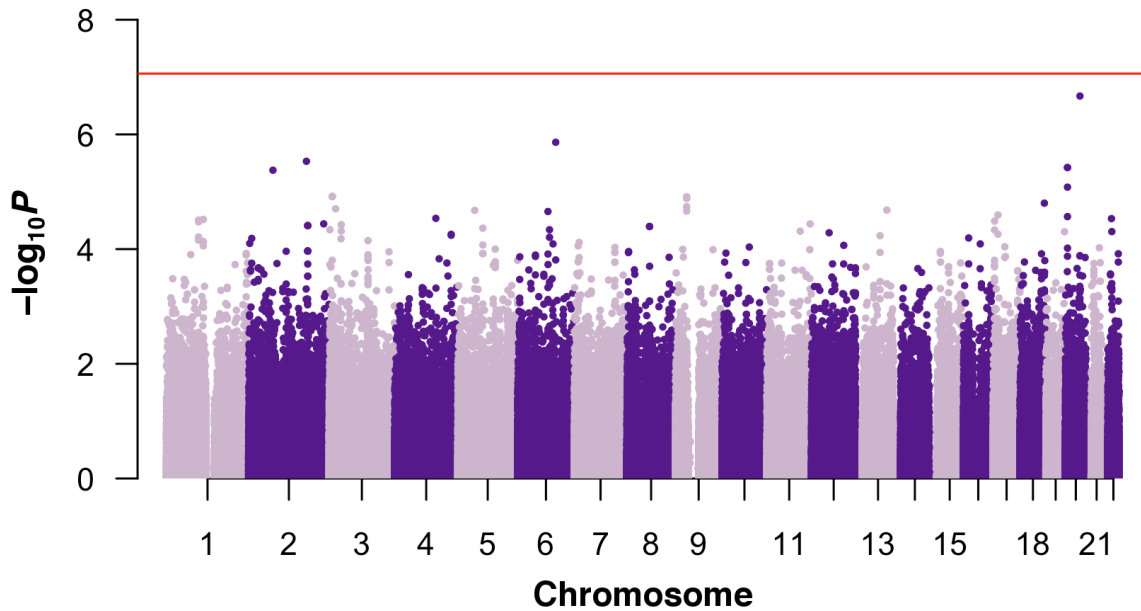


Figure 4.8. Manhattan plot of grade 3+ hypertension analysis. The distribution of $-\log_{10}$ transformed unadjusted P -values for the association with cumulative bevacizumab dose at the first occurrence of grade 3+ hypertension is plotted as a function of the chromosomal location of all tested SNPs ($N = 574,465$). No SNPs surpassed the Bonferroni-corrected significance threshold of $P = 8.7 \times 10^{-8}$.

Table 4.8. Top SNP associations of grade 3+ hypertension analysis

SNP	HR (95% CI)	P^1	MAF	Nearest gene	Function
rs1981431	0.3 (0.2–0.4)	2.1×10^{-7}	0.51	<i>SDC4</i>	intronic
rs13216979	3.8 (2.2–6.5)	1.4×10^{-6}	0.08	<i>HS3ST5</i>	upstream
rs752280	3.5 (2.1–6.0)	2.0×10^{-6}	0.11	<i>SP3</i>	downstream
rs3920632	2.9 (1.8–4.5)	3.8×10^{-6}	0.31	<i>FERMT1</i>	upstream
rs17348756	3.9 (2.2–6.9)	4.2×10^{-6}	0.10	<i>NOTO</i>	upstream
rs2542353	3.6 (2.0–6.3)	1.2×10^{-5}	0.09	<i>LHFPL4</i>	upstream
rs946847	2.8 (1.7–4.3)	1.2×10^{-5}	0.17	<i>C9orf25</i>	intronic
rs17058484	3.3 (1.9–5.6)	1.6×10^{-5}	0.12	<i>LOC339298</i>	upstream
rs10510491	3.7 (2.0–6.6)	2.0×10^{-5}	0.09	<i>EFHB</i>	downstream
rs9584088	3.1 (1.8–5.2)	2.1×10^{-5}	0.20	<i>GPC6</i>	upstream

¹Unadjusted P -value from Cox proportional hazards analysis under an additive genetic model and adjusted for age, BMI ≥ 25 , preexisting hypertension, and preexisting diabetes.

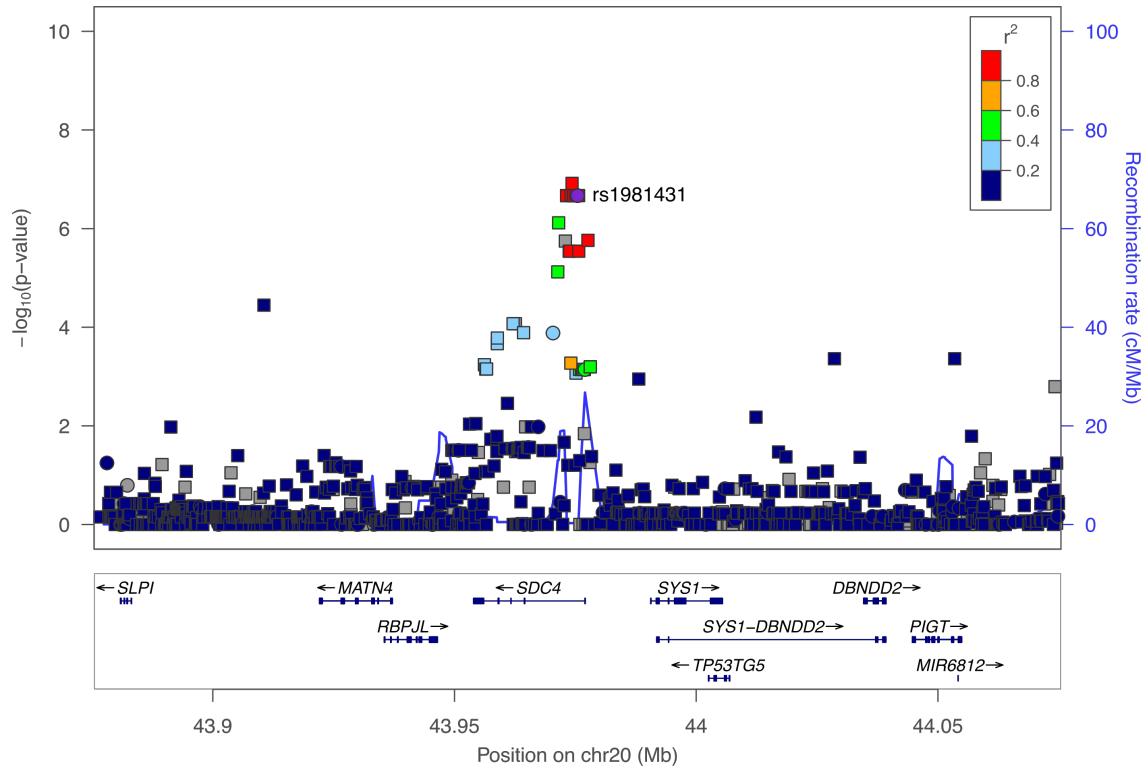
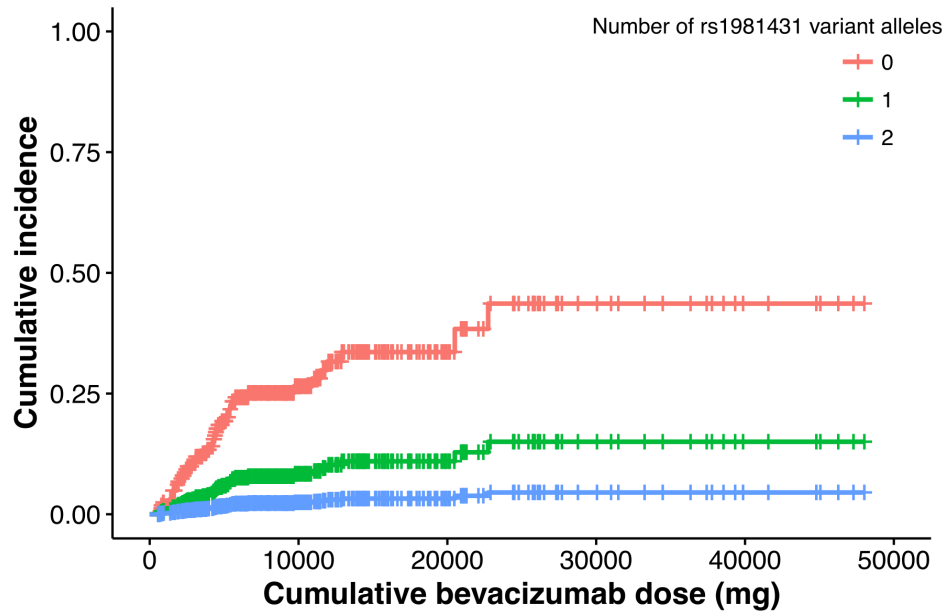


Figure 4.9. Associations with grade 3+ hypertension in the rs1981431 genomic region.

Associations with grade 3+ hypertension are shown on a $-\log_{10}P$ scale. Circles indicate genotyped SNPs; squares indicate imputed SNPs. Dot color indicates the strength of linkage disequilibrium (r^2) between rs1981431 (purple) and each SNP. Plot was produced using LocusZoom (<http://locuszoom.sph.umich.edu/>).



Genotype	<i>N</i> , subjects	<i>N</i> , events
rs1981431=0 (CC)	96	22
rs1981431=1 (CA)	218	20
rs1981431=2 (AA)	101	1

Figure 4.10. rs1981431 is associated with decreased incidence of grade 3+ hypertension.

The cumulative incidence of grade 3+ hypertension (HTN) as a function of cumulative bevacizumab dose at the first occurrence of toxicity is plotted for each genotype. The number of patients and grade 3+ HTN events per genotype are listed below. The variant allele decreased toxicity risk compared with the wild-type allele, with only one toxicity event occurring within 101 homozygous variant patients.

4.4.4 In silico functional analysis

The top SNP of the grade 2+ HTN analysis, rs2018541, is located 75 kb upstream of *MSH6*. Regulome data available for this genomic region suggests no known function in human umbilical vein endothelial cells (HUVEC) (Figure 4.11) nor in most cell types assayed by ENCODE and Roadmap, except for a predicted enhancer state in H1 BMP4 derived trophoblast cultured cells (Roadmap). Examination of imputed genotypes in strong LD ($r^2 > 0.8$) with rs2018541 identified no potentially functional SNPs associating with grade 2+ HTN.

Other SNPs with $P < 10^{-5}$ associations in the grade 2+ analysis include two SNPs between *CASC6* and *MAP3K7* and one intronic SNP in *ASB5*. rs711272 and rs1145786 are located 314 and 325 kb, respectively, upstream of *MAP3K7* but are not in strong LD with each other ($r^2 = 0.55$). The site at rs711272 is predicted to be conserved (GERP++: 4.1), though neither SNP is predicted to have regulatory function. The genomic region containing rs17679314 (*ASB5*) also does not contain any regulatory function in HUVEC, though it is predicted to have enhancer activity in HSMM cell derived skeletal muscle myotubes (Roadmap).

rs1981431 lies within an intron of *SDC4* near the first exon. rs1981431 is located in a predicted weak enhancer region in HUVEC, characterized primarily by H3K4Me1 and H3K79me2 histone modifications (Figure 4.12). rs1981431 has also been associated with differential expression of *SDC4*, with the A allele associated with increased expression in the cerebellum and decreased expression in lymphoblastoid cells (Table 4.9).

Other SNPs with $P < 10^{-5}$ associations in the grade 3+ analysis include rs13216979 (732 kb 5' of *HS3ST5*), rs752280 (218 kb 5' of *SP3*), rs3920632 (232 kb 5' of *FERMT1*), and rs17348756 (16 kb 5' of *NOTO*). rs13216979 (phyloP: 1.1, phastCons: 1) and rs752280 (GERP++: 2.1) are predicted to be conserved. The rs17348756 minor allele has been associated with decreased *SMYD5* expression in tibial nerve ($P = 6.5 \times 10^{-10}$) and transformed fibroblasts ($P = 9.9 \times 10^{-9}$)⁴¹. However, regulatory elements are absent from all the genomic regions containing these SNPs in all cell types assayed by ENCODE and Roadmap.

Examination of imputed genotypes of potentially functional SNPs in *SDC4* identified rs2741454 associating with grade 3+ HTN ($P = 1.2 \times 10^{-7}$, HR 0.2, 95% CI 0.1–0.4). rs2741454 is in strong LD with rs1981431 ($r^2 = 0.93$) and is located in an intronic region predicted to be a strong enhancer (Figure 4.12). The SNP maps to a DNase hypersensitive site and is predicted to be conserved (GERP++: 2.2) and deleterious (CADD: 14.1).

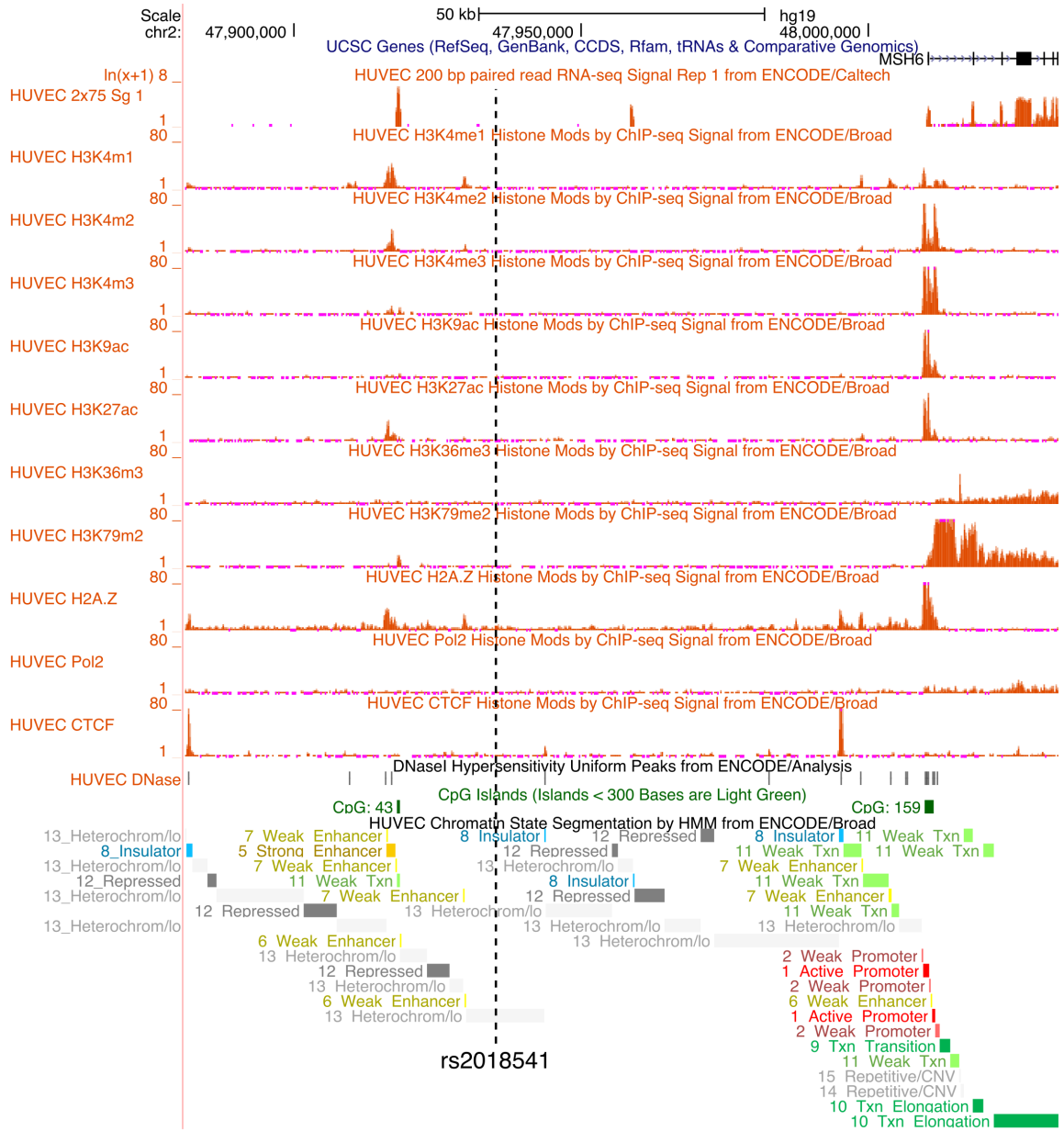


Figure 4.11. rs2018541 is in a genomic region 5' upstream of *MSH6* lacking predicted regulatory function. Tracks (top to bottom): UCSC Genes, HUVEC 200 bp paired read RNA-seq Signal Rep 1 from ENCODE/Caltech, HUVEC Histone Modifications by ChIP-seq Signal from ENCODE/Broad (H3K4me1, H3K4me2, H3K4me3, H3K9ac, H3K27ac, H3K36me3, H3K79me2, H2A.Z, Pol2, CTCF), HUVEC DNaseI Hypersensitivity Uniform Peaks from ENCODE/Analysis, CpG Islands, and HUVEC Chromatin State Segmentation by HMM from ENCODE/Broad.

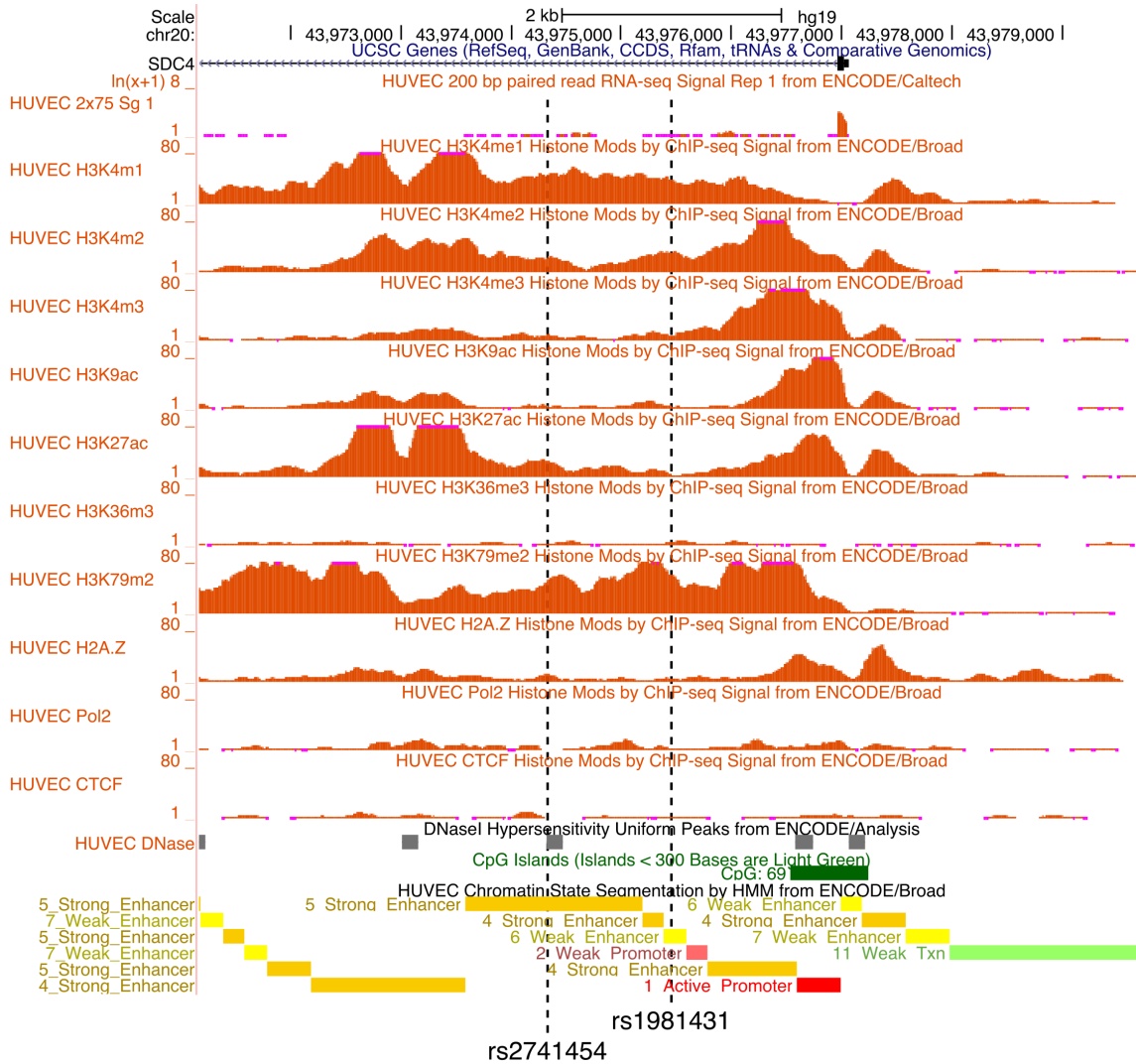


Figure 4.12. rs1981431 and rs2741454 are in a predicted enhancer region within an intron of *SDC4*. Tracks (top to bottom): UCSC Genes, HUVEC 200 bp paired read RNA-seq Signal Rep 1 from ENCODE/Caltech, HUVEC Histone Modifications by ChIP-seq Signal from ENCODE/Broad (H3K4me1, H3K4me2, H3K4me3, H3K9ac, H3K27ac, H3K36me3, H3K79me2, H2A.Z, Pol2, CTCF), HUVEC DNaseI Hypersensitivity Uniform Peaks from ENCODE/Analysis, CpG Islands, and HUVEC Chromatin State Segmentation by HMM from ENCODE/Broad.

Table 4.9. rs1981431 eQTL associations with *SDC4* expression

Tissue/Cell	<i>P</i>	Beta¹	Study
Brain – Cerebellum	3.9 x 10 ⁻⁷	0.33	GTEx V6p ⁴¹
Artery – Aorta	0.0052	-0.14	GTEx V6p ⁴¹
Artery – Tibial	0.067	-0.07	GTEx V6p ⁴¹
Lymphoblastoid cells	2.7 x 10 ⁻¹¹	-0.34	1000 Genomes ⁴²
Lymphoblastoid cells	7.6 x 10 ⁻⁹	-0.11	MuTHER ⁴³

¹Beta directions were adjusted to be consistent with rs1981431-A as the effect allele.

4.4.5 Replication analysis of top SNP associations

SNPs with associations of $P < 10^{-5}$ in both the grade 2+ HTN and grade 3+ HTN analyses were tested for replication in bevacizumab-treated patients from CALGB 80405 and CALGB 90401. Associations with grade 3+ HTN were also looked up in ECOG-5103 GWAS results. rs17679314 (*ASB5*) associated with early grade 2+ HTN ($P = 0.01$, OR 2.1, 95% CI 1.2–3.7) in CALGB 80405. The risk allele was observed in 19 (27%) of 70 cases (17 heterozygous, 2 homozygous) compared to 63 (16%) of 393 controls (all heterozygous). rs17348756 (*NOTO*) associated with grade 3+ HTN at a nominally significant level in ECOG-5103, but with an opposite direction of effect (HR 0.7). No other associations replicated in any cohort (Tables 4.10-4.12, Figures 4.13 and 4.14).

Table 4.10. Replication analysis of top SNP associations in CALGB 80405

Phenotype ¹	SNP	OR (95% CI)	P ²
Early grade 2+ HTN	rs2018541 (<i>MSH6</i>)	0.4 (0.1–1.0)	0.07
	rs711272 (<i>MAP3K7</i>)	1.4 (1.0–2.0)	0.08
	rs1145786 (<i>MAP3K7</i>)	1.2 (0.8–1.7)	0.40
	rs17679314 (<i>ASB5</i>)	2.1 (1.2–3.7)	0.01
Early grade 3+ HTN	rs1981431 (<i>SDC4</i>)	1.1 (0.6–2.0)	0.77
	rs13216979 (<i>HS3ST5</i>)	0.7 (0.1–2.5)	0.66
	rs752280 (<i>SP3</i>)	0.7 (0.2–1.8)	0.51
	rs3920632 (<i>FERMT1</i>)	0.8 (0.4–1.5)	0.49
	rs17348756 (<i>NOTO</i>)	0.9 (0.2–2.4)	0.82

¹Early HTN: HTN occurring within the first three treatment cycles (cumulative bevacizumab dose: 60 mg/kg).

²Unadjusted *P*-value from logistic regression under an additive genetic model and adjusted for preexisting HTN.

Table 4.11. Replication analysis of top SNP associations in CALGB 90401

Phenotype	SNP	HR (95% CI)	P ¹
Grade 2+ HTN	rs2018541 (<i>MSH6</i>)	0.9 (0.4–1.8)	0.76
	rs711272 (<i>MAP3K7</i>)	1.1 (0.7–1.6)	0.67
	rs1145786 (<i>MAP3K7</i>)	1.2 (0.9–1.8)	0.24
	rs17679314 (<i>ASB5</i>)	1.2 (0.7–2.1)	0.38
Grade 3+ HTN	rs1981431 (<i>SDC4</i>)	0.7 (0.4–1.3)	0.31
	rs13216979 (<i>HS3ST5</i>)	1.4 (0.6–3.6)	0.45
	rs752280 (<i>SP3</i>)	0.7 (0.3–1.7)	0.40
	rs3920632 (<i>FERMT1</i>)	0.8 (0.4–1.4)	0.40
	rs17348756 ² (<i>NOTO</i>)	NA	NA

¹Unadjusted *P*-value from Cox proportional hazards analysis under an additive genetic model and adjusted for age, BMI ≥ 25, and preexisting diabetes.

²No proxy SNP available.

Table 4.12. Lookup of top SNP associations with grade 3+ hypertension in ECOG-5103

SNP	HR	P¹
rs2018541 (<i>MSH6</i>)	0.9	0.77
rs711272 (<i>MAP3K7</i>)	1.1	0.62
rs1145786 (<i>MAP3K7</i>)	1.0	0.88
rs17679314 (<i>ASB5</i>)	0.8	0.38
rs1981431 (<i>SDC4</i>)	1.0	0.67
rs13216979 (<i>HS3ST5</i>)	1.1	0.51
rs752280 (<i>SP3</i>)	1.0	0.88
rs3920632 (<i>FERMT1</i>)	1.1	0.57
rs17348756 (<i>NOTO</i>)	0.7	0.04

¹Unadjusted *P*-value from Cox proportional hazards analysis under an additive genetic model and adjusted for age > 50, BMI > 30.

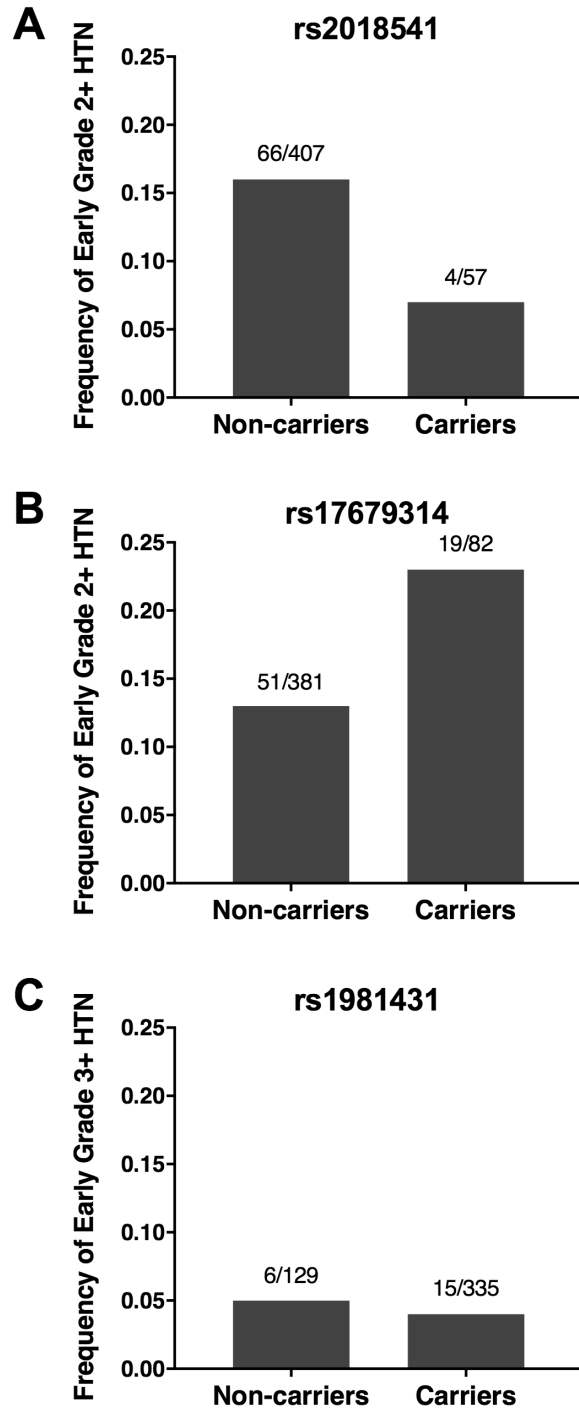


Figure 4.13. Frequency of early bevacizumab-induced hypertension in CALGB 80405 replication subjects stratified by carrier status of top discovery SNPs. Early grade 2+ hypertension (HTN) frequencies in carriers versus non-carriers of A) rs2018541 (*MSH6*) and B) rs17679314 (*ASB5*). C) Early grade 3+ HTN frequencies in carriers versus non-carriers of rs1981431 (*SDC4*). Fractions represent the number of HTN cases over the total number of subjects for each carrier status. Only the rs17679314 association met statistical significance ($P = 0.01$).

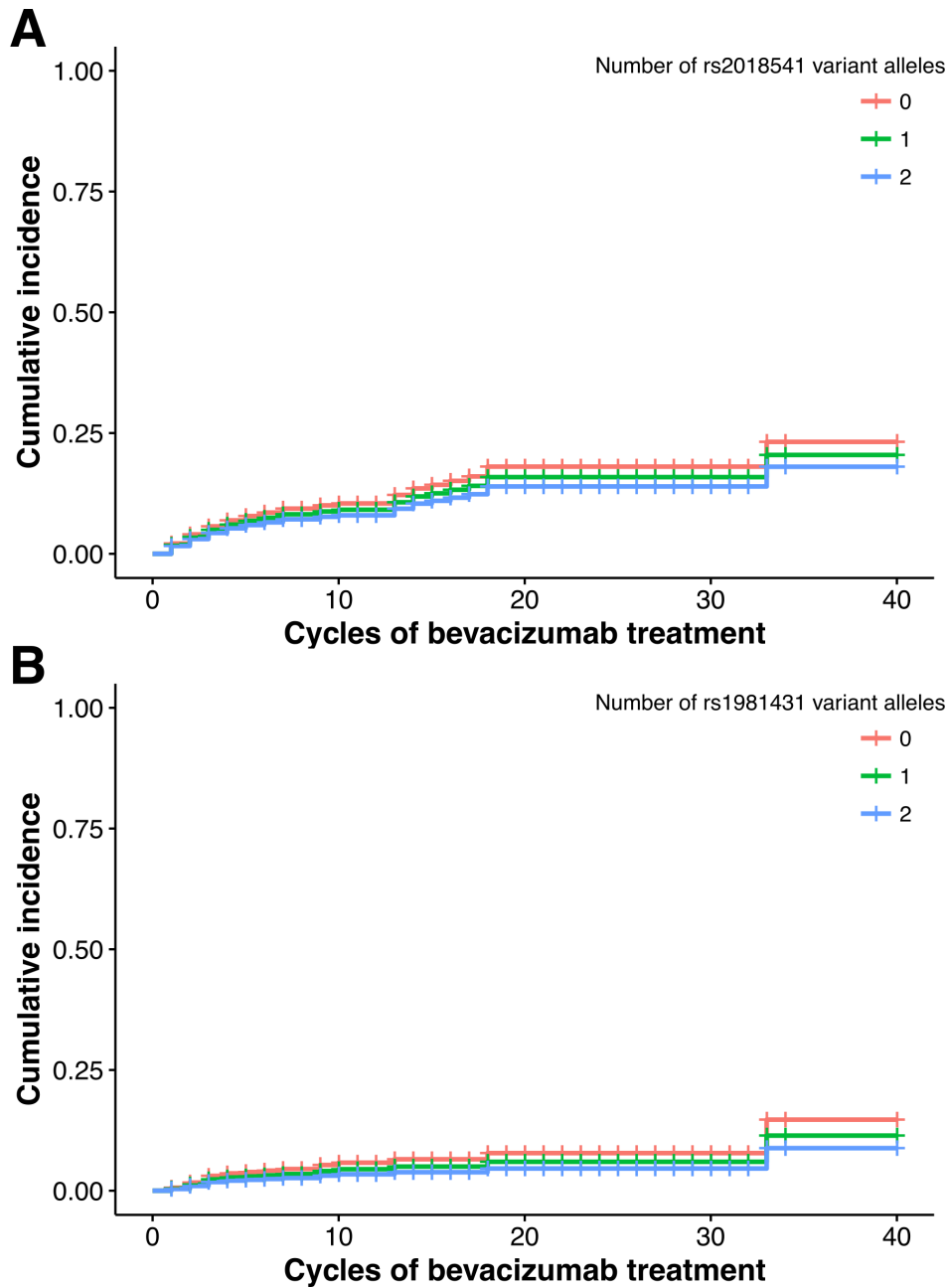


Figure 4.14. Cumulative incidence of bevacizumab-induced hypertension in CALGB 90401 replication subjects stratified by genotypes of top discovery SNPs. The cumulative incidence of A) grade 2+ hypertension (HTN) for rs2018541 (*MSH6*) and B) grade 3+ HTN for rs1981431 (*SDC4*) is plotted as a function of cumulative bevacizumab dose at the first occurrence of toxicity. A prescribed dose of 15 mg/kg bevacizumab was given each treatment cycle. Neither of these associations met statistical significance.

4.4.6 Analysis of previously reported SNP associations

Previously identified SNPs from published candidate gene and genome-wide association studies of bevacizumab-induced HTN (Table 4.13) were tested for associations with grade 2+ and grade 3+ HTN in CALGB 40502 (Tables 4.14 and 4.15). Only rs833069 (*VEGFA*), a proxy for rs2010963 ($r^2 = 0.97$), replicated at a nominally significant level ($P = 0.04$, HR 0.6, 95% CI 0.4–1.0) for association with grade 3+ HTN.

Table 4.13. Previously reported SNP associations with bevacizumab-induced hypertension

SNP	Gene	Function	Association with bev-induced HTN	Study
rs699947 (A/C)	VEGFA	promoter	CC: Decreased risk (early grade 2+, grade 2+)	Morita <i>et al</i> (2012) ⁷
rs833061 (C/T)	VEGFA	promoter	TT: Decreased risk (grade 3+)	Schneider <i>et al</i> (2008) ⁵
			TT: Decreased risk (early grade 2+)	Morita <i>et al</i> (2012) ⁷
rs2010963 (G/C)	VEGFA	5'-UTR	CC: Decreased risk (grade 3+)	Schneider <i>et al</i> (2008) ⁵
			C: Increased risk (all-grade)	Etienne-Grimaldi <i>et al</i> (2011) ⁶
			GG: Increased risk (grade 3+)	Gampenrieder <i>et al</i> (2016) ⁹
rs3025039 (T/C)	VEGFA	3'-UTR	CC: Decreased risk (grade 2+)	Morita <i>et al</i> (2012) ⁷
			CC: Increased risk (all-grade)	Sibertin-Blanc <i>et al</i> (2015) ⁸
rs2305949 (C/T)	KDR	intronic	T: Decreased risk (all-grade)	Lambrechts <i>et al</i> (2014) ¹²
rs1870377 (T/A)	KDR	nonsynonymous	A: Increased risk (grade 2+)	Jain <i>et al</i> (2010) ¹⁰
rs1680695 (T/G)	EGLN3	intronic	G: Increased risk (all-grade)	Lambrechts <i>et al</i> (2014) ¹²
rs4444903 (A/G)	EGF	5'-UTR	G: Increased risk (all-grade)	Lambrechts <i>et al</i> (2014) ¹²
rs11064560 (T/G)	WNK1	intronic	T: Increased risk (all-grade)	Lambrechts <i>et al</i> (2014) ¹²
rs6453204 (A/G)	SV2C	intronic	G: Increased risk (SBP > 160 mmHg, grade 3+)	Schneider <i>et al</i> (2014) ¹¹

Table 4.14. Associations of previously reported SNPs with grade 2+ hypertension in CALGB 40502

SNP	Proxy SNP	HR (95% CI)	<i>P</i> ¹
rs699947 (A/C)	rs833070 ($r^2 = 1.00$)	1.1 (0.9–1.4)	0.37
rs833061 (C/T)	rs833070 ($r^2 = 0.97$)	1.1 (0.9–1.4)	0.24
rs2010963 (G/C)	rs833069 ($r^2 = 0.97$)	0.9 (0.7–1.1)	0.56
rs3025039 (T/C)		1.1 (0.8–1.6)	0.78
rs2305949 (C/T)	rs2305948 ($D' = 0.98$)	0.9 (0.6–1.4)	0.89
rs1870377 (T/A)		1.0 (0.7–1.3)	0.88
rs1680695 (T/G)	rs1384372 ($r^2 = 0.93$)	1.0 (0.8–1.3)	0.70
rs4444903 (A/G)		0.9 (0.7–1.2)	0.83
rs11064560 (T/G)		1.0 (0.7–1.3)	0.37
rs6453204 (A/G)		0.9 (0.6–1.4)	0.65

¹Unadjusted *P*-value from Cox proportional hazards analysis under an additive genetic model and adjusted for age, BMI ≥ 25 , preexisting hypertension, and preexisting diabetes.

Table 4.15. Associations of previously reported SNPs with grade 3+ hypertension in CALGB 40502

SNP	Proxy SNP	HR (95% CI)	<i>P</i> ¹
rs699947 (A/C)	rs833070 ($r^2 = 1.00$)	1.2 (0.8–1.9)	0.35
rs833061 (C/T)	rs833070 ($r^2 = 0.97$)	1.2 (0.8–1.9)	0.35
rs2010963 (G/C)	rs833069 ($r^2 = 0.97$)	0.6 (0.4–1.0)	0.04
rs3025039 (T/C)		1.3 (0.7–2.4)	0.38
rs2305949 (C/T)	rs2305948 ($D' = 0.98$)	1.1 (0.6–2.1)	0.74
rs1870377 (T/A)		1.2 (0.7–2.0)	0.46
rs1680695 (T/G)	rs1384372 ($r^2 = 0.93$)	1.1 (0.7–1.8)	0.53
rs4444903 (A/G)		0.8 (0.5–1.2)	0.25
rs11064560 (T/G)		1.2 (0.8–2.0)	0.43
rs6453204 (A/G)		0.6 (0.3–1.2)	0.12

¹Unadjusted *P*-value from Cox proportional hazards analysis under an additive genetic model and adjusted for age, BMI ≥ 25 , preexisting hypertension, and preexisting diabetes.

Although the original *SV2C* SNP (rs6453204) from the Schneider *et al* GWAS in ECOG-5103 did not associate with HTN in CALGB 40502 using either a cumulative dose or binary model, four other SNPs in *SV2C*, including a missense variant, ranked within the top 100 associations of the primary genome-wide analysis of grade 3+ HTN in CALGB 40502 (Table 4.16).

Table 4.16. Top *SV2C* SNP associations with grade 3+ hypertension in CALGB 40502

SNP	HR (95% CI)	<i>P</i> ¹	MAF	Gene	Function
rs2937748	3.1 (1.8–5.4)	4.3 x 10 ⁻⁵	0.07	<i>SV2C</i>	intronic
rs2937746	3.1 (1.8–5.4)	8.5 x 10 ⁻⁵	0.07	<i>SV2C</i>	intronic
rs2358712	3.0 (1.7–5.2)	1.2 x 10 ⁻⁴	0.07	<i>SV2C</i>	intronic
rs31244	3.0 (1.7–5.2)	1.2 x 10 ⁻⁴	0.07	<i>SV2C</i>	missense

¹Unadjusted *P*-value from Cox proportional hazards analysis under an additive genetic model and adjusted for age, BMI ≥ 25, preexisting hypertension, and preexisting diabetes.

4.5 Discussion

The present study used a genome-wide analysis to discover common variants that may be predictive of bevacizumab-induced HTN. Although no genetic associations reached statistical significance following correction for multiple testing, several top loci are in genomic regions of biological interest and at least two top SNPs may have regulatory function.

The strongest grade 2+ HTN association is with a locus upstream of *MSH6*. *MSH6* encodes mutS homolog 6, a member of the DNA mismatch repair MutS family. Mutations in this gene have been primarily associated with Lynch syndrome⁴⁴, colorectal cancer⁴⁵, and

endometrial cancer⁴⁶. Of interest to bevacizumab treatment, one study observed significantly higher median serum VEGF concentrations in colorectal cancer patients with microsatellite unstable tumors (lacking protein expression of any of 4 mismatch repair genes: *MLH1*, *PMS2*, *MSH2*, *MSH6*) compared to patients with microsatellite stable tumors⁴⁷. Little evidence is available regarding the regulatory function of the associated SNP, warranting functional studies to examine changes in *MSH6* expression and how this may influence VEGF levels or other mechanisms related to blood pressure regulation.

rs17679314 (*ASB5*) also associated with grade 2+ HTN. *ASB5* encodes a member of the ankyrin repeat and SOCS box-containing (*ASB*) family of proteins and has been reported to play a role in the initiation of arteriogenesis⁴⁸. *ASB5* is also located near *VEGFC*, which encodes another VEGFR2-binding ligand, though no eQTL associations between rs17679314 (or its proxies) and *VEGFC* expression have been reported.

The strongest association with grade 3+ HTN was with rs1981431, an intronic SNP in *SDC4*. The hazards ratio of this association indicates a protective effect against bevacizumab-induced HTN. *In silico* analyses suggest that this SNP is located in an enhancer region in endothelial cells, and eQTL analyses have found rs1981431 to be associated with differential expression of *SDC4* in various tissues. *SDC4* encodes syndecan-4, a ubiquitous cell surface heparan sulfate proteoglycan⁴⁹. Heparan sulfate proteoglycans act as transactivating co-receptors of VEGFR2, leading to prolonged and enhanced VEGF signaling⁵⁰. A lack of syndecan-4 has been reported to affect VEGFR2 phosphorylation⁵¹. Upon stimulation with pro-angiogenic factors like VEGF, syndecan-4 expression is

upregulated on endothelial cells^{51,52}. SDC4 expression has been shown to increase VEGF-induced NO release⁵³, consistent with the observation of decreased eNOS phosphorylation in endothelial cells of *SDC4*^{-/-} mice⁵⁴.

Syndecan-4 has also been examined for its association with direct changes in blood pressure. *SDC4* variant rs1981429 (242 bp downstream of rs1981431; $r^2 = 0.99$) has been associated with essential HTN in a Finnish cohort⁵⁵. *SDC4*^{-/-} mice were shown to have increased arterial blood pressure⁵⁴; however, in a different study, *SDC4*^{-/-} mice exhibited lower systolic blood pressure following lipopolysaccharide injection⁵⁶. Although the high population MAF of rs1981431 suggests that it is unlikely to have a truly large effect on blood pressure, it may perhaps influence VEGF signaling only upon bevacizumab exposure. Further studies are required to determine the role of *SDC4* in the development of bevacizumab-induced HTN.

rs17348756 (*NOTO*), which also associated with grade 3+ HTN, has reported eQTL associations with decreased expression of *SMYD5*, a member of the Smyd family of methyltransferases. Human Smyd proteins have been implicated in diverse biological functions; Smyd2 mediates Hsp90 methylation⁵⁷ and Smyd3 catalyzes VEGFR1 methylation⁵⁸. Smyd5 has been shown to regulate inflammatory response genes⁵⁹ and hematopoiesis⁶⁰ in animal models but its function in humans remains largely unknown.

rs17679314 (*ASB5*), which associated with cumulative bevacizumab dose at the first occurrence of grade 2+ HTN in CALGB 40502, also associated with development of early

grade 2+ HTN in CALGB 80405. No other associations replicated in any of the replication cohorts. This could be attributed to differences in clinical trial design and dosing, demographic, clinical, and phenotypic differences between study populations, or the possibility of false positive findings. The sample size of CALGB 90401 had 63% and 91% power to detect associations at a nominal significance level of 0.05 for the strongest SNP associations from the grade 2+ and grade 3+ analyses, respectively, assuming similar effect sizes and directions as in the discovery phase⁶¹. Using toxicity information from only the first three treatment cycles, CALGB 80405 had 80% and 92% power, respectively, to detect associations of similar effects as in CALGB 40502 (G*Power 3⁶²).

Previously described associations in the published literature did not replicate in CALGB 40502, though a proxy SNP of rs2010963 nominally associated with grade 3+ HTN. This 5'-UTR variant of *VEGFA* has been previously associated with risk of grade 3+ or all-grade HTN, though with discordant effect directions^{5,6,9}. The association in CALGB 40502 agrees with Schneider *et al* and Gampenrieder *et al*, with the minor allele associating with decreased risk of HTN. Furthermore, the previous Schneider *et al* GWAS of bevacizumab-induced HTN in ECOG-5103 identified an intronic SNP (rs6453204) in *SV2C* associated with systolic blood pressure > 160 mmHg in the discovery cohort and with grade 3–4 HTN in the replication cohort¹¹. Four *SV2C* SNPs, including a missense variant, ranked in the top 100 associations in the CALGB 40502 grade 3+ HTN analysis. Although none of these variants are in LD with rs6453204, nor is there evidence of association between *SV2C* and HTN in the CALGB 80405 or CALGB 90401 cohorts, this finding contributes additional support of the potential role of *SV2C* in the development of bevacizumab-induced HTN. *SV2C* encodes

a synaptic vesicle glycoprotein, and Schneider *et al* postulate that the protein may influence blood pressure through the release of catecholamines from adrenal chromaffin cells and production of aldosterone through adrenocortical connections with the adrenal medulla.

Limitations of this study are similar to those of the exome sequencing study described in Chapter 2. Despite rigorous curation, the HTN phenotype may be confounded by other factors, especially preexisting HTN, which was significantly correlated with the development of grade 3+ on-treatment HTN ($P = 2 \times 10^{-4}$, HR 3.3). The size of the analyzed cohort is underpowered for detecting genome-wide associations, with only 0.4% power to detect the strongest observed SNP association from the grade 2+ analysis and 7% power to detect the strongest observed association from the grade 3+ analysis at Bonferroni-adjusted significance levels⁶¹. Assuming the same toxicity incidence rate, a sample size 2 to 4 times larger would be needed to achieve at least 80% statistical power. Replication is needed in additional cohorts to extend these current findings, and functional studies are also required to assess whether the identified SNPs and genes affect blood pressure regulation.

4.6 Conclusions

This genome-wide association study identified SNPs in or near novel genes (*MSH6*, *SDC4*, *ASB5*, *SMYD5*) that potentially modify the risk of developing bevacizumab-induced HTN. Additional validation studies are warranted to determine the role of these genes and variants in the pathogenesis of the toxicity. These findings will contribute to a better understanding of the genetic architecture and mechanism of bevacizumab-induced HTN.

4.7 References

1. Ferrara N, Hillan KJ, Gerber HP, Novotny W. Discovery and development of bevacizumab, an anti-VEGF antibody for treating cancer. *Nat Rev Drug Discov.* 2004;3(5):391–400.
2. Zhu X, Wu S, Dahut WL, Parikh CR. Risks of proteinuria and hypertension with bevacizumab, an antibody against vascular endothelial growth factor: systematic review and meta-analysis. *Am J Kidney Dis.* 2007;49(2):186–93.
3. Ranpura V, Pulipati B, Chu D, Zhu X, Wu S. Increased risk of high-grade hypertension with bevacizumab in cancer patients: a meta-analysis. *Am J Hypertens.* 2010;23(5):460–8.
4. Avastin [package insert]. South San Francisco, CA: Genentech, Inc.; 2016. Available from: https://www.gene.com/download/pdf/avastin_prescribing.pdf
5. Schneider BP, Wang M, Radovich M, Sledge GW, Badve S, Thor A, Flockhart DA, Hancock B, Davidson N, Gralow J, Dickler M, Perez EA, Cobleigh M, Shenkier T, Edgerton S, Miller KD, ECOG 2100. Association of vascular endothelial growth factor and vascular endothelial growth factor receptor-2 genetic polymorphisms with outcome in a trial of paclitaxel compared with paclitaxel plus bevacizumab in advanced breast cancer: ECOG 2100. *J Clin Oncol.* 2008;26(28):4672–8.
6. Etienne-Grimaldi MC, Formento P, Degeorges A, Pierga JY, Delva R, Pivot X, Dalenc F, Espié M, Veyret C, Formento JL, Francoual M, Piutti M, de Crémoux P, Milano G. Prospective analysis of the impact of VEGF-A gene polymorphisms on the pharmacodynamics of bevacizumab-based therapy in metastatic breast cancer patients. *Br J Clin Pharmacol.* 2011;71(6):921–8.
7. Morita S, Uehara K, Nakayama G, Shibata T, Oguri T, Inada-Inoue M, Shimokata T, Sugishita M, Mitsuma A, Ando Y. Association between bevacizumab-related hypertension and vascular endothelial growth factor (VEGF) gene polymorphisms in Japanese patients with metastatic colorectal cancer. *Cancer Chemother Pharmacol.* 2013;71(2):405–11.
8. Sibertin-Blanc C, Mancini J, Fabre A, Lagarde A, Del Grande J, Levy N, Seitz JF, Olschwang S, Dahan L. Vascular Endothelial Growth Factor A c.*237C>T polymorphism is associated with bevacizumab efficacy and related hypertension in metastatic colorectal cancer. *Dig Liver Dis.* 2015;47(4):331–7.
9. Gampenrieder SP, Hufnagl C, Brechelmacher S, Huemer F, Hackl H, Rinnerthaler G, Romeder F, Monzo Fuentes C, Morre P, Hauser-Kronberger C, Mlineritsch B, Greil R. Endothelin-1 genetic polymorphism as predictive marker for bevacizumab in metastatic breast cancer. *Pharmacogenomics J.* 2016. doi:10.1038/tpj.2016.25 [Epub ahead of print]

10. Jain L, Sissung TM, Danesi R, Kohn EC, Dahut WL, Kummar S, Venzon D, Liewehr D, English BC, Baum CE, Yarchoan R, Giaccone G, Venitz J, Price DK, Figg WD. Hypertension and hand-foot skin reactions related to VEGFR2 genotype and improved clinical outcome following bevacizumab and sorafenib. *J Exp Clin Cancer Res.* 2010;29:95.
11. Schneider BP, Li L, Shen F, Miller KD, Radovich M, O'Neill A, Gray RJ, Lane D, Flockhart DA, Jiang G, Wang Z, Lai D, Koller D, Pratt JH, Dang CT, Northfelt D, Perez EA, Shenkier T, Cobleigh M, Smith ML, Railey E, Partridge A, Gralow J, Sparano J, Davidson NE, Foroud T, Sledge GW. Genetic variant predicts bevacizumab-induced hypertension in ECOG-5103 and ECOG-2100. *Br J Cancer.* 2014;111(6):1241–8.
12. Lambrechts D, Moisse M, Delmar P, Miles DW, Leighl N, Escudier B, Van Cutsem E, Bansal AT, Carmeliet P, Scherer SJ, de Haas S, Pallaud C. Genetic markers of bevacizumab-induced hypertension. *Angiogenesis.* 2014;17(3):685–94.
13. The SEARCH Collaborative Group. SLC01B1 variants and statin-induced myopathy — a genomewide study. *N Engl J Med.* 2008;359(8):789–99.
14. Daly AK, Donaldson PT, Bhatnagar P, Shen Y, Pe'er I, Floratos A, Daly MJ, Goldstein DB, John S, Nelson MR, Graham J, Park BK, Dillon JF, Bernal W, Cordell HJ, Pirmohamed M, Aithal GP, Day CP. HLA-B*5701 genotype is a major determinant of drug-induced liver injury due to flucloxacillin. *Nat Genet.* 2009;41(7):816–9.
15. McCormack M, Alfirevic A, Bourgeois S, Farrell JJ, Kasperavičiūtė D, Carrington M, Sills GJ, Marson T, Jia X, de Bakker PIW, Chinthapalli K, Molokhia M, Johnson MR, O'Connor GD, Chaila E, Alhusaini S, Shianna KV, Radtke RA, Heinzen EL, Walley N, Pandolfo M, Pichler W, Park BK, Depondt C, Sisodiya SM, Goldstein DB, Deloukas P, Delanty N, Cavalleri GL, Pirmohamed M. HLA-A*3101 and carbamazepine-induced hypersensitivity reactions in Europeans. *N Engl J Med.* 2011;364(12):1134–43.
16. Chen P, Lin J-J, Lu C-S, Ong C-T, Hsieh PF, Yang C-C, Tai C-T, Wu S-L, Lu C-H, Hsu Y-C, Yu H-Y, Ro L-S, Lu C-T, Chu C-C, Tsai J-J, Su Y-H, Lan S-H, Sung S-F, Lin S-Y, Chuang H-P, Huang L-C, Chen Y-J, Tsai P-J, Liao H-T, Lin Y-H, Chen C-H, Chung W-H, Hung S-I, Wu J-Y, Chang C-F, Chen L, Chen Y-T, Shen C-Y. Carbamazepine-induced toxic effects and HLA-B*1502 screening in Taiwan. *N Engl J Med.* 2011;364(12):1126–33.
17. Rugo HS, Barry WT, Moreno-Aspitia A, Lyss AP, Cirrincione C, Leung E, Mayer EL, Naughton M, Toppmeyer D, Carey LA, Perez EA, Hudis C, Winer EP. Randomized phase III trial of paclitaxel once per week compared with nanoparticle albumin-bound nab-paclitaxel once per week or ixabepilone with bevacizumab as first-line chemotherapy for locally recurrent or metastatic breast cancer: CALGB 40502/NCCTG N063H (Alliance). *J Clin Oncol.* 2015;33(21):2361–9.
18. Common Terminology for Adverse Events v3.0 (CTCAE). Cancer Therapy Evaluation Program; 2003. Available from: <http://ctep.cancer.gov/reporting/ctc.html>

19. Aulchenko YS, Ripke S, Isaacs A, van Duijn CM. GenABEL: an R library for genome-wide association analysis. *Bioinformatics*. 2007;23(10):1294–6.
20. Price AL, Patterson NJ, Plenge RM, Weinblatt ME, Shadick NA, Reich D. Principal components analysis corrects for stratification in genome-wide association studies. *Nat Genet*. 2006;38(8):904–9.
21. Das S, Forer L, Schön herr S, Sidore C, Locke AE, Kwong A, Vrieze SI, Chew EY, Levy S, McGue M, Schlessinger D, Stambolian D, Loh P-R, Iacono WG, Swaroop A, Scott LJ, Cucca F, Kronenberg F, Boehnke M, Abecasis GR, Fuchsberger C. Next-generation genotype imputation service and methods. *Nat Genet*. 2016;48(10):1284–7.
22. Maitland ML, Bakris GL, Black HR, Chen HX, Durand JB, Elliott WJ, Ivy SP, Leier CV, Lindenfeld J, Liu G, Remick SC, Steingart R, Tang WHW, Cardiovascular Toxicities Panel, Convened by the Angiogenesis Task Force of the National Cancer Institute Investigational Drug Steering Committee. Initial assessment, surveillance, and management of blood pressure in patients receiving vascular endothelial growth factor signaling pathway inhibitors. *J Natl Cancer Inst*. 2010;102(9):596–604.
23. Therneau TM. A package for survival analysis in S. Version 2.39-2. 2016. Available from: <https://CRAN.R-project.org/package=survival>
24. R Core Team. R: A language and environment for statistical computing. Vienna, Austria: R Foundation for Statistical Computing; 2013. Available from: <https://www.R-project.org/>
25. Ward LD, Kellis M. HaploReg: a resource for exploring chromatin states, conservation, and regulatory motif alterations within sets of genetically linked variants. *Nucleic Acids Res*. 2012;40(Database issue):D930–4.
26. Boyle AP, Hong EL, Hariharan M, Cheng Y, Schaub MA, Kasowski M, Karczewski KJ, Park J, Hitz BC, Weng S, Cherry JM, Snyder M. Annotation of functional variation in personal genomes using RegulomeDB. *Genome Res*. 2012;22(9):1790–7.
27. Kumar P, Henikoff S, Ng PC. Predicting the effects of coding non-synonymous variants on protein function using the SIFT algorithm. *Nat Protoc*. 2009;4(8):1073–81.
28. Adzhubei IA, Schmidt S, Peshkin L, Ramensky VE, Gerasimova A, Bork P, Kondrashov AS, Sunyaev SR. A method and server for predicting damaging missense mutations. *Nat Methods*. 2010;7(4):248–9.
29. Davydov EV, Goode DL, Sirota M, Cooper GM, Sidow A, Batzoglou S. Identifying a high fraction of the human genome to be under selective constraint using GERP++. *PLoS Comput Biol*. 2010;6(12):e1001025.
30. Kircher M, Witten DM, Jain P, O’Roak BJ, Cooper GM, Shendure J. A general

framework for estimating the relative pathogenicity of human genetic variants. *Nat Genet.* 2014;46(3):310–5.

31. Auton A, Abecasis GR, Durbin RM, Bentley DR, Chakravarti A, Clark AG, Donnelly P, Flicek P, Gibbs RA, Green ED, Knoppers BM, Korbel JO, Lander ES, Lehrach H, Mardis ER, Marth GT, McVean GA, Nickerson DA, Schmidt JP, Sherry ST, Wang J, Wilson RK, Gibbs RA, Boerwinkle E, Doddapaneni H, Han Y, Korchina V, Kovar C, Lee S, Reid JG, Zhu Y, Wang J, Chang Y, Feng Q, Fang X, Guo X, Jian M, Jiang H, Jin X, Lan T, Li G, Li J, Li Y, Liu S, Liu X, Lu Y, Ma X, Tang M, Wang B, Wang G, Wu H, Wu R, Xu X, Yin Y, Zhang D, Zhang W, Zhao J, Zhao M, Zheng X, Lander ES, Gupta N, Gharani N, Toji LH, Gerry NP, Resch AM, Flicek P, Barker J, Clarke L, Gil L, Hunt SE, Kelman G, Kulesha E, Leinonen R, McLaren WM, Radhakrishnan R, Roa A, Smirnov D, Smith RE, Streeter I, Thormann A, Toneva I, Vaughan B, Zheng-Bradley X, Bentley DR, Grocock R, Humphray S, James T, Kingsbury Z, Lehrach H, Sudbrak R, Amstislavskiy VS, Borodina TA, Lienhard M, Mertes F, Sultan M, Timmermann B, Yaspo M-L, Mardis ER, Wilson RK, Fulton L, Fulton R, Sherry ST, Ananiev V, Belaia Z, Beloslyudtsev D, Bouk N, Chen C, Church D, Cohen R, Cook C, Garner J, Hefferon T, Kimelman M, Liu C, Lopez J, Meric P, O'Sullivan C, Ostapchuk Y, Phan L, Ponomarov S, Schneider V, Shekhtman E, Sirotkin K, Slotta D, Zhang H, McVean GA, Durbin RM, Balasubramaniam S, Burton J, Danecek P, Keane TM, Kolb-Kokocinski A, McCarthy S, Stalker J, Quail M, Schmidt JP, Davies CJ, Gollub J, Webster T, Wong B, Zhan Y, Campbell CL, Kong Y, Marcketta A, Gibbs RA, Yu F, Antunes L, Bainbridge M, Muzny D, Sabo A, Huang Z, Wang J, Coin LJM, Fang L, Guo X, Jin X, Li G, Li Q, Li Y, Li Z, Lin H, Liu B, Luo R, Shao H, Xie Y, Ye C, Yu C, Zhang F, Zheng H, Zhu H, Dal E, Kahveci F, Marth GT, Garrison EP, Kural D, Lee W-P, Fung Leong W, Stromberg M, Ward AN, Wu J, Zhang M, Daly MJ, DePristo MA, Handsaker RE, Altshuler DM, Bhatia G, Genovese G, Gupta N, Li H, Kashin S, Lander ES, McCarroll SA, Nemesh JC, Poplin RE, Yoon SC, Lihm J, Makarov V, Clark AG, Gottipati S, Keinan A, Rodriguez-Flores JL, Korbel JO, Rausch T, Fritz MH, Stütz AM, Flicek P, Beal K, Clarke L, Datta A, Herrero J, McLaren WM, Ritchie GRS, Smith RE, Zerbino D, Zheng-Bradley X, Sabeti PC, Shlyakhter I, Schaffner SF, Vitti J, Cooper DN, Ball EV, Stenson PD, Bentley DR, Barnes B, Bauer M, Keira Cheetham R, Cox A, Eberle M, Humphray S, Kahn S, Murray L, Peden J, Shaw R, Kenny EE, Batzer MA, Konkel MK, Walker JA, MacArthur DG, Lek M, Sudbrak R, Amstislavskiy VS, Herwig R, Mardis ER, Ding L, Koboldt DC, Larson D, Cerveira E, Ye K, Byrnes JK, Malhotra A, La Vega De FM, Romanovitch M, Baran Y, Rosenfeld JA, Zhang C, Plewczynski D, Gymrek M, Moreno-Estrada A, Simpson JT, Lappalainen T, Radew K, Shringarpure SS, Halperin E, Frederick Willems T, Erlich Y, Zakharia F, Montgomery SB, Hwang J, Shriver MD, Hyland FCL, Carroll AW, DeGorter MK, Craig DW, Lacroute P, Christoforides A, Maples BK, Homer N, Izatt T, Kurdoglu AA, Sinari SA, Squire K, Sherry ST, Xiao C, Sebat J, Antaki D, Gujral M, Noor A, Ye K, Burchard EG, Hernandez RD, Gignoux CR, Haussler D, Katzman SJ, James Kent W, Howie B, Ruiz-Linares A, Dermitzakis ET, Devine SE, Min Kang H, Kidd JM, Blackwell T, Caron S, Chen W, Emery S, Fritsche L, Fuchsberger C, Li B, Lyons R, Scheller C, Sidore C, Song S, Sliwerska E, Taliun D, Tan A, Welch R, Kate Wing M, Zhan X, Awadalla P, Hodgkinson A, Li Y, Shi X, Quitadamo A, Lunter G, McVean GA, Marchini JL, Myers S, Churchhouse C, Delaneau O, Gupta-Hinch A, Kretzschmar W, Iqbal Z, Mathieson I, Menelaou A, Rimmer A, Xifara DK, Oleksyk

TK, Fu Y, Liu X, Xiong M, Jorde L, Witherspoon D, Xing J, Browning BL, Browning SR, Hormozdiari F, Sudmant PH, Khurana E, Durbin RM, Hurles ME, Tyler-Smith C, Albers CA, Ayub Q, Balasubramaniam S, Chen Y, Colonna V, Danecek P, Jostins L, Keane TM, McCarthy S, Walter K, Xue Y, Balasubramanian S, Chen J, Clarke D, Fu Y, Harmanci AO, Jin M, Lee D, Liu J, Jasmine Mu X, Zhang J, Zhang Y, Li Y, Luo R, Zhu H, Alkan C, Dal E, Kahveci F, Marth GT, Garrison EP, Kural D, Lee W-P, Ward AN, Wu J, Zhang M, McCarroll SA, Handsaker RE, Banks E, Genovese G, Hartl C, Li H, Kashin S, Nemesh JC, Shakir K, Yoon SC, Lihm J, Makarov V, Degenhardt J, Korbel JO, Fritz MH, Meiers S, Raeder B, Rausch T, Stütz AM, Flicek P, Paolo Casale F, Clarke L, Smith RE, Stegle O, Zheng-Bradley X, Bentley DR, Barnes B, Keira Cheetham R, Eberle M, Humphray S, Kahn S, Murray L, Shaw R, Lameijer E-W, Batzer MA, Konkel MK, Walker JA, Ding L, Hall I, Ye K, Lacroute P, Cerveira E, Malhotra A, Hwang J, Plewczynski D, Radew K, Romanovitch M, Zhang C, Craig DW, Homer N, Church D, Xiao C, Sebat J, Bafna V, Michaelson J, Ye K, Devine SE, Gardner EJ, Kidd JM, Mills RE, Dayama G, Emery S, Jun G, Shi X, Quitadamo A, Lunter G, McVean GA, Chen K, Fan X, Chong Z, Chen T, Witherspoon D, Xing J, Eichler EE, Chaisson MJ, Hormozdiari F, Huddleston J, Malig M, Nelson BJ, Sudmant PH, Parrish NF, Khurana E, Blackburne B, Lindsay SJ, Ning Z, Walter K, Zhang Y, Abyzov A, Chen J, Clarke D, Lam H, Jasmine Mu X, Sisu C, Zhang J, Zhang Y, Gibbs RA, Yu F, Bainbridge M, Challis D, Evani US, Kovar C, Lu J, Nagaswamy U, Reid JG, Sabo A, Yu J, Guo X, Li W, Li Y, Wu R, Marth GT, Garrison EP, Fung Leong W, Ward AN, del Angel G, Gabriel SB, Gupta N, Hartl C, Poplin RE, Clark AG, Rodriguez-Flores JL, Flicek P, Clarke L, Smith RE, Zheng-Bradley X, MacArthur DG, Mardis ER, Fulton R, Koboldt DC, Craig DW, Christoforides A, Homer N, Izatt T, Sherry ST, Xiao C, Dermitzakis ET, Min Kang H, McVean GA, Balasubramanian S, Habegger L, Yu H, Flicek P, Clarke L, Cunningham F, Dunham I, Zerbino D, Zheng-Bradley X, Lage K, Berg Jespersen J, Horn H, Montgomery SB, DeGorter MK, Khurana E, Tyler-Smith C, Chen Y, Colonna V, Xue Y, Gerstein MB, Balasubramanian S, Fu Y, Kim D, Marcketta A, Desalle R, Narechania A, Wilson Sayres MA, Garrison EP, Handsaker RE, Kashin S, McCarroll SA, Rodriguez-Flores JL, Flicek P, Clarke L, Zheng-Bradley X, Erlich Y, Gymrek M, Frederick Willems T, Bustamante CD, Mendez FL, David Poznik G, Underhill PA, Lee C, Cerveira E, Malhotra A, Romanovitch M, Zhang C, Coin L, Shao H, Mittelman D, Tyler-Smith C, Banerjee R, Cerezo M, Chen Y, Fitzgerald TW, Louzada S, Massaia A, McCarthy S, Ritchie GR, Xue Y, Yang F, Gibbs RA, Kovar C, Kalra D, Hale W, Reid JG, Wang J, Dan X, Guo X, Li G, Li Y, Ye C, Zheng X, Flicek P, Clarke L, Zheng-Bradley X, Bentley DR, Cox A, Humphray S, Kahn S, Sudbrak R, Albrecht MW, Lienhard M, Larson D, Craig DW, Izatt T, Kurdoglu AA, Sherry ST, Xiao C, Haussler D, McVean GA, Durbin RM, Balasubramanian S, Keane TM, McCarthy S, Stalker J, Chakravarti A, Knoppers BM, Beiswanger C, Burchard EG, Cai H, Cao H, Durbin RM, Gerry NP, Gharani N, Gibbs RA, Gignoux CR, Henn B, Jones D, Jorde L, Kaye JS, Keinan A, Kent A, Kerasidou A, Li Y, Mathias R, McVean GA, Moreno-Estrada A, Ossorio PN, Parker M, Resch AM, Rotimi CN, Royal CD, Sandoval K, Su Y, Sudbrak R, Tian Z, Tishkoff S, Toji LH, Tyler-Smith C, Via M, Wang Y, Yang H, Yang L, Zhu J, Bodmer W, Bedoya G, Ruiz-Linares A, Cai Z, Gao Y, Chu J, Peltonen L, Garcia-Montero A, Orfao A, Dutil J, Martinez-Cruzado JC, Oleksyk TK, Barnes KC, Mathias RA, Hennis A, Watson H, McKenzie C, Qadri F, LaRocque R, Sabeti PC, Zhu J, Deng X, Sabeti PC, Asogun D, Folarin O, Happi C, Omoniwa O, Stremlau M, Tariyal R, Jallow M, Sisay Joof F, Corrah

- T, Rockett K, Kwiatkowski D, Kooner J, Tinh Hiên TN, Dunstan SJ, Thuy Hang N, Fannie R, Garry R, Kanneh L, Moses L, Sabeti PC, Schieffelin J, Grant DS, Gallo C, Poletti G, Saleheen D, Rasheed A, Brooks LD, Felsenfeld AL, McEwen JE, Vaydylevich Y, Green ED, Duncanson A, Dunn M, Schloss JA, Wang J, Yang H, Brooks LD, Durbin RM, Garrison EP, Min Kang H, Korbel JO, Marchini JL, McCarthy S, McVean GA. A global reference for human genetic variation. *Nature*. 2015;526(7571):68–74.
32. ENCODE Project Consortium. An integrated encyclopedia of DNA elements in the human genome. *Nature*. 2012;489(7414):57–74.
33. Rosenbloom KR, Sloan CA, Malladi VS, Dreszer TR, Learned K, Kirkup VM, Wong MC, Maddren M, Fang R, Heitner SG, Lee BT, Barber GP, Harte RA, Diekhans M, Long JC, Wilder SP, Zweig AS, Karolchik D, Kuhn RM, Haussler D, Kent WJ. ENCODE data in the UCSC Genome Browser: year 5 update. *Nucleic Acids Res*. 2013;41(Database issue):D56–63.
34. Kundaje A, Meuleman W, Bilenky M, Yen A, Kheradpour P, Zhang Z, Wang J, Amin V, Whitaker JW, Ward LD, Sarkar A, Sandstrom RS, Eaton ML, Pfenning A, Wang X, Claussnitzer Yaping Liu M, Alan Harris R, Epstein CB, David Hawkins R, Lister R, Hong C, Mungall AJ, Canfield TK, Scott Hansen R, Kaul R, Bansal MS, Farh K-H, Feizi S, Karlic R, Kim A-R, Lowdon R, Elliott G, Mercer TR, Polak P, Rajagopal N, Sallari RC, Siebenthall KT, Stevens M, Thurman RE, Wu J, Zhang B, Zhou X, Abdennur N, Adli M, Akerman M, Barrera L, Antosiewicz-Bourget J, Ballinger T, Barnes MJ, Bates D, Bell RJA, Bennett DA, Bianco K, Bock C, Boyle P, Brinchmann J, Caballero-Campo P, Camahort R, Carrasco-Alfonso MJ, Charnecki T, Chen H, Chen Z, Cheng JB, Cho S, Chu A, Chung W-Y, Cowan C, Athena Deng Q, Deshpande V, Diegel M, Ding B, Durham T, Echipare L, Edsall L, Flowers D, Genbacev-Krtolica O, Gifford C, Gillespie S, Giste E, Glass IA, Gnirke A, Gormley M, Gu H, Gu J, Hafler DA, Hangauer MJ, Hariharan M, Hatan M, Haugen E, He Y, Heimfeld S, Herlofsen S, Hou Z, Humbert R, Issner R, Jackson AR, Jia H, Jiang P, Johnson AK, Kadlec T, Kamoh B, Kapidzic M, Kent J, Kim A, Kleinewietfeld M, Klugman S, Krishnan J, Kuan S, Kutayavin T, Lee A-Y, Lee K, Li J, Li N, Li Y, Ligon KL, Lin S, Lin Y, Liu J, Liu Y, Luckey CJ, Ma YP, Maire C, Marson A, Mattick JS, Mayo M, McMaster M, Metsky H, Mikkelsen T, Miller D, Miri M, Mukame E, Nagarajan RP, Neri F, Nery J, Nguyen T, O’Geen H, Paithankar S, Papayannopoulou T, Pelizzola M, Plettner P, Propson NE, Raghuraman S, Raney BJ, Raubitschek A, Reynolds AP, Richards H, Riehle K, Rinaudo P, Robinson JF, Rockweiler NB, Rosen E, Rynes E, Schein J, Sears R, Sejnowski T, Shafer A, Shen L, Shoemaker R, Sigaroudinia M, Slukvin I, Stehling-Sun S, Stewart R, Subramanian SL, Suknuntha K, Swanson S, Tian S, Tilden H, Tsai L, Urich M, Vaughn I, Vierstra J, Vong S, Wagner U, Wang H, Wang T, Wang Y, Weiss A, Whitton H, Wildberg A, Witt H, Won K-J, Xie M, Xing X, Xu I, Xuan Z, Ye Z, Yen C-A, Yu P, Zhang X, Zhang X, Zhao J, Zhou Y, Zhu J, Zhu Y, Ziegler S, Beudet AE, Boyer LA, De Jager PL, Farnham PJ, Fisher SJ, Haussler D, Jones SJM, Li W, Marra MA, McManus MT, Thomson JA, Tlsty TD, Tsai L-H, Wang W, Waterland RA, Zhang MQ, Chadwick LH, Bernstein BE, Costello JF, Ecker JR, Hirst M, Meissner A, Milosavljevic A, Ren B, Stamatoyannopoulos JA, Wang T, Kellis M, Ernst J, Heravi-Moussavi A, Wang J, Ziller MJ, Schultz MD, Quon G, Wu Y-C, Pfenning AR, Claussnitzer

- M, Liu Y, Coarfa C, Harris RA, Shores N, Gjoneska E, Leung D, Xie W, Hawkins RD, Gascard P, Mungall AJ, Moore R, Chuah E, Tam A, Hansen RS, Sabo PJ, Carles A, Dixon JR, Kulkarni A, Li D, Neph SJ, Onuchic V, Ray P, Sinnott-Armstrong NA, Wu J, Zhang B, Zhou X, Beaudet AE, Boyer LA, De Jager PL, Farnham PJ, Fisher SJ, Haussler D, Jones SJM, Li W, Marra MA, McManus MT, Sunyaev S, Thomson JA, Tlsty TD, Tsai L-H, Wang W, Waterland RA, Zhang MQ, Chadwick LH, Costello JF, Ecker JR, Hirst M, Meissner A, Milosavljevic A, Ren B, Stamatoyannopoulos JA, Wang T. Integrative analysis of 111 reference human epigenomes. *Nature*. 2015;518(7539):317–30.
35. Lonsdale J, Thomas J, Salvatore M, Phillips R, Lo E, Shad S, Hasz R, Walters G, Garcia F, Young N, Foster B, Moser M, Karasik E, Gillard B, Ramsey K, Sullivan S, Bridge J, Magazine H, Syron J, Fleming J, Siminoff L, Traino H, Mosavel M, Barker L, Jewell S, Rohrer D, Maxim D, Filkins D, Harbach P, Cortadillo E, Berghuis B, Turner L, Hudson E, Feenstra K, Sobin L, Robb J, Branton P, Korzeniewski G, Shive C, Tabor D, Qi L, Groch K, Nampally S, Buia S, Zimmerman A, Smith A, Burges R, Robinson K, Valentino K, Bradbury D, Cosentino M, Diaz-Mayoral N, Kennedy M, Engel T, Williams P, Erickson K, Ardlie K, Winckler W, Getz G, DeLuca D, MacArthur D, Kellis M, Thomson A, Young T, Gelfand E, Donovan M, Meng Y, Grant G, Mash D, Marcus Y, Basile M, Liu J, Zhu J, Tu Z, Cox NJ, Nicolae DL, Gamazon ER, Im HK, Konkashbaev A, Pritchard J, Stevens M, Flutre T, Wen X, Dermitzakis ET, Lappalainen T, Guigo R, Monlong J, Sammeth M, Koller D, Battle A, Mostafavi S, McCarthy M, Rivas M, Maller J, Rusyn I, Nobel A, Wright F, Shabalina A, Feolo M, Sharopova N, Sturcke A, Paschal J, Anderson JM, Wilder EL, Derr LK, Green ED, Struwing JP, Temple G, Volpi S, Boyer JT, Thomson EJ, Guyer MS, Ng C, Abdallah A, Colantuoni D, Insel TR, Koester SE, Little AR, Bender PK, Lehner T, Yao Y, Compton CC, Vaught JB, Sawyer S, Lockhart NC, Demchok J, Moore HF. The Genotype-Tissue Expression (GTEx) project. *Nat Genet*. 2013;45(6):580–5.
 36. Yu CH, Pal LR, Moulton J. Consensus genome-wide expression quantitative trait loci and their relationship with human complex trait disease. *OMICS*. 2016;20(7):400–14.
 37. Staley JR, Blackshaw J, Kamat MA, Ellis S, Surendran P, Sun BB, Paul DS, Freitag D, Burgess S, Danesh J, Young R, Butterworth AS. PhenoScanner: a database of human genotype–phenotype associations. *Bioinformatics*. 2016;32(20):3207–9.
 38. Venook AP, Blanke CD, Niedzwiecki D, Lenz H-J, Taylor JR, Hollis DR, Sutherland S, Goldberg RM. Revisiting the Cancer and Leukemia Group B/Southwest Oncology Group 80405 Trial: a phase III trial of chemotherapy and biologic agents for patients with untreated advanced colorectal adenocarcinoma. *Clin Colorectal Cancer*. 2007;6(7):536–8.
 39. Venook AP, Niedzwiecki D, Lenz H-J, Innocenti F, Mahoney MR, O'Neil BH, Shaw JE, Polite BN, Hochster HS, Atkins JN, Goldberg RM, Mayer RJ, Schilsky RL, Bertagnoli MM, Blanke CD. CALGB/SWOG 80405: Phase III trial of irinotecan/5-FU/leucovorin (FOLFIRI) or oxaliplatin/5-FU/leucovorin (mFOLFOX6) with bevacizumab (BV) or cetuximab (CET) for patients (pts) with KRAS wild-type (wt) untreated metastatic

- adenocarcinoma of the colon or rectum (MCRC). *J Clin Oncol*. 2014;32:5s.
40. Kelly WK, Halabi S, Carducci M, George D, Mahoney JF, Stadler WM, Morris M, Kantoff P, Monk JP, Kaplan E, Vogelzang NJ, Small EJ. Randomized, double-blind, placebo-controlled phase III trial comparing docetaxel and prednisone with or without bevacizumab in men with metastatic castration-resistant prostate cancer: CALGB 90401. *J Clin Oncol*. 2012;30(13):1534–40.
 41. Aguet F, Brown AA, Castel S, Davis JR, Mohammadi P, Segre AV, Zappala Z, Abell NS, Fresard L, Gamazon ER, Gelfand E, Gludemans MJ, He Y, Hormozdiari F, Li X, Li X, Liu B, Garrido-Martin D, Ongen H, Palowitch JJ, Park Y, Peterson CB, Quon G, Ripke S, Shabalín AA, Shimko TC, Strober BJ, Sullivan TJ, Teran NA, Tsang EK, Zhang H, Zhou Y-H, Battle A, Bustamonte CD, Cox NJ, Engelhardt BE, Eskin E, Getz G, Kellis M, Li G, MacArthur DG, Nobel AB, Sabbati C, Wen X, Wright FA, GTEx Consortium, Lappalainen T, Ardlie KG, Dermitzakis ET, Brown CD, Montgomery SB. Local genetic effects on gene expression across 44 human tissues. *BioRxiv* 074450 [Preprint]. 2016. Available from: <https://doi.org/10.1101/074450>
 42. Lappalainen T, Sammeth M, Friedländer MR, Hoen PAC', Monlong J, Rivas MA, González-Porta M, Kurbatova N, Griebel T, Ferreira PG, Barann M, Wieland T, Greger L, van Itersen M, Almlöf J, Ribeca P, Pulyakhina I, Esser D, Giger T, Tikhonov A, Sultan M, Bertier G, MacArthur DG, Lek M, Lizano E, Buermans HPJ, Padioleau I, Schwarzmayr T, Karlberg O, Ongen H, Kilpinen H, Beltran S, Gut M, Kahlem K, Amstislavskiy V, Stegle O, Pirinen M, Montgomery SB, Donnelly P, McCarthy MI, Flicek P, Strom TM, Consortium TG, Lehrach H, Schreiber S, Sudbrak R, Carracedo Á, Antonarakis SE, Häsler R, Syvänen A-C, van Ommen G-J, Brazma A, Meitinger T, Rosenstiel P, Guigo R, Gut IG, Estivill X, Dermitzakis ET. Transcriptome and genome sequencing uncovers functional variation in humans. *Nature*. 2013;501(7468):506–11.
 43. Grundberg E, Small KS, Hedman ÅK, Nica AC, Buil A, Keildson S, Bell JT, Yang T-P, Meduri E, Barrett A, Nisbett J, Sekowska M, Wilk A, Shin S-Y, Glass D, Travers M, Min JL, Ring S, Ho K, Thorleifsson G, Kong A, Thorsteindottir U, Ainali C, Dimas AS, Hassanali N, Ingle C, Knowles D, Krestyaninova M, Lowe CE, Di Meglio P, Montgomery SB, Parts L, Potter S, Surdulescu G, Tsaprouni L, Tsoka S, Bataille V, Durbin R, Nestle FO, O'Rahilly S, Soranzo N, Lindgren CM, Zondervan KT, Ahmadi KR, Schadt EE, Stefansson K, Smith GD, McCarthy MI, Deloukas P, Dermitzakis ET, Spector TD. Mapping cis- and trans-regulatory effects across multiple tissues in twins. *Nat Genet*. 2012;44(10):1084–9.
 44. Miyaki M, Konishi M, Tanaka K, Kikuchi-Yanoshita R, Muraoka M, Yasuno M, Igari T, Koike M, Chiba M, Mori T. Germline mutation of MSH6 as the cause of hereditary nonpolyposis colorectal cancer. *Nat Genet*. 1997;17(3):271–2.
 45. Kolodner RD, Tytell JD, Schmeits JL, Kane MF, Gupta RD, Weger J, Wahlberg S, Fox EA, Peel D, Ziogas A, Garber JE, Syngal S, Anton-Culver H, Li FP. Germ-line msh6

- mutations in colorectal cancer families. *Cancer Res.* 1999;59(20):5068–74.
46. Wijnen J, de Leeuw W, Vasen H, van der Klift H, Møller P, Stormorken A, Meijers-Heijboer H, Lindhout D, Menko F, Vossen S, Möslein G, Tops C, Bröcker-Vriends A, Wu Y, Hofstra R, Sijmons R, Cornelisse C, Morreau H, Fodde R. Familial endometrial cancer in female carriers of MSH6 germline mutations. *Nat Genet.* 1999;23(2):142–4.
 47. Hansen TF, Jensen LH, Spindler KLG, Lindebjerg J, Brandslund I, Jakobsen A. The relationship between serum vascular endothelial growth factor A and microsatellite instability in colorectal cancer. *Colorectal Dis.* 2011;13(9):984–8.
 48. Boengler K, Pipp F, Fernandez B, Richter A, Schaper W, Deindl E. The ankyrin repeat containing SOCS box protein 5: a novel protein associated with arteriogenesis. *Biochem Biophys Res Commun.* 2003;302(1):17–22.
 49. Elfenbein A, Simons M. Syndecan-4 signaling at a glance. *J Cell Sci.* 2013;126(Pt 17):3799–804.
 50. Jakobsson L, Kreuger J, Holmborn K, Lundin L, Eriksson I, Kjellén L, Claesson-Welsh L. Heparan sulfate in trans potentiates VEGFR-mediated angiogenesis. *Dev Cell.* 2006;10(5):625–34.
 51. De Rossi G, Nourshargh S, Whiteford JR. Syndecan-4 is required for VEGF-induced angiogenesis. *Angiogenesis.* 2014;17(3):715.
 52. Weston GC, Haviv I, Rogers PA. Microarray analysis of VEGF-responsive genes in myometrial endothelial cells. *Mol Hum Reprod.* 2002;8(9):855–63.
 53. Zhang Y, Li J, Partovian C, Sellke FW, Simons M. Syndecan-4 modulates basic fibroblast growth factor 2 signaling in vivo. *Am J Physiol Heart Circ Physiol.* 2003;284(6):H2078–82.
 54. Partovian C, Ju R, Zhuang ZW, Martin KA, Simons M. Syndecan-4 regulates subcellular localization of mTOR Complex2 and Akt activation in a PKCalpha-dependent manner in endothelial cells. *Mol Cell.* 2008;32(1):140–9.
 55. Kunas T, Nikkari ST. Contribution of syndecan-4 genetic variants to hypertension, the TAMRISK study. *BMC Res Notes.* 2014;7:815.
 56. Ishiguro K, Kadomatsu K, Kojima T, Muramatsu H, Iwase M, Yoshikai Y, Yanada M, Yamamoto K, Matsushita T, Nishimura M, Kusugami K, Saito H, Muramatsu T. Syndecan-4 deficiency leads to high mortality of lipopolysaccharide-injected mice. *J Biol Chem.* 2001;276(50):47483–8.
 57. Hamamoto R, Toyokawa G, Nakakido M, Ueda K, Nakamura Y. SMYD2-dependent HSP90 methylation promotes cancer cell proliferation by regulating the chaperone complex formation. *Cancer Lett.* 2014;351(1):126–33.

58. Kunizaki M, Hamamoto R, Silva FP, Yamaguchi K, Nagayasu T, Shibuya M, Nakamura Y, Furukawa Y. The lysine 831 of vascular endothelial growth factor receptor 1 is a novel target of methylation by SMYD3. *Cancer Res.* 2007;67(22):10759–65.
59. Stender JD, Pascual G, Liu W, Kaikkonen MU, Do K, Spann NJ, Boutros M, Perrimon N, Rosenfeld MG, Glass CK. Control of proinflammatory gene programs by regulated trimethylation and demethylation of histone H4K20. *Mol Cell.* 2012;48(1):28–38.
60. Fujii T, Tsunesumi S-I, Sagara H, Munakata M, Hisaki Y, Sekiya T, Furukawa Y, Sakamoto K, Watanabe S. Smyd5 plays pivotal roles in both primitive and definitive hematopoiesis during zebrafish embryogenesis. *Sci Rep.* 2016;6:29157.
61. Chow S, Shao J, Wang H. *Sample size calculations in clinical research.* 2nd ed. Chapman & Hall/CRC Biostatistics Series; 2008.
62. Faul F, Erdfelder E, Lang A-G, Buchner A. G*Power 3: a flexible statistical power analysis program for the social, behavioral, and biomedical sciences. *Behav Res Methods.* 2007;39(2):175–91.

Chapter 5: Conclusions and Perspectives

5.1 Summary

Bevacizumab is commonly used in combination with chemotherapy to treat numerous types of solid tumors¹. The monoclonal antibody targets vascular endothelial growth factor A (VEGF) and downregulates angiogenic effects mediated by VEGF receptor 2 (VEGFR2/*KDR*) signaling². A common dose-limiting toxicity of bevacizumab treatment is the development of hypertension (HTN)^{3,4}, which can lead to serious cardiovascular complications and organ damage. Interindividual variation in the time to onset and severity of HTN may be due in part to genetic factors. A number of prior studies have identified significant associations between incidence rates of HTN during bevacizumab treatment and common SNPs in *VEGFA*, *KDR*, and *SV2C*⁵⁻¹⁰, but these findings are inconsistent and still require validation. To identify novel mechanisms contributing to bevacizumab-induced HTN, the research in this dissertation explored additional genetic variation in non-VEGF pathways and of rare variants with potentially large phenotypic effects. *In silico* and *in vitro* functional analyses were performed to examine the potential roles of the identified genes and variants in the mechanism of bevacizumab-induced HTN.

A discovery-based sequencing analysis of whole exomes and candidate gene regulatory regions was performed to identify genomic regions associated with severe, early-onset bevacizumab-induced HTN in colorectal cancer patients (CALGB 80405) with extreme toxicity phenotypes (Chapter 2). This is the first study we know of to date using sequencing to examine bevacizumab-induced HTN. SNP-based and gene-based association methods

were used to analyze common variants, rare and low frequency variants, or variants of all frequencies. A targeted candidate gene analysis identified an intergenic region between *SLC29A1* and *HSP90AB1* containing four top SNPs in the association analysis, one of which replicated in two independent patient cohorts. Based on publicly available bioinformatic data, these SNP regions are enriched for regulatory elements that may potentially increase *SLC29A1* expression; these predictions still need to be functionally validated. Additional exploratory analyses were conducted to examine exome-wide associations within variants filtered by different functional criteria, but these analyses did not yield significant or biologically interesting results.

The evidence that SNPs near *SLC29A1* could alter *SLC29A1* expression led to the hypothesis that variation in *SLC29A1* expression contributes to interindividual variability in bevacizumab-induced HTN. *SLC29A1* encodes endothelial nucleoside transporter 1 (ENT1), which regulates extracellular adenosine levels and therefore adenosine signaling¹¹. Both adenosine and VEGF signaling induce activation of endothelial nitric oxide synthase (eNOS)¹²⁻¹⁴, which produces nitric oxide (NO). NO functions as a vasodilator and reduced levels of NO have been implicated in HTN resulting from VEGF inhibition¹⁵.

To better understand how changes in adenosine and VEGF signaling may contribute to bevacizumab-induced HTN, the effects of ENT1 and bevacizumab on vasodilatory signaling pathways were examined in human umbilical vein endothelial cells (HUVEC) (Chapter 3). Bevacizumab had no direct effect on adenosine receptor activity, as indicated by the insensitivity of cAMP generation to bevacizumab treatment. Pharmacological inhibition of

ENT1 in HUVEC increased adenosine receptor signaling and NO synthesis. Overexpression of SLC29A1 disrupted adenosine signaling and resulted in decreased NO levels that were further reduced upon exposure to bevacizumab, with enhanced sensitivity under conditions of elevated SLC29A1 expression. Preliminary data suggest that the effects of ENT1 inhibition and SLC29A1 overexpression on levels of prostacyclin (PGI₂), another vasodilatory molecule, follow the same trends as NO levels. However, while NO is generated as a result of both adenosine and VEGF signaling, PGI₂ synthesis appears to be driven primarily by VEGF signaling and is less affected by changes in adenosine. We have proposed a mechanism based on these early results suggesting that due to the synergistic effects of decreased adenosine signaling and decreased VEGF signaling on vasodilatory molecule production, increased basal expression of ENT1 may sensitize patients to a rise in blood pressure during bevacizumab exposure. Additional functional assessment and *in vivo* and clinical studies are needed to further test this hypothesis.

Alongside the sequencing analysis, a genome-wide association study (GWAS) using genotyping array data was conducted in a larger, independent cohort of bevacizumab-treated breast cancer patients (CALGB 40502, Chapter 4). While the sequencing analysis used a binary outcome of extreme toxicity phenotypes, the GWAS used a time-to-event outcome that accounted for cumulative bevacizumab dose and study discontinuation for non-HTN causes. Associations of the cumulative dose at first occurrence of either grade 2+ HTN or grade 3+ HTN were tested. The top associations of these respective analyses were SNPs near or within *MSH6* and *SDC4*, both of which have been previously implicated in the regulation of VEGF. Other top associations of potential biological interest include a SNP in

ASB5 and a SNP associated with *SMYD5* expression. *SDC4* (syndecan-4) is of especially great interest, as it has been shown to increase VEGF-induced eNOS activity and NO release^{16,17}. A proxy SNP of this *SDC4* variant has been associated with the development of primary HTN¹⁸. Additional studies are required to determine the specific role that these genes play in the pathogenesis of bevacizumab-induced HTN.

Cross-study comparison of the top SNPs of the sequencing and GWAS studies yielded few replicated associations at a statistically significant level. Top associations were also examined in additional bevacizumab-treated cohorts (CALGB 90401, ECOG-5103) if genotype data was available. From the sequencing study, rs9381299 (*SLC29A1-HSP90AB1*) associated with early grade 3+ HTN in CALGB 40502 and with SBP > 180 in ECOG-5103. From the GWAS, rs17679314 (*ASB5*) associated with early grade 2+ HTN in CALGB 80405. Limited statistical power (in both discovery and replication cohorts), the possibility of false positive findings, differences in trial design and bevacizumab dosing, and clinical differences between study populations (colorectal vs. breast vs. prostate) may explain why most associations failed to replicate. CALGB 40502 and ECOG-5103 were comprised of all women while CALGB 90401 enrolled only men; sex differences could have also influenced our findings, although sex did not associate with toxicity incidence in CALGB 80405 (the only study including both males and females). Especially because no associations in any of our discovery analyses achieved genome-wide significance, replication is needed in additional cohorts to extend these current findings. Aggregate effects and interactions of our novel risk variants and previously described risk variants on bevacizumab-induced HTN should also be examined in larger populations. A meta-analysis across multiple

studies is likely needed to overcome sample size limitations inherent in most clinical study populations.

5.2 Challenges and future directions

One challenge of the genetic studies presented in this dissertation lies in the difficulty of identifying true drug-induced HTN. Preexisting HTN was significantly correlated with on-treatment HTN in both the CALGB 80405 exome sequencing cohort and in CALGB 40502. This association is possibly confounding, and genetic models in both studies were adjusted for preexisting HTN to minimize this effect. However, this association has been previously reported¹⁹⁻²¹ and may possibly be informative. In CALGB 80405, hypertensive patients were required to be normotensive upon study initiation, and even while on antihypertensive medications many still developed the toxicity. Similarly in CALGB 40502, some patients who developed grade 2+ HTN and would presumably be prescribed antihypertensive medications later worsened to grade 3+ HTN. This suggests that some patients may be genetically predisposed to an especially sensitive response to bevacizumab, such that even pharmacologically controlled HTN is further exacerbated upon bevacizumab treatment. Although the present studies had limited data and too few subjects to test this hypothesis, a future study stratifying by the class of antihypertensive medication could elucidate a more specific mechanism of the toxicity.

Our functional evidence for the potential involvement of the *SLC29A1*-encoded nucleoside transporter in bevacizumab-induced HTN suggests that variation in other parts of the adenosine signaling pathway may have similar effects on the toxicity. Other equilibrative

(ENT2, ENT3, ENT4) and concentrative (CNT1, CNT2, CNT3) nucleoside transporters also mediate adenosine transport across cell membranes²². Extracellular adenosine concentrations are further regulated by CD39 (*ENTPD1*) and CD73 (*NT5E*) ectonucleotidases, which sequentially hydrolyze ATP to adenosine, adenosine kinase (*ADK*), which phosphorylates adenosine to AMP, and adenosine deaminase (*ADA*), which degrades adenosine to inosine²³. Adenosine also signals through four receptor subtypes, A₁ (*ADORA1*), A_{2A} (*ADORA2A*), A_{2B} (*ADORA2B*), and A₃ (*ADORA3*), which exert varying effects across multiple tissues, though endothelial cells predominantly express only the A₂ receptors²⁴. None of these genes or variants in these genes strongly associated with bevacizumab-induced HTN in our studies, but adenosine signaling pathway genes and their regulatory regions should be examined in future studies of this toxicity.

Altered adenosine signaling and nucleoside transport should also be further investigated at a functional level. Changes in ENT1 expression have been previously reported to directly affect adenosine deaminase and A_{2A} receptor expression²⁵, and NO has been shown to reduce *SLC29A1* promoter expression²⁶. Decreased *SLC29A1* expression and ENT1 transport activity have been previously described during preeclampsia, which is characterized by high blood pressure^{27,28}, and gestational diabetes, which is associated with endothelial dysfunction^{26,29}. Such changes are accompanied by observations of increased adenosine concentrations, increased CD39 and CD73 activity²⁷, reduced A_{2A} receptor expression and enhanced A_{2B} receptor signaling^{28,30}, and upregulation of soluble VEGFR1 (sFlt-1)^{31,32}, which binds to VEGF as bevacizumab does. Expression and activity of these proteins and of other nucleoside transporters, as well as nucleoside transporter

recycling³³, should be considered in future functional studies of bevacizumab, as multiple aberrations of the adenosine signaling pathway could result in a more sensitive response. Similar changes in sensitivity to bevacizumab treatment could also occur as a result of epigenetic regulation of these genes. Changes in adenosine transport rates, receptor binding affinities, or enzyme kinetics modulated by genetic effects or drug interactions should also be considered during functional studies of bevacizumab treatment.

We briefly considered the direct relationship between adenosine and VEGF. Hypoxia upregulates adenosine-induced VEGF release from HUVEC via enhanced A_{2B} receptor signaling³⁴ and also downregulates ENT1 expression and activity³⁵, similar to the changes observed during preeclampsia and gestational diabetes. Adenosine-induced VEGF expression was not observed during normoxic conditions in HUVEC³⁴, so hypoxic conditions may be necessary to test the effects between *SLC29A1* variation and VEGF inhibition on VEGF expression in endothelial cells. However, there is limited evidence that under normoxia, adenosine still plays a role in maintaining basal levels of VEGF through various muscle cell types³⁶. In a cohort of bevacizumab-treated pancreatic patients (CALGB 80303³⁷), two intronic *SLC29A1* SNPs trended with changes in basal levels of VEGF, though these results were not significant. Measurements of both adenosine and VEGF levels in patients who develop bevacizumab-induced HTN would be greatly informative in determining whether modulation of adenosine signaling and the interaction of adenosine and VEGF are truly involved in this toxicity.

Our findings may have implications for combination therapy of bevacizumab with other drugs. Although there was stronger evidence supporting the association of the identified *SLC29A1-HSP90AB1* SNPs with *SLC29A1* than with *HSP90AB1*, Hsp90 also regulates eNOS activity³⁸. Therefore, Hsp90 inhibitors for cancer treatment could have great inhibitory effects on NO signaling if used with VEGF inhibitors or adenosine receptor antagonists. The relationship between adenosine and VEGF signaling may also be relevant to cancer immunotherapies. Adenosine, in addition to promoting angiogenesis, is known to accumulate in the tumor microenvironment and create an immune-suppressed niche that favors tumor growth²³. Mechanisms contributing to this include inhibition of cytokine production, deregulation of immune cell proliferation and differentiation, and suppression of T-cell activity²³. A₂ receptors are expressed on nearly all immune cells³⁹, and use of adenosine receptor antagonists, which would mimic the effects of increased ENT1 expression, have been proposed to improve response to immunotherapies^{39,40}. Coadministration of VEGF inhibitors with Hsp90 inhibitors or adenosine receptor antagonists might be expected to increase the risk of therapy-induced HTN, and the study of such drug interactions may be informative in further elucidating these mechanisms.

5.3 Conclusions

This dissertation describes novel genetic loci that potentially modify the risk of developing bevacizumab-induced HTN. These findings will advance understanding of the genetic architecture of bevacizumab-induced HTN and may be extended to the study of HTN resulting from treatment with other angiogenesis inhibitors as well as other possible

causes of HTN. Our functional studies provide evidence for the involvement of adenosine signaling in the pathophysiological mechanism of bevacizumab-induced HTN.

These new biological insights may support the development of improved and novel strategies to treat bevacizumab-induced HTN and aid in the selection of appropriate treatment for cancer patients. Since bevacizumab treatment is held or discontinued upon development of HTN, it is clinically important to manage complications to prolong effective therapy. Frequent monitoring of blood pressure and prophylactic antihypertensive patients in sub-populations of patients at risk for bevacizumab toxicity may help prevent adverse events. Blood pressure elevation itself has been previously proposed as a biomarker for VEGF inhibitor efficacy; if true, this group may be at a therapeutic benefit if their HTN can be well controlled.

This research also highlights challenges that are frequently encountered in genetic studies of adverse drug reactions. Larger and more well-powered studies are crucial for the discovery and replication of genetic associations, but obtaining adequate numbers of cases is particularly difficult in pharmacogenomics, as serious adverse drug reactions are typically rare and can only be detected within a drug-treated disease population. Available study populations are further limited by a lack of well-curated drug response phenotype data. Improved adverse event tracking, standardized phenotype description, and more efficient mechanisms for data sharing and biobank access will increase sample sizes for such studies. Functional validation is also necessary for understanding the consequences of genetic variation but is still challenging, particularly for the study of noncoding variants.

Advancement of gene editing technologies and large-scale efforts to characterize regulatory elements of the genome, including recent expansion of the ENCODE Project, will greatly help in interpreting targets identified from high-throughput genomics studies.

In summary, the results presented in this dissertation provide novel targets that require additional study using genetic and pharmacological approaches. Further research on the risk factors and mechanisms of bevacizumab-induced HTN are necessary to minimize the number of patients impacted by this dose-limiting toxicity.

5.4 References

1. Avastin [package insert]. South San Francisco, CA: Genentech, Inc.; 2016. Available from: https://www.gene.com/download/pdf/avastin_prescribing.pdf
2. Ferrara N, Hillan KJ, Gerber HP, Novotny W. Discovery and development of bevacizumab, an anti-VEGF antibody for treating cancer. *Nat Rev Drug Discov*. 2004;3(5):391–400.
3. Zhu X, Wu S, Dahut WL, Parikh CR. Risks of proteinuria and hypertension with bevacizumab, an antibody against vascular endothelial growth factor: systematic review and meta-analysis. *Am J Kidney Dis*. 2007;49(2):186–93.
4. Ranpura V, Pulipati B, Chu D, Zhu X, Wu S. Increased risk of high-grade hypertension with bevacizumab in cancer patients: a meta-analysis. *Am J Hypertens*. 2010;23(5):460–8.
5. Schneider BP, Wang M, Radovich M, Sledge GW, Badve S, Thor A, Flockhart DA, Hancock B, Davidson N, Gralow J, Dickler M, Perez EA, Cobleigh M, Shenkier T, Edgerton S, Miller KD, ECOG 2100. Association of vascular endothelial growth factor and vascular endothelial growth factor receptor-2 genetic polymorphisms with outcome in a trial of paclitaxel compared with paclitaxel plus bevacizumab in advanced breast cancer: ECOG 2100. *J Clin Oncol*. 2008;26(28):4672–8.
6. Etienne-Grimaldi MC, Formento P, Degeorges A, Pierga JY, Delva R, Pivot X, Dalenc F, Espié M, Veyret C, Formento JL, Francoual M, Piutti M, de Crémoux P, Milano G. Prospective analysis of the impact of VEGF-A gene polymorphisms on the pharmacodynamics of bevacizumab-based therapy in metastatic breast cancer patients. *Br J Clin Pharmacol*. 2011;71(6):921–8.
7. Morita S, Uehara K, Nakayama G, Shibata T, Oguri T, Inada-Inoue M, Shimokata T, Sugishita M, Mitsuma A, Ando Y. Association between bevacizumab-related hypertension and vascular endothelial growth factor (VEGF) gene polymorphisms in Japanese patients with metastatic colorectal cancer. *Cancer Chemother Pharmacol*. 2013;71(2):405–11.
8. Sibertin-Blanc C, Mancini J, Fabre A, Lagarde A, Del Grande J, Levy N, Seitz JF, Olschwang S, Dahan L. Vascular Endothelial Growth Factor A c.*237C>T polymorphism is associated with bevacizumab efficacy and related hypertension in metastatic colorectal cancer. *Dig Liver Dis*. 2015;47(4):331–7.
9. Gampenrieder SP, Hufnagl C, Brechelmacher S, Huemer F, Hackl H, Rinnerthaler G, Romeder F, Monzo Fuentes C, Morre P, Hauser-Kronberger C, Mlineritsch B, Greil R. Endothelin-1 genetic polymorphism as predictive marker for bevacizumab in metastatic breast cancer. *Pharmacogenomics J*. 2016. doi:10.1038/tpj.2016.25 [Epub ahead of print]

10. Jain L, Sissung TM, Danesi R, Kohn EC, Dahut WL, Kummar S, Venzon D, Liewehr D, English BC, Baum CE, Yarchoan R, Giaccone G, Venitz J, Price DK, Figg WD. Hypertension and hand-foot skin reactions related to VEGFR2 genotype and improved clinical outcome following bevacizumab and sorafenib. *J Exp Clin Cancer Res.* 2010;29:95.
11. Baldwin SA, Beal PR, Yao SYM, King AE, Cass CE, Young JD. The equilibrative nucleoside transporter family, SLC29. *Pflugers Arch.* 2004;447(5):735–43.
12. San Martín R, Sobrevia L. Gestational diabetes and the adenosine/L-arginine/nitric oxide (ALANO) pathway in human umbilical vein endothelium. *Placenta.* 2006;27(1):1–10.
13. Hood JD, Meininger CJ, Ziche M, Granger HJ. VEGF upregulates ecNOS message, protein, and NO production in human endothelial cells. *Am J Physiol Heart Circ Physiol.* 1998;274(3 Pt 2):H1054–8.
14. Bouloumié A, Schini-Kerth VB, Busse R. Vascular endothelial growth factor up-regulates nitric oxide synthase expression in endothelial cells. *Cardiovasc Res.* 1999;41(3):773–80.
15. Facemire CS, Nixon AB, Griffiths R, Hurwitz H, Coffman TM. Vascular endothelial growth factor receptor 2 controls blood pressure by regulating nitric oxide synthase expression. *Hypertension.* 2009;54(3):652–8.
16. Zhang Y, Li J, Partovian C, Sellke FW, Simons M. Syndecan-4 modulates basic fibroblast growth factor 2 signaling in vivo. *Am J Physiol Heart Circ Physiol.* 2003;284(6):H2078–82.
17. Partovian C, Ju R, Zhuang ZW, Martin KA, Simons M. Syndecan-4 regulates subcellular localization of mTOR Complex2 and Akt activation in a PKCalpha-dependent manner in endothelial cells. *Mol Cell.* 2008;32(1):140–9.
18. Kunnas T, Nikkari ST. Contribution of syndecan-4 genetic variants to hypertension, the TAMRISK study. *BMC Res Notes.* 2014;7:815.
19. Isobe T, Uchino K, Makiyama C, Ariyama H, Arita S, Tamura S, Komoda M, Kusaba H, Shirakawa T, Esaki T, Mitsugi K, Takaishi S, Akashi K, Baba E. Analysis of adverse events of bevacizumab-containing systemic chemotherapy for metastatic colorectal cancer in Japan. *Anticancer Res.* 2014;34(4):2035–40.
20. Wicki A, Hermann F, Prêtre V, Winterhalder R, Kueng M, von Moos R, Rochlitz C, Herrmann R. Pre-existing antihypertensive treatment predicts early increase in blood pressure during bevacizumab therapy: the prospective AVALUE cohort study. *Oncol Res Treat.* 2014;37(5):230–6.
21. Hamnvik OP, Choueiri TK, Turchin A, McKay RR, Goyal L, Davis M, Kaymakcalan MD,

- Williams JS. Clinical risk factors for the development of hypertension in patients treated with inhibitors of the VEGF signaling pathway. *Cancer*. 2015;121(2):311–9.
22. Young JD, Yao SYM, Baldwin JM, Cass CE, Baldwin SA. The human concentrative and equilibrative nucleoside transporter families, SLC28 and SLC29. *Mol Aspects Med*. 2013;34(2-3):529–47.
 23. Antonioli L, Blandizzi C, Pacher P, Haskó G. Immunity, inflammation and cancer: a leading role for adenosine. *Nat Rev Cancer*. 2013;13(12):842–57.
 24. Chen J-F, Eltzschig HK, Fredholm BB. Adenosine receptors as drug targets — what are the challenges? *Nat Rev Drug Discov*. 2013;12(4):265–86.
 25. Bone DBJ, Choi DS, Coe IR, Hammond JR. Nucleoside/nucleobase transport and metabolism by microvascular endothelial cells isolated from ENT1-/- mice. *Am J Physiol Heart Circ Physiol*. 2010;299(3):H847–56.
 26. Farías M, San Martín R, Puebla C, Pearson JD, Casado JF, Pastor-Anglada M, Casanello P, Sobrevia L. Nitric oxide reduces adenosine transporter ENT1 gene (SLC29A1) promoter activity in human fetal endothelium from gestational diabetes. *J Cell Physiol*. 2006;208(2):451–60.
 27. Salsoso R, Farías M, Gutiérrez J, Pardo F, Chiarello DI, Toledo F, Leiva A, Mate A, Vázquez CM, Sobrevia L. Adenosine and preeclampsia. *Mol Aspects Med*. 2017. doi:10.1016/j.mam.2016.12.003 [Epub ahead of print]
 28. Escudero C, Casanello P, Sobrevia L. Human equilibrative nucleoside transporters 1 and 2 may be differentially modulated by A2B adenosine receptors in placenta microvascular endothelial cells from pre-eclampsia. *Placenta*. 2008;29(9):816–25.
 29. Vásquez G, Sanhueza F, Vásquez R, González M, San Martín R, Casanello P, Sobrevia L. Role of adenosine transport in gestational diabetes-induced L-arginine transport and nitric oxide synthesis in human umbilical vein endothelium. *J Physiol*. 2004;560(Pt 1):111–22.
 30. Acurio J, Troncoso F, Bertoglia P, Salomon C, Aguayo C, Sobrevia L, Escudero C. Potential role of A2B adenosine receptors on proliferation/migration of fetal endothelium derived from preeclamptic pregnancies. *Biomed Res Int*. 2014;2014:274507.
 31. Powe CE, Levine RJ, Karumanchi SA. Preeclampsia, a disease of the maternal endothelium: the role of antiangiogenic factors and implications for later cardiovascular disease. *Circulation*. 2011;123(24):2856–69.
 32. Iriyama T, Sun K, Parchim NF, Li J, Zhao C, Song A, Hart LA, Blackwell SC, Sibai BM, Chan L-NL, Chan T-S, Hicks MJ, Blackburn MR, Kellems RE, Xia Y. Elevated placental adenosine signaling contributes to the pathogenesis of preeclampsia. *Circulation*.

2015;131(8):730–41.

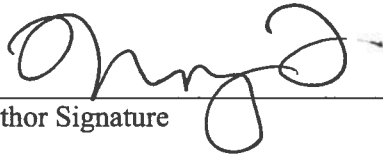
33. Leiva A, Pardo F, Ramírez MA, Farías M, Casanello P, Sobrevia L. Fetoplacental vascular endothelial dysfunction as an early phenomenon in the programming of human adult diseases in subjects born from gestational diabetes mellitus or obesity in pregnancy. *Exp Diabetes Res.* 2011;2011:349286.
34. Feoktistov I, Ryzhov S, Zhong H, Goldstein AE, Matafonov A, Zeng D, Biaggioni I. Hypoxia modulates adenosine receptors in human endothelial and smooth muscle cells toward an A2B angiogenic phenotype. *Hypertension.* 2004;44(5):649–54.
35. Casanello P, Torres A, Sanhueza F, González M, Farías M, Gallardo V, Pastor-Anglada M, San Martín R, Sobrevia L. Equilibrative nucleoside transporter 1 expression is downregulated by hypoxia in human umbilical vein endothelium. *Circ Res.* 2005;97:16–24.
36. Adair TH. Growth regulation of the vascular system: an emerging role for adenosine. *Am J Physiol Regul Integr Comp Physiol.* 2005;289(2):R283–96.
37. Kindler HL, Niedzwiecki D, Hollis D, Sutherland S, Schrag D, Hurwitz H, Innocenti F, Mulcahy MF, O'Reilly E, Wozniak TF, Picus J, Bhargava P, Mayer RJ, Schilsky RL, Goldberg RM. Gemcitabine plus bevacizumab compared with gemcitabine plus placebo in patients with advanced pancreatic cancer: phase III trial of the Cancer and Leukemia Group B (CALGB 80303). *J Clin Oncol.* 2010;28(22):3617–22.
38. García-Cardena G, Fan R, Shah V, Sorrentino R, Cirino G, Papapetropoulos A, Sessa WC. Dynamic activation of endothelial nitric oxide synthase by Hsp90. *Nature.* 1998;392:821–4.
39. Cekic C, Linden J. Purinergic regulation of the immune system. *Nat Rev Immunol.* 2016;16(3):177–92.
40. Leone RD, Lo Y-C, Powell JD. A2aR antagonists: Next generation checkpoint blockade for cancer immunotherapy. *Comput Struct Biotechnol J.* 2015;13:265–72.

Publishing Agreement

It is the policy of the University to encourage the distribution of all theses, dissertations, and manuscripts. Copies of all UCSF theses, dissertations, and manuscripts will be routed to the library via the Graduate Division. The library will make all theses, dissertations, and manuscripts accessible to the public and will preserve these to the best of their abilities, in perpetuity.

Please sign the following statement:

I hereby grant permission to the Graduate Division of the University of California, San Francisco to release copies of my thesis, dissertation, or manuscript to the Campus Library to provide access and preservation, in whole or in part, in perpetuity.

A handwritten signature in black ink, appearing to be 'Ming', written over a horizontal line.

Author Signature

3/30/2017
Date